Regulation of LFA-1 on T cells by phosphoinositide signalling

Kristoffer Haurum Johansen

National Institute of Allergy and Infectious Disease, NIH &

Department of Pathology, University of Cambridge

This dissertation is submitted to University of Cambridge

for the degree of *Doctor of Philosophy*

Clare Hall

June, 2021

Declaration

This dissertation is the result of my own work and includes nothing which is the outcome of work done in collaboration except as declared in the Preface and specified in the text.

It is not substantially the same as any that I have submitted, or, is being concurrently submitted for a degree or diploma or other qualification at the University of Cambridge or any other University or similar institution except as declared in the Preface and specified in the text. I further state that no substantial part of my dissertation has already been submitted, or, is being concurrently submitted for any such degree, diploma or other qualification at the University of Cambridge or any other University or similar institution except as declared in the Preface and specified in the text.

This dissertation does not exceed the word limit set by the Faculty of Biology of 60,000 words excluding appendices, bibliography, footnotes, tables and equations.

Kristoffer Haurum Johansen, 2021

To the loves of my life, Line & Albert — in hope that the future will be as bright as now.

Regulation of LFA-1 on T cells by phosphoinositide signalling

Submitted by Kristoffer Haurum Johansen

Summary

Lymphocyte Function-Associated Antigen 1 (LFA-1) is the major integrin in T cells and binds Intercellular Adhesion Molecule 1 and 2 (ICAM-1 and ICAM-2) expressed on endothelial cells and antigen presenting cells. LFA-1 affinity for ICAM is increased following chemokine and T cell receptor (TCR) engagement by inside-out signalling. This process coordinates T cell migration, adhesion, and activation of T cells. LFA-1 activation is mediated by phosphoinositide 3-kinase (PI3K) and the downstream phosphoinositide PtdIns(3,4,5)P_3 (PIP_3).

To investigate how PI3K regulates LFA-1, I optimised CRISPR/Cas9-mediated mutagenesis in T cells, and designed a retroviral library of CRISPR/single guide RNAs targeting all known and potential PIP_3-binding proteins. Using this library, I screened the targeted genes for effects on ICAM-1-binding by a flow cytometry-based ICAM-1-binding assay, using *Cas9*-expressing primary mouse T cells. I identified multiple proteins regulating LFA-1-mediated adhesion to ICAM-1, including the RAP1/RAS GTPase-activating protein RASA3. I found that RASA3 is a critical negative regulator of LFA-1 activation and that RASA3 is inhibited by PI3K signalling. T cells without RASA3 have greatly increased ICAM-1-binding.

Mice with conditional deletion of *Rasa3* in T cells have altered T cell homeostasis including increased numbers of mature thymocytes in the thymus, but decreased T cells in lymph nodes, spleen, and especially in the blood. Further, *Rasa3* deletion in T cells resulted in reduced germinal centre and antigen-specific antibody responses to immunisation, likely as a result of decreased T follicular helper (T_{FH}) cell numbers.

The presented results thus describe a novel genetic screen in T cells which has uncovered a critical role for RASA3 as a PI3K-regulated inhibitor of T cell adhesion and migration that is required for T cell homeostasis and function.

Acknowledgements

The journey of a lifetime. Thanks to all; scientific collaborators, mentors, friends, and family.

About four years and six months ago I was fortunate to commence this journey of unknowns. I travelled to the capital of the western world, Washington D.C. to start my PhD project in the lab of Dr. Pamela L. Schwartzberg at the National Institutes of Health. At that time, she was to me purely a well-renowned brilliant scientist with whom I had spoken on the phone once and exchanged a dozen emails. Pam turned out to be much more than I could have hoped for – a joy to work with, a great friend, and a vast human reservoir of immunological knowledge. Pam supported me through ups and downs (and an odd presidency…), nurtured my scientific curiosity, taught me how to conduct vigorous science, introduced me to many kings and queens of the immunological community, and provided a fantastic environment for a young scientist to grow. Pam, thank you for it all, looking forward to future collaborations and your future visits to us in Europe!

On the other side of the Atlantic ocean, in a country with an equally interesting political (read odd) landscape, Great Britain, the king of OkkenVikings was ready to steer my Viking ship of T cell integrin immunology to conquer further unknown scientific territory. Professor Klaus Okkenhaug at the Department of Pathology, University of Cambridge, whom I knew from a research rotation six years ago, hosted me for the last two and a half years of my PhD. Klaus has been no less than a perfect mentor and friend. From social fun trips in our inflatable kayaks on the River Cam, long runs and half marathons, to thoughtful discussions about anything from the intricate mechanisms of TCR-mediated PI3K activation and integrins in T_{reg} cells to Scandinavian politics and dreams of distant skiing slopes. I am eternally grateful, and the way you have taken me, Line, and Albert in as extended family has been a joy. It is begrudgingly that I will leave the lab this summer, but we will stay in touch.

Which brings us to Line. Line, you have been the guiding light that has carried me through the sometimes tough patches, and more so the endless adventures and experiences this PhD has brought about. Also thanks for fixing my Table of Contents and reminding me to back up. Lately (6 months ago), our family journey has been enriched with little baby Albert; energy bomb of joy, temperamental sleep thief, everything we could ever have wished for and more. Our love to you is eternal.

Many thanks to my family in Denmark for enduring; Anton, Rasmus, John and Marianne, I have many times missed you a lot, and always been able to seek support and advice from you. Thank you for always being there for me; I can't wait to be back in Denmark close to you all again.

This brings us to my now extended family; all the wonderful colleagues and friends I have been fortunate to get to know these last years.

Bonnie, thanks for being a wonderful friend, for teaching me everything CRISPR and beyond, and for endless discussions about work and life. Silvia, thank you for being who you are, and bringing Italian proverbs and slanter to the table. Thanks to Dom for carrying the RASA3 torch after I left NIH, and Jenn, Julie, Julio, and Robin; I miss you all, and thanks for all your help and assistance!

Thank you to Carly for amazing climbing, hiking, fun and eventful times, you were like a long lost sister to me. Eli, my roomie and friend, and the rest of the Ducklettes for pretending like we could be rock stars and scientists at the same time. Keith, Pavol, Keyla, Javier, Nick, and the rest of the NIH crew for being more fun than I could have asked for.

At the other side of the pond thanks to Christina for being the wonderful lab mate you are - in and out of work, *Muchas gracias muchacha*! Anita for being a great friend, Julie for being an absolutely amazing masters student and the rest of the extended OkkenVikings family; Grace, Anne, Iqbal, Julius, Andrew, Fabien, Leandra, Fiore, Anna (Great part II student!), Alberto; it would not have been possible without you all. Rahul and James for being amazing mentors; always been a huge help and delight to discuss science and life with you. Also Theodor, Sofia, Sherden, Lasse, Sven; great friends for life!

To collaborators, mentors, and the OxCam PhD family that have always been great; Dr. Chung Park for imaging *Rasa3* KO T cells in vivo, Dr. Tibor Verez and Edward Schrom with LN whole tissue imaging, Dr. Ronald Germain, Professor Doreen Cantrell, Dr. Larry Samelson, Dr. John Kehrl for helpful discussions, Professor Wolfgang Bergmeier for providing mice and advice, Dr. James Phelan for assistance with CRISPR/Cas9 screening, and Dr. Meritxell Nus and James Harrison for providing *Bcl6*-flox x $Cd4^{Cre}$ mice.

A special note of thanks to all the technicians that have helped me throughout; animal technicians at NHGRI, NIH and Gurdon, University of Cambridge, as well as core facility managers. I have been fortunate to work with the best! Joanna and Carl at the flow core in Department of Pathology in Cambridge, and Stacie and Martha at the flow core at NHGRI, NIH; I have used and abused your help, and I am eternally indebted.

Thank you to all my Danish friends for staying in touch, to many of you for visiting me; Holti & Emilie, Marco & Yaffah, Rasmus, Oskar & Nanna, Stine & Camilla, Sasha, Anna, Emma & Simon, Andreas & Jonas. Lastly a big thanks to all who I have not mentioned but are dear to me!

Lastly a big thank you to Wellcome Trust and NIH for funding the research, and to NIH and University of Cambridge for providing me the ideal scientific environments to pursue my PhD.

Table of acknowledgement of assistance during the course of the thesis

Training and mentoring **(initial training of basic techniques, and mentoring/brainstorming throughout)**	
Dr. Bonnie Huang	CRISPR/Cas9 screening and optimisation, cloning, general T cell work
Dr. Silvia Preite	Immunisations and flow cytometry
Dr. Jennifer Cannons	Biochemistry, *in vitro* assays
Dr. Senta Kapnick	T cell culture
Dr. Christina Courreges	Western blotting
Dr. Anne-Katrien Stark	Flow cytometry
Dr. Fabien Garcon	ICAM-1-binding assay
Data obtained from technical service providers **(sequencing, cell sorting, animal husbandry, facilities)**	
Stacie Anderson and Martha Kirby, at NHGRI, NIH	Cell sorting
Joanna Cerveira & Carl Bradford, Pathology, Uni. of Cambridge	Cell sorting
Gurdon Institute, Biomedical Services	Animal husbandry
Animal facility, NHGRI, NIH	Animal husbandry
Gurdon Institute sequencing facility	Sanger sequencing
Imaging facility, NHGRI, NIH	Confocal Imaging
Imaging facility, Pathology, Uni. of Cambridge	Confocal imaging
Data produced jointly **(Either because of technical help needed, or where help was desirable due to limited hands)**	
Dr. Silvia Preite, Julie Reilley, Dr. Jennifer Cannons, Dr. Dominic Golec, Dr. Grace Cooper, Dr. Christina Courreges	Processing of tissues
Dr. Silvia Preite	Some immunisation experiments
Dr. Christina Courreges	Recording of flow cytometry
Dr. Tibor Verez and Dr. Edward Schrom	Help with Ce3D imaging and analysis
Data/materials provided by someone else **(Data produced by others, and included in thesis or appendices)**	
Dr. Dominic Golec & Dr. Bonnie Huang	Repeats of OT-II transfer experiment
Dr. Bonnie Huang & Dr. James Phelan	Next-gen sequencing of CRISPR screens
Dr. Silvia Preite & Dr. Dominic Golec	Immunisation repeat
Dr. Chung Park & Dr. Dominic Golec	Cell transfer/migration studies (discussed in thesis)
Julie Hagedorn Thomsen	Confocal imaging (I supervised, Julie did most of the imaging)

Contents

List of Figures

List of Tables

Abbreviations

Abbreviaton	full name
4E-BP1	4E binding protein 1
ADAM17	disintegrin and metalloprotease 17
ADAP	Adhesion and degranulation promoting adaptor protein
AID	Activation-induced cytidine deaminase
APC	Antigen-presenting cells
BTK	Bruton's kinase
CALDAGEF-I	RAS guanyl releasing protein 2
CCL	CC-chemokine ligand
CCR	CC-chemokine receptor
CRISPR	Clustered regularly interspaced short palindromic repeats
crRNA	CRISPR RNA
cSMAC	Central supramolecular clusters
CSR	Class switch recombination
CTL	Cytotoxic $CD8^+$ T lymphocytes
CXCL	CXC-chemokine ligand
CXCR	CXC-chemokine receptor
DAG	Diacylglycerol
DC	Dendritic cells
DHR	Dock Homology Domains
DN	Double negative
DOCK	Dedicator of cytokinesis
DP	Double positive
dSMAC	Distal supramolecular clusters
DZ	Dark zone
dLN	draining popliteal lymph node
EAE	experimental autoimmune encephalomyelitis
EBI2	Epstein-Barr virus induced molecule-2
ERM	Ezrin, radixin, and Myosin
FACS	Fluorescence-activated cell sorting
FDC	Follicular dendritic cells
FERM3	Fermitin family homolog 3
FOXO1	Forkhead box protein O1
FRC	Fibroblastic reticular cell
FUT	Fucosyltransferase 7
FYB	Adhesion and degranulation promoting adaptor protein
GAGs	Glycosaminoglycans
GAP	GTPase activating proteins
GC	Germinal centers
GEF	Guanine exchange factor
GlcNAc6ST1/2	N-acetylglucosamine 6-O-sulphotransferase 1/2
GPR183	Epstein-Barr virus induced molecule-2
GRB2	Growth factor receptor-bound protein 2
GST	Glutathione S Transferase
HDR	homology-directed repair
HEV	High endothelial venules
ICAM	Intercellular Adhesion Molecules
ICOSL	Inducible costimulatory ligand
IFNγ	Interferon γ
Ig	Immunoglobulin
IP3	Inositol triphosphate
IP4	$Ins(1,3,4,5)P_4$
IPEX	Immunodysregulation polyendocrinopathy enteropathy X-linked
IRF4	Interferon regulatory factor 4
IS	Immunological synapse
ITAM	immunoreceptor tyrosine-based activation motifs
ITK	IL-2-inducible kinase
iT_{reg}	Inducible T_{reg}
IVC	Individually ventilated cages
IVC	Individually ventilated cages
JAM	Junctional adhesion molecules
LAT	Linker for Activation of T cells
LFA-1	Lymphocyte function-associated Antigen-1
LM-OVA	Listeria monocytogenes ovalbumin
LN	Lymph node
LPP3	Lipid phosphate phosphatase 3
LZ	Light zone
MACS	magnetic-activated cell sorting
MAP	Mitogen-activated protein
MHC	Major histocompatibility complex
mLN	Mesenteric LNs
mTORC1	mTOR complex 1
NHEJ	Non homologous end joining
NT	Non-targeting
OSBPL	Oxysterol binding protein related proteins
PAM	Protospacer adjacent motif
PAMP	Pathogen-associated molecular pattern
PBP	PIP3-binding proteins
PD1	Programmed cell death protein 1
PDK1	3-Phosphoinositide-dependent protein kinase-1
PFA	Paraformaldehyde
PH	Pleckstrin homology
PI3K	Phosphoinositide 3-kinase
PIP_2	Phosphatidylinositol (4,5)-bisphosphate
PIP_3	Phosphatidylinositol (3,4,5) P3
PKC	Protein Kinase C
PLC	Phospholipase C

pLN	Peripheral lymph node
PNAd	Peripheral node addressins
PP	Peyer's patches
pSMAC	Peripheral supramolecular clusters
PtdIns	Phosphatidylinositol
PI	Phosphoinositide
PTEN	phosphatase and tensin homolog
RASA3	RAS P21 Protein Activator 3
RASGRP2	RAS guanyl releasing protein 2
RIAM	Rap1-GTP-interacting adaptor molecule
S1P	Sphingosine 1-phosphate
S1PR1	Sphingosine 1-phosphate receptor 1
scICAM-1	soluble complexed ICAM-1
S6K	S6 kinase
SAP	Signalling lymphocytic activation molecule associated protein
sgRNA	Single guide RNA
shRNA	Short hairpin RNA
SKAP1	SRC kinase associated phosphoprotein 1
SLAM	Signaling lymphocytic activation molecule
SLO	Secondary lymphoid organ
SLP76	SH2-domain-containing leukocyte protein of 76 kDa
SMAC	supramolecular clusters
SMH	Somatic hypermutations
SOS	Son of Sevenless
SP	single positive
SWAP70	Switch associated protein 70
TACE	Tumor Necrosis Factor converting enzyme
TCR	T cell receptor
TEM	Transendothelial migration
T_{FH}	T follicular helper
T_{FR}	T follicular regulatory
T_H	T helper
TNFα	Tumour necrosis factor α
tracrRNA	Trans-activating RNA
T_{reg}	Regulatory T
tT_{reg}	Thymic T_{reg}
VCAM-1	Vascular cell adhesion molecule-1
VLA-4	Very late antigen 4
WB	Western Blot
ZAP-70	Zeta-chain-associated protein kinase 70

Chapter 1

Introduction

1. Introduction

The immune system guards the body against invading microorganisms, including viruses, bacteria, fungi, and parasites, as well as cells that have run their course or gone awry, including cancer cells. Innate immune responses defend against most infections swiftly (within minutes or hours of infection), and will combat most invaders whilst recruiting other immune cells by secreting cytokines and chemokines. Innate immune cells, including macrophages, neutrophils and monocytes, recognise *pathogen-associated molecular patterns* (PAMP) that are broadly shared by pathogens. The second line of defence is the adaptive immune system. Contrary to the innate immune response, adaptive immune responses are specific to distinct antigens. Adaptive immune responses kick in more slowly (in days or weeks) and are involved in combating resilient infections, as well as the development of memory towards the pathogen, which enables a faster mobilisation of a stronger adaptive response in case of re-infection. Adaptive immune responses are mediated by B cells, that secrete soluble antibodies specific to foreign antigen, and T cells, that recognise fragments of antigen presented on infected or cancer cells in the context of MHC molecules. All of these processes are tightly regulated, and dysregulated immune responses may lead to autoinflammatory (in the context of innate immune cells) or autoimmune diseases (in the context of adaptive immune cells). To ensure timely and efficient activation of adaptive immune cells, ingenious systems have developed through evolution controlling the selective development and survival of non-self-reactive naïve B and T cells. Important for these tightly regulated processes are a plethora of surface receptors, and regulators thereof.

In this chapter I will introduce the ins and outs of T cell biology (Chapter 1.1), with a focus on migration, and regulation of integrins (Chapter 1.3). I will describe how *phosphoinositides* (PIs) are regulated (Chapter 1.2), and how these signalling lipids regulate crucial T cell functions, including integrin-mediated T cell adhesion (Chapter 1.4). Chapter 1.5 introduces how CRISPR/Cas9 has revolutionised the way we study signal transduction, and how this can be applied to study signalling networks in T cells in a fraction of the time it would take with conventional genetically modified animals. Finally, I will introduce what this PhD project sought out to investigate, and the hypotheses and aims of the PhD (Chapter 1.6).

1.1 T cell biology

1.1.1 T cell development

T cells develop in the thymus from hematopoietic stem cells originating from the bone marrow. The thymus is an organ situated anterior of the heart specialised in T cell development (therefrom the name T cells). In the thymus, progenitor T cells commit to their T cell lineage, giving rise to a pool of $CD3^-$, $CD4^-CD8^-$ *double negative* (DN) thymocytes. Most precursor cells commit to become conventional α:β T cells, giving rise to ~95% of the mature T cells whereas the remaining ~5% turn into γ:δ T cells. DN thymocytes committed to the α:β lineage undergo 4 DN stages (DN1-4) [1]. These DN stages start differentiation at the cortico-medullary junction (DN1) and progress through DN2 whilst migrating to the subcapsular region where DN3-4 occurs [2]. In DN1 cells *T cell receptor* (TCR) related genes are in the germline configuration. DN2 cells initiate TCRβ VDJ rearrangement, which continues in DN3 cells. DN3 cells that successfully produce a rearranged β-chain coupled to an invariant pre-T α chain (giving rise to a pre-TCR), progress to become DN4 cells. DN4 cells proliferate, arrest β-chain rearrangement, and upregulate both CD4 and CD8 giving rise to *double positive* (DP) thymocytes [1].

DP thymocytes, now in the deeper thymic cortex, initiate a process of positive selection. DP thymocytes, that are able to recognise self-peptide in the context of *major histocompatibility complex* (MHC) molecules on thymic stromal cells, survive (hence positive selection). DP thymocytes, that do not successfully undergo positive selection will rearrange their α-chain and retry the interaction selection process, and eventually undergo apoptosis. DP thymocytes that bind self-peptide:MHC too strongly (and hence would risk activating in response to self-antigens in the periphery), are deleted by a process termed negative selection. DP thymocytes with an appropriate, intermediate affinity are thus able to bind MHC, but are not reactive to self-peptides. During positive selection DP thymocytes with a TCR capable of engaging with MHC class I downregulate CD4 to become $CD8^+$ *single positive* (SP) thymocytes, whereas DP thymocytes capable of binding MHC class II downregulate CD8 to become $CD4^+$ SP thymocytes. These immature SP thymocytes migrate to the medulla of the thymus, where they undergo further negative selection through interactions with thymic *antigen-presenting cells*

(APCs) and undergo further maturation to become mature thymocytes, that express CD62L (also known as L-selectin) and *sphingosine 1-phosphate receptor 1* (S1PR1) [1, 3]. Expression of S1PR1 allows the mature thymocytes to egress the thymus through the blood as newly developed naïve T cells.

1.1.2 T cell recirculation, adhesion, and migration

Following T cell development, T cells migrate to the lymphatic system, where they recirculate as naïve T cells between *secondary lymphoid organs* (SLO) such as *lymph nodes* (LN), *Peyer's patches* (PP) and spleen through blood and lymphatic vessels by a process termed homing. As the frequency of naïve T cells specific to a given antigen is very low (~100 T cells specific to a given antigen [4, 5]), the probability of random encounter with a T cells cognate antigen is very low. To mitigate this conundrum, T cell homing is tightly regulated, and intricate lymphoid systems are in place guiding the T cells through LN allowing for sampling of antigen in a concentrated coordinated manner from *dendritic cells* (DC). These transient interactions with APCs are interrupted when the T cell recognises its cognate antigen, after which the T cell is activated. These activated T cells can proliferate more than 1000-fold and acquire effector functions, preparing to migrate to the site of infection (Figure 1-1a).

1.1.2.1 Homing and migration of naïve T cells

Recirculation to and migration within LNs and other SLOs

During circulation through the blood, T cells are subject to extreme physical forces as a result of the rapid flow of blood (1-70 dyn/cm^2) [6, 7]. To exit the circulation at the correct place at the right time, tight regulation of expression and avidity of adhesion receptors is necessary to allow for *transendothelial migration* (TEM) into LNs (as well as PPs) through thick specialised postcapillary venules (termed *high endothelial venules* (HEVs)) for naïve T cells and central memory T cells, and into inflamed tissues for effector T cells [8]. These adhesion receptors form stable bonds with their ligands expressed on these specialized endothelial cells. During naïve T cell recirculation, the initial interactions preceding TEM are mediated in part by the interaction of CD62L on T cells, with *peripheral node addressins* (PNAds) expressed on HEV associated endothelial cells. PNAds are sialylated mucins (sialomycins; often CD34 or

GlyCAM-1) containing a sulphated form of Sialyl Lewis X tetrasaccharides [9, 10] (Figure 1-1b, step 1). These sialylations are a product of multiple HEV-specific enzymes, including *N-acetylglucosamine 6-O-sulphotransferase 1/2* (GlcNAc6ST1/2) and *fucosyltransferase 7* (FUT7) [11-13]. The resulting CD62L/PNAd interaction induces rolling of the T cells, which allows binding of chemokines immobilised on HEV-expressed *glycosaminoglycans* (GAGs) [14] by chemokine receptors. *Peripheral LN* (pLN) homing is mainly regulated by *CC-chemokine ligand 21* (CCL21) and CCL19 immobilized on HEV, which engages *CC-Chemokine Receptor 7* (CCR7) on naïve T cells [15-17]. Chemokine stimulation then rapidly induces *Lymphocyte function-associated antigen 1* (LFA-1) on the T cell, which binds *Intercellular Adhesion Molecules* (ICAMs) expressed on the endothelial cells resulting in arrest of the T cell (Figure 1-1b, step 2). The arrested T cell will then migrate along the endothelial barrier for several minutes until they localise dedicated "exit ramps" where they undergo TEM through the endothelial barrier into the LN parenchyma (Figure 1-1b, step 3-4) [18]. Together,

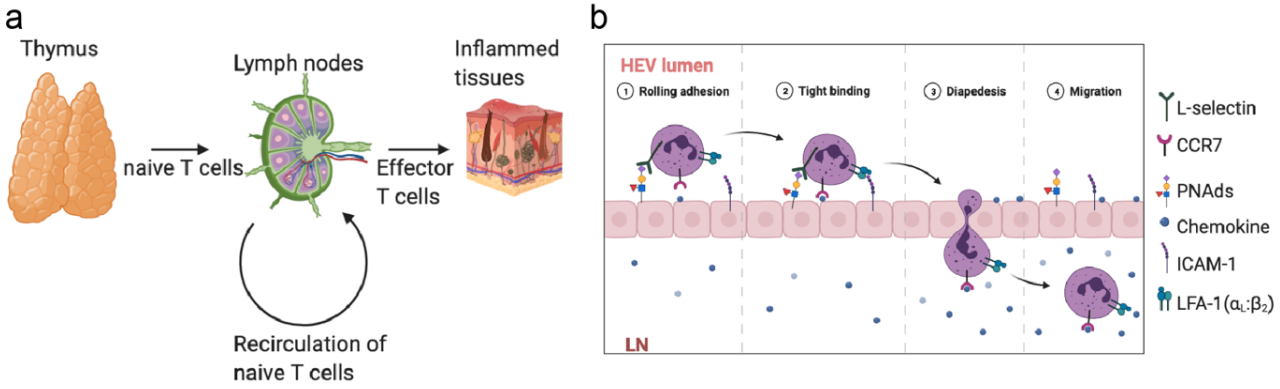

under steady state HEVs thus function as a selective gateway to the LNs, attracting naïve and resting memory T cells, but blocking entry of other leukocytes such as neutrophils [19].

Figure 1-1. T cell life cycle and LN entry. **a**, Schematic of the T cell life cycle from development in the thymus to recirculation between SLOs (including LNs) and eliciting effector functions in inflamed tissues. **b**, schematic of LN entry showing the 4 steps of TEM; 1. Rolling/initial adhesion, 2. Tight binding mediated by integrins, 3. Diapedesis/TEM through the endothelial barrier and exit through "exit-ramps", 4. Migration in the paracortex. Figure prepared in BioRender.

The majority of naïve T cells enter LNs through HEVs (Figure 1-2, step 1), however it has recently been shown, that naïve T cells, which have exited a primary LN through efferent lymphatics, can enter secondary LNs through afferent lymphatics and enter the paracortex of these secondary LNs in a CCR7-dependent manner (Figure 1-2, step 2) [20]. This challenges

the dogma that primarily effector memory T cell subsets use this route of entry to home to LNs [21]. However, effector subsets are often migrating through afferent lymphatics draining tissues such as skin, whereas the naïve T cell subsets arriving through afferent lymphatics are primarily migrating from other LNs. Similarly, some transmigrating DCs migrate through afferent lymphatics in a CCR7-dependent manner, whereas other DC subsets enter LNs through HEVs similar to the majority of naïve T cells [8].

Following LN entry through HEVs, T cells are momentarily trapped in the perivascular space just below the HEVs allowing them to interact with DCs accumulated around the HEVs [18, 22]. Subsequently T cells migrate along the T cell zone *fibroblastic reticular cells* (FRCs) in an apparently stochastic manner through the paracortex [18]. FRCs express high levels of chemokines CCL21 and CCL19 which regulate T cell motility, as well as the homeostatic cytokine IL-7 [23]. Accordingly, studies of CCR7-deficient mice have found that CCR7 is required for efficient retention of lymphocytes in the paracortex and is thereby thought to increase duration of APC-T cell interactions before T cells exit and progress to other SLOs [24]. CCR7 thus both regulates T cell LN entry, and the localisation of T cells in the paracortex of the LNs. LN-bound and resident DCs are similarly accumulated along the T cell zone FRCs, where they continuously probe the lymph for antigen [25, 26], which in turn are presented to T cells scanning for antigen along these FRC networks (Figure 1-2, step 3).

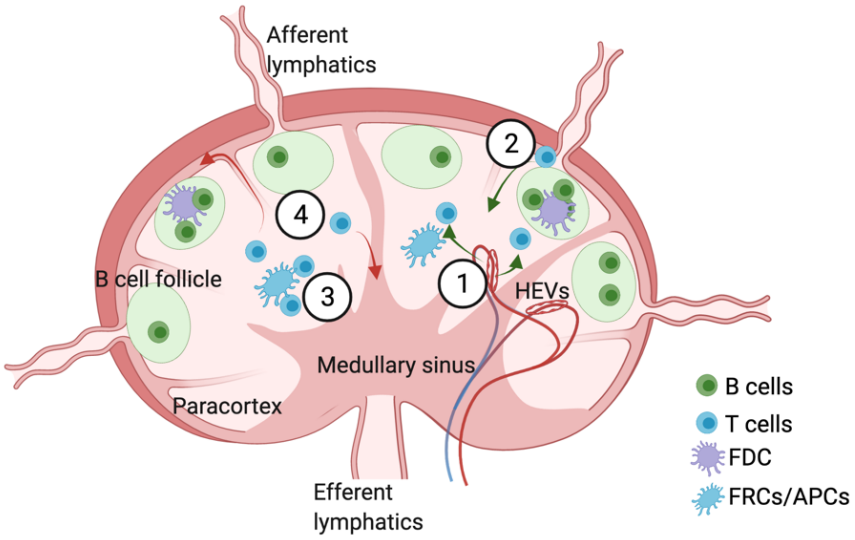

Figure 1-2. T cell LN migration. Simplified diagram showing entry through HEVs (1), entry through afferent lymphatic vessels (2), scanning of APCs for cognate antigen (3), and egress through efferent lymphatics (4). Figure made in BioRender.

Eventually non-stimulated naïve T cells egress from the LNs through efferent lymphatics (Figure 1-2, step 4). This process is also tightly regulated. *Sphingosine 1-phosphate* (S1P) concentrations are kept low in the LN by S1P lyases [27], whereas sphingosine kinases expressed by endothelial cells produce S1P in the blood [28]. As a result of being in a S1P-depleted environment S1PR1 is upregulated (S1P stimulation results in internalisation of S1PR1). The resulting S1P gradient and expression of S1PR1 in naïve T cells that have been in the LNs long enough to upregulate the receptor, allows the T cells to egress through cortical sinuses, from which the T cells will flow through the medullary sinuses into the efferent lymph [29, 30]. Following egress through efferent lymphatics, the lymphatics connect LNs in series, but eventually merge with the thoracic duct allowing the T cells to recirculate through the blood.

Migration to and within the spleen

The spleen is specialised in filtering blood-borne pathogens, and thus plays a major role in infectious disease. The spleen is the SLO, through which most cells pass and understanding splenic recirculation is therefore crucial [31]. Contrary to other SLOs the spleen does not contain HEVs, and instead spleen entry is dependent on different regulatory mechanisms. T cells (and other lymphocytes) enter the spleen with the blood into the red pulp and marginal

zone. Therefrom, the T cells migrate through marginal zone bridging channels into the T cell zone in the white pulp in a one-directional CCR7-dependent manner supported by the perivascular splenic stroma [16, 31]. Similar to T cells in LNs, T cells in the spleen express high levels of the S1P receptor, S1PR1, likely as a consequence of low S1P presence in the spleen compared to blood [32]. However, the role of S1P in egress from the spleen is less clear. An elegant study using a reporter mouse expressing GFP-tagged S1PR1 on macrophages (allowing for quantification of internalised S1PR1 as a measure for S1P levels) to study S1P levels in subregions of tissues allowed for quantification of S1P levels in the spleen. The study found that *lipid phosphate phosphatase 3* (LPP3)-deficient mice have high levels of S1P in the red pulp, whereas S1P in WT mice is low in the red pulp. This suggests that LPP3 is involved in degrading S1P entering with the blood into the spleen. Similarly, in the white pulp low levels of S1P were observed and this also seemed to be regulated by LPP3. These findings indirectly hint that S1P-dependent T cell sensing is at least partially involved in splenic egress [33].

1.1.2.2 Chemokine-mediated attraction of T cells

Chemokine-mediated attraction of T cells is a highly complex and redundant process mediated by multiple chemokine receptors for each T cell subset. Each chemokine receptor is further induced by multiple different chemokine ligands. Chemokines are small (8-12 kDa) peptides that bind specialised Gαi-protein-coupled receptors (chemokine receptors). Binding of chemokines induces migration of the lymphocyte towards the chemokine gradient by chemotaxis. Some chemokines are primarily involved in migration of lymphocytes to, and development of, lymphoid structures (homeostatic chemokines), whereas others are involved in attraction of lymphocytes to inflammatory tissues (inflammatory chemokines). The respective roles of chemokines and their receptors in T cells are summarised in Table 1-1.

Table 1-1. Chemokine receptors in T cells

RECEPTOR	LIGAND	PREDOMINANT ROLE IN T CELLS	REFERENCES
CCR1	CCL3, CCL5, CCL7, CCL23	Attraction of T_H1 to inflammatory sites	[34, 35]
CCR3	CCL5, CCL7, CCL11, CCL13, CCL26	Attraction of T_H2 to inflammatory sites	[35, 36]

CCR4	CCL2, CCL4-5, CCL17, CCL22	Attraction of T_H2, T_H17 and T_{reg} to inflammatory sites	[36, 37]
CCR5	CCL3-5	Attraction of T_H1 to inflammatory sites	[38-40]
CCR6	CCL20	Attraction of T_H17 and T_H22 to inflammation in gut, LN, liver	[41]
CCR7	CCL19, CCL21	Homing to SLO of naive and CM T cells	[42]
CCR8	CCL1, CCL8	Positioning of T_H2 in specialised areas in SLO	[37]
CCR10	CCL27-28	Attraction of T_{reg} and T_H22 to inflamed skin	[43, 44]
CXCR3	CXCL9-11, CXCL4L1	Attraction of T_H1 and $CD8^+$ T cells to inflammatory sites	[45]
CXCR4	SDF1	T cell survival and homing	[40]
CXCR5	CXCL13	T_{FH} and T_{FR} cell positioning in GCs in LNs	[46]
CX3CR1	CX3CL1 (Fractalkine)	T cell migration	[47]

Chemokine-mediated induction of chemokine receptors results in activation of intracellular Gα-proteins by exchange of GDP with GTP, which results in separation of the Gα protein from Gβγ proteins. These separated proteins can then activate downstream effector proteins, including *phospholipase C* (PLC) β [48]. PLCβ cleaves the *phosphatidylinositol(4,5)-bisphosphate* (PIP_2) into *diacylglycerol* (DAG) and *inositol triphosphate* (IP_3), which act as lipid second messengers. As second messengers DAG activates *Protein Kinase C* (PKC), which triggers chemotaxis, including LFA-1-mediated locomotion [49, 50]. IP_3 triggers calcium release, which further activates PKC, as well as induces transcriptional changes in the cells and the calcium dependent RAP1 *guanyl exchange factor* (GEF), *RAS guanyl releasing protein 2* (RASGRP2; also known as CALDAGEF-I) [48, 51, 52]. Further, G-protein activation results in activation of the class IB *phosphoinositide 3-kinase* (PI3K), PI3Kγ, resulting in increased levels of *phosphatidylinositol(3,4,5)-trisphosphate* (PIP_3) along the leading edge of the migrating cell [48, 53]. PI3K signalling will be discussed further in Chapter 1.2; briefly, PI3Kγ signalling downstream of chemokine receptor signalling supports survival of T cells [54], induces transcriptional changes [55], actin polymerisation [56], and is involved in activation of the integrin LFA-1 [49].

Under steady state, CCR7 and *CXC-chemokine receptor* (CXCR) 4 are the main receptors involved in migration to and within LNs. As described above (Chapter 1.1.2.1) CCR7 is induced by the homeostatic chemokines CCL19 and CCL21 presented by HEVs [17] or

secreted by FRCs. CXCR4 is similarly expressed by naïve T cells. CXCR4 responds *to CXC-chemokine ligand* (CXCL) 12 (also known as SDF1α) presented on HEVs, as well as CXCL13, which is more abundant in PPs than LNs, however CXCR4 is only modestly involved in homeostatic migration of T cells [57]. Interestingly, T cells in the LNs have been shown to desensitise and internalise CCR7, which possibly allows the naïve T cells to recirculate to the blood towards S1P gradients [58].

1.1.2.3 Differentiation and homing of antigen-encountered T cells

CD4⁺ T cells

Naïve CD4⁺ T cells are activated by peptide presented on MHC class II on APCs and differentiate to distinct effector CD4⁺ *T helper* (T_H) subsets characterised by their ability to produce and secrete particular cytokines. Broadly, T_H1 cells are involved in inflammatory responses against intracellular pathogens and primarily produce *Interferon γ* (IFNγ), *Tumour necrosis factor α* (TNFα), and IL-2 that among other functions assist by stimulating and activating macrophages and CD8⁺ T cells. T_H2 cells are important in defences against extracellular pathogens, including parasites, and protect tissues and secrete high levels of IL-4, that assist B cell responses by inducing differentiation and antibody production. T_H2 cells also secrete other cytokines involved in activation of mast cells and eosinophils. Additional T_H subsets have been described, including gut-associated T_H17 cells, which produce IL-17 and aid in the defence against gut associated pathogens; and IL-9 secreting T_H9 cells involved in protection against helminth infections. Lastly, of particular importance to this thesis are *T follicular helper* (T_{FH}) cells found in B cell follicles of LNs where they assist B cell responses. T_{FH} cells will be described in detail in Chapter 1.1.4.

In most circumstances polarising cytokines present in the microenvironment during activation direct the naïve CD4⁺ T cells to a particular differentiated T_H subset [59], however evidence suggests that the differentiation profile can also be affected by the type of APC activating the T cell, as well as by the level of stimuli [59]. These activated effector subsets of CD4⁺ T cells secrete cytokines in their dedicated milieu. Most T_H subsets are destined to migrate and elicit their functions at the site of inflammation, whereas certain T_H cells (such as T_{FH} cells) are destined to support inflammatory responses directly in the SLO.

A subset of $CD4^+$ T cells (5-10%) develop as *regulatory T* (T_{reg}) cells, that are characterised by their expression of the transcriptional repressor FoxP3 and IL2R (CD25) [60]. They either develop in the thymus (*thymic T_{reg}* cells (tT_{reg} cells)) or in the periphery (*inducible T_{reg}* cells (iT_{reg} cells)), and are critical for maintaining tolerance. Mice lacking T_{reg} cells due to a mutation affecting FoxP3 levels develop a fatal lymphoproliferative disease (Scurvy mice) with massive proliferation of effector $CD4^+$ T cells [61], and a similar disease exists in human, where dysregulated FoxP3 leads to *immunodysregulation polyendocrinopathy enteropathy X-linked* (IPEX) syndrome [62, 63]. T_{reg} cells are thus necessary to suppress and balance aberrant immune responses to exogenous and self-antigens. Mechanistically, T_{reg} cells suppress T cell responses through multiple mechanisms, including secretion of immunosuppressive cytokines (i.e. IL-10 and IL-35), direct interactions with effector T cells, as well as suppressed DC functions [64].

$CD8^+$ T cells

Naïve $CD8^+$ T cells are activated following engagement of their TCR with peptide presented in the context of MHC class I on many cell types, including APCs, such as mature DCs. For effective activation of $CD8^+$ T cells, the peptide-presenting DC has to be licensed by $CD4^+$ T_H cells or supported by $CD4^+$ T cells during APC interaction [65, 66], and this explains why $CD8^+$ T cell responses sometimes are $CD4^+$ T_H-dependent [67]. Following effective activation, $CD8^+$ T cells expand and upregulate effector molecules such as granzymes, and perforins to become effector *cytotoxic $CD8^+$ T lymphocytes* (CTL).

Memory T cells

Following first antigen-encounter, naïve T cells proliferate and differentiate to acquire effector functions to generate helper $CD4^+$ T cells or CTLs, whereas a smaller subset acquire memory phenotypes. Memory T cells can be classified as long-lived self-renewing *central memory T* (T_{CM}) cells, that reside in SLOs and readily activate upon re-encounter of their antigen, whereas *effector memory T* (T_{EM}) cells are tissue-resident memory T cells reactivating upon encountering antigen presented directly in the tissues.

Migration of effector subsets

Whereas naïve T cells preferentially home to LNs and other SLOs, activated T cells downregulate CCR7, and upregulate other chemokine receptors depending on the specific subset of T cells [68]. This allows for controlled attraction of dedicated T cell subsets to their designated site of inflammation and infection. Antigen-stimulated T cells downregulate L-selectin, and glycosylate *P-selectin glycoprotein ligand-1* (PSGL-1) resulting in functional PSGL-1 ligand which allows for binding of L-, P-, and E-selectins upregulated on inflamed endothelial tissues [reviewed in 69]. Other integrins are also involved in migration along, and adhesion to vascular endothelium as well as TEM of antigen-stimulated T cells. Of particular importance in effector subsets are VLA-4/VCAM-1, and α4β7/MAdCAM-1 interactions that mediate migration to distinct inflammatory sites [reviewed in 70, 71].

1.1.3 T cell activation and signal transduction

Precise regulation of T cell activation is crucial to control infections, without inducing autoimmunity. T cell stimulation is therefore a tightly regulated process involving multiple safeguards and pathways that converge in effective activation. A naïve T cell is activated by recognition by the TCR of its cognate antigen presented by MHC-complexes on APCs. In the absence of costimulation, the activated T cell results in anergy, which ensures the T cells is only activated by APCs and thereby protects against autoimmunity. Stimulation through the TCR in presence of costimulation on the other hand results in induction of rapid proliferation and differentiation to effector T cell subsets.

1.1.3.1 Signal 1: TCR stimulation

In conventional α/β T cells, the TCR complex consists of a heterodimeric complex of TCRα and TCRβ, as well as 4 CD3 subunits; CD3γ/δ/ε/ζ. The TCRα/β heterodimer is responsible for binding of its cognate peptide/MHC complex, whereas the CD3 subunits are responsible for conducting the downstream activation through their cytosolic YXXL/I *immunoreceptor tyrosine-based activation motifs* (ITAMs) [72]. In conjunction, CD4/CD8 co-receptors are recruited to the TCR complex by their binding of MHC. As a result of the engagement of TCR, the ITAMs on the CD3 subunits are phosphorylated by recruited protein tyrosine kinases such

as LCK and FYN. This is a complex, highly regulated process commencing with recruitment and activation of LCK. LCK is recruited to the TCR through its interaction with CD4/CD8 co-receptors [73, 74]. LCK has 2 major regulatory tyrosine phosphorylation sites (Tyr394, and Tyr505) that determine the activation state of LCK. pTyr394 stabilises the active conformation of LCK, whereas pTyr505 is inhibitory. Dephosphorylation of Tyr505 by the transmembrane phosphatase CD45 is thus required for the activation, however the exact mechanism regulating activation of LCK is complex, and a matter of debate [75, 76]. LCK (and FYN) activation results in phosphorylation of the ITAMs, including ITAMs on CD3ζ that recruit the *Zeta-chain-associated protein kinase 70* (ZAP-70) tyrosine kinase via its dual SH2 domains. ZAP-70 is then activated by LCK- and FYN-mediated phosphorylation [77]. ZAP-70 subsequently phosphorylates the transmembrane scaffolding protein, *Linker for Activation of T cells* (LAT), and *SH2-domain-containing leukocyte protein of 76 kDa* (SLP76). These phosphorylated tyrosines in LAT/SLP76 function as docking sites for further scaffolding proteins, which in turn recruit downstream proteins. Among these recruited scaffolding proteins are *growth factor receptor-bound protein 2* (GRB2), and *adhesion and degranulation promoting adaptor protein* (ADAP; also known as FYB) [78].

This LAT/SLP76 signalosome will recruit and activate effectors, including PLCγ1, *IL-2-inducible kinase* (ITK), and VAV1. These LAT/SLP76 signalosomes further oligomerise forming large signalling complexes by the TCR complex [78]. PLCγ1 activation is dependent on interaction with phospho-SLP76 interactions with LAT [79], and as described in Chapter 1.1.2.2, PLCγ1 activation results in production of DAG and IP_3, which triggers Ca^{2+} release and activation of Ca^{2+} regulated proteins, including calcineurin. DAG further activates PKC, and *mitogen-activated protein* (MAP) kinases via RasGRP1 [80]. VAV1 activates RAC signalling and downstream actin remodelling. MAP kinases are also activated following GRB2 recruitment to LAT, which acts as scaffold for the RAS *guanine exchange factor* (GEF), *Son of Sevenless* (SOS), thereby activating RAS [80]. Together these multiple signals converge in activation of transcription factors that initiate transcriptional programs required for T cell activation. Downstream of TCR stimulation, PI3K is further rapidly activated. However, the specific mechanisms by which PI3K is recruited and activated by TCR is still controversial [81, 82].

TCR signalling is negatively regulated by most phosphatases, excluding CD45 and SHP2. One such regulatory phosphatase is PTPN22, which dephosphorylates ERK, ITAMs, LCK, and ZAP-70 [83]. In a similar manner, SHP1 inhibits TCR signalling by dephosphorylating LCK and ZAP-70 [84, 85]. PTPN22 and SHP1 are consequently critical for homeostasis, and loss of either PTPN22 or SHP1 leads to autoimmune disease underlining the importance of the need for tight regulation of TCR signalling [86].

1.1.3.2 Signal 2: Costimulation

CD28-mediated costimulation is the main costimulatory signal involved in naïve T cell priming. It is induced by binding of B7 proteins (CD80 and CD86) on the APCs, and the downstream signalling is mediated by two cytoplasmic motifs; YMNM and PYAP. YMNM mediates activation of PI3K [87, 88] and downstream activation of PI3K effector proteins, resulting in proliferation and survival of activated T cells (discussed in detail in Chapter 1.2). YMNM and PYAP motifs are further directly involved in recruitment of adaptor proteins in a similar fashion to TCR activation. GRB2 is recruited to the PYAP motif, where it can recruit SOS which activates RAS, and VAV1. CD28 further recruits PKCθ in a PI3K independent manner [89]. Most, if not all, of these signals from CD28 are not exclusive, and can all be activated by TCR stimulation alone. However, CD28 more readily activates VAV1, and more readily activates PI3K/ITK/TEC-induced activation of PLCγ which results in Ca^{2+} release [82]. Further, CD28 activates LCK separately of TCR stimulation [90]. Together this supports a quantitative role for CD28 costimulation rather than a qualitative role with separate signalling pathways [91]. CD28 therefore seems to lower the threshold for T cell activation rather than independently coupling to signalling networks.

CD28 costimulation is not just crucial during T cell priming; conditional KO of CD28 following T cell priming results in decreased T_{FH} cells differentiation, and decreased T_H1 expansion following influenza challenge, indicating a crucial role for CD28 costimulation in effector $CD4^+$ T cells [92]. Similarly, CD28 signalling is essential for T_{reg} cell development, homeostasis, and function [93]. However, following differentiation of effector $CD8^+$ T cells, CD28 costimulation seems more modest. CD28 ablation before secondary *Listeria monocytogenes ovalbumin* (LM-OVA) challenge reduced CTL degranulation and IFNγ

production slightly [94]. Yet, in stimulation of memory $CD8^+$ T cells, CD28 is crucial for the recall response [94]. Although multiple other costimulatory receptors exist, CD28 is the main costimulatory molecule on naïve T cells, and the other costimulatory receptors are not discussed further.

1.1.4 T cell assistance to humoral immune responses

T cells provide essential help to antibody responses and the interactions between T and B cells are necessary for effective responses to infections and vaccinations. These interactions take place in specialised structures of the SLOs termed *germinal centers* (GC). GCs form in B cell rich follicles following immunogenic T-dependent antigen challenge [95]. Within these GCs, GC B cells proliferate extensively, and diversify their *immunoglobulin* (Ig) repertoire by *somatic hypermutations* (SMH) [96]. This leads to a diverse Ig repertoire, and B cells with high affinity to the antigen, as well as production of plasma cells that secrete high affinity antibodies.

1.1.4.1 Initial GC formation

Initiation of the GC reaction happens in the B cell follicles containing naïve IgM^+IgD^+ B cells. Naïve B cells that encounter antigen in these follicles, either presented by *follicular dendritic cells* (FDC) or soluble antigen arriving in the follicle [97-99], are pre-activated resulting in alteration of expression of migratory receptors involved in intranodal localisation. Consequently, the cells upregulate CCR7 and *Epstein-Barr virus induced molecule-2* (EBI2; also known as GPR183), which allows the pre-activated B cell to migrate towards CCL21/CCL19 gradients in the T cell zone and the EBI2 ligand, oxysterol [100-102]. Concurrently, T_{FH} cell differentiation is initiated before the initial interaction with the B cells. Naïve $CD4^+$ T cells are primed in the T cell zone by DCs. Primed T cells destined to become T_{FH} cells are called pre-T_{FH} cells and upregulate the transcriptional repressor BCL6 and CXCR5 following the initial priming. The pre-T_{FH} cells also downregulate CCR7 and upregulate EBI2 [103, 104]. The oxysterol ligand is produced by lymphoid stromal cells in the T:B cell border, and the enzymes involved are repressed in the B cell zone FDCs. This results in a gradient attracting the B and T cells to the border [105] assisted by the opposing expression of CCR7 and CXCR5 on B and T cells [102, 106].

The pre-T_{FH} and pre-activated B cells will thus meet in the B:T cell zone, where they will interact in a *signalling lymphocytic activation molecule* (SLAM)-*associated protein* (SAP) and integrin-dependent manner [107, 108]. Peptide presented by the B cells to the pre-T_{FH} cells provides proliferation and survival signals that allow the pre-T_{FH} cells to fully differentiate into T_{FH} cells. The B cells further receive signals to distinguish themselves as early GC B cells. These early GC B cells and T_{FH} cells migrate into the B cell follicle, where the GC B cells seed the early GC along the network of FDC around day 4 of the GC reaction [109]. Some of the activated B cells will following their initial interactions with the T cells migrate to the medullary cords where they reside as short-lived plasmablasts that produce the initial low affinity antibodies.

A critical aspect of these initial contacts between B cells and T cells at the T:B zone border, is cell migration and location bringing B and T cells into contact, and as I will describe in Chapter 1.1.4.4 integrins are critical to this process.

1.1.4.2 Mature GC formation

The early GC B cells seeding in the B cell follicle start proliferating rapidly in response to T_{FH} secreted cytokines (e.g. IL-21, IL-4) and costimulatory receptor signals (e.g. CD40L) [110]. As a result, the GC will develop, and GC B cells will outcompete naïve B cells in the forming GC follicle. This process supports SHM and affinity maturation of the GC B cells. The mature GC will eventually consist of a *light zone* (LZ) consisting of T_{FH} cells, FDCs, and GC B cells, and a *dark zone* (DZ) containing GC B cells with fewer T_{FH} cells [96]. The GC B cells thus cycle between the DZ, where they primarily undergo clonal expansion and SHM, and the LZ, where affinity maturation, differentiation, and *class switch recombination* (CSR) primarily take place [111]. Of note, CSR also occurs before GC formation, and recent studies suggest it primarily happens prior to GC formation [112]. DZ GC B cells express CXCR4 which guides the DZ GC B cells to the CXCL12-rich DZ [113], and higher *activation-induced cytidine deaminase* (AID) required for SHM [110], whereas the LZ GC B cells are can be identified based on high CD86 and lower CXCR4, and migrate to the LZ towards the CXCR5 ligand CXCL13 [96].

In the LZ, high affinity GC B cells pick up antigen from the FDCs and present it to T_{FH} cells, which in turn provide proliferative signals, whereas low affinity GC B cells will pick up less antigen from the FDCs [96]. In these LZs the GC B cells are competing for signals from the relatively sparse T_{FH} cells. This creates a competitive environment, where high affinity, class switched GC B cells will get sufficient signals from T_{FH} cells [110]. Besides selecting for GC B cells that have undergone rounds of SHM to high affinity antibodies, CSR from IgM to IgG (IgG more effectively mounts immune responses) is necessary to mount effective humoral immunity. In the early phase of GC formation, CSR is relatively inefficient, and most early GC B cells are still IgM^+. Recent studies support a model where class switched IgG^+ GC B cells outcompete IgM^+ GC B cells in a process very similar to SHM [114]. Following successful affinity maturation and class switching, creating GC B cells with high affinity IgG, GC B cells with high *inducible costimulatory ligand* (ICOSL) (as a result of ample T_{FH} CD40 signalling) will differentiate to become long-lived plasma cells [115]. These plasma cells migrate to the bone marrow and tissues. A fraction will differentiate to become B memory cells [110].

So how do the abundant GC B cells find the sparse T_{FH} cells in the packed GC? Interactions are relatively short between B cells and T_{FH} cells [115, 116]. A recent study found that GC B cells upregulate CCL22 and CCL17 following stimulation of CD40 by CD40L, and this in turn attracts T_{FH} cells through binding of CCR4 and increases the duration of T:B cell interactions [117].

1.1.4.3 T_{FR} cells

A subset of $CXCR5^+$ $PD1^+$ T follicular cells called *T follicular regulatory* (T_{FR}) cells express FoxP3, and act as a counterbalance to the T_{FH} cells in the GC by suppressing their functions and limiting the GC response [118-120]. These T_{FR} cells are transcriptionally and functionally distinct from T_{FH} and T_{reg} cells but are maintained in the GC in a similar manner to T_{FH} cells [120]. There is still some debate of whether all T_{FR} cells derive from T_{reg} cells, although it seems that the majority derive from tT_{reg} cells [120]. However, under the right conditions, T_{FR} cells can also derive from naïve T cells in the LNs in an antigen-dependent manner suggesting some plasticity [121]. These naïve T cell-derived T_{FR} cells would be expected to be specific to the immunised antigen, whereas the tT_{reg}-derived T_{FR} cells are likely not specific to the immunised

antigen to the same extent [121]. Nevertheless, T_{FR} cells and T_{FH} cells seem to have different TCR specificities with the T_{FR} cell TCR repertoire resembling the T_{reg} repertoire to a greater extent than the T_{FH} repertoire [122]. T_{FR} cells develop following challenge and co-opt the T_{FH}-like expression pattern of CXCR5 and *programmed cell death protein 1* (PD1) in a NFAT-dependent manner [123], which allows the T_{FR} cells to enter the GC towards the CXCL13 gradients. In the GC, T_{FR} cells suppress the GC response through multiple mechanisms that are incompletely understood; it is clear that CTLA-4 is required for efficient suppression [124], likely by occupying CD80/CD86 on APCs and stripping the receptor from the surface, thereby limiting the costimulatory potential of the APCs [125]. Further, T_{FR} cells produce suppressive cytokines such as IL-10 and TGFβ [126, 127]. It is however clear that T_{FR} cells are required to suppress aberrant responses, and T_{FR} cell ablation exacerbates humoral autoimmune syndromes such as Lupus [123] and aberrant B cell proliferation [128, 129]. Intriguingly, there are indications that the ratio of T_{FR}:T_{FH} cells is a predictor of the extent of the humoral response and as T_{FH} cells proliferate to a greater extent than T_{FR} cells during an immune response, T_{FR} cells possibly suppress the T_{FH} cells until there is enough T_{FH} cells in the GC to overcome the T_{FR}-mediated suppression [130].

1.1.4.4 T_{FH} development – including PI3K and LFA-1 mediated signalling

T_{FH} cells development is tightly regulated, and relies on multiple factors, although the initial DC mediated priming event commits the T cell to the T_{FH} lineage [131]. Multiple costimulatory signals have been implicated in T_{FH} development, including CD28 and ICOS. Induction of CD28 results in upregulation of ICOS, as well as PD1, OX40, and CXCR5. ICOS subsequently supports the maintenance of T_{FH} cells and GC reaction [132]. ICOS signalling is important for GC responses, and ICOS-deficient mice have limited GC responses with no migration of T_{FH} cells to the B cell follicles [133]. ICOS-ICOSL interactions between T_{FH} cells and GC B cells induces further ICOS on the surface of the T_{FH} cells which again can assist the GC B cells [115]. ICOS costimulation, like CD28 costimulation, induces PI3K signalling (discussed further in Chapter 1.3), and mice expressing a mutant version of ICOS that disrupts ICOS-mediated PI3K activation mount defective GC responses with poor affinity maturation and

class switching of GC B cells [134]. Similarly, kinase-dead *Pik3cd*^{D910A} mice (PI3Kδ catalytic subunit) cannot develop T_{FH} cells, and therefore do not mount effective GCs. Interestingly, this deficiency seems to solely affect the T cells, as transfer of WT T cells to *Pik3cd*^{D910A} mice rescues the defective GC response [135]. Further, KO of the phosphatase that opposes PI3K signalling, *phosphatase and tensin homolog* (PTEN) in primed T cells (*Ox40*^{Cre}) resulted in increased GC responses and antibody titres [135]. Comparably, hyperactive *Pik3cd*^{E1020K} had increased GC responses, both under steady state, and in response to immunisation. However, this led to poor class switching and disorganized GCs. This seemed to in part be a result of aberrant signalling independent of ICOS [136, 137]. ICOS-mediated PI3K signalling regulates T_{FH} signalling and development in multiple ways. Importantly, PI3K activation results in AKT-mediated inactivation of *Forkhead box protein O1* (FOXO1). FOXO1 represses *Bcl6* expression, and AKT activation thus results in reduced FOXO1-mediated repression of the *Bcl6* locus [138]. In contrast, AKT activation reduces FOXO1-mediated expression of the transcription factor KLF2 that regulates expression of multiple genes involved in T_{FH} cell signalling and location including CXCR5 and S1PR1 [137]. Together these transcriptional regulatory pathways are thus highly complex, and the exact mechanisms dictating T_{FH} cell differentiation downstream of PI3K is still a matter of active research [137, 139]. Similarly to ICOS, OX40 (which also activates PI3K signalling) is also important during T_{FH} cell development, and OX40-deficient T cells generally have defective $CD4^+$ T cell responses [140], and stimulation or overexpression of OX40 skews $CD4^+$ T cells towards a T_{FH}-like phenotype [141, 142].

LFA-1 in T_{FH} development and functions

Recently, it has been suggested that the level of tonic signalling in T cells (signalling from self-peptide/MHC complexes) affects the T_{FH} response. By applying a set of mouse models with high or low tonic signalling, it was found that T_{FH} cells develop and function at a higher capacity if the $CD4^+$ T cells are stimulated under low tonic signals [143]. These data suggest that systems that increased baseline TCR signalling strength under steady state might negatively affect T_{FH} development and functionality during GC reactions. Interestingly, another study showed that T_{FH} cells in the GC undergo antigen-dependent selection resulting in expansion of high affinity clones. Further, this study found that the amount of antigen present

on GC B cells correlates with the proliferative potential of T_{FH} cells in the GC [144]. Together these studies suggest that TCR strength both before and after T_{FH} priming have to be tightly regulated for efficient immune responses.

In light of these findings, it is perhaps not surprising that the major T cell integrin LFA-1 and its ligand ICAM-1 are involved in forming stable GC B cell:T_{FH} cell interactions and that they mediate the interaction strength [107, 145, 146]. Actually, activated GC B cells have increased surface levels of ICAM-1 and ICAM-2 compared to naïve B cells, and ablation of ICAM-1 and ICAM-2 results in defective GC B cell responses due to defective clonal competition at the T:B cell border (and not defective initial B cell activation) [146]. Similarly, T_{FH} cells have elevated and active LFA-1 which is required for efficient T_{FH} cell development. LFA-1 seems to be especially important for early T_{FH} cell differentiation and activation enhances BCL6 expression in $CD4^+$ T cells. Blockade of LFA-1 at the peak of immunisation also affected T_{FH} cell persistence in the GC to some extent [147]. Accordingly, *dedicator of cytokinesis* (DOCK) 8 controls T_{FH} cell localisation in the GC in a LFA-1 dependent manner, and KO of DOCK8 impairs T_{FH} cell migration into the GC [148]. Together these findings point to LFA-1 having a critical role in the GC response and effective T_{FH} functions. Interestingly, a hyperactive LFA-1 mutant also has impaired humoral responses to TNP-CGG/Alum immunisation suggesting neither too much or too little LFA-1 activity is beneficial for the GC response [149]. The details of how increased levels of LFA-1, or increased LFA-1 activity on T_{FH} cells, affects the GC response have however not been investigated.

1.2 PI3K in T cells

Phosphatidylinositol (PtdIns) constitute a minor fraction of the inner leaflet of the cellular membrane in all eukaryotic cells and are extensively involved in signalling pathways. Phosphorylated PtdIns are called *phosphoinositols* (PIs) and are phosphorylated at three positions (D3, D4, D5) of the inositol ring by PI kinases and dephosphorylated by PI phosphatases. The D3-phosphorylated position is involved in multiple signalling pathways by selectively recruiting proteins with specificity to the specific phospholipid product in the inner leaflet of the cell membrane. PI3Ks are responsible for phosphorylation of this D3 position,

and the three PI3K subclasses are highly selective to specific substrates. As only 4% of the lipids are PtdIns, and only ≈1% of PtdIns are phosphorylated, this evidently is a highly regulated system, where changes in phosphorylation have major downstream effects [150].

Class I PI3Ks, which are the focus of this thesis, specifically phosphorylate $PI(4,5)P_2$ to generate PIP_3. PIP_3 is bound by the *pleckstrin homology* (PH)-domain and in some cases other domains (see Chapter 1.2.3). Proteins with PH domains are hence recruited to the membrane, thereby initiating downstream signal transduction. The class I PI3K subfamily comprises class IA PI3Ks (PI3Kα, PI3Kβ, and PI3Kδ) and the class IB PI3K (PI3Kγ). The class I PI3Ks are heterodimeric proteins consisting of a regulatory domain (class IA PI3Ks: p85; class IB PI3K: p101) and a catalytic domain (p110α (PI3Kα), p110β (PI3Kβ), p110δ (PI3Kδ), or p110γ (PI3Kγ)) [151].

Class II PI3Ks consist of 3 catalytic isoforms, C2α, C2β, and C2γ, that phosphorylate PtdIns to generate PI(3)P, and PI(4)P to generate $PI(3,4)P_2$. The role of class II PI3Ks in T cells is not as well described as class I PI3Ks, but they have been shown to be involved in clathrin-mediated endocytosis and vesicular trafficking [152] as well as cell migration [153] in other cell types. C2β has been implicated in PI(3)P generation in T cells, which in turn results in activation of potassium channel, KCa3.1 aiding intake of Ca^{2+} [154].

Class III PI3Ks is a heterodimeric protein consisting of the catalytic VPS34 and a regulatory (VPS15) subunit. VPS34 phosphorylates PtdIns to generate PI(3)P, which recruits proteins that contain FYVE or PX domains [155]. VPS34-deficient T cells have defects in endocytosis and autophagy; and mice with conditional T cell KO of VPS34 are lymphopenic and suffer from inflammatory wasting syndrome with age [156]. These mice also have impaired cellular metabolism and fail to effectively mount T_H1 responses, wherefor autoimmune *experimental autoimmune encephalomyelitis* (EAE) cannot readily be induced in these mice [157].

This chapter describes the roles of class I PI3Ks in T cells, and further investigates the proteins involved in the downstream signalling pathways. For the remainder of this thesis, unless otherwise specified, PI3K will refer to class I PI3Ks.

1.2.1 PI3K in T cells - differentiation, effector functions, and migration

In T cells PI3Kδ is the dominant class I PI3K isoform (Figure 1-3a). PI3Kδ is activated downstream of the TCR as well by costimulatory and cytokine receptors, including LFA-1-mediated "outside-in" signalling [158], that stimulate the phosphorylation of tyrosines within YXXM motifs that bind to the SH2 domains of the p85 subunit [159] (Figure 1-3b). PI3Kγ is also expressed in T cells and predominantly mediates signals downstream of G protein-coupled receptors such as chemokine receptors [151] (Figure 1-3b).

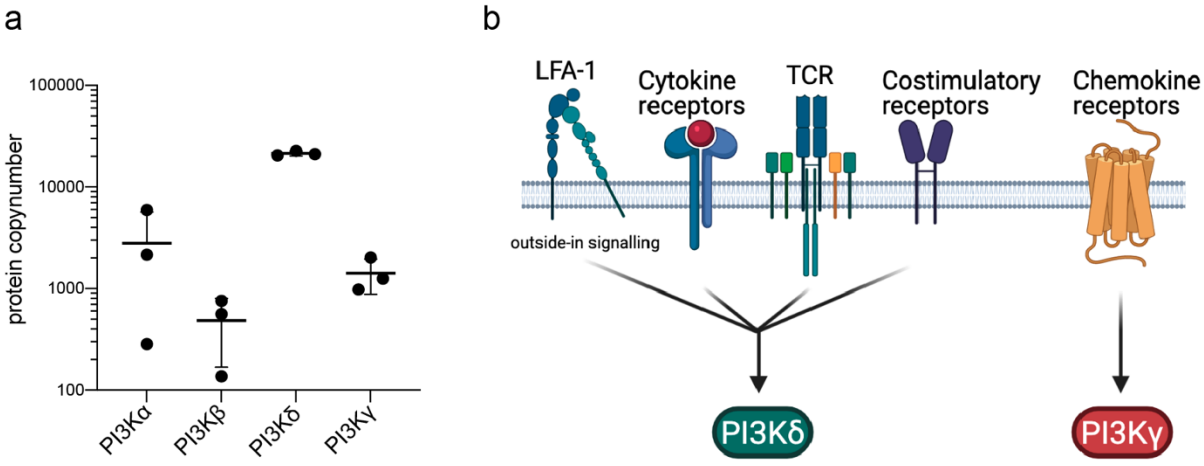

Figure 1-3. PI3K activation in T cells **a,** Protein copy numbers of class I PI3K isoforms (3 WT $CD4^+$ T cells protein copynumbers, Error bars: mean±SD); data from former PhD student Rafeah Alam from the Okkenhaug laboratory. **b**, Simplified schematic of the differential regulation of PI3Kδ activated by TCR, cytokines, LFA-1, and costimulatory signalling, and PI3Kγ regulated by chemokine receptors in T cells. Figure made in BioRender.

1.2.1.1 PI3K in T cell development and differentiation

Class I PI3K signalling is important during T cell development. The *Pik3cd*$^{-/-}$*Pik3cg*$^{-/-}$ double-knockout leads to near complete ablation of β-selection in the thymus, whereas loss of either p110δ or p110γ only causes minor developmental defects [160-162]. This is largely a result of signalling from CXCR4-mediated activation of p110γ and pre-TCR-mediated activation of p110δ, and both signals appear sufficient to generate the necessary PIP_3 for β-selection [163]. Similar involvement of PIP_3 signals for β-selection were observed following deletion of the PIP_3 phosphatase PTEN, which bypasses the need for pre-TCR stimulation [164]. PTEN KO

mice also show impaired negative selection and develop autoimmunity implicating PI3K signalling in central tolerance [165]. Similarly, kinase-dead *Pik3cd*^{D910A} mice have increased numbers of T_{reg} cells in the thymus implicating p110δ in tT_{reg} selection [166]. In humans, loss of p110δ function leads to more profound defects in B cell development, while limited T cell developmental defects are also observed [167-169].

1.2.1.2 PI3K signalling in T cells

PI3K signalling is important for multiple effector T cell functions both in $CD4^+$ and $CD8^+$ T cells. By generating PIP_3, PH domain-containing proteins with high affinity for PIP_3 are recruited to the membrane. Most research to date has focused on AKT-mediated signalling; AKT is recruited to the membrane and brought together with *3-phosphoinositide-dependent protein kinase-1* (PDK1). PDK1 in turn phosphorylates AKT on Thr308 which activates the kinase activity of AKT [170]. Thr308-phosphorylated AKT phosphorylates *mTOR complex 2* (mTORC2), which further phosphorylates AKT on Ser473 resulting in complete activation of AKT allowing for AKT phosphorylation of all its substrates [171]. AKT in turn phosphorylates several downstream proteins, including the FOXO transcription factors. AKT-mediated phosphorylation of FOXOs results in nuclear exclusion and degradation, thereby reducing expression of FOXO transcriptional targets, including *Rag1/2*, *Il7r*, *Bcl6, Klf2, and FoxP3* [172-179]. This is a major mechanism by which PI3K indirectly controls gene expression.

AKT further indirectly activates the serine/threonine kinase mTOR. AKT phosphorylates Tuberin (TSC2), which results in inactivation of the protein. TSC2 under normal circumstances inactivates the small GTPase RHEB, which in its active form activates *mTOR complex 1* (mTORC1). Thereby AKT activates mTORC1 which phosphorylates *S6 kinase* (S6K) and *4E binding protein 1* (4E-BP1) [171]. S6K activation inhibits PI3K activity, and this has been suggested to results in a negative feedback loop through mTOR following PI3K activation in cancer cells [180]. In T cells mTORC1 activity suppresses PI3K activity by increasing PTEN levels, and this is thought to act as a further negative feedback loop [181]. The resulting mTOR activity induces metabolic changes and affects differentiation [182, 183], as well as survival and proliferation signals necessary for efficient proliferation of T cells [184]. However, evidence from $CD8^+$ T cells suggest a non-obligatory role for PI3Kδ in regulating mTOR,

implying these pathways are more complicated than so [185]. AKT also phosphorylates multiple other proteins, including GSK3 involved in survival and differentiation of T cell subsets [186].

Together these activated pathways affect survival, proliferation, and differentiation of T cells. Consequently, $CD4^+$ T cells with deficient PI3K signalling (either due to KO, or the kinase-dead mutation *Pik3cd*^{D910A}) show impaired T_H1, T_H2, T_H17, T_{reg} cell differentiation and functions, and decreased proliferation in response to TCR stimulation [166, 187-196].

Similarly, PI3Kδ signalling has been implicated in $CD8^+$ T cell functions. Several CTL effector molecules were not expressed to the same extent after inhibition of AKT [191]. This also corresponds to the fact that p110δ is necessary for the expression and secretion of IFNγ, both in $CD8^+$ T cells and $CD4^+$ T cells [189, 191]. Further, degranulation of granzymes and the expression of FasL are reduced in *Pik3cd*$^{-/-}$ $CD8^+$ T cells resulting in reduced tumour clearance in a subcutaneous MC38 tumour model [197]. However, other studies have shown that the role of PI3K in tumour clearance is potentially more complicated, as PI3Kδ inhibition affects T_{reg} cells to a greater extent than CTLs. Therefore, in some tumour models PI3Kδ inhibition or deficiency results in increased tumour clearance making it a potential therapeutic target [198].

The role of PI3Kγ in T cell differentiation and function is less clear. Some studies suggest that PI3Kγ signalling is required for effective TCR/CD28-mediated activation and proliferation of T cells [54, 199], although the exact mechanism of PI3Kγ activation downstream of TCR or CD28 is not understood. Furthermore, PI3Kγ is implicated in migration to inflammatory tissues and during homeostatic migration towards chemokines [200, 201].

1.2.2 PI3K-mediated regulation of naïve T cell migration and homeostasis

Expression of homing molecules CD62L and CCR7 on the surface of naïve T cells is critical for orchestrating naïve T cell trafficking to LNs as described in Chapter 1.1.2.1. Their expression on naïve T cells is regulated by PI3Kδ signalling with FOXO1 being a particularly important player. Transcriptional activity of FOXO1 is high in naïve T cells and results in robust expression of CD62L and CCR7 through control of KLF2 levels, a transcription factor that drives expression of these key homing molecules [202]. PI3Kδ-mediated signals upon T

cell activation result in phosphorylation and inactivation of FOXO1, thereby reducing FOXO1-mediated transcription of KLF2 and its target genes including CD62L, CCR7, S1PR1 [203, 204]. As a result of this reduced expression of homing molecules, activated T cells are diverted from entering LNs and instead biased towards migration into peripheral tissues, where they elicit their effector function. Loss of S1PR1 also helps sequester effector T cells in inflamed tissues. Besides regulating CD62L levels transcriptionally, PI3Kδ activation results in proteolytic cleavage of the CD62L ectodomain (CD62L shedding) by *Tumour necrosis factor converting enzyme* (TACE)/*disintegrin and metalloprotease 17* (ADAM17), all of which traffic to the membrane as a result of TCR stimulation [205-207]. This process is PI3Kδ dependent and is mediated by MAPK ERK1/2-phosphorylation of TACE/ADAM17 [208-211] (Figure 1-4). PI3Kδ cross-talks with the RAS pathway, resulting in ERK activation, which in turn is considered to phosphorylate TACE/ADAM17; this is thought to be the mechanism leading to CD62L shedding. Consequently, PI3Kδ signals are central in regulating T effector cell migration, and the resulting transcriptional changes support migration to inflamed tissues (Figure 1-4).

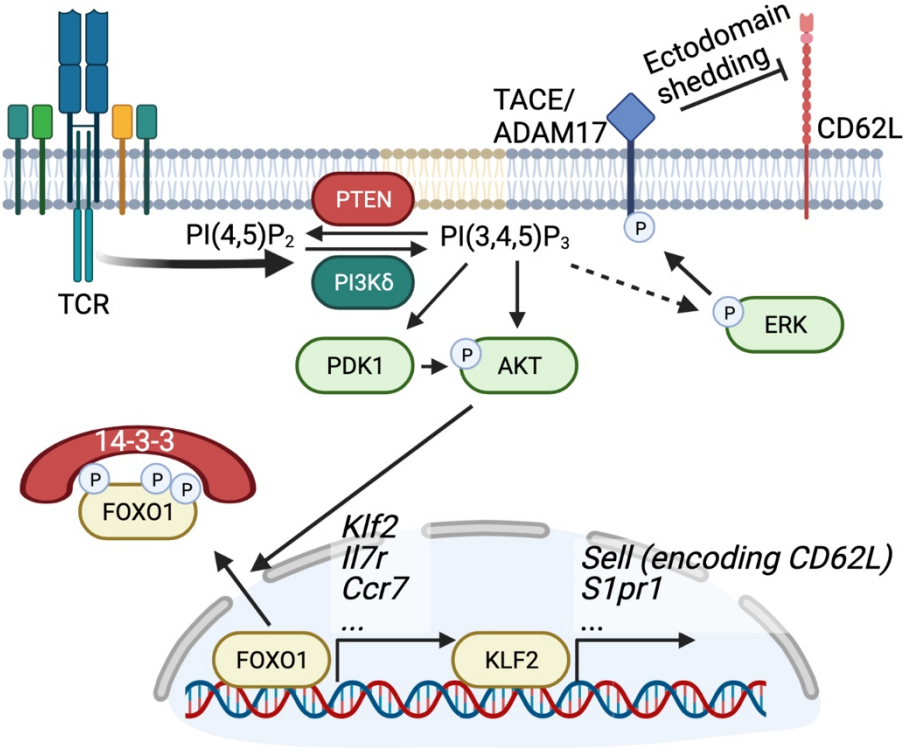

Figure 1-4. PI3Kδ-mediated regulation of CD62L, CCR7, and S1PR1. PI3K-mediated PIP_3 production leads to recruitment of PDK1 and AKT, leading to AKT activation. AKT phosphorylates FOXO1, which allows for binding of the 14-3-3 leading to cytosolic sequestration of FOXO1. FOXO1 promotes transcription of *Klf2* (as well as *Il7r*, *Ccr7*). Decreased expression of the transcription factor KLF2 in turn results in decreased transcription of *Sell*, encoding CD62L, and *S1pr1*. Figure made in BioRender.

1.2.2.1 CCR7 expression, CD62L-shedding and LFA-1 activation – three birds, one stone?

It is intriguing that PI3K signalling regulates multiple processes involved in T cell migration. PI3K-mediated CD62L-shedding and reduced CD62L, S1P1, and CCR7 expression results in decreased LN entry and is an important step in T cell differentiation to effector subsets. Concurrently, as PI3K-signalling increases integrin affinity, PI3K signals can regulate migration and adhesion, including TEM into LNs. Consequently, inhibition of PI3K or disruption of PI3K signalling will affect all of these rheostats of migration, not always in predictable ways. Hence, PTEN-deficient T cells with high PIP_3 levels are excluded from LNs after adoptive transfer [212]. Nevertheless, *activated PI3K delta Syndrome* (APDS) patients

(see Chapter 1.2.4) suffer from lymphadenopathy and this is reversed upon treatment with a PI3Kδ inhibitor [213].

Studies of migration of PI3K-deficient T cells, as well as use of inhibitors in mice has progressed our understanding of T cell distribution *in vivo*. Thus, p110γ-deficient T cells exhibit reduced migration towards chemokines, whereas p110δ-deficient T cells respond to chemokines like WT cells [214]. Similarly, p110γ selective inhibitors affect responses to chemokines, whereas p110α/β/δ selective inhibitors do not affect responses to chemokines, except at very high concentrations as a result of off-target effects [215]. Following LN entry, p110γ-deficient T cells migrate interstitially similarly to WT T cells, and chemokine-induced interstitial migration seems independent of PI3K signalling [216]. However, treatment with Wortmannin as well as disruption of regulatory p85 subunits of class IA PI3K have shown that these cells migrated at lower velocities than WT cells, yet T cell location within the LN did not seem altered [217] At steady state, PI3Kδ does not contribute to T cell migration or chemokine-dependent migration, as *Pik3cd*^{D910A} T cells migrated like WT T cells in an endothelial cell-coated transwell assays or following adoptive transfer [218]. However, following antigenic challenge, p110δ was required for efficient migration to the site of inflammation and presence of antigen, consistent with a key role of PI3Kδ in regulating integrin affinity [218]. Disruption of p110δ results in increased track velocities of OT-II CD4$^+$ T cells in LN slices with OVA-pulsed DCs, as a result of decreased interaction times with the peptide-presenting DCs in the slices [219]. Similar results have been observed for p110γ-deficient T cells that are deficient in antigen-dependent and chemokine-dependent migration of effector CD4$^+$ and CD8$^+$ T cells [200, 201]. Interestingly, CD28 seems to also be important for homing of antigen-stimulated T cells to non-lymphoid tissues, whereas CD28 (Y173F), which is uncoupled from PI3Kδ, was defective. This suggests that CD28-mediated activation of PI3K is involved in migration of activated T cells to non-lymphoid sites [220]. Consequently, when inhibiting PI3Kδ, homeostatic migration of naïve T cells seems unperturbed (as these have low PI3K activity in the first place), whereas activated T cells show decreased antigen-dependent migration into non-lymphoid tissues.

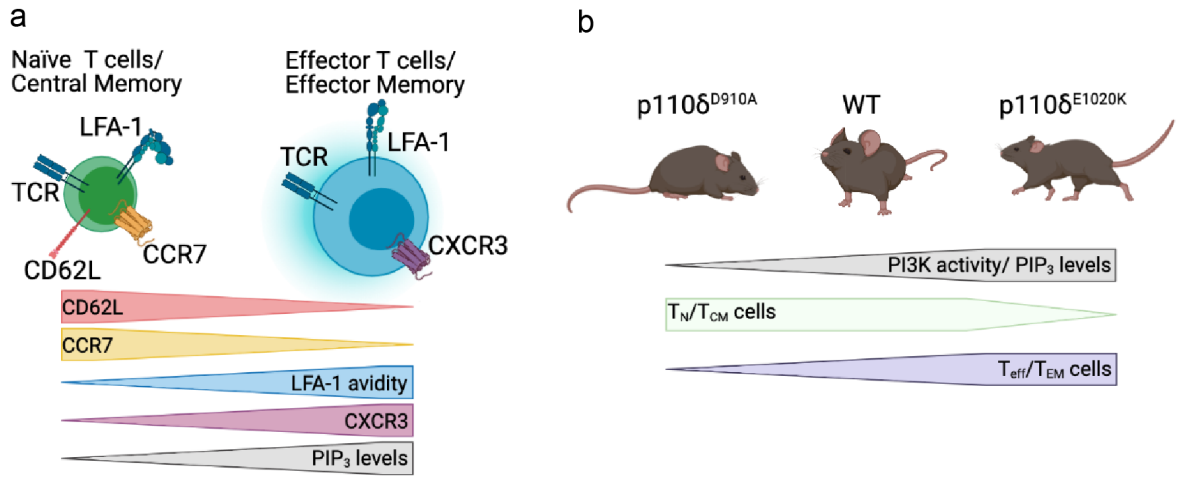

Figure 1-5. Involvement of PI3K signalling in T cell migration. **a,** Diagram of relative surface levels of CD62L, CCR7, CXCR3, and avidity of LFA-1 in naïve T cells/ T_{CM} cells and T_{eff}/T_{EM} cells. **b**, Spectrum of PI3K activity in PI3K mutant mouse models, and how this affects the levels of naïve T cells/T_{CM} and T_{eff}/T_{EM} cells. Figure made in BioRender.

Central memory T cells (T_{CM}) that are $CD62L^{+}CCR7^{+}LFA\text{-}1^{+}$ are consequently supported by PI3Kδ inhibition, whereas effector T cells (T_{eff}) and effector memory T cells (T_{EM}) ($CD62L^{-}CCR7^{-}LFA\text{-}1^{++}$) are inhibited (Figure 1-5a). This is evidenced by the fact that APDS patients have reduced T_{CM} cells and increased T_{eff} cells [221, 222], whereas *Pik3cd*^{D910A} mice have normal memory T cells, but reduced T_{eff} cells [192] (Figure 1-5b). These PI3K-dependent alterations of T cell memory responses are possibly affected by altered expression of migratory receptors, however, differentiation of *Pik3cd*^{D910A} T cells to T_{eff} is largely defective, implicating PI3K more broadly in differentiation and migration.

1.2.3 PIP_3-binding proteins

The majority of work focusing on signalling downstream of PI3K has focused on a handful of PIP_3-binding proteins; AKT, PDK1, TEC kinases, and VAV1. In reality these signalling pathways are much more complex, as upwards of >80 proteins bind specifically to PIP_3. The understanding of PI binding has become increasingly clear, but for several reasons it is still debated which proteins are regulated by PI3K. Firstly, the fact that a protein has affinity to PIP_3, does not mean it has biological relevance. Secondly, most roles downstream of PI3K can in part be attributed to AKT-mediated signalling [151].

Most PIP_3-binding proteins have PH domains. They are 120 amino acid domains with high sequence homology discovered in 1993 [223, 224]. PH domains were initially thought to primarily bind $PI(4,5)P_2$ [225], but it has since become evident that some of the PH domains are specifically recruited to other PIs, including PIP_3. PIP_3 thus alters the activation states of these proteins, which in most cases results in protein activation.

PI-binding properties of different PH domains have recently become clearer through a series of clever studies. Park *et al*. applied confocal microscopy to track YFP-tagged PH domains in NIH3T3 fibroblasts during induction of PIP_3-production, and identified ~30 PIP_3-binding PH-domains recruited to the membrane and developed a machine learning algorithm for prediction of PIP_3-binding PH domains [226]. Another approach applied mass spectrometry (MS) to identify proteins with affinity to various PIs. Jungmichel *et al*. applied SILAC MS to study the PI interactome in HeLaS3 cells and found that 12 % of PH domains (38 proteins) have high affinity to PIP_3 [227], but also identified a high number of non-PH domain proteins with affinity to PIP_3 (162 non-PH proteins with binding above the set threshold) including DOCK family proteins, that also elsewhere have been shown to have affinity to PIs [228]. Together, these studies have significantly expanded the knowledge of PIP_3 specificity.

Several protein families were found to bind PIP_3, including many small GTPase regulating proteins such as Rho *GTPase exchange factors* (GEFs) (i.e. ArhGEFs, AKAP13) and *GTPase activating proteins* (GAPs) (i.e. ArhGAPs), ARF GEFs (ACAP3), RAS/RAP1 GAPs (RASA2, RASA3), that either activate the GTPase function of small GTPases (GAPs) or exchange hydrolysed GDP for GTP (GEFs). Other proteins identified included *Switch associated protein 70* (SWAP70), Cytohesins, *Oxysterol binding protein related proteins* (OSBPLs), *Dedicator of cytokinesis* (DOCKs), VAV1, and PLEK/PLEKHA/PLEKHB proteins.

When combining these studies of PIP_3-binding proteins with proteins that have been identified to have PIP_3 affinity, I found 90 PH domain containing proteins with affinity to PIP_3 based on proteins with PH domains in Uniprot and PFAM databases. Further, I identified 162 PIP_3-binding proteins without PH domains with PIP_3 affinity based on the PIP_3-affinity screens presented above. Most of the PIP_3-binding proteins are relatively unknown, and only a handful have been described in the literature. Nonetheless, many of the proteins comprising PH

domains with affinity for PIP_3 are found in both naïve T cells and activated T cells, and it is therefore likely that some of these proteins are involved in T cell homeostasis and function (Figure 1-6).

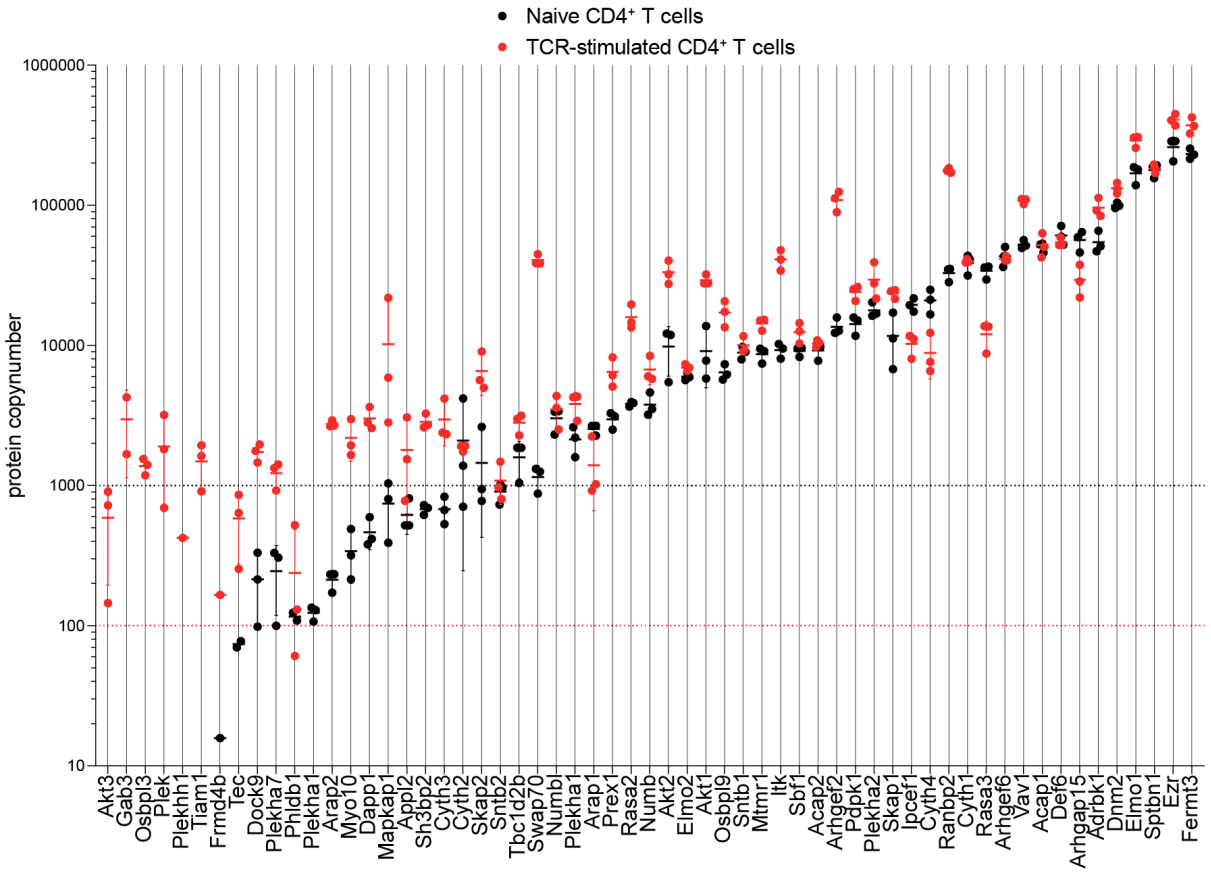

Figure 1-6. Protein copy numbers of PIP_3-binding PH-domain-containing proteins. Proteins are shown in order of copy numbers in naïve T cells (black) with copy numbers from 24h TCR stimulated cells shown as well (red); data from former PhD student Rafeah Alam from the Okkenhaug laboratory.

1.2.4 Activated PI3Kδ syndrome

Activating mutations in PI3Kδ have been identified as the cause of a novel immunodeficiency syndrome called APDS [221, 222, 229-231]. These patients are susceptible to airway infections and chronic viral infections and have enlarged LNs and spleens as well as autoimmune traits, including cytopenia [230]. The most frequent PI3Kδ mutant leading to APDS is E1021K in patients and E1020K in mouse models generated by several groups to recapitulate the phenotypes of the patients. These mice are also susceptible to airway infections, and have

enlarged LNs and spleen, as well as aberrant production of autoantibodies [136, 232, 233]. It is clear from these patients and mice that PI3Kδ regulation has to be tightly regulated. Too much PI3K signalling is not a positive thing. Thus, the pathway has to be dynamically regulated to ensure optimal lymphocyte development and function [234, 235].

1.2.5 Inositol signalling

Besides PI3Ks, a range of PI4K, PI5K, and PI phosphatases are involved in tight regulation of PI levels in the membrane. All known PI kinases and phosphatases are shown in Table 1-2 as well as their substrates and products.

Only few studies have investigated PI(3)P-binding, but it is clear that some FYVE domains [236] as well as some PX domains have affinity to PI(3)P [237, 238]. Further, a subset of PH domains have been shown to have PI(3)P affinity [227]. As PI kinases are specific to a subset of PIs the PI kinase functions are dependent on there being sufficient substrate. As an example class I PI3K requires PI(4,5)P_2 and are therefore dependent on sufficient production of this PI. This paints a picture of a complex process involving regulation of the different PI isoforms. This is not the main focus of this thesis, but it is of interest that there are signalling proteins that have affinity to other PIs than PIP_3 or PI(3)P [239], and it would thus be of interest to broadly investigate roles of these proteins in general immune functions as potential signalling proteins.

Table 1-2. Phosphoinositol kinases and phosphatases and their substrates and products. Grouped and colour coded based on PI lipid substrate and product.

Group	Gene	Substrate	Product
Inositol lipid kinases			
PI3 Kinases	PIK3CA, PIK3CB, PIK3CD, PIK3CG	PI(4,5)P2	PIP3
	PIK3C2A, PIK3C2B, PIK3C2G	PI, PI(4)P	PI(3)P, PI(3,4)P2
	PIK3C3	PI	PI(3)P
PI4 Kinases	PI4KIIa, PI4KIIb, PI4KIIIa, PI4KIIIb	PI	PI(4)P
	PIP4K2a, PIP4K2b, PIP4K2g	PI(3)P, PI(5)P	PI(3,4)P2, PI(4,5)P2
PI5 Kinases	PIKfyve	PI	PI(5)P
	PIP5Ka, PIP5Kb, PIP5Kg	PI(4)P, PI(4,5)P2	PI(4,5)P2, PIP3

inositol lipid phosphatases			
PI3 pptases	PTEN	PIP3, PI(3,4)P2	PI(4,5)P2, PI(4)P
	TRIPa, TRIPb, TRIPg	PIP3	PI(4,5)P2
	MTM1	PI(3)P	PI
	MTMR1, MTMR2, MTMR3, MTMR4, MTMR6, MTMR7, MTMR8	PI(3)P, PI(3,5)P2	PI, PI(5)P
PI4 pptases	INPP4A, INPP4B	PI(3,4)P2	PI(3)P
	TMEM55A, TMEM55B	PI(4,5)P2	PI(5)P
PI5 pptases	SHIP1	PIP3	PI(3,4)P2
	SHIP2	PIP3, PI(4,5)P2	PI(3,4)P2, PI(4)P
	SKIP	PIP3	PI(3,4)P2
	OCRL, SYNJ1, SYNJ2, PIPP	PI(4,5)P2	PI(4)P
	Inpp5a	IP3	IP2
	Inpp5b	PI(4,5)P2	PI(4)P
	Inpp5e	PIP3, (PI(3,5)P2)	PI(3,4)P2, (PI(3)P)
	Fig4	PI(3,5)P2	PI(3)P
	Sac2	PIP3, PI(4,5)P2	PI(3,4)P2, PI(4)P
	Sac1	PI(3)P, PI(4)P	PI
Phospholipids in order of complexity			
PI	PI(3)P	PI(3,4)P2	PIP3
	PI(4)P	PI(3,5)P2	
	PI(5)P	PI(4,5)P2	

1.3 Lymphocyte function-associated antigen 1 – the major T cell integrin

Integrins are transmembrane, heterodimeric proteins that are involved in cell-cell and cell-extracellular matrix interactions as well as binding of soluble ligands. In mammals, the heterodimeric transmembrane structure of integrins is composed of one of 18 α subunits and one of 8 β subunits, that can form 24 different combinations. Integrins may undergo conformational priming (activation) due to intracellular signalling events ("Inside-out" signalling) resulting in high affinity binding of their ligands, and are often involved in cell-cell

interactions and/or migration. Further, integrins mediate signal transduction, where binding of their ligands stimulates intracellular signalling pathways ("outside-in" signalling). In T cells, the major integrin is LFA-1, and its crucial role in T cell biology has become clear from decades of brilliant studies on its regulation, function, and role for T cell functions, development and location.

In this subchapter, I describe what LFA-1 (and some of the other important T cell integrins) does, how it is regulated, and why it is important in T cell biology.

1.3.1 Integrins in T cells

T cells are known to express at least 15 of the 24 known integrins depending on their differentiation and activation state [240, 241] (Figure 1-7a). Like other integrins, LFA-1 ($\alpha L\beta 2$) is a heterodimeric protein and is composed of integrin αL (CD11a; encoded by *Itgal*) and integrin β2 (CD18; encoded by *Itgb2*). LFA-1 is expressed by all T cell subsets and specifically binds ICAMs and *junctional adhesion molecules* (JAMs) [242, 243]. Under steady state, LFA-1 is found in a closed conformation with low affinity to its ligands. Following inside-out activation by chemokines, cytokines, or TCR-stimulation, LFA-1 rapidly changes conformation from its low affinity closed/bent conformation to an intermediate affinity extended conformation, where the extracellular domain is partly open, but the cytosolic domain remains closed. This intermediate affinity extended conformation allows for binding to ICAM-1. ICAM-1-binding results in further increases in affinity through outside-in signalling, ultimately resulting in the high affinity open-extended conformation [Reviewed in 240, 244]. These conformational activation steps (from hereon called LFA-1 activation) happen in seconds following chemokine stimulation, and within minutes following TCR stimulation. The process of LN entry is highly dependent on LFA1; LFA-1-deficient mice have greatly reduced T cell adhesion to HEVs, in particular in pLNs and therefore limited to no T cell migration to the LNs occur [245, 246]. After T cells enter the LNs, the role of LFA-1 is less clear. Studies of the role of LFA-1 in interstitial T cell migration indicate that LFA-1 is required for retention of T cells in the parenchyma and T cells lacking LFA-1 egressed the LN rapidly [247]. Further, LFA-1 modulates the interaction times with APCs and facilitates their scanning [248]. However, other studies using LFA-1-deficient T cells [249] or DCs lacking ICAMs altogether

[250, 251], suggest that interstitial and intranodal motility of T cells and DCs in the absence of antigen is much less dependent on integrins than is the entry into and egress out of the LNs themselves. These studies are somewhat contradictory, and together paint a picture of the role of LFA-1 in intranodal migration as dependent on the biological context.

Multiple other integrins have been described in literature in subsets of T cells (Figure 1-7a), and their expression levels vary based on the activation state of the T cells (Figure 1-7b). *Very late antigen 4* (VLA-4) (integrin α4/CD49d encoded by *Itga4* and integrin β1/CD29 encoded by *Itgb1*) binds *vascular cell adhesion molecule-1* (VCAM-1) and is expressed in antigen-stimulated subsets of T cells [252]. VLA-4/VCAM-1 interactions are especially important for homing of T cells through the blood-brain barrier and VLA-4 expression correlates with severity of EAE [253]. Another important integrin in T cells is α4β7 (also known as LPAM-1) which binds MAdCAM-1 and is involved in homing to gut-associated lymphoid tissues [254].

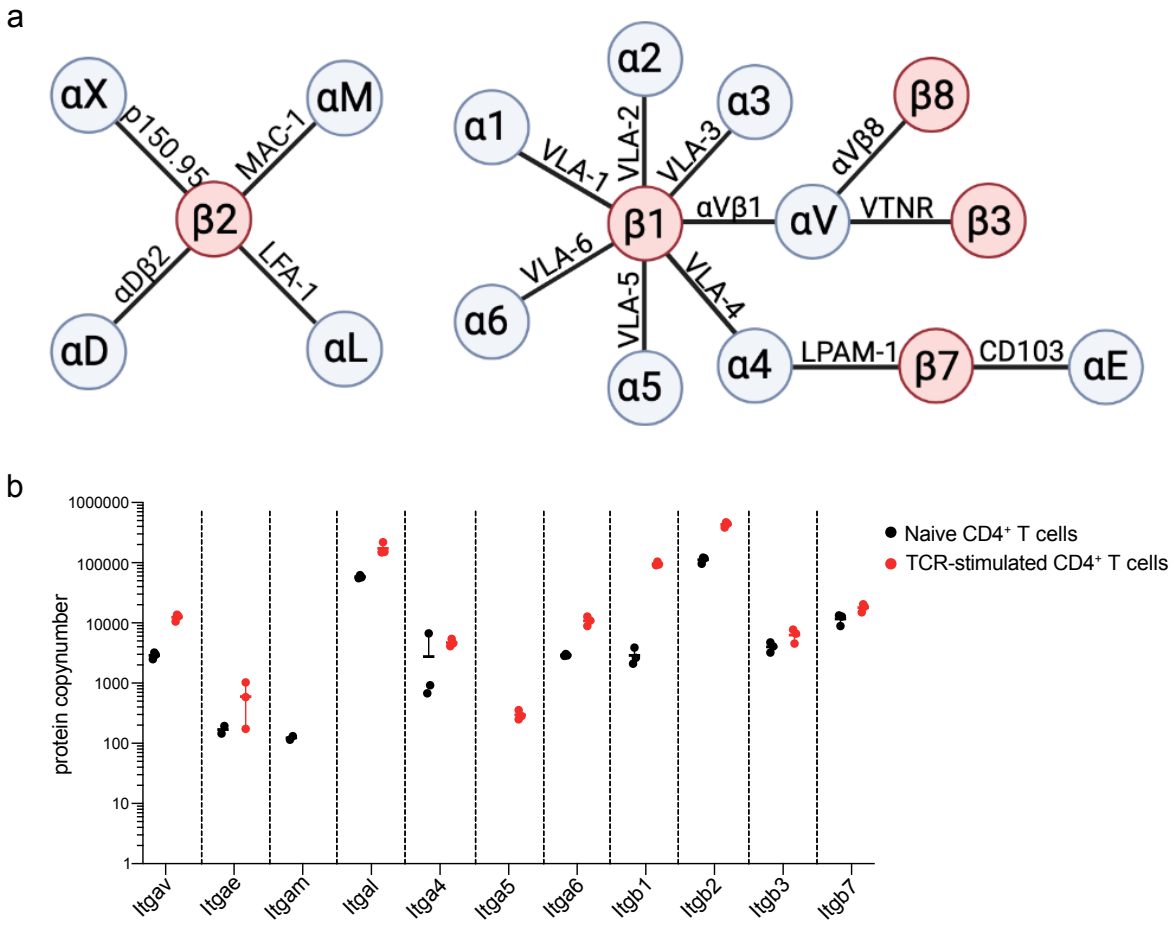

Figure 1-7. Integrins expressed in T cells. **a**, Schematic of integrin chains expressed in T cells with α integrin chains in blue, and β integrin chains in red. Lines indicate which integrin chains form heterodimeric integrins, and names over lines are commonly used names of the resulting integrin. Figure made in BioRender. **b**, Proteomics copy numbers of integrins found in naïve and 24 hour TCR stimulated $CD4^+$ T cells (log10 scale axis); data from former PhD student Rafeah Alam from the Okkenhaug laboratory.

1.3.2 Integrin affinity regulation in T cells

Inside-out signalling in T cells is a complex process mediated by a range of proteins that collectively result in increased LFA-1 affinity and avidity. As described in Chapter 1.1.3.1, TCR stimulation results in activation of PLCγ mediated by the pSLP76/LAT complex resulting in downstream activation of PLCγ1/2, which in turn mediates calcium release and activation of the RAP1-GEF, RASGRP2. RASGRP2 then activates RAP1 by exchanging GDP for GTP [255]. Of note however, RASGRP2 is not expressed in mouse lymphocytes, suggesting other RAP1 GEFs are involved in the regulation. Another pathway leading to RAP1 activation is recruitment of the CRKL-C3G complex by the WAVE2-ARP2/3-ABL complex and activating phosphorylation of CRKL by LCK/ZAP70 [256-258]. This results in activation of the RAP1-GEF, C3G, thus further activating the small GTPase, RAP1A/B. Active GTP-bound RAP1A and RAP1B is critical for the process of LFA-1 activation [259-262].

Chemokine receptors are GPCRs that following chemokine binding induce a multitude of signals some of which converge in activation of RAP1 via the activation of PLCβ as described in Chapter 1.1.2.2. Besides activating the PLC-dependent signalling-cascade, chemokine receptors also induce activation of PI3Kγ resulting in initiation of PI3K-mediated signals (discussed further below).

GTP-bound RAP1 interacts with *Rap1-GTP-interacting adaptor molecule* (RIAM) [263-265] and RAPL [261]. In turn, this complex mediates activation [265] and plasma-membrane binding of TALIN1 [264]. The *Fermitin family homolog 3* (FERM3; F3) domain of TALIN1 in turn binds the β chain of LFA-1, thereby mediating activation of LFA-1 [266, 267]. RIAM has a PH domain that preferentially interacts with PIP_2. By binding PIP_2, RIAM is thought to act as a proximity detector mediating binding of activated RAP1 and TALIN1 to the membrane [268]. Another PH-domain containing protein involved in the process is *SRC kinase associated*

phosphoprotein 1 (SKAP1; also known as SKAP55). SKAP1 is constitutively associated with ADAP and has been shown to also mediate binding of RAP1 to the plasma membrane through its PH domain [269, 270]. Together SKAP1/ADAP integrates with the RIAM-RAPL-RAP1 complex during TCR-induced LFA-1 activation and likely stabilises this complex [271]. During LFA-1 activation KINDLIN3 binds the cytoplasmic tail of β integrins and is required for stabilisation of the high affinity conformation of LFA-1 [272-274]. TALIN1 thus mediates conformational maturation to an intermediate affinity of LFA-1, whereas binding of both KINDLIN3 and TALIN1 to the β-chain is thought to result in the high affinity conformation of LFA-1 [272].

Several negative regulators of LFA-1 activation exist, including RAP1 GAPs, as well as RhoH, which is required to keep LFA-1 in a non-adhesive state [275]. RhoH is also required for TCR signalling through its interactions with ZAP70 and LCK [276, 277]. Interestingly, chemokine-induced LFA1 activation is suppressed by RhoH, whereas RhoH enhances TCR-induced LFA-1 activation [278]. Further, RAP1 GAP proteins are expected to negatively regulate LFA-1 by inactivating RAP1-mediated LFA-1 activation. Interestingly the E3 ubiquitin protein-ligase CBL-B also acts as a negative regulator of LFA-1, potentially by ubiquitination and inactivation of CRKL [279] or by blocking association of 14-3-3 with the LFA-1 β-chain [280]. These findings are intriguing in the context of some of the data presented in this thesis.

Together these intricate regulatory mechanisms integrate migratory signals, such as chemokines and TCR engagement with integrin activation. Consequently, LFA-1 affinity is turned on and off in a concise manner by multiple microenvironmental cues.

1.3.2.1 VLA-4 affinity regulations; How is it different from LFA-1?

The vast majority of mechanistic work relating to integrins in T cells has been focusing on regulation of LFA-1. It is therefore not completely clear how other integrins are regulated, and to what extent signalling components mediate regulation of multiple integrins. VLA-4 is perhaps the second most studied of the T cell integrins, and there are a handful of studies investigating VLA-4 activation. RAP1 activity has been shown in mouse models to also be involved in regulation of VLA-4 activation in a similar manner to LFA-1 activation

downstream of both TCR and chemokine activation [259, 281]. Surprisingly however, RAP1 does not seem to be crucial for VLA-4 mediated VCAM-1-binding in human T cells [282]. Similar observations are found for T cells defective for RIAM (which associates with RAP1), where ICAM-1-binding seems more defective than VCAM-1-binding (although both are affected) [283]. KINDLIN3 and TALIN1 seem to also be involved in VCAM-1 binding, however these proteins seem much less critical for VCAM-1- than ICAM-1-binding in human T cells [273]. These findings do not necessarily indicate that the signalling pathways are exclusive but should caution scientists to not think of integrin signalling as one linear pathway affecting all integrins similarly. It will be interesting to see to what extent different signals converge on different types of integrins.

1.3.2.2 Outside-in signalling by LFA-1

Following engagement of LFA-1 by ICAM-1/2, the integrin further induces downstream signals in a process termed "outside-in" signalling that is responsible for the final conformational step from the intermediate affinity LFA-1 (extension of LFA-1) to the high affinity conformation of LFA-1 (further extension of the headpiece and segregation of the α and β chains). LFA-1 does not contain an intracellular signalling domain, so these downstream signals are dependent on recruitment of signal-transducing proteins to the cytosolic surface of the integrin [284]. Surprisingly, ZAP70 and LCK are constitutively associated with LFA-1 during activation and are directly involved in the outside-in signalling; siRNA-mediated knockdown of ZAP70 results in greatly reduced high affinity LFA-1 [285]. Similarly, RAP1/RAPL [286] as well as KINDLIN-3/TALIN1 [287, 288] seem to be involved in both the initial activation of LFA-1 as well as the subsequent outside-in activation of the high affinity conformation, which can be evaluated using direct artificial activation using cations such as Mn^{2+}. Similar mechanisms are at play during VLA-4-mediated outside-in signals, and ZAP70-mediated disruption of a VAV1-TALIN1 complex was further found to be important in this process [289]. Further, a whole range of adaptor and downstream signalling proteins have been implicated in mediating downstream signals from LFA-1, and many of the proteins seem to overlap between inside-out and outside-in signalling, including scaffolding proteins such as ADAP, CRKL, SKAP1 and SLP76, as well as cytoskeletal and catalytic proteins such as

VAV1, *Ezrin, radixin, and Myosin* (ERM) proteins, and Vinculin [Reviewed in 290]. These pathways thus involve a multitude of proteins, and the importance and relevance of all these proteins is still being studied extensively. An important consequence of the outside-in signalling is that it also results in activation of signalling pathways leading to altered transcription, survival and cytoskeletal remodelling.

Cytoskeletal remodelling in T cells is important for T cell spreading, polarisation and chemotaxis, and the Rho family of small GTPases are critical in this process. The Rho GTPase RAC1 has been shown to be regulated by VAV1 downstream of LFA-1 in a PI3K dependent manner and therethrough mediate cytoskeletal remodelling [291]. These processes are essential for LFA-1 or VLA-4-dependent migration, but surprisingly migration under flow on ICAM-1 and VCAM-1 is quite different; T cells migrate against flow on ICAM-1-coated plastic, whereas they migrate downstream on VCAM-1 [292] suggesting that cytoskeletal remodelling is different between LFA-1- and VLA-induced signals. Interestingly, LFA-1 induction activates PI3K in a CRKL-mediated manner [158, 293], whereas these signalling pathways are not induced downstream of VLA-4 activation to the same extent, which might explain these differences.

Affinity vs avidity of integrins – note of caution

When studying integrins such as LFA-1, regulation can either be modulated by direct changes to affinity, changes in avidity through surface clustering of the integrins, or by levels of expression or presence at the surface. Studies investigating LFA-1-mediated adhesion often do not clearly distinguish these mechanisms and it is often unclear whether particular mechanisms affect LFA-1 affinity or avidity.

In human T cells, antibodies specific to the intermediate or high affinity conformation of LFA-1 can be used to measure affinity, however similar affinity-specific antibodies are not as well established for mouse T cells. Binding of ICAM-1 can be used as a proxy for LFA-1 activity, and here binding to soluble ICAM-1 molecules is more dependent on affinity changes and LFA-1 surface expression, whereas binding of ICAM-1-coated surfaces (immobilised ICAM-1) or conjugate-formation is dependent both on changes to overall avidity as a result of increased affinity, surface expression, and clustering.

1.3.3 LFA-1 and phosphoinositides in the immunological synapse

During T cell conjugation with APCs, the involved receptors, and intracellular signalling complexes are segregated into distinct structural zones in the so-called *immunological synapse* (IS) [72]. This allows for dynamic integration of signals in a spatiotemporal manner, allowing for fine-tuning of signalling events in T cell activation in the interface between the cells [294, 295].

In the early immature IS, chemokine-mediated LFA-1 is activated in a PI3Kγ-dependent manner, which initiates the adhesive contact between the T cell and APC and this allows for scanning of TCR complexes and thus supports the initial activation [296]. In these early IS structures, LFA-1 is found in the centre of the synapse with the TCR and its associated signalling complexes at the periphery [297, 298]. The IS subsequently reorganises into *supramolecular clusters* (SMACs) consisting of distinct clusters of receptors, adhesion molecules, and signalling proteins [299]. These mature IS structures have TCR/pMHC

complexes and intracellular signalling proteins localised in the *central SMAC* (cSMAC). LFA-1 redistributes to the *peripheral* and *distal SMAC* (pSMAC and dSMAC) (Figure 1-8a) [297].

VLA-4 is also enriched in the pSMAC and has been implicated in T cell activation through its regulation of SLP76 mobility to the TCR [300]. SLP76 is restrained by VLA-4 in the pSMAC, which is thought to catalyse closer contact with upstream activators in TCR activation and decrease the amount of SLP76 that is internalised in the cSMAC during termination of TCR signalling [300, 301].

PIs are important in the spatial regulation of signalling proteins within the IS. PIP_3 is especially accumulated at the pSMAC, and both $PI(4,5)P_2$ and PIP_3 are cleared from the cSMAC (Figure 1-8b). This is sustained by continuous PI3K signalling and recruitment of PIP_3-binding proteins [302-304]. PI3K-dependent actin remodelling is also thought to be regulated in the peripheral IS, which mediates synaptic force and thereby potentiates CTL-mediated target killing [305].

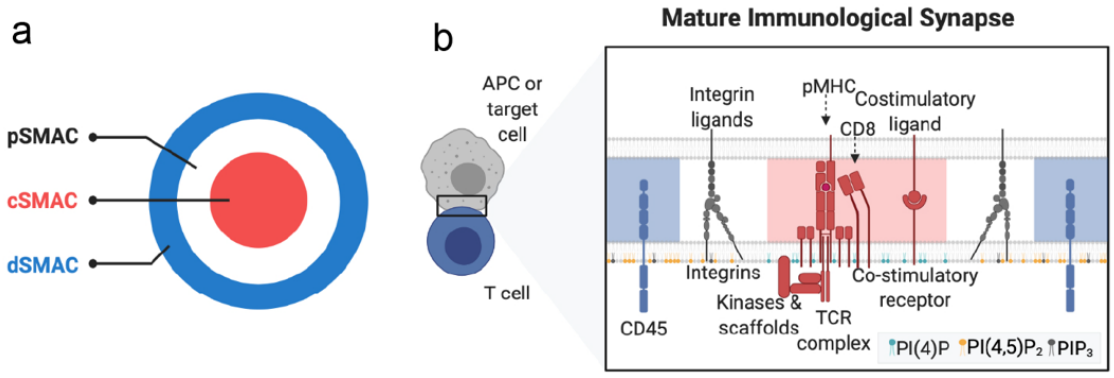

Figure 1-8. Phospholipids in the immunological synapse. **a**, shows the bulls eye of the synapse in the Z-plane. **b**, Schematic of the immunological synapse showing approximate location of critical receptors in the dSMAC, pSMAC, and cSMAC as well as approximate composition of PI(4)P, $PI(4,5)P_2$ and $PI(3,4,5)P_3$ in the inner leaflet of the T cell. Figure made in BioRender with help from Julie Thomsen.

1.3.4 Integrin-regulation by PI3K

Early studies of PI3Ks roles in $CD4^+$ T cell activation found that broad inhibition of PI3Ks with Wortmannin reduced antigen-specific interactions between DO11.10 $CD4^+$ T cells and OVA-pulsed B cells as well as T cell adhesion to immobilised ICAM-1 (ICAM-1-coated plastic) [306, 307]. Further, Wortmannin was found to inhibit CD28-induced activation [308],

and Wortmannin and LY294002 (class I PI3K inhibitor) inhibits CD7-induced activation of β1-integrin-mediated adhesion (VLA1-6) to immobilised fibronectin [309]. In accordance, overexpression of a hyperactive p110-CAAX mutant increased ICAM-1-binding in response to PDBu/Ionomycin [310]. These early findings all supported a role for PI3K in activation of integrins downstream of TCR-engagement.

Fabien Garcon from the Okkenhaug laboratory sought to investigate how PI3Kδ was involved in regulating LFA-1-mediated ICAM-1-binding. Kinase-dead *Pik3cd*^{D910A} CD4^{+} T cells had reduced affinity towards ICAM-1 after stimulation with anti-CD3. As a consequence, OT-II transgenic *Pik3cd*^{D910A} CD4^{+} T cells did not form conjugates with OVA$_{323-339}$-pulsed B cells as well as WT OT-II T cells. *Pik3cd*^{D910A} mutant T cells had reduced RAP1-GTP, indicating a role for PI3Kδ in RAP1-GTP activation. Interestingly, the activation of LFA-1 was less dependent on AKT suggesting other PIP_3-binding proteins were responsible for the PI3K-mediated activation of LFA-1 [219].

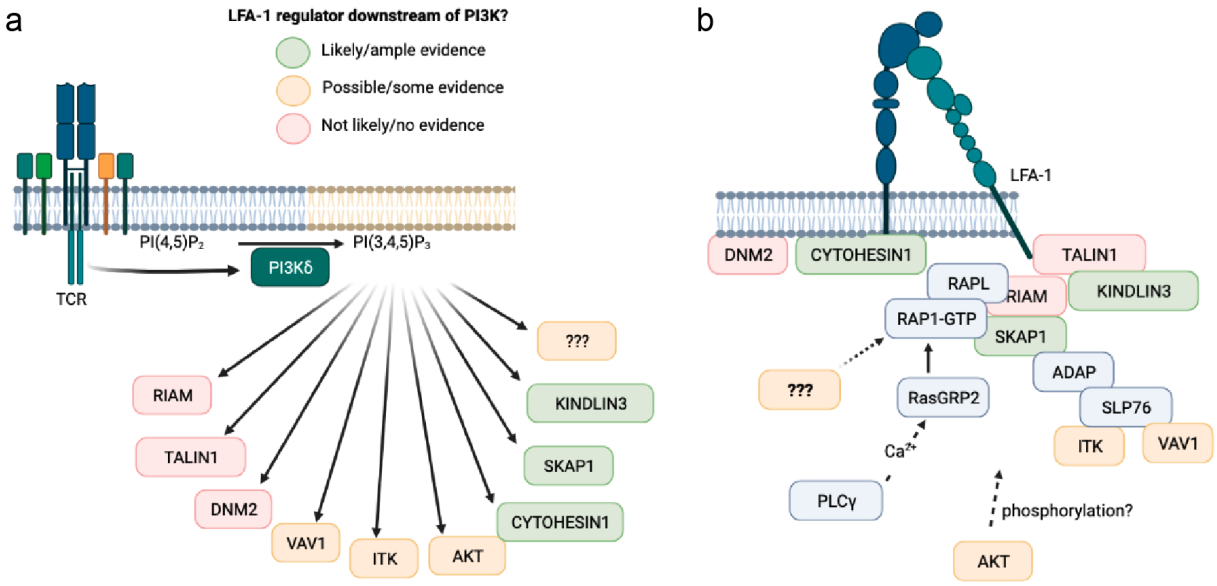

Figure 1-9. LFA-1 regulators downstream of PI3Kδ. **a**, Schematic of proteins that have been implicated in LFA-1 regulation, and the likelihood that they are regulated by PI3K based on the literature. Red proteins have PH domains but are unlikely to be regulated by PI3K. Orange proteins have some evidence suggesting that PI3K regulates their functions and are to some extent involved in LFA-1 regulation. Green proteins have ample evidence that they are regulated by PI3K and have been implicated in LFA-1 regulation in multiple papers. **b**, Simplified

schematic of how the proteins in (**a**) are involved in regulation of LFA-1, showing interaction partners and approximate location. Figure made in BioRender.

Treatment of lymphocytes with Wortmannin or LY294002 decreases SDF1α, CCL19, and CCL21-mediated adhesion to ICAM-1. However, this decrease seemed to be a consequence of decreased avidity rather than decreased affinity, due to decreased chemokine-induced LFA-1 mobility in the membrane following PI3K inhibition [311]. Indeed, Nombela-Arrieta *et al.* found that chemokine-dependent migration of T cells is largely PI3Kγ independent and mediated by DOCK2 [312]. They also found that interstitial migration and S1P-mediated egress was independent of PI3Kγ [313]. Further, PI3K signalling does not seem necessary for chemokine-induced VLA4 activity [314]. PI3Kδ signalling is moreover not required for chemokine-induced LFA-1 activation [219]. Therefore, PI3Kδ activity downstream of TCR-stimulation increases LFA-1 affinity, whereas PI3Kγ-signalling seems dispensable for chemokine-induced LFA-1 affinity regulation.

Nevertheless, multiple proteins involved in the process of LFA-1 activation, including CYTOHESIN-1, SKAP1, and KINDLIN-3, have the potential to be regulated by PIP_3 (Figure 1-9a-b). The intracellular ARF-GEF protein, CYTOHESIN-1, was described early on to bind β2 integrins (e.g. LFA-1, MAC-1) and activate LFA-1-mediated adhesion to immobilised ICAM-1. The PI3K-mediated membrane recruitment of the PH domain of CYTOHESIN-1 was found to partially facilitate the CYTOHESIN-1-mediated activation of LFA-1 [315-317]. CYTOHESIN-1 binds directly to the cytoplasmic tail of β2 integrin, and this interaction as well as the ARF-GEF functionality of its SEC7 homology domain have been shown to regulate the activation of LFA-1 in T cells and LFA-1 mediated TEM [318, 319]. Moreover, CYTOHESIN-1 further regulates activation of RhoA and integrin activation in DCs [320]. Surprisingly, CYTOHESIN-1 seems to have opposing roles in regulation of MAC-1 (αMβ2) integrin-mediated adhesion to fibrinogen by neutrophils, suggesting a more complex involvement of CYTOHESIN-1 in regulation of integrin activation [321]. This potentially hints at a differential role of PI3K-signalling in regulating integrins in different immune subsets depending on their integrin expression.

Another PH-domain-containing protein, SKAP1, involved in LFA-1 activation has been characterised by Rudd and others. They found that the ADAP/SKAP1 module mediated by RIAM is necessary for TCR-induced inside-out LFA-1 activation and clustering by mediating formation of RAP1/RAPL complexes as well as membrane recruitment of these essential proteins involved in LFA-1 activation [269, 271, 322, 323]. The SKAP1 PH domain was found to be required for membrane recruitment, and this in turn was necessary for the recruitment of RAPL to the membrane [270]. A SKAP1 mutant that was constitutively associated with the membrane by addition of a myristoylation site, disrupted the requirement for PI3K signalling in binding immobilised ICAM-1 suggesting that PI3K-mediated activation of LFA-1 is dependent on ADAP/SKAP1/RIAM signalling. Indeed, although RIAM contains a PH domain with high affinity for PI monophosphates *in vitro*, SKAP1 is required for recruitment of RAP1/RIAM to the membrane during LFA-1 activation [323]. In accordance, K152E mutation of SKAP1 eliminated PIP_3-binding *in vitro* and as a result impaired immobilised ICAM-1-binding [324]. Unexpectedly, this mutant did not abolish SKAP1/ADAP/RIAM/RAPL binding to the membrane, suggesting redundancy in the pathways resulting in membrane-recruitment of these proteins. Surprisingly, SKAP1 mutants lacking the PH domain do not significantly alter its role in integrin-mediated adhesion, suggesting the mechanism by which PI3K regulates SKAP1 is still incompletely understood [269, 324, 325]. Further, earlier unpublished data from the Okkenhaug laboratory has not found an effect of SKAP1 KO on ICAM-1-binding (not shown).

Mutations of the crucial LFA-1 regulator, KINDLIN-3, are the cause of leukocyte adhesion deficiency III (LAD-III), a rare autosomal disorder, resulting in severe bleeding and life-threatening infections as a result of defective β1- and β2-integrin-mediated adhesion [326, 327]. Studies by Hogg *et al*. suggest that KINDLIN-3 has higher affinity to PIP_3 than PIP_2 [328]. They also found that the PIP_3-binding was necessary for the function of KINDLIN-3, as KINDLIN-3 mutants that specifically did not bind PIP_3 failed to rescue adhesion of LAD-III cells to ICAM-1. This study therefore suggests that KINDLIN-3 is at least partially regulated by PI3K, though this has yet to be confirmed in lymphocytes.

Consistent with several studies indicating a key role for PI3K signalling in regulating integrin affinity/avidity, and multiple other proteins have been implicated in PI3K mediated integrin

regulation indirectly (Figure 1-9a-b). A whole range of integrin-regulating proteins contain PH domains, and some have affinity for PIP_3, however whether integrin-regulation by these proteins is directly affected by PI3K signalling is still unclear. It is important to note that PIP_2 is up to 100X more abundant on the plasma membrane than PIP_3. Therefore, a given protein needs to have high selectivity for PIP_3 over PIP_2 in order to be directly regulated by PI3Ks. DNM2 which is known for its role in regulating vesicular traffic, has been suggested to also regulate integrin affinity directly via FAK/PYK2- and C3G (also known as RAPGEFI)-mediated RAP1 activation [329]. DNM2 has a PH domain, however it does not appear to have affinity for PIP_3 in screens of PIP_3-binding [227], and it is therefore unlikely that it is regulated by PI3K. The Schwartzberg laboratory and others have also shown that TEC kinases are involved in regulating cytoskeletal remodelling and LFA-1-mediated adhesion [330, 331]. In T cells, the highest expressed TEC kinases are ITK and RLK, and *Itk* KO cells have decreased adhesion to ICAM-1. RLK does not contain a PH domain, whereas ITK contains a PH domain that binds selectively to PIP_3 [332], but the role of this in T cell integrin-mediated adhesion is unclear. Similar results have been described for VAV1 implicating it in clustering of LFA-1, but it is not known if this effect is PI3K-dependent [333, 334]. It seems likely that both TEC kinases and VAV1 are more important for LFA-1 clustering, and thereby increased avidity, than affinity regulation as these proteins are known to be important for cytoskeletal remodelling, and recruitment of proteins to the synapse [331]. Intriguingly, DOCK proteins which do not contain PH domains, have been suggested to have affinity to PIP_3 via so-called *Dock Homology Domains* (DHR1) [228]. However, the extent of direct PIP_3 affinity, and whether the affinity is a result of DOCK-proteins interacting with the PH-domain-containing ELMO proteins is still debated [302, 335]. DOCK2 was described earlier in the introduction in the context of chemokine-stimulated LFA-1 activation but does not seem to affect TCR-induced LFA-1 activation, as it seems to be involved in TCR-induced RAC-dependent TCR clustering, without affecting LFA-1 translocation to the IS [302, 336]. However, it is possible that this is context-specific, and some subsets thus might be more or less dependent on DOCK2 for efficient LFA-1 activation.

The fact that such a high proportion of LFA-1 regulators contain PH domains, underpins the importance of PI3K-mediated signalling in regulating LFA-1, and it is likely that there are more proteins involved. Multiple possible mechanisms of PI3K-mediated regulation are plausible;

firstly, it is possible that PI3K activity directly activates the PIP_3-binding LFA-1 regulators by inducing a conformational change in the proteins. Secondly, PIP_3 can colocalise proteins that interact and activate each other. Thirdly, it is possible that microclusters of PIP_3 colocalise with LFA-1 spatiotemporally during LFA-1 activation. Similarly, it is possible that PIP_3 inactivates negative regulators of LFA-1 by similar mechanisms, i.e. conformational inactivation, colocalisation of negative regulators with other proteins that inhibit them, or by sequestering the negative regulators from LFA-1 during activation as has been suggested for regulation of platelet integrins [337]. The main goal of this PhD project has been to screen for such unknown regulators of LFA-1 activation downstream of PI3K using a *clustered regularly interspaced short palindromic repeats* (CRISPR)/Cas9-based screen of predicted PIP_3-binding proteins for effects on ICAM-1-binding. As I will present in the results section (Chapter 3) I have identified multiple novel regulators and studied one of these in detail, the small dual RAP1/RAS GAP, RASA3.

1.4 RASA3 – a dual RAS/RAP1 GAP

The PIP_3-binding protein with the highest affinity to PIP_3 identified by Jungmichel *et al*. was RASA3 [227], which is expressed at high levels in both $CD4^+$ and $CD8^+$ T cells (Figure 1-6). This protein has been a major focus of my PhD project, and here I present what is currently known about it from studies on platelets and other cell types.

RAS P21 Protein Activator 3 (RASA3) (also known as $GAP1^{IP4BP}$) was identified as a dual RAS/RAP1 GAP from the GAP1 subfamily and was initially considered specific for soluble *Ins(1,3,4,5)P4* (IP_4) in platelets [338-340]. These initial studies hinted a role of IP_4 in regulating RASA3 activity *in vitro*. The GAP1 family consist of four proteins; RASA2 (also known as $GAP1^m$), RASA3, RASA4 (also known as CAPRI), and RASAL. The GAP1 proteins all have 2 C2 domains (C2A and C2B), a GAP domain, a PH/*Bruton's kinase* (BTK) domain, and a C terminal region with no known homology (Figure 1-10a). The sequence encoding RASA3 is highly conserved in mammals, and has >95% protein homology between humans and mice thus suggesting an important role for RASA3 [341].

RASA3 seems to be the GAP1 protein with highest RAP1 GAP specificity *in vitro*. Exactly how RASA3 elicits its dual GAP functions, remains unknown, but it seems to have higher catalytic activity towards RAP1 than RAS [342]. When examining the RAS and RAP1 catalytic activity of the RASA3 GAP domain without the C2 domains or PH domain, RASA3 loses its GAP activity towards RAP1, but still has catalytic activity towards RAS, suggesting its RAP1 activity is dependent on the C2 domains and/or PH domain to stabilise structural rearrangements that allow for binding of RAP1 [342, 343]. Multiple mutants of the GAP domain that alter its GAP specificities have been identified including a RASA3^{R317Q} mutant, which disrupts the GAP domain, as well as a RASA3^{P489V} mutant that decreases the RAP1 GAP specificity without affecting the RAS GAP activity [344] (Figure 1-10a). The different regulators of LFA-1 with PH domains have little or no similarity (Figure 1-10b).

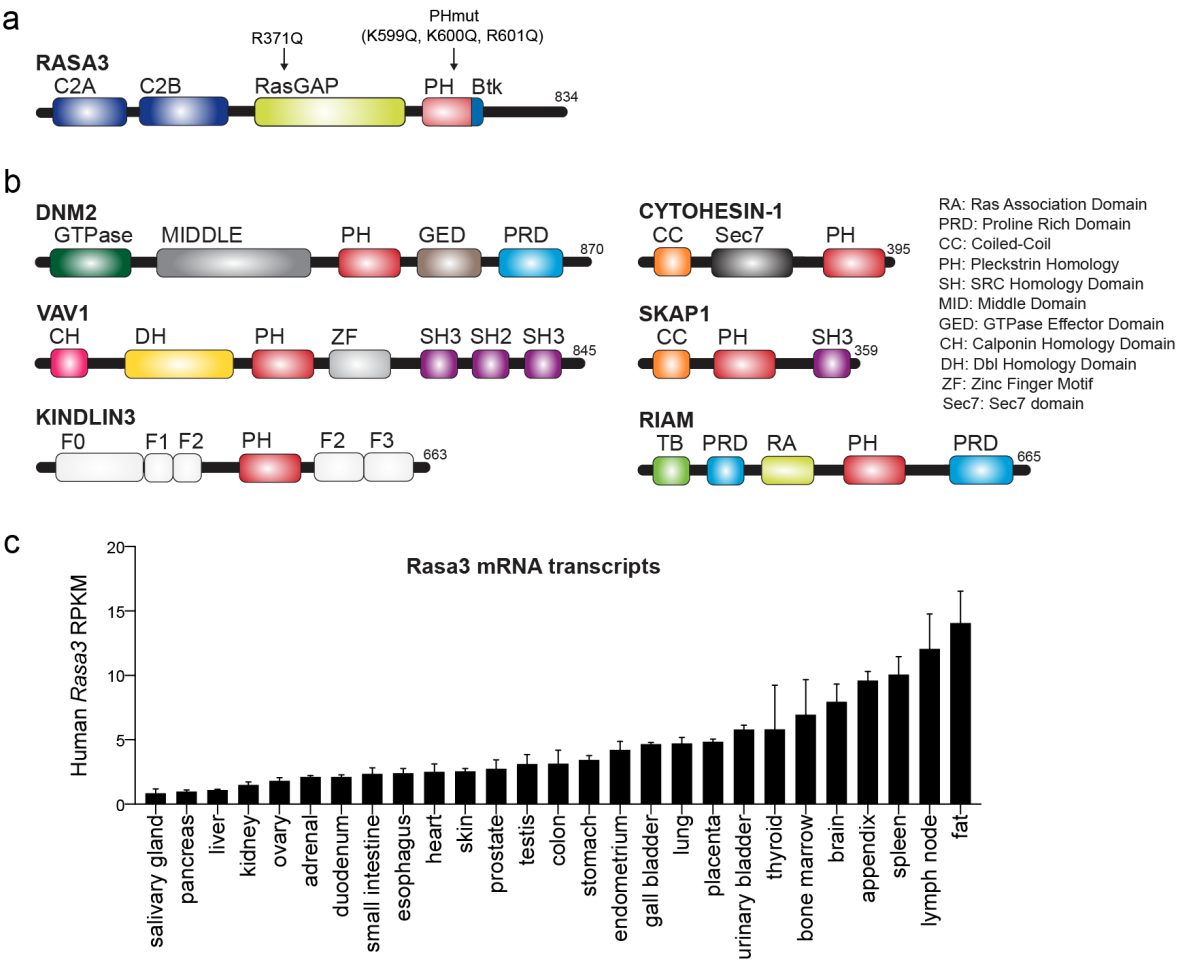

Figure 1-10. PH domain proteins involved in LFA-1 regulation. **a**, RASA3 domain structure as well as the location of the R371Q mutation which disrupts the GAP function of RASA3 and a PH mutant (K599Q, K600Q, R601Q)

that disrupts binding to PIs in the membrane. **b**, Domain structures of other proteins that have been implicated in LFA-1 regulation that contain PH domains. **c**, Expression of *Rasa3* in human tissues mined from [345].

The C2 domains of other GAP1 proteins seem to be involved in regulation of the GAP domain in a Ca^{2+}-dependent manner, as well as association with lipids in the membrane. Nonetheless the role of the C2 domains of RASA3 is not known, whereas the PH domain is necessary for binding to the membrane through its interaction with PIs [346]. Studies of the PI specificity of RASA3 indicate that RASA3 binds both PIP_2 and PIP_3 [347], however, other studies have indicated that RASA3 has considerably higher association with the membrane in presence of PIP_3 than with PIP_2 [337, 348]. By creating a RASA3 mutant with K599Q, K600Q, R601Q, the PI binding of RASA3 is disrupted due to a neutralised core of the PH domain [337, 346], which allows for probing the role of PIP_3-binding in RASA3 function and localisation (Figure 1-10a). Together these studies suggest that RASA3 localisation is sensitive to PI3K activity and that PI3K activity regulates the activity of RASA3. However, it is still debated exactly how RASA3 is biochemically regulated.

Rasa3 is expressed in multiple tissues in humans and mice, and is found at high levels in leukocytes, thymus, LNs, and spleen, suggesting an important role for RASA3 in the immune system (Figure 1-10**c**) [345, 349]. Full KO of *Rasa3* in mice is embryonically lethal [349-351] due to a severe bleeding disorder, and point mutations of *Rasa3* lead to unstable protein resulting in severe bleeding disorders causing mortality before day 30 [349]. Based on these observations, the RASA3 role in platelet function and development has been most studied. In platelet development, RASA3 was found to be important in controlling RAP1 inactivation during megakaryocyte differentiation and release of pro-platelets. RASA3 was found to regulate their integrin αIIbβ3-mediated adhesion, and RASA3 loss resulted in severely defective platelet development [349, 350]. Subsequent studies have further identified RASA3 as the main regulator of RAP1 activity through inside-out and outside-in signalling in platelets and thereby a critical regulator of αIIbβ3 integrin activity [352]. RASA3 was found to not affect RAS in platelets [352]. A recent study further identified RASA3 as a critical regulator of endothelial cell β1 integrins and thereby involved in vascular lumen structure [353]. Together these studies suggest an important role in RAP1-mediated integrin regulation in multiple cell types.

Interestingly, RASA3 was found to be inhibited by PI3K in platelets independently of AKT [337, 352, 354], but exactly how PI3K regulates the activity of RASA3 remains unknown. It is possible that RASA3 is sequestered from the integrins as a result of its high affinity to PIP_3. Alternatively, PIP3-binding inactivates RASA3 through a conformational rearrangement or by bringing the protein close to an unidentified binding partner, kinase or other modifying protein that alter the RASA3 activity. It is intriguing how PI3K activity would negatively regulate a protein such as RASA3, since it is the only known protein that seems to be negatively regulated by PIP_3-binding.

So far only one study has investigated the role of RASA3 in T cells: Wu *et al*. found RASA3 in a screen of proteins that are highly expressed in pathogenic T_H17 cells and showed that its loss results in decreased severity of *Experimental Autoimmune Encephalomyelitis* (EAE). They found that RASA3 binds CBL-B and *interferon regulatory factor 4* (IRF4), and thereby promoted the ubiquitination and degradation of IRF4 which is necessary for T_H17 development [355]. Thus, conditional *Rasa3* KO in T cells ($Rasa3^{fl/fl}$ x $Cd4^{Cre}$) resulted in reduced pathogenic T_H17 development and decreased EAE pathogenesis, and a skewing of T cell development to a T_H2 cell program [355]. Thus, RASA3 seems to also play a role in T cell biology, however Wu *et al*. did not investigate how RASA3 is involved in integrin regulation and T cell migration.

1.5 Using CRISPR/Cas9 to characterise genes in T cells

CRISPR/Cas9 has disrupted the way scientists approach research questions in all fields of biology. By enabling easy, swift, and precise manipulation of the genetic code, scientists can probe the roles of novel genes with an unprecedented speed and precision. The Nobel-prize awarded to Jennifer Doudna and Emmanuelle Charpentier for their discoveries of CRISPR/Cas9 celebrates the beginning of a biological revolution. In immunology, the application of CRISPR/Cas9 has allowed immunologists to investigate which genes are necessary for cancer immune evasion [356], immune-mediated cancer elimination and tumour infiltration, infection of host cells [357-359], development of immune cell subsets and their functions [360, 361], as well as allowed for genetic engineering of highly efficient chimeric

antigen receptor T cells for fighting cancers [362]. In this chapter I highlight some of the most important discoveries in T cell biology applying CRISPR/Cas9 and discuss challenges of using the tool for screening genes involved in T cell biology.

1.5.1 Using CRISPR/Cas9 in immune cells

CRISPR was discovered in bacteria as a defence mechanism used to disrupt invading foreign DNA particles (i.e. viral, bacteriophage, bacterial DNA) by guiding a nuclease to the foreign genomic DNA [363-365]. Multiple CRISPR nucleases have since been discovered that can cut the foreign DNA, however, the most studied nuclease is the single subunit type II CRISPR nuclease, Cas9. Cas9 is guided to the foreign DNA by a guide RNA composed of a *trans-activating RNA* (tracrRNA), which facilitates binding of the Cas9 enzyme, and a CRISPR RNA (crRNA), which engages the target DNA and the bound tracrRNA in the Cas9 enzyme, thus guiding the enzyme to its target. The gRNA-bound Cas9 enzyme binds gRNA-complementary genomic DNA sequence upstream of a *protospacer adjacent motif* (PAM) [366], and cleaves the DNA inducing a double-stranded DNA break [365, 366]. The creative finding that initially catalysed the applicability of CRISPR/Cas9 in common scientific research was the combination of the tracrRNA with the crRNA to create a so-called *single guide RNA* (sgRNA) [367]. Introducing this sgRNA and the Cas9 enzyme into eukaryotic cells allowed scientists to cut the genome any sequence upstream of a PAM sequence specific to the chosen Cas9 enzyme (NGG for *Streptococcus pyogenes* Cas9) with high specificity and efficacy [368]. The double-stranded break will then be repaired by either *non homologous end joining* (NHEJ) or *homology-directed repair* (HDR). NHEJ is error-prone and often results in random insertions or deletions; in turn these errors often result in frameshift mutations or deletions that result in a KO of the targeted gene, and CRISPR/Cas9 was thus adapted as a gene KO tool in mammalian cells [369-372]. By introducing a DNA template alongside the Cas9 enzyme and sgRNA, Cas9 can also be adapted as a gene editing tool. The template DNA can then be used as template for HDR-mediated repair, thereby replacing the DNA by the break. Together, these tools quickly transformed the way scientists study the genome and led to numerous tools harnessing the sequence-specific selectivity of the gRNA/Cas9 complex.

In this thesis, I have applied CRISPR/Cas9 as a tool for knocking out genes in primary mouse T cells. The greatest challenge in effectively knocking out genes using this tool in primary T cells is the introduction of the gRNA and the Cas9 enzyme. Primary T cells can be transduced efficiently using γ-retroviral particles [373, 374], whereas most methods of electroporation significantly decrease viability. When using electroporation, a *ribonuclear protein* (RNP) consisting of Cas9 complexed with the sgRNA *in vitro* are electroporated into the cells [375, 376]. Another caveat of the electroporation approach is that the sgRNA sequence is not incorporated into the genome, which makes it difficult to dissect which genes were targeted in pooled CRISPR screens as discussed in Chapter 1.5.2. Dr. Bonnie Huang from the Schwartzberg laboratory optimised CRISPR KO in T cells using mouse T cells from genetically engineered *streptococcus pyogenes* Cas9-expressing mice [377, 378]. This allowed us to circumvent having to introduce the Cas9 enzyme. Thus, we just had to introduce the sgRNA in a γ-retroviral backbone to get efficient KO. Dr. Huang also found that using an "all-in-one" vector approach where the vector contains both the sgRNA and the Cas9 enzyme resulted in reduced efficacy of both transductions and gene targeting compared to using Cas9 mice with a smaller retrovirus containing only the sgRNA [379]. One caveat of using γ-retroviral delivery to KO genes in mouse T cells is that retroviral delivery necessitates actively cycling and proliferating cells [374]. As a result, only activated T cells can be transduced efficiently, which limits the questions CRISPR can help answer. There are ways to circumvent this, i.e. transduction of naïve T cells with lentivirus (can infect non-dividing cells), which will give low transduction efficiencies, but possibly could work under the right conditions, or transduction of hematopoietic stem cells, followed by transfer *in vivo* and then isolating the developed T cells from the periphery of the mice [380]. More recently, newer electroporation methods have improved the introduction of sgRNAs into primary T cells, however this cannot easily be used for CRISPR screening.

1.5.2 CRISPR/Cas9 screening

Earlier, for investigating the roles of genes in T cell biology it was common to use *short hairpin RNAs* (shRNAs) to screen the role of genes in various biological functions. However, there are several pros of using CRISPR/Cas9 to screen for gene functions. Firstly, some biological effects might only appear in a full KO where no residual protein is left, and whilst successful

CRISPR/Cas9 KO can result in complete ablation of the protein in the edited cells, shRNAs only reduces the expression. Secondly, studies have suggested that CRISPR/Cas9 has fewer off-targets, and greater specificity than shRNAs [381-383]. Nonetheless, there are still situations where shRNA knockdown is favourable to CRISPR/Cas9-mediated KO; for example, if the targeted genes are essential, but a knockdown would not kill the cells. CRISPR screening can be done in several ways, but the two most common concepts are arrayed CRISPR screens and pooled CRISPR screens.

Arrayed CRISPR screening applies individually cloned sgRNA-vectors to KO genes in multiwell formats. This is costly, as it takes up a high amount of reagent, and time consuming, as every gene has to be screened individually. However, arrayed screens allow for screening of phenotypes using techniques such as imaging, proteomics, and other similar technical methods that cannot be detected by sequencing directly [359].

In pooled CRISPR screens sgRNAs are introduced by viral integration in the target cell genomes allowing for sequencing as readout of genes that affect the phenotype. The sgRNA-oligos are synthesized, mixed, and cloned into the viral vector of choice in a pooled fashion, and the target cells are transduced with the virus resulting in genomic integration of the oligo encoding the sgRNA into the target cell genome. The transduced cells are subsequently used for the desired assay of choice, and the readout conducted by next generation sequencing of the integrated sgRNAs. The fact that sequencing is the readout limits the assays that can be conducted. It is possible to screen functional readouts by either growth assays, in vivo competition assays, or cell-sorting-based assays where cells are sorted and sequenced to quantify sgRNAs that affect the proportions in the sorted populations [359]. Pooled screens are also faster, and can be done much easier for large scale libraries.

Multiple innovative approaches have allowed for screens involving *single-cell RNA* (scRNA) sequencing that allow one to pick up sgRNAs in the scRNA sequencing pipeline involving barcodes in the sgRNA vectors [384-386]. Similarly, techniques such as Procode CRISPR/Cas9 screening has expanded the way we can do CRISPR/Cas9 pooled screening by circumventing the need for sequencing through viral expression of peptide barcodes that can be picked up by antibodies (and thereby be detected by flow cytometry or Cytof) [387].

1.6 Hypotheses and aims

1.6.1 Identification of noncanonical PIP_3-binding proteins in LFA-1 regulation

It is clear that PI3K is important for the regulation of LFA-1 activity, however we still do not fully understand how PI3K activity regulates LFA-1. There are multiple proteins that regulate LFA-1 that are potentially regulated by PI3K, and previous results from the laboratory of Dr. Fabien Garçon and Professor Okkenhaug suggested that the regulation is at least partially independent of AKT, and somehow involves RAP1 activation [219] (Figure 1-11). Yet, investigating the role of PI3K effector proteins in this process in an unbiased way has not been done.

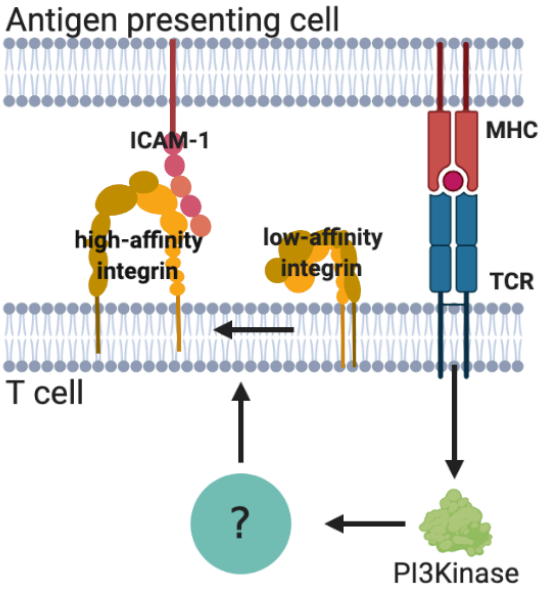

Figure 1-11. PI3K-mediated regulation of LFA-1: what are the downstream mediators? PI3K regulates LFA-1-mediated binding of ICAM-1 in T cells, but it is still not understood what downstream signalling proteins mediate this process. Figure made in BioRender

My aims for this thesis were therefore to:

1. Identify novel regulators of LFA-1 using CRISPR/Cas9 by screening PI3K effector proteins (results presented in **Chapter 3**).

2. Biochemically characterise the most interesting hits from the CRISPR/Cas9 screen to determine the biochemical role of the protein in T cells (results presented in **Chapter** 4).
3. Understand the role of the hits from aim 2 in T cell homeostasis *in vivo* and T-dependent humoral immunity (results presented in **Chapter 5**).

Chapter 2

Materials and Methods

2. Materials and Methods

2.1 Mice

2.1.1 Housing and Husbandry

The breeding and experiments carried out at NIH were done in accordance with the US American Animal Welfare Act and NIH policies, whereas the procedures and breeding of the mice used for in United Kingdom were conducted in accordance with Commonwealth Home Office regulations and University of Cambridge guidelines (Home office license P0AB4361E). For all experiments, mice were kept in *individually ventilated cages* (IVC) cages in a specific pathogen-free environment. At the NIH, mice were kept in the NHGRI Animal Core Facility, whereas in the UK mice were kept at the Gurdon Mouse Facility, Anne McLaren Building, and MIRA Facility at University of Cambridge. Mice were used at ages of 8-12 weeks unless otherwise stated and were euthanised according to Home Office regulations by CO_2 followed by cervical dislocation or cervical dislocation followed by destruction of brain. For a complete list of mouse strains used and the abbreviations used in this thesis, see Table 2-1.

Table 2-1. Mouse strains used in this thesis

Strain name	**Abbreviation**	**MGI number**
C57BL6	WT	MGI:2159736
Rasa3$^{tm1.1Wber}$	*Rasa3*^{fl}	MGI:5756029
Gt(ROSA)26Sor$^{tm1.1(CAG-cas9*,-EGFP)Fezh}$/J	*Cas9*$^{+}$	MGI:5583855
B6.Cg-Tg(Cd4-cre)1Cwi/BfluJ	*Cd4*^{Cre}	MGI:5566534
C57BL/6-Tg(TcraTcrb)1100Mjb/J	OT-I	MGI:3054907
Pik3cd^{tm1Bvan}	*Pik3cd*^{D910A}	MGI:2385595
Pik3cd$^{tm1.1Klog}$	*Pik3cd*^{E1020K}	MGI:6202025
B6.Cg-Tg(TcraTcrb)425Cbn/J	OT-II	MGI:3046083
B6.129S(FVB)-Bcl6$^{tm1.1Dent}$/J	*Bcl6*^{fl}	MGI:3871652

2.1.2 Mouse strains

C57BL/6 (MGI:2159736), OT-I (MGI:3054907), OT-II (MGI:3046083) [388], constitutive *Cas9*$^{+}$ (MGI:5583855) [378], *Cd4*^{Cre} (MGI:5566534), and CD45.1 (MGI:4819849) mice were obtained from Jackson Laboratory. *Pik3cd*^{D910A} (MGI:2385595) [389] and *Pik3cd*^{E1020K} (MGI:6202025) [136, 232] mice were bred at University of Cambridge or the NIH. *Rasa3*^{fl} (MGI:5756029) [352] mice were kindly provided by Professor Wolfgang Bergmeier's laboratory, University of North Carolina and were rederived into *Cd4*^{Cre} C57BL/6 mice in the NHGRI Animal Core Facility. The *Rasa3*^{fl} mice were subsequently shipped to University of Cambridge, pathogen tested, and released for breeding and experiments. *Bcl6*$^{fl/fl}$ mice (MGI:3871652) [390] used in Cambridge were kindly provided by Dr. Meritxell Nus' laboratory and *Bcl6*$^{fl/fl}$ mice used at NIH were bred at the NIH. Cas9 mice were bred to OT-I mice, and *Rasa3*$^{fl/fl}$ mice were bred to *Cas9*, OT-I, OT-II and/or *Cd4*^{Cre} mice. For adoptive transfer experiments C57BL/6 mice were bred to CD45.1^{+} mice to generate WT CD45.1/2^{+} mice used as recipients, and WT CD45.1^{+} mice for transfer.

2.1.3 Genotyping

At NIH I performed genotyping by conventional PCR for *Rasa3*^{fl} with Fwd: GTCATCCATGGGTTTCCTAAGCACTTCC and Rev: AAAACACACTGAGGTTCAGAC ACGCTCC primers, *Cd4*^{Cre} with Fwd: CCTGGAAAATGCTTCTGTCCGTTTG and Rev: ACGAACCTGGTCGAAATCAGTGCG primers, and *Cas9*$^{+}$ (according to JAX protocol) and by flow cytometry staining of bleeds for Vα2 and Vβ5 for OT-I/OT-II. At University of Cambridge, genotyping was performed by Transnetyx genotyping service using real-time PCR.

2.2 *In vivo* models

2.2.1 NP-OVA immunisation of mice

I performed immunisations as previously described [136]. Mice were immunised subcutaneously in the hock with 20 μg NP-OVA (Biosearch Technologies) emulsified in alum

(Imject™ Alum, Thermo Scientific). Analysis of resting and draining LNs was performed 8 days later. For Ce3D imaging NP-OVA/AddaVax immunisations was performed intramuscularly into the calf muscle of the hind legs by Dr. Dominic Golec and Dr. Tibor Verez at NIH. For some of the presented experiments immunisations were performed by Dr. Silvia Preite, Dominic Golec, or Dr. Bonnie Huang as specified in figure legends.

2.3 T cell cultures

2.3.1 Preparation of single cell suspensions from mouse tissues

Mice were euthanised and pLN (axillary, cervical, brachial, and inguinal), *mesenteric LNs* (mLN), spleen, PPs, bone marrow, and thymus were carefully dissected and stored in PBS on ice. Tissues were in most experiments prepared to a single cell suspension by mashing the tissues through 40 μm or 70 μm cell strainers. Isolated single cell suspensions of splenocytes and isolated blood was treated with ammonium-chloride-potassium lysis buffer for 5min followed by 2X wash with PBS to get rid of red blood cells. Following successful preparation of cells, cells were counted by automated cell counting using a Nucleocounter NC-3000 (Chemometec) or a Vi-Cell (Beckman Coulter). Cells were prepared for subsequent assays or analysis as described below.

2.3.1.1 Cell enrichment by magnetic-activated cell sorting

For certain experiments, cells were enriched using *magnetic-activated cell sorting* (MACS) by negative selection. This was done either with MojoSort (Biolegend), EasySep (Stem Cell), or MACS Cell Separation (Miltenyi) kits. MACS was done according to manufacturer's protocol. For most experiments MojoSort kits were used; here cells were prepared in MACS buffer (PBS + 0.5% BSA + 1 mM EDTA) at $1x10^8$ cells/mL, stained 15min on ice with biotin-conjugated antibodies followed by addition of magnetic Streptavidin-beads and stained for 15min on ice. Tubes with stained cells were placed in a MojoSort magnet and incubated 5min after which the supernatant with untouched enriched cells was transferred to a fresh tube. Beads were washed

with MACS buffer and incubated for 5min and supernatant isolated to increase yield. I consistently got >90% purity from the negative selection kits, as determined by flow cytometry.

2.3.2 *In vitro* activation of T cells

For activation of T cells *in vitro* I either added peptide directly to single cell suspensions of splenocytes activate TCR transgenic T cells, or enriched total T cells (or $CD4^+$ or $CD8^+$ T cells) and activated cells on plate bound anti-CD3 with soluble anti-CD28.

Activation of TCR transgenic T cells

To activate OT-I TCR transgenic $CD8^+$ T cells *in vitro*, single cell suspensions of splenocytes were plated at $2x10^6$ cells/mL with 10 nM SIINFEKL peptide (unless otherwise stated) in R10 medium (RPMI-1640 + 10% heat-inactivated FBS + 2 mM L-glutamine + 1% Pen/Strep + 0.5 mM β-ME) and incubated in a humidified 37˚C, 5% CO_2 incubator. Activation was visually confirmed by light microscopy at 24-48h after activation, and unless cells were blasted for viral transduction, cells were kept for 72h (Day 3) before activated $CD8^+$ T cells were counted and plated in fresh media with 10 ng/mL rhIL-2 at $1x10^6$ cells/mL. Cells were resuspended in fresh media every subsequent day with fresh rhIL-2 until day of assay.

Activation of T cells with plate-bound antibodies

To activate polyclonal T cells *in vitro*, appropriate size tissue culture wells were coated with anti-CD3 (2C11, BioXCell or Biolegend) at 1 μg/mL (unless otherwise stated) in PBS overnight at 4˚C or 2h at 37˚C. Wells were washed 2X with PBS followed by 1X in R10 before T cells were plated. T cells from LNs or spleen (or a mix) MACS was performed as described in Chapter 2.3.1.1, to negatively enrich either total T cells, $CD4^+$, or $CD8^+$ T cells. Cells were plated in the anti-CD3 coated wells at $1x10^6$ cells/mL with 2 μg/mL soluble anti-CD28 (37.51, BioXCell or Biolegend). For transductions, cells were activated with 5 μg/mL anti-CD3 and 5 μg/mL anti-CD28. Cells were kept on anti-CD3/28, and activation was visually confirmed by light microscopy at 24-48h after activation. Unless cells were blasted for viral transduction, cells were kept for 72h (Day 3) before activated T cells were counted and plated in fresh media with 10 ng/mL rhIL-2 at $1x10^6$ cells/mL. Cells were resuspended in fresh media every subsequent day with fresh rhIL-2 until day of assay.

2.3.3 Retroviral transduction of primary murine T cells

293T cells (ATCC) were cultured in EMEM (ATCC) + 10% FBS + 2 mM L-glutamine (Thermofisher Scientific). Cells were transfected with Mirus TransIT®-293 (Mirus) according to manufacturer's instructions with pCL-Eco packaging plasmid and retroviral plasmid of interest as I have previously described [379]. Virus was harvested at 24 and 48h post transfection and spun at 1000 G for 5min at 4˚C to remove cellular debris. OT-I x Cas9 splenocytes were prepared for transduction as previously described [379]. Briefly, splenocytes ($1x10^6$ cells/mL) were activated with 10 nM SIINFEKL peptide in RPMI + 10% FBS + 2 mM L-glutamine (R10 medium) and transduced with viral supernatant + 10 IU/mL rhIL2 and 8 μg/mL Polybrene (Sigma) by spinfection (2000 RPM, 1.5h, 32˚C) at 24h and 40h after activation for sgRNA. Similar transduction protocols were used for overexpression of proteins, however, for these experiments, cells were activated with 5 μg/mL plate-bound anti-CD3 and 5 μg/mL soluble anti-CD28. I co-authored a protocol publication on how to use this technique for Cas9-mediated KO in T cells (Figure 2-1) [379].

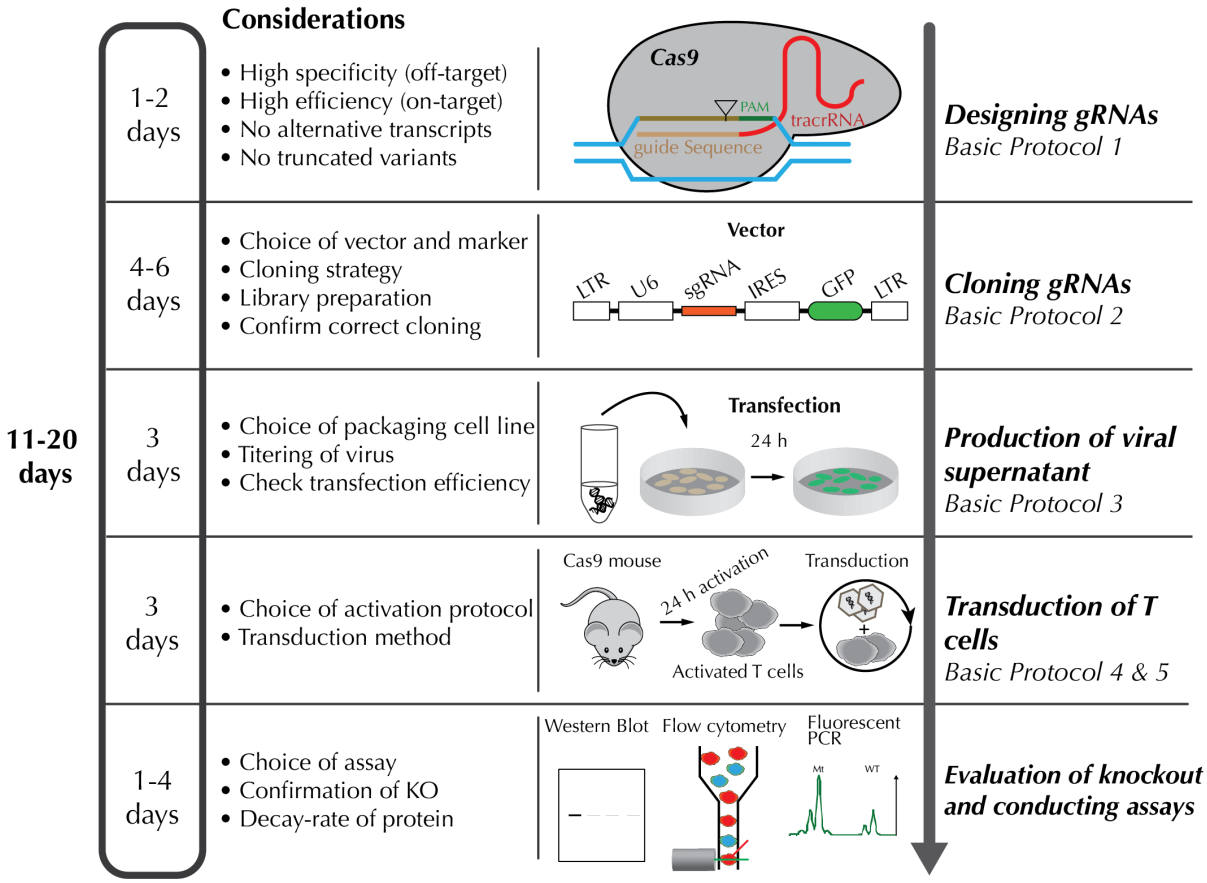

Figure 2-1. Protocol for KO of genes in T cells by CRISPR/Cas9. This diagram shows the usual workflow I use to KO genes in primary mouse T cells using CRISPR/Cas9, from designing the sgRNA to assay in the T cells. diagram was published in [379].

2.4 Flow cytometry

2.4.1 Surface staining of cells for flow cytometry analysis

For staining, cells from spleen, LNs, and PPs were prepared to single cell suspensions in *fluorescence-activated cell sorting* (FACS) buffer (PBS + 0.5% BSA + 1 µM EDTA) as described in Chapter 2.3.1. For phenotyping pLNs, left and right inguinal, brachial and axillary LNs were pooled (6 LNs/mouse). Cells were stained at 2-5x10^6 cells/ml in 96-well round or V-bottom plates with a surface antibody cocktail containing fluorophore-conjugated antibodies, Fc-blocking antibodies (anti-CD16/32, 2.4G2, BioXCell) and LIVE/DEAD® Fixable Aqua Dead Cell Stain Kit or LIVE/DEAD® Fixable Near-IR Dead Cell Stain Kit (Life

Technologies), 50 μL/sample. Cells were stained for 30-60min on ice, followed by 2X washes in FACS buffer. For intracellular staining, fixation was proceeded as described in Chapter. 2.4.2.

In some experiments for staining of CXCR5, a 3-step sandwich stain was performed using 1:100 purified rat, anti-mouse CXCR5 antibody (BD Bioscience) in FACS buffer + 2% FBS + 2% mouse serum for 60min on ice. Cells were washed 2X and stained with 1:1000 secondary biotin-conjugated Affinipure Goat, anti-rat (Jackson Immunoresearch) 30min on ice, washed 2X and stained with a surface cocktail mix as above containing tertiary fluorophore-conjugated streptavidin. Alternatively, 1:50 CXCR5-biotin was used as primary antibody for 60min on ice, followed by surface cocktail containing fluorophore-labelled streptavidin. A complete list of antibodies used can be found in Table 2-2.

Table 2-2. List of antibodies used for flow cytometry staining

Specificity	**Clone**	**Fluorophore**	**Concentration**	**Supplier**	**Catalog #**	**LOT #**
B220	RA3-6B2	PerCPCY5.5	1:100	BioLegend	103236	B209575
B220	RA3-6B2	BV785	1:200	BioLegend	103246	B249689
B220	RA3-6B2	PerCPCY5.5	1:100	BioLegend	103236	B209575
Biotin-SP AffiniPure Fab Goat Anti-Rat IgG (H+L)		biotin	1:1000	Jackson Immunoresearch	112-067-003	---
CD11a/CD18	H155-78	PE/CY7	1:200	BioLegend	141012	B201657
CD138	281-2	BV605	1:400	BioLegend	142516	B232065
CD138	281-2	BV510	1:300	BioLegend	142521	B293283
CD19	1D3	APC-CY7	1:100	BioLegend	115530	B253924
CD19	1D3	APC-CY7	1:100	BioLegend	152406	B241294
CD24	M1/69	ef450	1:200	eBioscience	48-0242-80	2062723
CD25	PC61	FITC	1:100	BioLegend	102006	B152996
CD25	PC61	PE	1:200	BioLegend	102008	B191542
CD25	PC61.5	APC	1:200	eBioscience	17-0251-82	2154040
CD3	145-2C11	BV421	1:200	BioLegend	100335	B237072
CD4	GK1.5	BUV737	1:200	BD Biosciences	612761	0058133
CD4	RM4-5	BV605	1:400	BioLegend	100548	B244808

CD4	GK1.5	PE	1:300	BioLegend	100408	B217033
CD4	GK1.5	FITC	1:200	eBioscience	11-0041-85	E022407
CD44	IM7	AF700	1:200	eBioscience	56-0441-82	4329936
CD44	IM7	eF450	1:200	eBioscience	48-0441-82	E08502-1651
CD45.1	A20	PEDazzle	1:200	BioLegend	110748	B297341
CD45.1	A20	BV421	1:300	BioLegend	110732	B198258
CD45.1	A20	FITC	1:200	eBioscience	11-0453-81	4291919
CD45.2	104	APC/Fire750	1:200	BioLegend	109852	B277826
CD45.2	104	BV711	1:200	BioLegend	109847	B291921
CD45.2	104	BV785	1:200	BioLegend	109839	B253092
CD45.2	104	AF700	1:100	BioLegend	109822	B202497
CD45.2	104	BUV737	1:200	BD Biosciences	564880	7270780
CD8	53-6.7	BUV395	1:200	BD Biosciences	563786	9352024
CXCR5	2G8	purified	1:100	BD Biosciences	551961	6343832
CXCR5	2G8	biotin	1:50	BD Biosciences	551960	7068617
CXCR5	2G8	biotin	1:50	BD Biosciences	551960	7068617
CXCR5	2G8	Biotin	1:50	BD Biosciences	551960	4318735
FAS	Jo2	BV421	1:200	BD Biosciences	557653	6214949
FAS	Jo2	BV421	1:200	BD Biosciences	562633	7047594
FoxP3	FJK-16s	ef450	1:200	eBioscience	48-5773-82	1988692
GL7	GL7	APC	1:400	BioLegend	144606	B207559
GL7	GL7	AF647	1:400	BioLegend	144606	B259840
GL7	GL7	Alexa 647	1:500	BioLegend	144606	B259840
IgD	11-26C	PerCP-efluor710	1:200	eBioscience	46-5993-82	2061510
IgG1	X56	BB515	1:200	BD Biosciences	565104	8113631
IgG1	X56	APC	1:200	BD Biosciences	550874	7128657
IgG1	X56	BV421	1:200	BD Biosciences	742475	282615
IgM	R6-60.2	PECy7	1:100	BD Biosciences	552867	6083739
IgM	R6.60.2	BV711	1:100	BD Biosciences	564026	8120585
IgM	11/41	PerCP-efluor710	1:200	eBioscience	46-5993-82	2061510
IgM	MA-69	PECy7	1:100	BioLegend	408610	B317875
LD aqua		530	1:300	eBioscience		---
LD eF780		APC-eF780	1:2000	eBioscience		---

NP		PE	1:200	Biosearch technologies	N-5070-1	---
PD1	29F.1A12	BV605	1:200	BioLegend	135220	B306642
PD1	29F.1A12	BV785	1:200	BioLegend	135225	B311640
PD1	29F.1A12	BV605	1:200	BioLegend	135220	B306642
Streptavidin		APC	1:500	BD Biosciences	554067	
Streptavidin		PerCPcy5.5	1:100	eBioscience	45-4317-82	2198664
Streptavidin		AF647	1:200	BioLegend	405237	B304665
TCRvβ5.1, 5.2	MR9-4	PE	1:200	BioLegend	139503	B269714
TCRβ	H57-597	BV650	1:200	BD Biosciences	742483	0231553
TCRβ	H57-597	FITC	1:100	eBioscience	11-5961-85	4302124
CD62L	MEL-14	AF647	1:300	BioLegend	104421	B239264
Affinipure goat anti-human IgG		APC		Jackson Immunoresearch	109-135-098	146588
CD3	17A2	BV605	1:200	BioLegend	100237	B225359
CD4	H129-19	FITC	1:200	BioLegend	130308	B182345
CD8	53-6.7	PE	1:200	eBioscience	12-0081-82	E01037-1633
CD62L	MEL-14	BV421	1:200	BioLegend	104435	B263401
CD44	IM7	PECy7	1:200	BioLegend	103030	B171969
CD11a	2D7	PE	1:200	BD Pharmingen	553121	M063071
GL7 Antigen	GL7	PerCPCY5.5	1:200	Biolegend	144610	B306885
Fas	Jo2	BUV737	1:200	BD Biosciences	741763	0329586
Va2	B20.1	APC	1:200	eBioscience	17-5812-82	2142951
Vb5	MR9-4	PE	1:200	BD Biosciences	553190	8345781
ICOS	17G9	BV421	1:200	BD Biosciences	564070	7233528
ICOS	15F9	PECY5	1:200	Biolegend	107708	B241135

2.4.2 Intracellular staining for flow cytometry

For intracellular staining of transcription factors, including FoxP3, surface markers were stained as above, followed by IC staining using the FoxP3-staining kit (eBioscience). Firstly, cells were fix/permed with 100 μL intracellular fixation buffer, for 30min at RT in dark, washed 2X in 200 μL permeabilization buffer, and stained with intracellular antibodies in permeabilization buffer for 30-45 min on ice. Cells were then washed 2X in permeabilization

buffer and resuspended in FACS buffer for acquisition by flow. When staining cells with fluorescent protein expression, cells were fixed in 100 μL 4% *paraformaldehyde* (PFA) in PBS for 15 min, RT, in the dark, prior to continuing with FoxP3-staining kit as this was found to better preserve the fluorescent proteins.

2.4.3 Fluorescence activated cell sorting

For FACS of lymphocytes, cells were surface-stained as described in Chapter 2.4.1 and resuspended in FACS buffer. Cells were filtered through 40 μm filters prior to sort, and were sorted directly into R10 media. Cell purity was confirmed by running a fraction of the sorted samples on the sorter in acquisition mode. Cells were counted post sort and used for downstream applications.

2.4.4 Flow cytometer setup and data analysis

As this project was performed on 2 continents and 3 institutes, I ended up using multiple different types of instruments. The Cytoflex S, Attune, and LSR II cytometers are conventional cytometers that acquire the emission intensities in predefined fluorescent channels for each cell, and fluorescence is compensated as has been done traditionally. The Aurora spectral analyser acquires the complete fluorescent spectrum from each cell, and the complete spectrum is subsequently unmixed in the software to quantify the signal for each dye independently.

Beckman Coulter – Cytoflex Flow cytometer

For most experiments with simple staining panels a Cytoflex S with 4 lasers (405 nm, 488 nm, 561 nm, 640 nm) was used for acquisition with its high-throughput plate-reader. CytExpert (Beckman Coulter) software was used for acquisition.

Thermofisher – Attune NxT Flow cytometer

An Attune NxT with 4 lasers (405 nm, 488 nm, 561 nm, 640 nm) was used in a few experiments if Cytoflex S was fully booked or down for maintenance. Attune NxT software was used for acquisition.

BD – LSR II cytometer

At NIH, for early experiments during the PhD I used a 4 laser LSR II cytometer (405 nm, 488 nm, 561 nm, 640 nm) for acquisition. FACSDIVA (BD) was used for acquisition.

Cytek – Aurora Spectral analyser

For big multidimensional panels (>10 colours), an Aurora spectral analyser with 5 lasers (Ultraviolet, Violet, Blue, Green, Red) was used for acquisition. Acquisition was done with SpectroFlow software (Cytek).

Gating and data analysis

For analysis of acquired data, cells were gated on FSC-A/SSC-A, excluding doublets (FSC-A/FSC-A/FSC-W), and gating on live cells (negative for L/D marker), except for ICAM-1-binding assays, where LD staining was omitted as fixation was done as part of time-course; gating strategy is described in figure legends. All flow cytometry analysis was done in FlowJo 10.7.1 (Treestar).

2.5 *In vitro* assays

2.5.1 Flow cytometry-based ICAM-1-binding assay

Flow cytometry-based ICAM-1-binding was adapted from previous publications [219, 391, 392]. To prepare *soluble complexed ICAM-1* (scICAM-1), 40 μg/mL recombinant mouse ICAM-1-Fc (796-IC-050, R&D) and 1:6.25 dilution of APC-anti-human Fcγ specific IgG $F(ab')_2$ (109-135-098, Jackson Immunoresearch) were mixed in PBS and incubated on ice >30min. $1x10^6$ T cells per sample were coated with 1 μg/mL anti-CD3ε (2C11) in 1 mL FACS buffer for 30min on ice. Cells were washed and resuspended in 39.8 μL ice-cold ICAM-1-binding buffer (PBS + 0.5% BSA + 0.5 mM Mg^{2+} + 0.9 mM Ca^{2+}). 7.9 μL ice-cold scICAM-1 was added, and the cells were activated by crosslinking CD3ε with 12.5 μL anti-Armenian hamster IgG (5 μg/mL) and placing the samples at 37˚C. 10 μL (~$1.5x10^5$ cells) were taken per timepoint and fixed in 500 μL 4% PFA for 5min. Samples were washed in FACS buffer and if total T cells were used, samples were stained with anti-CD4 and anti-CD8 before acquisition with a Cytoflex S high throughput plate reader. For some experiments, T cells were stimulated

with CXCL10 (250 ng/mL), or SDF1α (250 ng/mL) at 37˚C. For VCAM-1-binding assays, VCAM-1-Fc (643-VM, R&D) was used as above to make soluble complexed VCAM-1 (scVCAM-1). *In vitro* activated T cells were rested for 2h without rhIL-2 before assay.

2.5.2 ELISA of serum

ELISA for total and antigen-specific Ig was performed as previously described [136]. Half area plates (Nunc) coated with αIg antibodies, 5 μg/mL NP_4-BSA or NP_{20}-BSA (Biosearch Technologies) in PBS (overnight, 4˚C) were prepared, washed 4X with PBS + 0.05% Tween 20, blocked with PBS + 1% BSA (2h, RT), and serial dilutions of serum in PBS + 1% BSA from NP-OVA immunized mice were applied (3h, RT), followed by 4X washes with PBS + 0.05% Tween 20 and by incubation with 1:500 alkaline phosphatase-conjugated Ig isotype-specific antibodies (Southern Biotech). Bound antibody was detected with pNPP substrate (Sigma-Aldrich) and absorbance was measured at 405 nm with a microplate reader (Molecular Devices). For total Ig ELISAs, wells were coated with 5 μg/mL anti-mouse Ig-isotype-specific antibodies (Southern Biotech) instead of NP-BSA. Values were calculated according to Ig standards (Southern Biotech) or reference serum from NP-OVA immunized mice.

2.5.3 CRISPR/Cas9 screen for regulators of ICAM-1-binding

I introduced CRISPR screening and pros and cons of types of screening in Chapter 1.5 and the libraries used, and in Chapter 3.4 I describe in detail how I curated the libraries. Further, cloning of the libraries is described in chapter 2.8.2. Here the ICAM-1-binding screen is described in detail.

For transduction of OT-I transgenic T cells with the PI3K-effector library activated ~200x10^6 OT-I x *Cas9* splenocytes with 10 nM SIINFEKL peptide as described in Chapter 2.3.2. 24h later I transduced ~50x10^6 OT-I x *Cas9* splenocytes (>20,000-fold coverage of library) as described in Chapter 2.3.3. Following transduction, cells were kept in fresh R10 media with 10 IU/mL rhIL2 and resuspended at 1x10^6 cells in fresh media with rhIL2 every day until day 5. On day 5, 85x10^6 GFP^+ T cells (>35,000-fold coverage of library) were sorted and seeded in fresh R10 with 10 IU/mL rhIL-2. Day 6, 100x10^6 GFP^+ T cells were rested for 2h without rhIL2

and coated with 1 μg/mL anti-CD3 (2C11) for 30min on ice. $26x10^6$ cells (>10,000-fold coverage of library) were pelleted for quantification of sgRNA frequencies going into the assay. The cells were then mixed with ice-cold scICAM-1 (prepared as described above), and incubated 37˚C for 2min with 5 μg/mL crosslinking anti-Armenian hamster IgG, followed by fixation of the cells in 2% PFA at RT, 5min. Cells were washed 3X, and sorted ~$19x10^6$ scICAM-1^{neg} (no ICAM-1-binding) and ~$12x10^6$ scICAM-1^{pos} (ICAM-1-binding) cells. Cells were resuspended in 100 μL PBS + 200 mM NaCl + 2 mg/mL of proteinase K and incubated at 47˚C overnight to reverse crosslinking of DNA. Genomic DNA was subsequently purified by DNeasy kit (Qiagen) from scICAM-1^-, scICAM-1^+, and day 6 transduced cells, and used for PCR amplification of ~600 bp amplicons surrounding the sgRNA sequence by guide_ID primers. Amplicons were further PCR amplified adding indexing primers to the samples for multiplex next-gen sequencing. Amplicons were purified by E-gel (Thermo) and quantified by Qubit (Thermo). Sequencing was then performed on Illumina NextSeq 500 with the 500/550 High Output V2 kit (75 cycles) (FC-404-2005, Illumina) according to manufacturer's instructions. Coverage for each sgRNA was ≥2000X for each sample after the sorts and ≥1000X sequencing depth for each sample.

sgRNA counts were obtained from FASTQ files and normalised to $2.5x10^6$ using a custom script as previously described [393, 394]. L2FC between scICAM-1^{neg} and scICAM-1^{pos} samples were calculated for each experiment, then averaged across experiments and waterfall plot of L2FC with SEM was prepared using a custom script. False-discovery rates were calculated by MAGeCK v0.5.9.3 [368, 395] using non-targeting sgRNAs for normalisation, and a volcano plot was prepared using a custom script I adapted from MAGeCKflute. The single sgRNA effects were also prepared using MAGeCKflute.

2.5.4 Quantitative Reverse Transcription PCR

FACS sorted $CD4^+$ T cells and $CD8^+$ T cells were activated by plating on anti-CD3 antibody-coated plates (1 μg/mL, 2C11, Biolegend) with 2 μg/mL of anti-CD28 antibody (37.51, Biolegend) in biological triplicates. Cell pellets were lysed in Tri Reagent and frozen at day 0-7. RNA was purified by RNeasy-Trizol purification (Qiagen), and RNA concentration was quantified by Nanodrop. Reverse-transcribed cDNA was synthesized from 200 ng of RNA with

Superscript IV (Thermofisher) using random hexamers following manufacturer's instructions. Quantitative RT-PCR was performed in technical triplicates according to manufacturer's instructions with PowerUp qPCR SYBR-green mix using HPRT and *Rasa3* qPCR primers (see Appendix 7.2) on a Viia 7 Real-Time PCR machine (Thermofisher). *Rasa3* transcripts were quantified by the ΔΔCt method, using HPRT as internal housekeeping gene normalised to day 0 for $CD4^+$ and $CD8^+$ T cells, respectively. $2^{-\Delta\Delta Ct}$ calculated as follows: $2^{-\Delta\Delta Ct} = 2^{-(Ct_{Rasa3,DayX} - Ct_{Hprt,DayX}) - (Ct_{Rasa3,Day0} - Ct_{Hprt,Day0})}$.

2.6 Biochemistry

2.6.1 PCR of deleted exons

To evaluate KO of *Rasa3*, $CD19^+CD4^-CD8^-$ B cells, $CD4^+CD8^-CD19^-$ $CD4^+$ T cells, and $CD4^-CD8^+CD19^-$ $CD8^+$ T cells were stained and sorted from *Rasa3*$^{fl/fl}$ (control) and *Rasa3*$^{fl/fl}$ x *Cd4*^{Cre} as described in Chapter 2.4, and genomic DNA was purified by DNeasy genomic DNA purification kit (Qiagen). Primers were designed with primers flanking the floxed exon (Fwd: Rasa3flox_Fwd, Rev: Rasa3flox_Rev, see oligos in Appendix 7.2). For PCR amplification, OneTaq polymerase (NEB) was used and amplified as shown in Table 2-3 and imaged on a 1.5% agarose gel using a GelDoc (Syngene).

Table 2-3. PCR amplification of Rasa3-flox region

	Denaturation	95	10 min
Cycle x35	Denaturation	95	30 sec
	Anneal	53	60 sec
	Extend	72	90 sec
	Extend	72	10 min
	Hold	4	

2.6.2 Western Blots

For *Western blot* (WB) analysis, $1x10^6$ cells were resuspended in 25 μL ice-cold 1X RIPA lysis buffer (150 mM NaCl, 1% NP40, 0.5% sodium deoxycholate, 0.1% SDS, 25 mM Tris pH 7.4)

containing protease inhibitors (cOmplete ULTRA tablets, Roche) and lysed on ice for 30min. Following lysis, samples were centrifugated at max speed, 4˚C to pellet lipids, protein aggregates, and DNA and supernatant was transferred to new tubes. Lysates were then mixed with 4X NuPage LDS sample buffer (Life Technologies) containing 10% β-mercaptoethanol and boiled at 70˚C for 10min and frozen at -80˚C until preparing western blots or loaded straight away.

For WB analysis, samples were loaded on a 4-12% Bolt Bis-Tris minigel (Invitrogen) and run at 90V for 120min (or until sample front reached bottom of gel). Protein was then transferred by wet transfer to an activated PVDF membrane (Immobilon-FL, Milipore) by running for 1h at 40V on ice. Transfer was assessed by Ponceau Red staining of the membrane and washed to get rid of the stain before drying for 1h. Membrane was then activated with methanol, and blocked for 1h in Intercept Blocking buffer (Licor), shaking at RT. The membrane was then stained with primary antibody in Intercept Blocking buffer + 0.2% Tween 20 on a shaker overnight at 4˚C. RAP1A/B (4938, Cell Signaling), Anti-RASA3 Ab (ab153846, Abcam, 1:1000), anti-pERK (4370, Cell Signaling, 1:1000), anti-ERK (9107, Cell Signaling, 1:1000). Next day, blots were washed 4x5min in TBST and incubated with secondary anti-mouse or anti-rabbit (IRDye800CW, or IRDye680RD, Licor) at 1:10000 in Intercept Blocking buffer + 0.2% Tween 20 + 0.01% SDS for 1h at RT. Membranes were then washed 4x5min in TBST, dried, and imaged on an Odyssey CLx (Licor).

2.6.3 Rap1 activation assay

Preparation of RalGDSRBD-GST protein

RAP1-GTP pulldowns were performed as previously described [219]. pGEX-RalGDS-RBD-GST plasmid was overexpressed in Rosetta-pLys bacteria and production of RalGDS-RBD-GST was induced with 0.1 mM IPTG in 2X-YT broth to OD_{600}=0.7, lysed in MTPBS buffer (150 mM NaCI, 16 mM Na_2HPO_4, 4 mM NaH_2PO_4, pH 7.4) + 100 μg/mL lysozyme + DNase (3U) + 0.1% Triton X100 + protease inhibitor cocktail (Sigma) + 1 mM PMSF and purified by glutathione-agarose beads (Sigma). Lysates were incubated with 10 mL glutathione-agarose beads (Thermofisher) for 2h, washed 3X with ice-cold MTPBS+0.1% Triton X100 (1000G, 4min), and protein was eluted with 4X 7.5 mL MTPBS + 10 mM reduced glutathione. Eluted

RalGDS-RBD-GST protein was upconcentrated in Amicon Ultra 15 mL columns and eluted by size exclusion chromatography (see Figure 2-2) followed by further upconcentration with Amicon Ultra 15 mL columns, snapfrozen, and stored in PBS + 150 mM NaCl at -80˚C for later use.

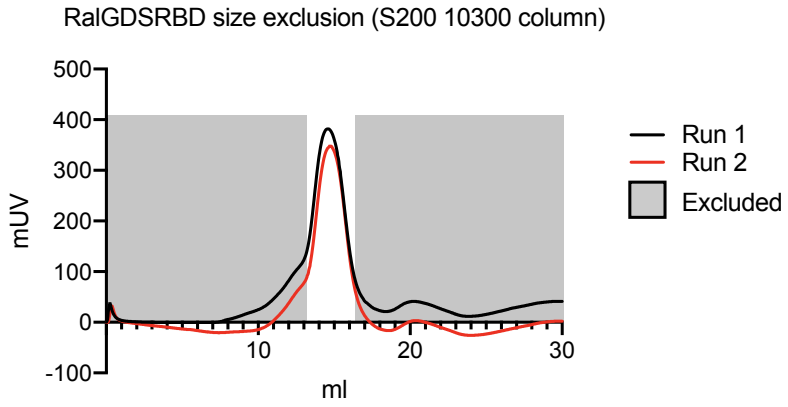

Figure 2-2. Size exclusion chromatography of overexpressed RalGDSRBD-GST protein. S200 10300 column was precalibrated with standards and protein eluted around 15ml was 40 kDa as expected for RalGDSRBD-GST.

RAP1-GTP pulldown assay

A single cell suspension of $20x10^6$ isolated total T cells/timepoint were isolated from WT and *Cd4*^{Cre} x *Rasa3*$^{fl/fl}$ mice, and T cells resuspended in 10 mL were coated with 10 µg/mL of anti-CD3 (2C11, Biolegend) on ice, 30min. Cells were washed twice and resuspended in RPMI + 0.5% FBS + 10 mM HEPES, and $20x10^6$ cells per timepoint were preheated for 2min at 37˚C, before crosslinking of CD3 with 10 µg/mL anti-hamster IgG (127-005-099, Jackson Immunoresearch). Following crosslinking, cells were spun down at 6000xRPM, 4 ˚C, 15Sec and lysed in ice-cold lysis buffer (20 mM Tris pH 7.5, 150 mM NaCl, 5 mM $MgCl_2$, 1% NP40, 5 mM β-glycerophosphate, 10% glycerol, 1 mM DTT, protease inhibitor cocktail (Sigma)) containing 10 µg RalGDS-RBD-GST per sample. Lysates were aspirated through 25G needles 5X, and incubated on ice for 5min, followed by centrifugation at max speed, 5min, 4˚C. RAP1-GTP pulldown lysates were then incubated with 10 µL Glutathione Sepharose 4B beads (17-0756-01, GE Healthcare) for 45min at 4˚C, washed 3X in ice-cold lysis buffer, and boiled in 1X sample buffer. Samples were separated on 4-12% polyacrylamide gels (Bolt Bis-Tris mini, Thermofisher) and immunoblots of pulldown lysates (and total lysates from before pulldown)

were transferred to PVDF membranes (Immobilon-FL, Millipore) and incubated with anti-RAP1A/B antibody (4938, Cell Signaling), followed by anti-Rabbit secondary (IRDye 800 CW, Licor), and imaged using Odyssey CLx (Licor) as described in Chapter 2.6.1.

2.7 Imaging

2.7.1 Imaging of subcellular localisation

These experiments were performed by Julie H. Thomsen under my supervision.

Coverslips were cleaned with ethanol for 5min and washed with PBS before coating with anti-CD3ε (10 μg/mL, Clone 2C11), and/or ICAM-1-Fc (2 μg/mL, #796-IC, R&Dsystems) in PBS or 0.01% poly-L-lysine in dH_2O overnight at 4˚C followed by 2X wash with PBS and blocking with R10 media for >10min. $CD4^+$ T cells transduced with desired constructs were rested for 2h in reduced T cell medium (RPMI + 0.5% HI FBS + 2 mM L-glutamine + 1% Pen/Strep + 0.5 mM β-ME). Where Idelalisib was used, 1 μM Idelalisib (Selleckchem, S2226) (or DMSO for controls) was added during the second hour of resting. $0.4x10^6$ cells were seeded on CD3 and ICAM-1-coated coverslips, and $0.8x10^6$ cells were seeded on poly-L-lysine coated coverslips for 15min at 37˚C followed by fixation with 4% PFA at RT 15min. After fixation, samples were quenched with 15 mM glycine for 2x5min, permeabilized with 0.1% saponin for 10min, followed by blocking 15min in blocking buffer (PBS + 1% BSA + 0.01% saponin). Slides were incubated with 1:1000 primary anti-GFP antibody (A86774, Antibodies.com) in blocking buffer for 1h. Coverslips were washed 3x3min in blocking buffer and mounted on glass slides using 7 μL Fluoromount-G (SouthernBiotech) with 5 μg/mL DAPI.

Images were acquired using a Zeiss AxioObserver.Z1 inverted microscope (Zeiss) with a LSM 700 confocal laser scanning system equipped with two photomultiplier tubes and a beam splitter (DBS1) using Zen acquisition software (Zeiss 2010 B SP1). Pinhole size was set to 1 AU for all lasers and all images were acquired with a Plan-Apochromat 63x/1.40 oil immersion objective using identical laser settings within an experiment. Analysis of PM localization was done in Fiji ImageJ 1.8.0 (NIH) by quantifying intensity in 3 distinct membrane regions and 3

distinct cytosol regions and dividing the mean PM intensity with the mean cytosol intensity for each analysed cell.

2.7.2 Imaging of T cell conjugates

These experiments were performed by Julie H. Thomsen under my supervision.

MACS purified B cells (EasySep, pan-B cell isolation kit, StemCell) were resuspended in B cell medium (RPMI + 10% HI FBS + 1% Pen/Strep + 0.05 mM β-ME) and were activated with 10 μg/mL lipopolysaccharide (LPS) (Sigma-Aldrich) for 24h. MACS-purified naïve OT-II $CD4^+$ T cells were rested for 2h in reduced T cell medium before conjugate formation. For experiments with inhibitors 1 μM Idelalisib or similar amount of DMSO were included for 1h. T cells were prepared at $2x10^6$ cells/mL. Meanwhile, activated B cells were washed with PBS and stained with 1 μM CellTracker™ dye in RPMI. B cells were incubated with the CellTracker dye for 30min at 37ºC, and washed twice in B cell medium. After the second wash, B cells were pulsed with 10 μM $OVA_{323-339}$ for 1h at 37ºC. Following peptide-pulsation, B cells were washed twice in B cell medium before they were resuspended in reduced T cell medium at $2x10^6$ cells/mL. For cell seeding, T and B cells were mixed 1:1 and a total of $1x10^6$ cells were seeded per poly-L-lysine coated coverslip. To allow better conjugate formation, cell seeded coverslips were shortly spun down (300g, 1 min, 37ºC) followed by incubation. After 30min incubation, mixed cells were fixed with 4% PFA for 15 min at RT and stained with antibodies as described in Chapter 2.7.1.

2.7.3 Ce3D imaging of LNs

These imaging experiments were performed by Dr. Tibor Veres and Dr. Dominic Goleç, and analysed by Edward Schrom and me.

LNs were stained and optically cleared as previously described [396]. Volume staining was performed using the following antibodies/dilutions: B220-eFluor 615 (ThermoFisher, clone RA3-6B2) 1:80; CD4-Alexa Fluor 488 (BioLegend, clone RM4-5) 1:80, PD-1-BV421 (BioLegend, clone RMP1-30) 1:80, FoxP3-eFluor 570 (ThermoFisher, clone FJK-16s) 1:50, Bcl6-Alexa Fluor 647 (BD Biosciences, clone K112-91) 1:50; CD35-BV510 (BD Biosciences, clone 8C12) 1:300. Confocal imaging was performed on an inverted Leica SP8 microscope

using a 40x 1.3 NA oil immersion objective. 3D image stacks were analysed using Imaris 9.2.1 (Bitplane). GC surfaces were delineated as $BCL6^+$ volumes at a smoothing resolution of 10μm. Within GCs, T cells were delineated as $CD4^+$ volumes at a smoothing resolution of 0.569μm. Among GC-T cells, GC-T_{FH} cells were identified as $BCL6^+$ $PD1^+$ T cells. To determine the relevant $BCL6^+$ and $PD1^+$ cutoffs, three separate $0.333*10^6$ μm^3 control volumes were sampled from the B cell follicle (not intersecting any GCs) in each image, T cells were segmented as $CD4^+$ volumes, and the 95^{th} – 99^{th} percentiles of BCL6 and PD1 expression among these non-GC-T cells were calculated. From these delineations of GC regions and GC-T_{FH} cells, the volume of each GC and the density of GC-T_{FH} cells were calculated.

2.8 Cloning of vectors

Numerous plasmids were cloned throughout the PhD. This section details how I constructed these vectors, and references primers used (sequences can be found in Appendix 7.2). All cloning was confirmed by Sanger sequencing, molecular biology reagents for cloning were from NEB unless otherwise stated, and cloning strategy was designed using Snapgene V4.2 and NEBbuilder.

2.8.1 Cloning of gRNA vectors

Cloning of MRIG backbone

For retroviral delivery of sgRNAs I used an optimised retroviral backbone, MRIG [158, 379], containing a mU6-sgRNA fragment and SV40-spCas9 fragment from pQCiG2 subcloned into MIGR1 (Addgene 27490) upstream of IRES-GFP which was cloned by Dr. Bonnie Huang. I further prepared a MRIA vector (with Ametrine instead of GFP) by PCR amplifying the Ametrine ORF from pAmetrine-N1 (Addgene 54505), and subcloning by traditional restriction digestion into MRIG using NcoI and SalI sites.

Subcloning of gRNA into MRIG backbone

Individually cloned oligos were designed with a partial mU6 and TracrRNA sequence at 5' and 3' ends respectively. Oligos were designed using Benchling as described in [379] or selected

from the published Brie library [368]. Single oligos were PCR amplified (primer: guide_amp_Fwd and guide_amp_Rev) and purified using qiaQuick PCR kit (Qiagen). BamHI-HF and MfeI-HF digested, shrimp alkaline phosphatase-treated MRIG was gel purified and ligated with amplicons from above. Ligation of sgRNA oligos was performed by traditional restriction ligation and transformed into 20 µL HB101 competent bacteria (Zymo).

2.8.2 Cloning of gRNA libraries and plasmids

All sgRNAs used in the thesis can be found on
https://drive.google.com/file/d/19mibsjHj4B4z4odbZcdZxh0iAWxW7o1B/view?usp=sharing

PIP_3-binding proteins library

Oligos for CRISPR/Cas9-mediated KO targeting genes encoding PIP_3-binding and PH-domain containing proteins (described in chapter 3.4.1) were either designed using Benchling [379] or selected from the Brie Library [368]. The sgRNAs per gene were included in the library as well as positive and negative controls for ICAM-1-binding and 30 non-targeting sgRNAs from the Brie library adding up to a total of 2298 sgRNAs [368].

For the *PIP_3-binding proteins* (PBP) library oligos were ordered as individual oligos (IDT): 5'-ggagaaaagccttgtttg-N20-gttttagagctaggatcctagc (N20 is the sgRNA sequence) and combined at equimolar ratios. Pooled oligos were PCR amplified in duplicate reactions with PCR program in Table 2-4 (primer: guide_amp_Fwd and guide_amp_Rev) using Herculase II polymerase (Agilent) and purified using QiaQuick PCR kit (Qiagen).

Table 2-4. PCR program for amplification of sgRNA libraries

	Step	**Temp**	**Time**
	Denaturation	95	2min
Cycle x10	Denaturation	95	20sec
	Anneal	56	30sec
	Extend	72	60sec
	Extend	72	10min
	Hold	4	

BamHI-HF and MfeI-HF digested, shrimp alkaline phosphatase-treated MRIG was gel purified and ligated with amplicons from above. Ligation of pooled amplicons was performed by HiFi assembly at 1:5 backbone:insert molar ratio and 1 µL of a 1:5 dilution of the HiFi assembly was electroporated into 20 µL Stbl4 bacteria (Thermo), in quadruplicates, with a Genepulser II using these parameters: 1.2 kV, 25 uF, 200 ohm, 0.1 cm cuvette, time constant T = RC = 200 ohm x 25 uF = 5000 us = 5 ms. Bacteria were shaken in SOC media for 1.5h at 37˚C to recover and plated on bioassay plates (Nunc) prepared with freshly prepared LB/Agar-ampicillin and incubated at 30˚C for 24h. 319000 colonies were counted ensuring a representation of ~140 colonies/sgRNA in the PBP library. Simulations show that this gives a >99.5% chance of including all sgRNAs in the library (Figure 2-3a). Colonies were scraped of the plates and plasmid was purified with EndoFree Maxiprep kits (Qiagen).

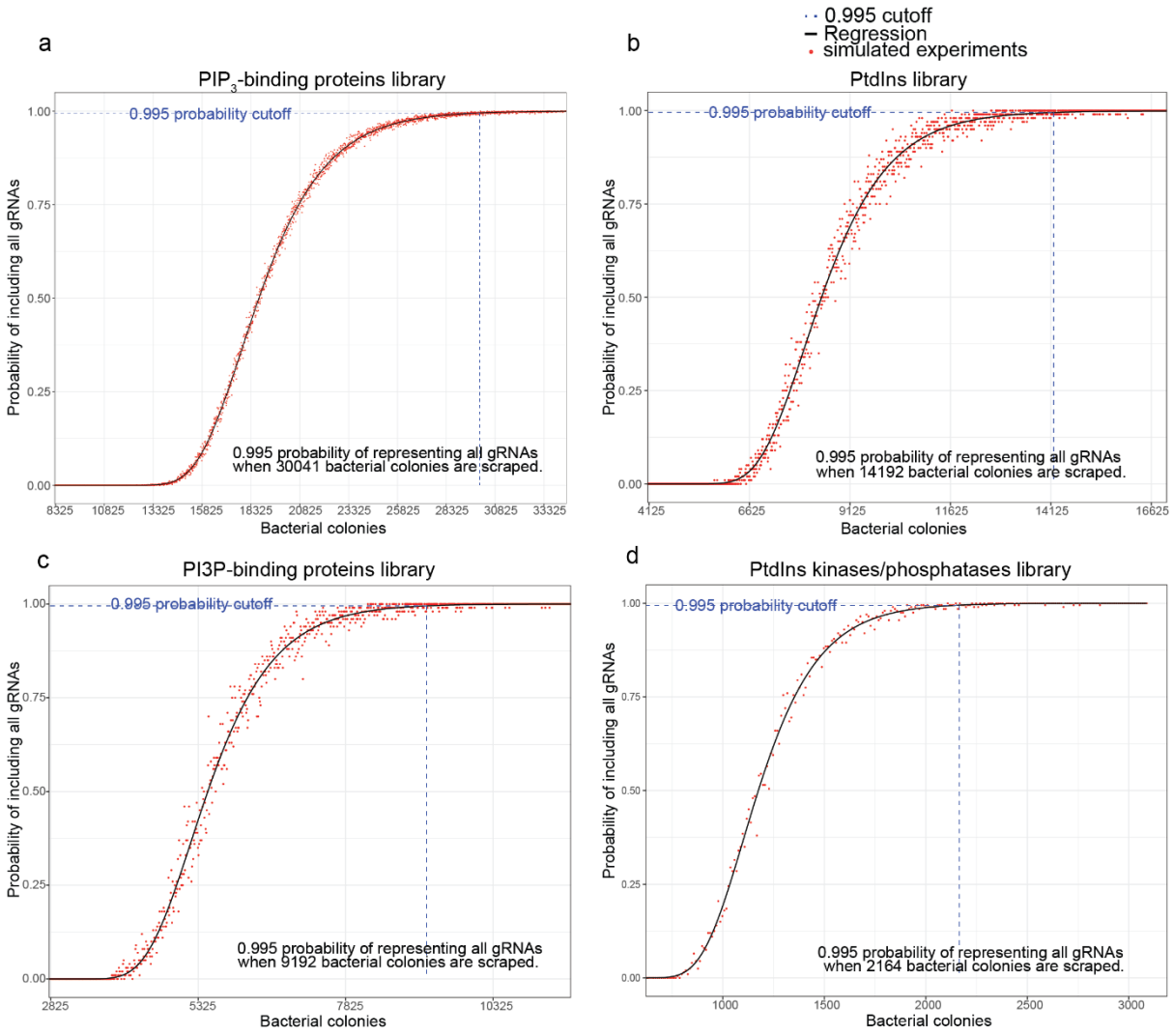

Figure 2-3. Simulation of probability of including all sgRNAs in PBP library. **a-d,** Simulations were performed for the PIP_3-binding proteins library (**a**), the PI-binding proteins library (**b**), the PI(3)P-binding proteins library (**c**), and the PI kinase/phosphatase library (**d**). Simulations were done with a custom-made R script and show the number of colonies required to get 0.995 probability (blue line) assuming colonies are picked randomly.

Cloning of total phospholipid-binding protein-targeting libraries

Oligos for CRISPR/Cas9-mediated KO targeting genes encoding other phospholipid-binding containing proteins (described in Chapter 3.4) were designed and cloned as described for the PBP library above, however minor alterations were applied for these libraries as described here:

Firstly, I cloned 3 libraries individually;

- 1 library containing sgRNAs targeting genes encoding PI(3)P-binding proteins identified in the literature, and proteins containing PX or FYVE domains (that have propensity to bind PI3P). 780 sgRNAs targeting 195 genes
- 1 library targeting genes encoding proteins containing other PtdIns-binding domains; BAR domains, A/ENTH domains, C2 domains, PDZ domains, or Tubby domains. 1140 sgRNAs targeting 285 genes
- 1 library targeting all PI kinases and phosphatases + 30 non-targeting sgRNA. 206 sgRNAs targeting 44 genes

Secondly, the gRNAs were ordered as a pool of oligos from oligo-arrays (TwistBioscience), and lastly, the oligos contained longer 5' and 3' overhangs for HiFi: 5'caattggagaaaagccttgtttg-N20-gttttagagctaggatcctagcaagtt-3'.

The resulting libraries had PI3P library: 39435 colonies, PI library: 28680 colonies, PI kinases/phosphatases: 16133 colonies, which for each library gives >99.5% chance of including all sgRNAs at least once (Figure 2-3b-d). These libraries were otherwise prepared as described for PBP libraries above, and purified using Endofree Megaprep kits (Qiagen).

2.8.3 Cloning of Rasa3-expression constructs

mRuby and mRuby-hRasa3 retroviral constructs

To construct an mRuby retroviral construct (murine mRuby retroviral 1; MRR1), I inserted *mRuby* (EcoRI-PacI) from pmRuby-N1 (Addgene 54581) by amplifying mRuby using mRuby_fwd and mRuby_rev followed by HiFi assembly (NEB) into linearised (*EcoRI*+*PacI*) MIGR1 backbone (Addgene 27490).

Human *Rasa3* (Addgene 70516) was subsequently PCR amplified (PCR primers: Rasa3_Fwd_mRuby+Rasa3_Rev_mRuby) to add a flexible nonrecombinant linker [397] and overhangs for HiFi assembly, and inserted into linearised (*PacI*+*SalI*) MRR1 by HiFi assembly (NEB) to make a mRuby-hRasa3 construct.

MGR1 and MGR1-hRasa3-GFP retroviral constructs

To generate a construct with a RASA3-GFP fusion protein I inserted a fresh Kozak sequence (kozak_fragment) by HiFi assembly of linearised (*EcoRI*+*NcoI*) MIGR1 to generate a MIGR1 backbone without IRES (MGR1). I then inserted linearised hRasa3 (PCR primers: hRasa3-GFP_Fwd and hRasa3-GFP_Rev) into linearised MGR1 (PCR primers: MGR1_Fwd+MGR1_Rev) by HiFi assembly.

2.8.4 Mutagenesis of Rasa3-expression constructs

$RASA3^{PHmut}$ (primer: hRasa3_K599Q_K600Q_R601Q_mut) and $RASA3^{R371Q}$ (primer: hRasa3_R371Q_mut) variants were generated by site-directed mutagenesis (QuikChange II XL, Agilent).

2.9 Data analysis and statistics

I analysed most data in GraphPad Prism or R. For flow cytometry data, I tested groups for normality by a D'Agostino & Pearson normality test for n>8, and Shapiro-Wilk normality test for n<8, as well as evaluated distribution by QQ plots. If any of the compared data did not clearly appear normally-distributed, I used Mann-Whitney U-test when comparing two groups, and corrected for multiple comparisons within an experiment by Holm-Šídák's multiple comparisons correction and One-way ANOVA with Holm-Šídák's multiple comparisons when comparing multiple groups. If two compared groups of data both appeared parametric, an

unpaired two-tailed Student's *t* test was used. For ICAM-1-binding assays, I used two-way ANOVA with Holm-Šídák's multiple comparisons to compare ICAM-1-binding of samples in a timepoint to the control group. I performed CRISPR/Cas9 data analysis with MaGeCK and custom scripts and *P* values are false discovery rates corrected by the Benjamini and Hochberg method using MaGeCK [395, 398]. For adoptive transfers, I used One-sample *t* tests to compare each sample to 1 (equal migration of KO and WT cells to tissue). I considered *P* values $P < 0.05$ statistically significant and marked $P<0.05$: *; $P\leq0.01$: **; $P\leq0.001$: ***, $P\leq0.0001$: ****, as well as showed exact *P* values between 0.1-0.05. For linear regression of GC:T_{FH} cell numbers, I performed a global linear regression, and the global linear model was compared by an Akaike Information Criterion Comparison to individual regression models for the individual sample groups. Ce3D images were analysed by Dr. Edward Schrom and me.

2.10 Oligo sequences

Primer sequences for cloning and qRT-PCR primers are listed in Appendix 7.2. All sgRNAs used in the thesis can be found on

https://drive.google.com/file/d/19mibsjHj4B4z4odbZcdZxh0iAWxW7o1B/view?usp=sharing

Chapter 3

Identifying novel PI3K effector proteins involved in LFA-1 regulation by CRISPR/Cas9-mediated mutagenesis

3. Identifying novel PI3K effector proteins involved in LFA-1 regulation by CRISPR/Cas9-mediated mutagenesis

3.1 Introduction

I initially sought to adapt CRISPR/Cas9 techniques optimised by Dr. Huang in the laboratory of Dr. Schwartzberg at NIH to screen for genes downstream of PI3K involved in regulating LFA-1. Based on work by Dr. Garcon in the Okkenhaug laboratory we had evidence suggesting that LFA-1 was regulated in part by PI3K effector proteins independently of AKT, and that this at least was partially dependent on regulation of RAP1 activity. Dr. Huang had optimised CRISPR/Cas9-mediated KO in primary mouse $CD4^+$ T cells stimulated with anti-CD3/CD28 using an optimised retroviral plasmid based on pQCIG2 and MIGR1 called MRIG (see Chapter 2.8.1 for cloning) before I commenced the PhD.

In this chapter I present optimisation of transduction of $CD8^+$ T cells activated with SIINFEKL peptide, and repeats of findings from Garcon *et al*. showing that PI3Kδ is required for optimal LFA-1 regulation. I further present data on combining an ICAM-1-binding assays with CRISPR/Cas9 mutagenesis to investigate the roles of genes in LFA-1 regulation. As I wanted to investigate PI3K-mediated regulation of LFA-1, I here present the CRISPR sgRNA libraries I designed targeting all proteins with potential to be downstream of PI3K. Lastly, I present data from a CRISPR screen using the described library investigating the role of these PI3K effector proteins in LFA-1 regulation as well as validation of the findings from the CRISPR screen with individually cloned sgRNAs.

3.2 CRISPR/Cas9-mediated KO in SIINFEKL-pulsed OT-I CD8$^+$ T cells

To conduct CRISPR/Cas9 KO in peptide-stimulated TCR-transgenic T cells, I sought to optimise this process. Timing of retroviral transductions is known to be crucial for transduction efficacy [373, 399]. In the literature (and based on experience from Dr. Huang) anti-CD3/CD28 stimulation 24h prior to first transduction is optimal [373, 379]. As stimulation with peptide is possibly not as potent, and perhaps slower than CD3/CD28 stimulation due to the fact that the peptide has to be picked up and presented from APCs from the spleen, I sought out to determine the optimal timepoints for my transduction. The devised protocol included peptide-stimulation by addition of SIINFEKL peptide directly to single cell suspensions of OT-I transgenic *Cas9*-expressing (OT-I x *Cas9*$^{+/+}$) splenocytes followed by spinfection (viral transduction by centrifugation) at two subsequent timepoints followed by culturing the T cells in rhIL2-containing media until day 6 where the assay would be conducted (Figure 3-1a). I compared spinfection at 24+48h with spinfection at 40+60h post activation, and found that the T cells transduced 24+48h post activation had a greater loss of the targeted p110δ protein at day 6 compared to transductions at 40+60h with all three tested sgRNAs (Figure 3-1b). Also transductions at 24+48h gave 70-90% transduced cells as evident by GFP expression in cells by day 6 (Figure 3-1c).

For the downstream assay I intended to use for assaying LFA-1 activation, a requirement is fixation of the cells to stop the reaction before acquisition by flow cytometry. To ensure the fixation did not decrease my ability to pick up the GFP signal in the transduced cells by flow cytometry, I transduced cells at 24/48h with *Itgal*-targeting sgRNAs (encoding CD11a/LFA-1 subunit), stained LFA-1 at day 6, and compared 4% PFA fixed cells with non-fixed cells. It was clear that the majority of GFP$^+$ sgRNA-transduced cells had lost LFA-1, both in fixed and non-fixed samples (Figure 3-1c). GFP signal is slightly decreased following fixation, but the same percentage of transduced cells can be picked up by flow cytometry without skewing the results, suggesting that PFA fixation does not negatively affect the downstream results. Notably, The *Itgal* sgRNA-transduced GFP$^-$ population has a fraction of cells that seem to lose LFA-1 expression (Figure 3-1c). This is possibly due to earlier expression of the retroviral

construct in some cells (resulting in Cas9-mediated cutting), but subsequent epigenetic suppression of expression. This result suggests it is not ideal to compare results from GFP$^+$ cells with internal GFP$^-$ T cells, and therefore preferred to compare with cells transduced with a *non-targeting* (NT) sgRNA.

To allow for double KO of two targeted genes, I cloned a MRIA vector (MRIG with Ametrine instead of GFP) and optimised transduction with a *Cd45*-targeting sgRNA in the MRIG vector and an *Itgal*-targeting sgRNA in the MRIA vector. ~50 % of Ametrine/GFP double positive cells lost both targeted proteins, indicating that this technique could be used to KO two genes simultaneously in future experiments (Figure 3-1d).

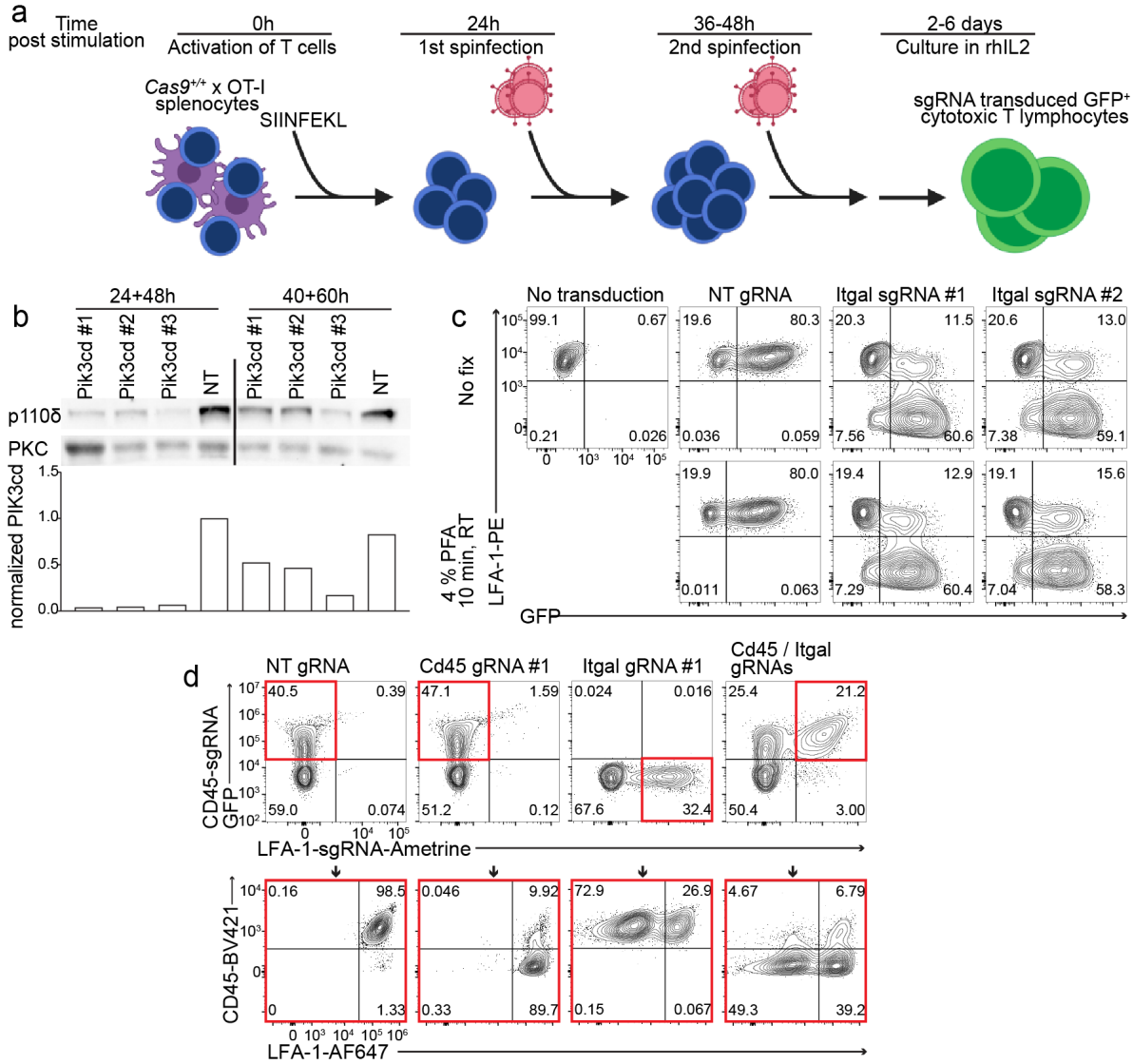

Figure 3-1. Optimisation of CRISPR/Cas9 KO in CD8⁺ T cells. **a,** Diagram of transduction protocol for KO of genes in SIINFEKL-activated OT-I x *Cas9*$^{+/+}$ CD8⁺ T cells. **b**, Western blot of Day 6 CTLs after activation with SIINFEKL followed by transductions at 24+48h (left) or 40+60h (right) after activation with indicated sgRNAs (NT: non targeting). Graphs show p110δ levels normalised to PKC loading control and the 24+48h transduced NT control. **c**, OT-I x *Cas9*$^{+/+}$ T cells transduced with the indicated sgRNAs with or without 4% PFA fixation followed by flow cytometry analysis of *Itgal* (LFA-1) and GFP. Gated on singlets, live, CD8. **d**, Double transductions of OT-I x *Cas9*$^{+/+}$ T cells with *Cd45* sgRNA in MRIG vector (GFP) and *Itgal* (LFA-1) sgRNA in MRIA vector (Ametrine). **a**-**d**, Experiments were performed once, 1 replicate.

Together these findings allowed me to go ahead with CRISPR/Cas9-mediated KO in either peptide-stimulated T cells or aCD3/CD28-stimulated T cells. The exact optimised protocols for CRISPR/Cas9 KO were published with Dr. Huang and Dr. Schwartzberg [379].

3.3 PI3Kδ regulates LFA-1-mediated ICAM-1-binding

To investigate LFA-1 activity in a high throughput manner I opted for a flow cytometry-based ICAM-1-binding assay previously used in the literature and in the Okkenhaug laboratory (Figure 3-2a) [219, 391, 392]. The assay relies on stimulated T cells binding soluble complexed recombinant ICAM-1 which has been fluorescently labelled (scICAM-1).

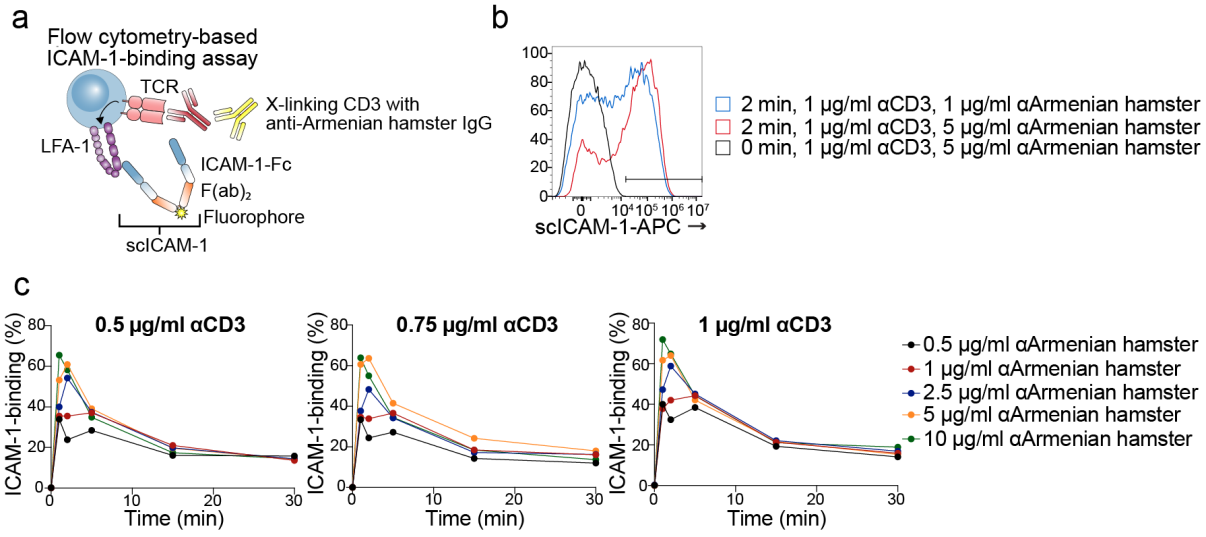

Figure 3-2. Flow cytometry-based ICAM-1-binding assay. **a**, Diagram of flow cytometry-based ICAM-1-binding assay used throughout thesis; see chapter 2.5.1 for protocol. **b-c**, Optimisation of ICAM-1-binding assay with varying concentrations of αCD3 or anti-Armenian hamster IgG for crosslinking of CD3 of SIINFEKL-stimulated

OT-I T cells after 6 days in culture. Histograms of the 2min peak timepoint for 1 μg/mL αCD3 + 1 or 5 μg/mL anti-Armenian Hamster IgG are shown (**b**) as well as time course graphs quantifying the ICAM-1-positive T cells (**c**). **b-c**, Experiments were performed once, 1 replicate per sample.

To ensure I would to able to identify both positive and negative regulators of LFA-1 activation, I wanted to optimise the assay to ensure I was activating the cells sufficiently without overstimulating the cells. I therefore titrated the concentrations of anti-CD3 and anti-Armenian hamster IgG used for crosslinking of CD3 on the T cells in presence of the fluorescently labelled scICAM-1 (Figure 3-2b-c). I found that several concentrations of anti-CD3 could activate LFA-1 (Figure 3-2c), and determined that a concentration of 1 μg/mL anti-CD3 with 5 μg/mL anti-Armenian hamster IgG ensured good activation of LFA-1 but still allowed me to pick up treatments resulting in increases in ICAM-1-binding (Figure 3-2b-c). I further managed to optimised the assay to work with 12 samples simultaneously using a multi-channel pipettor, and determined that for future gating I would set my ICAM-1-binding gate based on the 0-min timepoint to ensure reproducibility (Figure 3-2b).

To investigate the role of PI3K activity in LFA-1 regulation, and confirm previous findings showing that PI3K inactivation (either by inhibition or kinase dead mutant *Pik3cd*^{D910A}) decreases ICAM-1-binding [219], I used my optimised ICAM-1-binding assay to assay ICAM-1-binding of T cells from *Pik3cd*^{D910A} and *Pik3cd*^{E1020K} (hyperactive PI3K) mice. Naïve (CD44$^-$ CD4$^+$ and CD8$^+$) T cells (directly *ex vivo*) or previously anti-CD3/CD28-stimulated day 6 T cell blasts were stimulated by crosslinking CD3 and then monitored for binding of soluble complexed ICAM-1 (scICAM-1). The *Pik3cd*^{D910A} (kinase-dead PI3Kδ) T cells showed reduced ICAM-1-binding (Figure 3-3). Conversely, both *ex vivo* CD4$^+$ and CD8$^+$ naïve T cells and T cell blasts from *Pik3cd*^{E1020K} (hyperactive PI3Kδ) mice exhibited greatly increased ICAM-1-binding (Figure 3-3) at all assayed timepoints. Thus, TCR-induced ICAM-1-binding is dependent on PI3Kδ activity as previously described, and increased PI3Kδ activity results in increased ICAM-1-binding consistent with their increased PIP_3 levels.

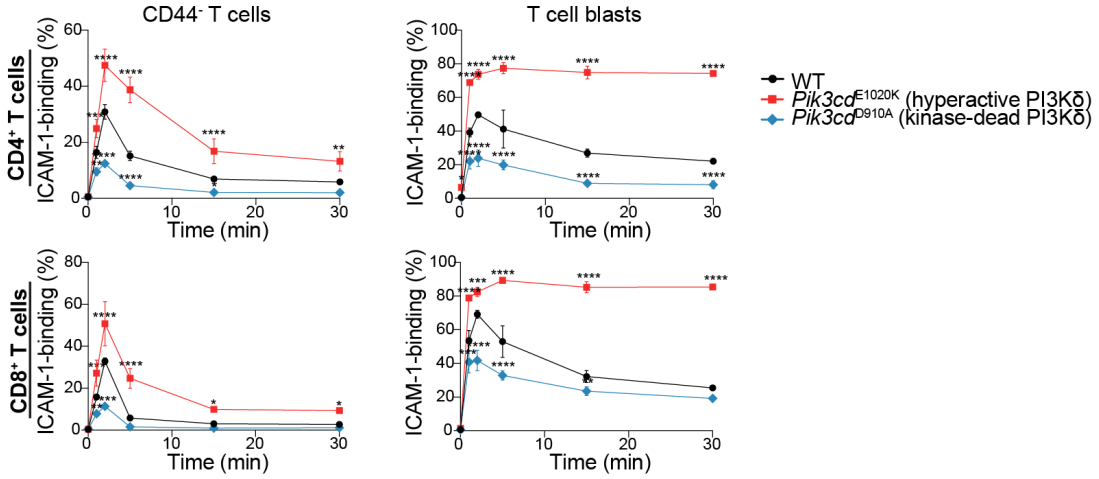

Figure 3-3. ICAM-1-binding is dependent on PI3K activity. Flow cytometry-based ICAM-1-binding assay was performed on *Pik3cd*^{D910A} (kinase-dead), WT, or *Pik3cd*^{E1020K} (hyperactive PI3Kδ) T cells directly *ex vivo* stained with CD44 (left) and on cells activated with anti-CD3/anti-CD28 for 2 days and expanded with rhIL2 until day 6 (right). Data are representative of 3 independent experiments and are means ± SD of 3 mice. **P*<0.05; ***P*<0.01, ****P*<0.001, *****P*<0.0001 as determined by two-way ANOVA with Holm-Šídák's multiple comparison test comparing samples in a timepoint to respective NT or WT control.

To formally establish that these PI3K effects on ICAM-1-binding are mediated via LFA-1 and to identify proteins downstream of PI3Kδ that regulate ICAM-1-binding, I utilized CRISPR-based mutagenesis to screen potential candidate genes (Figure 3-4a). To validate the approach and verify LFA-1-dependence of the assay, I first used retroviral delivery of CRISPR/Cas9 sgRNAs to knockout *Pik3cd* (encoding the p110δ subunit of PI3Kδ), *Pten* (encoding the PIP_3-phosphatase that antagonises PI3K signalling) or *Itgal* (encoding the CD11a subunit of LFA-1). OT-I x *Cas9*$^{+/+}$ CD8$^+$ T cells were stimulated, transduced with individual sgRNAs, and expanded in IL2. Using this technique, I consistently obtained high transduction efficacy and gene-targeting, with >90% of designed sgRNAs resulting in efficient gene-targeting (see examples in Figure 3-1). After restimulation with anti-CD3, ICAM-1-binding was monitored by flow cytometry.

Knocking out *Itgal* resulted in the majority of cells lacking expression of LFA-1 and almost completely ablated ICAM-1-binding (Figure 3-4b-d); the few cells that bound ICAM-1 still expressed LFA-1 (Figure 3-4e). Furthermore, similar to the results presented above from *Pik3cd*^{D910A} and *Pik3cd*^{E1020K} mice, knocking out *Pik3cd* decreased ICAM-1-binding, whereas

knocking out *Pten* increased ICAM-1-binding, without affecting LFA-1 surface levels (Figure 3-4b-d). Thus, my CRISPR/Cas9-mediated targeting strategy recapitulated results obtained using T cells from gene-targeted mice and confirmed that LFA-1-mediated ICAM-1-binding is dependent on regulation of PIP_3 levels by PI3K and PTEN.

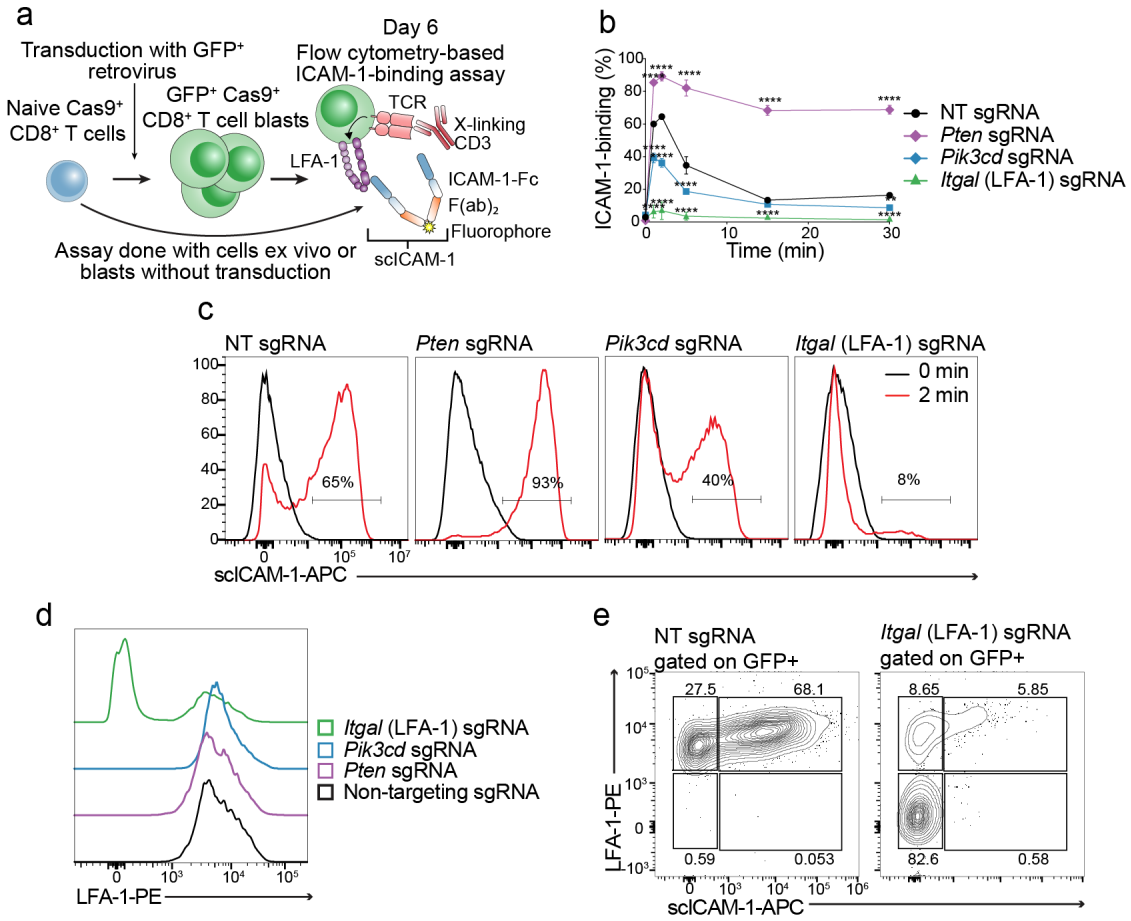

Figure 3-4. Screening of regulators of ICAM-1-binding with CRISPR/Cas9. **a**, Diagram for flow cytometry-based ICAM-1-binding assays used in (**b-e**). **b**, **c**, *Cas9*$^{+/+}$ x OT-I CD8$^+$ T cells were transduced with non-targeting control (*NT*), *Pten*, *Pik3cd*, and *Itgal*-targeting sgRNA and ICAM-1-binding of GFP$^+$ transduced cells was quantified on day 6. **c**, Representative ICAM-1-binding flow cytometry plots at 0 and 2min timepoints from (**b**). **d**, LFA-1 levels on the surface of GFP$^+$ cells from (**b**) quantified by flow cytometry. **e**, ICAM-1-binding of NT or *Itgal* sgRNA-transduced cells stained with LFA-1 antibody showing ablation of LFA-1 expression and ICAM-1-binding in *Itgal* KO T cells. Data are representative of 3 independent experiments (**b-e**). Data in (**b**) are means ±

SD of 3 sgRNAs (**c**). *P<0.05; **P<0.01, ***P<0.001, ****P<0.0001 as determined by two-way ANOVA with Holm-Šídák's multiple comparison test comparing samples in a timepoint to respective NT or WT control.

Together these findings highlight the importance of PI3K in LFA-1 affinity regulation, and confirm that this flow cytometry-based ICAM-1-binding assay is excellent for CRISPR/Cas9-mediated screening of regulators of LFA-1.

3.4 Designing libraries for CRISPR/Cas9-mediated mutagenesis

To understand how PI3Kδ regulates LFA-1 I wanted to use my optimised assay to screen all genes that were downstream of PI3K. To investigate the PI3K signalling pathways specifically, I thus decided to clone multiple libraries; one library for my CRISPR/Cas9 screen of LFA-1 regulators targeting all PIP_3-binding proteins, as well as a broader library targeting all proteins that have potential to be regulated by other PIs; that is all PI-binding proteins excluding PIP_3, the idea being that these two libraries combined would allow for future screens investigating more broadly how PI-binding proteins are involved in immune cell signalling. During my PhD I used the PIP_3-binding library (PBP) to screen for PIP_3-binding proteins affecting LFA-1, as described below.

3.4.1 Curation of lists of phosphoinositide-binding proteins

Library targeting PIP_3-binding proteins

To probe effector proteins downstream of PI3K, I initially designed a library targeting PIP_3-binding proteins to investigate in a CRISPR screen for effects on ICAM-1-binding (Figure 3-5a-b). I curated a list of potential PIP_3-binding proteins to KO as follows: Firstly I identified 402 PH-domain-containing proteins (annotated in the InterPro database [400]) of which 89 proteins have been shown experimentally to have affinity for PIP_3 based on proteomics [227] and functional imaging studies [226] as described in Chapter 1.2.3 (Figure 3-5a). Additionally, a thorough scan through the literature for proteins that had been shown to be PIP_3-binding were included in the group (Figure 3-5a, 1st box). Many of the genes were human genes, and to include these genes in the library I converted the human genes to their mouse orthologs by blasting the proteins and picking the top mouse hits for each gene (Figure 3-5a, 2nd box). As

there is still some controversy regarding which PH-domains do or do not bind PIP_3, I included all PH domain-containing proteins in our criteria for library generation. In addition, 162 proteins were included that do not have PH domains, but which nevertheless have been suggested to have some affinity for PIP_3 [226, 227] (Figure 3-5a, 3rd box). I used this list of proteins to design a library of 2298 sgRNAs targeting 570 genes, along with sgRNAs targeting genes encoding the PI-modifying enzymes PTEN, p110α (subunit of PI3Kα), p110γ (subunit of PI3Kγ), and p110δ (subunit of PI3Kδ), as well as those encoding RAP1 and the LFA-1 subunit, CD11a. Non-targeting sgRNAs were included as additional controls. From the final list of genes, sgRNAs were picked from the Brie library [368] four sgRNAs were designed per gene, synthesised, and cloned as a pool into the pMRIG retroviral vector as described in Chapter 2.8.1 and [379] (Figure 3-5a, 4th box). The resulting library targeting PIP_3-binding proteins was used for the CRISPR screen in this thesis (Figure 3-5b).

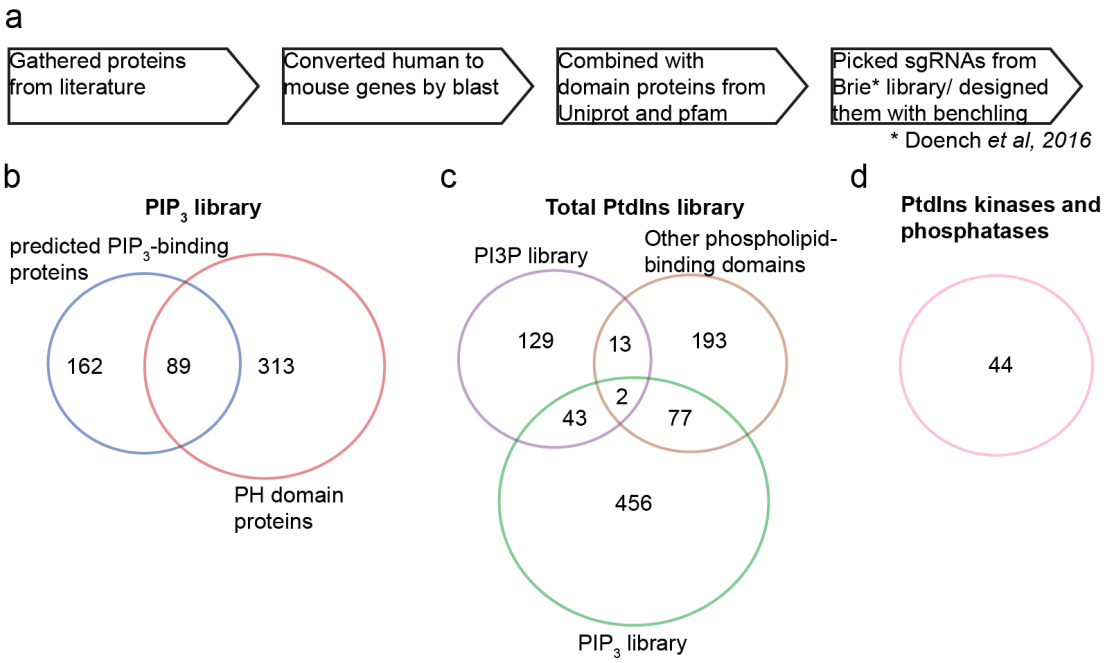

Figure 3-5. Curation of gene lists for CRISPR libraries. Pipeline for construction of libraries based on literature on affinity for phospholipids, as well as domain structure. **b**, Representation of proteins targeted in PIP_3-binding proteins targeting CRISPR/Cas9 library. **c**, Representation of sgRNAs in total library containing the PI(3)P

library, the PIP_3 library, and the rest of the phospholipid-binding domains. **d**, Genes targeted in sub-library targeting PI kinases and phosphatases.

Sub-libraries targeting PI-binding proteins

To also be able to screen for genes that are regulated by other phospholipids in various immunological contexts, I designed a set of smaller sub-libraries. I designed one library targeting predicted PI(3)P-binding proteins as signalling downstream of VPS34 (class III PI3K that synthesises PI(3)P) have been implicated in regulation of autophagy and is produced and upconcentrated on endosomes and phagosomes where it is involved in vesicular trafficking [155]. The library included sgRNAs targeting all FYVE domain proteins, PX domain proteins, and other proteins identified to have affinity for PI(3)P [227] (Figure 3-5c). Combined with the PIP_3-library, which contains sgRNAs against PH domain proteins, this would target the majority of PI3P-binding proteins. This library targeted 42 FYVE-containing proteins, 48 PX containing proteins, and 97 PI(3)P-binding proteins. A third library was designed targeting proteins with domains that have high affinity to other phospholipids based on the literature. This library included sgRNAs against genes encoding proteins containing BAR domains (17 genes), A/ENTH domains (10 genes), C2 domains (136 genes), PDZ domains (85 genes), and Tubby-like domains (7 genes) that all are involved in PI-binding (Figure 3-5c). Lastly, I cloned a sub-library containing sgRNAs against all PI kinases and phosphatases (Figure 3-5d) (see Chapter 1.2.5 and Table 1-2).

By combining the PIP_3 library, PI(3)P library, and PI library it is with these libraries possible to screen for roles of PI-binding genes in general in an unbiased manner. As the libraries are modular, it further allows for screening with smaller libraries for more specific questions. This is especially useful when conducting CRISPR/Cas9 screening in vivo, where obtaining library coverage is difficult. The kinase and phosphatase library allows for similar screening, and can be combined with the other libraries as a control library for identifying the roles of the individual PI lipids in specific immunological contexts.

3.5 Screening for regulators of LFA-1 downstream of PI3K

To screen for genes involved in regulation of LFA-1 downstream of PI3K I designed and optimised a pooled CRISPR/Cas9-mediated KO screen using the optimised ICAM-1-binding assay. To successfully use CRISPR/Cas9 for pooled screening using the ICAM-1-binding assay, I had to ensure I could successfully pick up the individual sgRNAs by sequencing following fixation. I adapted ChipSeq protocols for reverse-crosslinking of the fixed DNA, and used a modified protocol to enable successful sequencing following fixation. Further, based on the ICAM-1-binding profile of T cells by flow cytometry, I found that the peak of ICAM-1-binding was 2min after CD3-crosslinking, so decided to go for this timepoint for the CRISPR screen.

After optimisation, I transduced OT-I x *Cas9*$^{+/+}$ CD8^{+} T cells with the library as described in Chapter 2.3.3, expanded the transduced T cells, and sorted GFP^{+} cells at day 5 in culture to ensure I could do the assay with transduced cells. On day 6 I restimulated with anti-CD3 in presence of scICAM-1. Two min after activation, cells were fixed in 2% PFA, and ICAM-1-binding (scICAM-1^{pos}) and non-binding (scICAM-1^{neg}) cells were isolated by cell sorting ensuring high coverage of the library (Figure 3-6). I then amplified sgRNA sequences from the two populations, as well as from cells prior to the ICAM-1-binding assay and the total library and performed next-generation sequencing of the amplified sgRNA region to quantify sgRNA abundance in each population. This allowed me to compare sgRNA abundance between scICAM-1-binding and non-binding cells as well as sgRNA abundance lost during in culture by comparing sgRNA abundance in the cells prior to sequencing with sgRNA abundance in the total library. Calculating the ratio of sgRNAs between populations thereby allowed me to identify genes that affect ICAM-1-binding or genes that affect survival and growth in culture. Thus, if an sgRNA was enriched in the ICAM-1-binding population and lost in the ICAM-1-non-binding population, the targeted gene blocks ICAM-1-binding, whereas sgRNAs enriched in the ICAM-1-non-binding population and lost in the ICAM-1-binding population are required for ICAM-1-binding. High sgRNA coverage (>1000x) of the libraries was maintained throughout the assay.

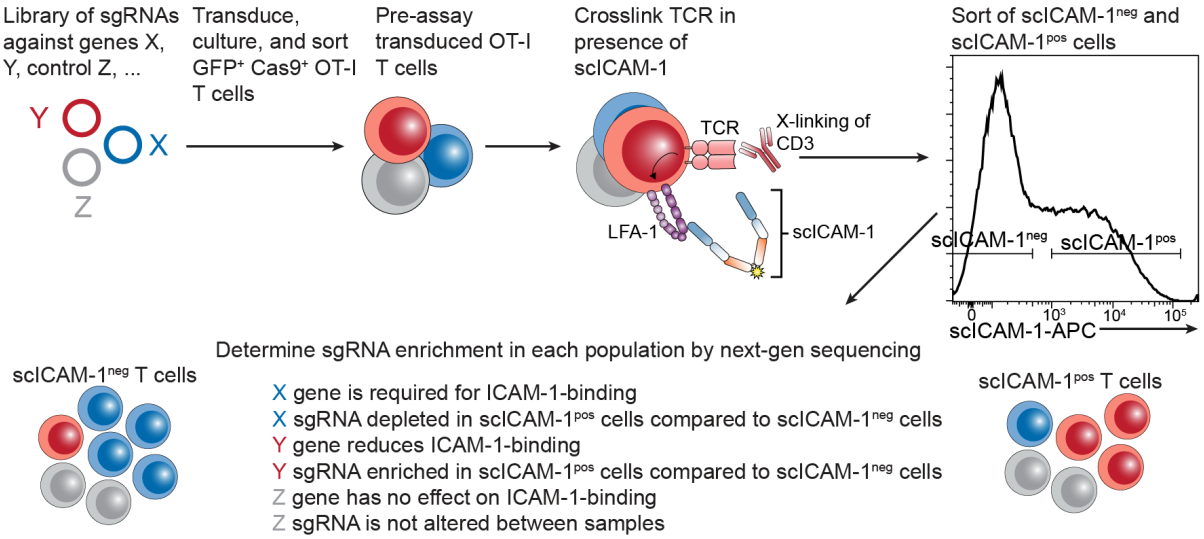

Figure 3-6. CRISPR/Cas9-mediated identification of regulators of ICAM-1-binding. Diagram of CRISPR-screen used to identify genes affecting ICAM-1-binding. *Cas9*$^{+/+}$ x OT-I CD8^{+} T cells were transduced with the CRISPR/Cas9 library targeting PIP_3-binding proteins, and sgRNAs were quantified in scICAM-1^{neg} (not binding ICAM-1) and scICAM-1^{pos} (ICAM-1-binding) GFP^{+} cells on day 6.

To evaluate the effects of targeting genes downstream of PI3K on T cells, I first compared sgRNA frequencies in T cells just prior to the ICAM-1-binding assay to the frequency in the library. This comparison revealed that a number of sgRNAs were depleted during the 6 days in culture (Figure 3-7a-b), suggesting that the corresponding genes are required for T cell expansion or survival. These included a number of ribosomal genes, including the 40S subunit *Rps19,* and the 60S subunit *Rpl38*; genes involved in assembly of the spliceosome and pre-mRNA-splicing, including *Nhp2l1* (also known as *Snu13*), chromatin remodelling, including *Supt16*; proteasomal genes, including the ubiquitination gene *Uba1*; cell cycle-associated genes, including *Chek1*, *Ect2*, *Mcm5*, *Fam35a*; and signalling-related genes, including *Dnm2*, *Pisd*, *Osbpl5*, and *Shc1*. Conversely, a few sgRNAs were enriched during the 6 days in culture, including those targeting *Pten,* consistent with previous data showing a growth advantage to cells lacking this tumour suppressor [401], and *Grb10*, which negatively regulates PI3K/mTOR signalling [402]. It is important to emphasise that the cells were transduced after activation, and thus the genes that are identified in this screen are not necessarily affecting activation of the T cells, or early proliferation, but are rather necessary for survival in the later stages of effector T cell proliferation and survival *in vitro*. Nonetheless, these findings highlight the

importance of PIP_3 in cell processes required for survival and proliferation [166, 389, 401, 403, 404].

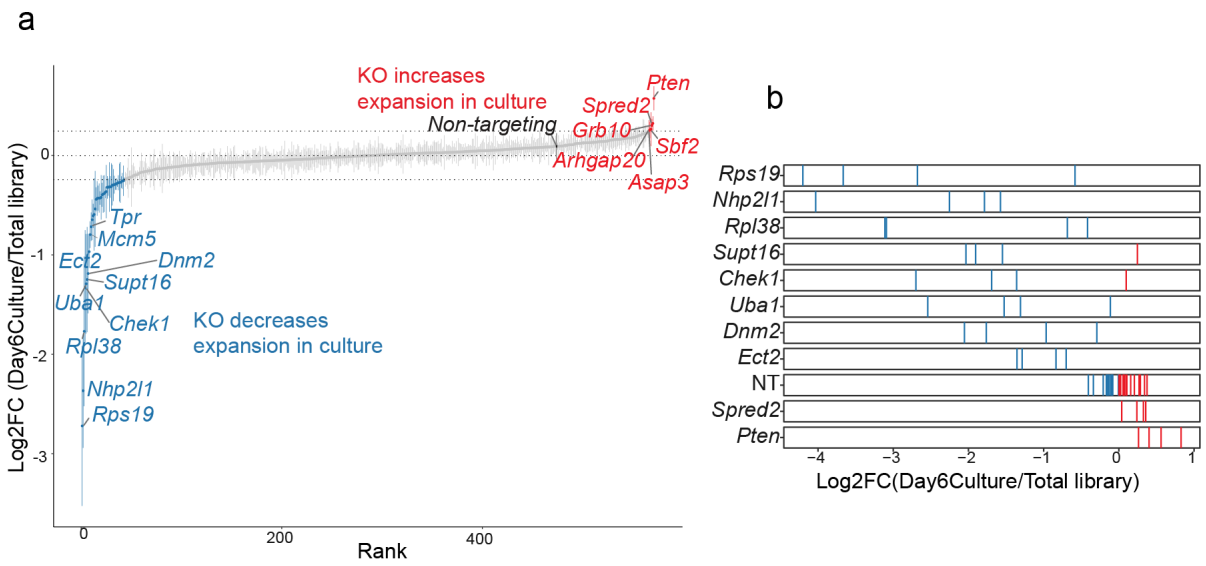

Figure 3-7. PIP_3-binding proteins involved in expansion in culture. **a-b**, sgRNAs abundance in cells following 6 days in culture with rhIL2 compared to sgRNA abundance in library used for transduction. (**a**) Waterfall plot of Day 6 culture sgRNA abundance/Total library sgRNA abundance as Log2 fold change (Log2FC). Error bars show mean±SEM. Dotted lines: ±SD (L2FC of total dataset). sgRNAs lost in culture (blue) target genes that are necessary for expansion, whereas sgRNAs that increase in culture (red) target genes that suppress expansion. (**b**) Plot shows individual sgRNAs of top and bottom hits from (**a**). Analysis and visualisation adapted from MAGeCK [395]. CRISPR/Cas9 screen was done twice and data is average of both experiments with assistance with the sequencing from Dr. Huang and Dr. Phelan.

I then compared the frequencies of sgRNAs between the sorted scICAM-1^{neg} (ICAM-1-binding) and scICAM-1^{pos} cells (ICAM-1-non-binding) (Figure 3-6 and Figure 3-8a-c). As I compared cells from the sort, any gene that would have been lost in culture would be equally depleted in the scICAM-1^{neg} and scICAM-1^{pos} cells. I observed no effect with non-targeting sgRNAs, and saw equal abundance in the scICAM-1^{neg} and scICAM-1^{pos} cells (Figure 3-8b-c). As expected, sgRNAs targeting *Pik3cd* and *Itgal* were underrepresented in the scICAM-1^{pos} population, consistent with these being required for ICAM-1-binding as observed in (Figure 3-3 and Figure 3-4). *Pten* sgRNAs were enriched in the scICAM-1^{pos} population, in accordance with PTEN being the PIP_3 phosphatase and thus negatively regulating PI3K activity (Figure 3-8a-c). One of the sgRNAs targeting *Pten* turned out to not affect PTEN levels by WB of T

cells following *Pten* KO (Figure 3-8d). This fits with the observation that that particular sgRNA did not affect ICAM-1-binding (Figure 3-8c).

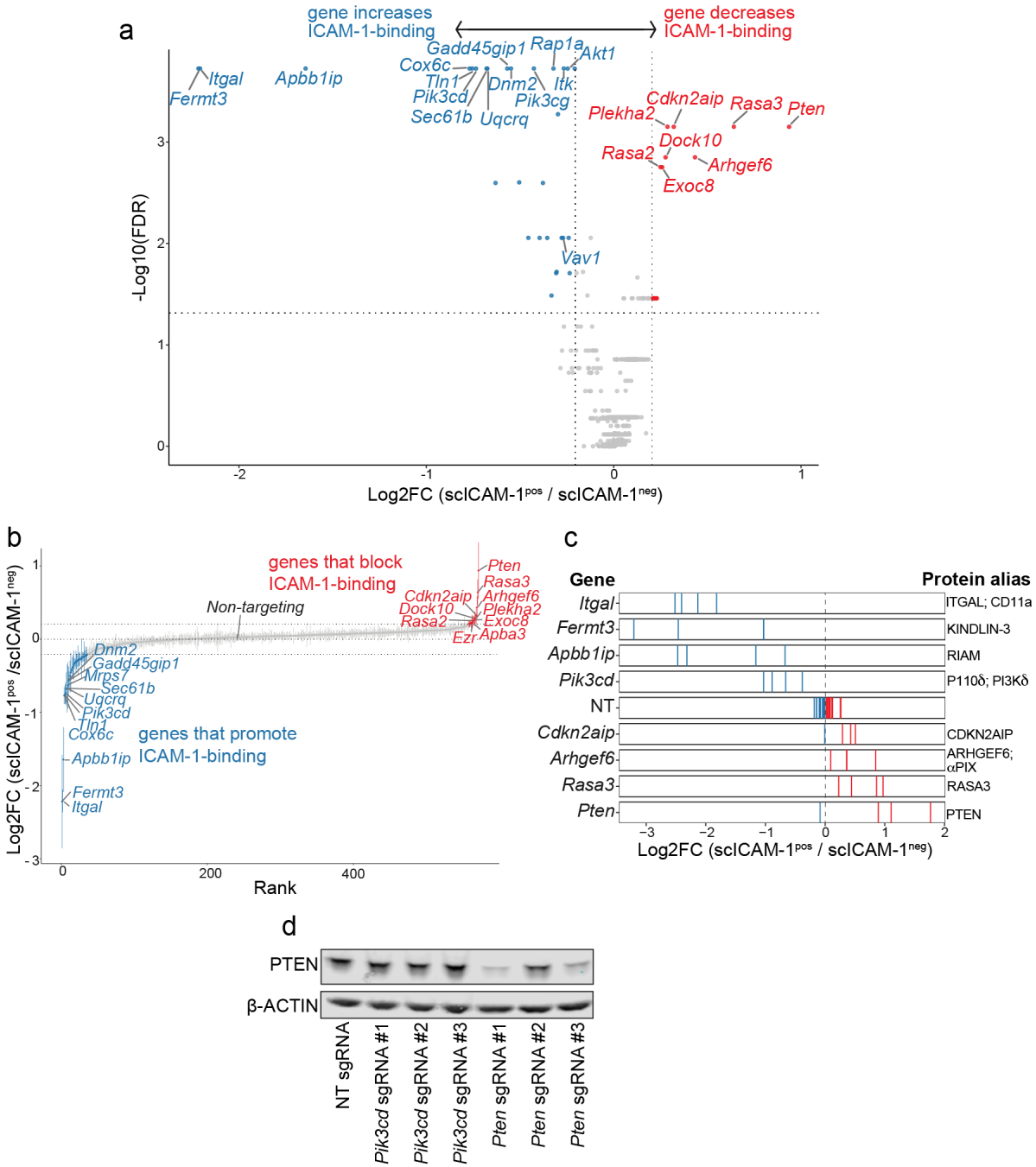

Figure 3-8. ICAM-1-regulators downstream of PI3K. **a**, Volcano-plot of genes from CRISPR screen (analysis and visualisation adapted from MAGeCK [395]) with 10 top and bottom 10 hits, as well as *Pik3cg*, *Rap1a*, *Itk*, *Akt1*, and *Vav1* (FDR: False discovery rate). **b**, Waterfall plot shows the relative abundance of sgRNAs between the scICAM-1^{neg} and scICAM-1^{pos} cells. Dotted lines: ±SD (L2FC of total dataset). Gene names shown are 10 top and

bottom hits, as well as *Itgal*. **c**, Representation of Log2FC(scICAM-1^{pos}/scICAM-1^{neg}) of individual sgRNAs (blue (negative) and red (positive) lines) from top and bottom hits from screen as well as non-targeting sgRNAs. Gene names, and protein aliases are presented. Data in (**a-c**) are L2FC of 4 sgRNAs averaged across two experiments ± SEM. Sequencing was performed with assistance by Dr. Huang and Dr. Phelan. **d**, T cells were transduced with NT, *Pik3cd*, or *Pten* sgRNAs and cells were lysed and western blotted for PTEN with β-ACTIN control.

Among other hits I found enriched in the scICAM-1^{neg} population were multiple genes encoding known positive regulators of integrins, including *Fermt3* (encoding KINDLIN-3) [405], *Apbb1ip* (encoding RIAM) [264], *Tln1* (encoding TALIN-1) [264, 405, 406], *Dnm2* (encoding DYNAMIN-2) [329, 407], *Vav1 [408, 409]*, and *Pik3cd* (encoding p110δ) (Figure 3-8a-c). KINDLIN-3 [410, 411], RIAM [268], DYNAMIN-2 [412] and VAV1 [413] all have PH domains, and of these, the PH domains of KINDLIN-3 [410, 411], RIAM [268], and VAV1 [334, 413] have been shown to have affinity for PIP_3. These hits provided confidence in the assay, while revealing multiple potential contributors to PI3K-mediated LFA-1 regulation. The observation that sgRNAs targeting different parts of a given gene had consistent effects on ICAM-1-binding added further confidence in the results and minimised the risk of off-target effects by the Cas9 enzyme (Figure 3-8c). Of note, AKT1 and 2 were not among the top hits in our screen, although AKT1 did reach statistical significance (Figure 3-8a).

Intriguingly, the screen also identified multiple previously unknown positive regulators of ICAM-1-binding (Figure 3-8a-c). These included multiple mitochondrial proteins including the Cytochrome C-related genes *Cox6c* and *Uqcrq*, as well as proteins involved in formation of the mitochondrial ribosome including *Mrps7* and *Mrpl16*; these findings suggested the potential importance of mitochondrial activity in LFA-1 function (Figure 3-9a). Genes encoding proteins involved in protein transport, such as *Sec61b* and *Dnm2* were also identified as positive regulators (Figure 3-9b). Further, a range of genes that have been involved in TCR signalling were identified, including *Kindlin3*, *Apbb1ip* (encoding RIAM), *Itk*, *Vav1*, *Pik3cd (encoding p110δ)*, and *Pik3cg* (encoding p110γ) (Figure 3-9c). The fact that multiple positive regulators affecting different classes of proteins were identified highlights the importance of PI3K signalling and PH domains in a broad range of cellular processes.

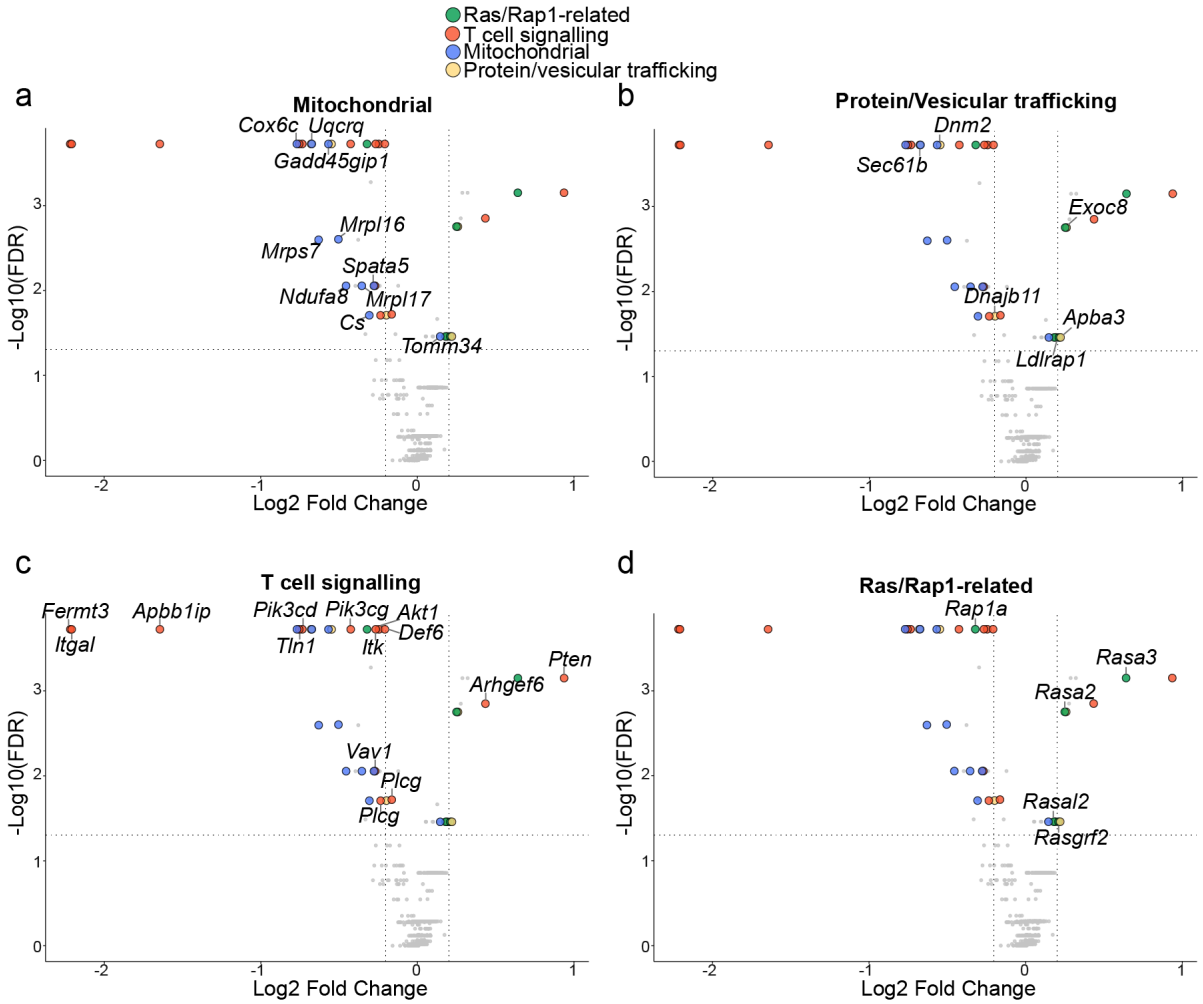

Figure 3-9. Categorised hits from CRISPR/Cas9 screen. **a-d**, Hits from the CRISPR screen presented in Figure 3-8 categorised as mitochondrial genes (blue, **a**), protein and vesicular trafficking-related genes (yellow, **b**), T cell signalling related genes (orange, **c**), and genes involved in regulation of RAS or RAP1 signalling (green, **d**).

To validate positive regulators of ICAM-1-binding identified in our screen, I subcloned individual sgRNAs targeting a variety of known PIP_3-binding proteins that were highly expressed in T cells. Targeting with individually cloned sgRNAs confirmed that sgRNAs directed against the positive regulator *Fermt3* (encoding KINDLIN-3) almost completely eliminated ICAM-1-binding, whereas sgRNAs targeting *Dnm2* and *Pik3cd* decreased ICAM-1-binding to a lesser extent (Figure 3-10a-b, d). To distinguish between genes that affect levels of LFA-1 on the surface of T cells and genes that affect LFA-1 adhesion, I evaluated CD11a levels on the surface by flow cytometry. Whereas *Fermt3* KO T cells had similar levels of surface LFA-1 as T cells transduced with non-targeting sgRNA, *Dnm2* KO T cells had

decreased surface CD11a (Figure 3-10e), suggesting that DNM2 mainly contributes to adhesion by regulating cell surface localization of integrins and other proteins.

Conversely, in the library prepared from scICAM-1^{pos} cells, I uncovered multiple negative regulators of ICAM-1-binding, including *Pten, Rasa3, Arhgef6* (also known as PIXα or COOL2), *Cdkn2aip*, and *Dock10* (Figure 3-8a-c). Among these, *Rasa3* was the highest scoring gene after *Pten*. KO of *Rasa3* by individual sgRNAs confirmed increased ICAM-1-binding (Figure 3-10a, c, f), without affecting LFA-1 surface levels (Figure 3-10g), suggesting that RASA3 is a previously unrecognized regulator of ICAM-1-binding by T cells. I validated the KO of RASA3 by sorting GFP^{+} sgRNA transduced cells, and western blotting for RASA3, and found that it is greatly decreased in all the sgRNA-transduced cells confirming the KO of the *Rasa3* gene (Figure 3-10h).

Together the screen thus identified multiple genes that affect expansion of T cells in culture in presence of rhIL-2, and more importantly, identified a range of positive and negative regulators of ICAM-1-binding that are potentially regulated by PI3K.

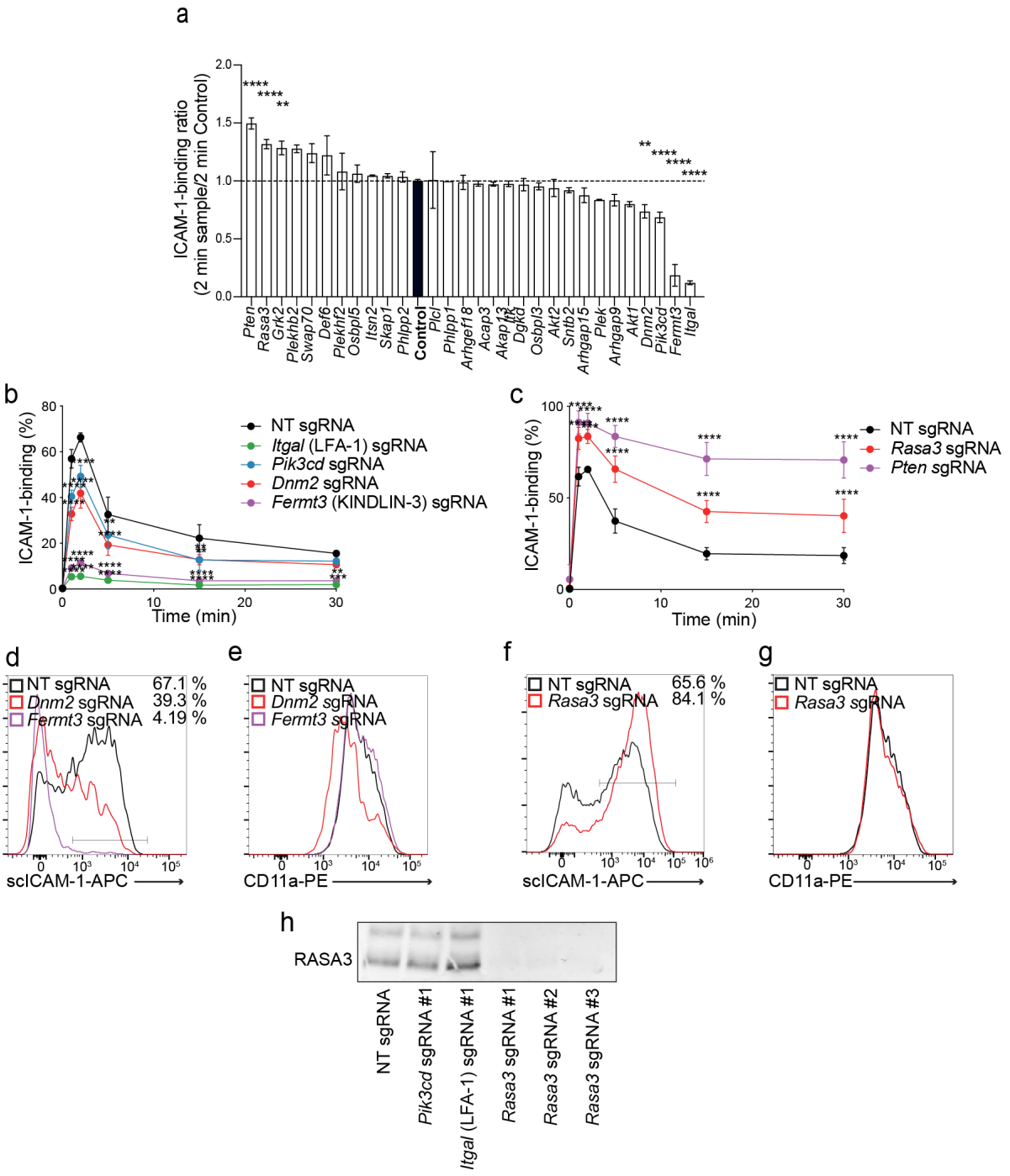

Figure 3-10. Validation of hits from CRISPR/Cas9 screen. **a**, Individual sgRNAs subcloned against highly expressed genes and top hits affecting ICAM-1-binding. ICAM-1-binding was evaluated per gene individually 2min after CD3-crosslinking (Error bars: SD, n=3-9 per target). **b**,**c**, Representative top positive (**b**) and negative (**c**) regulators from the screen were targeted with individually cloned sgRNAs and ICAM-1-binding was assessed by flow cytometry of day 6 *Cas9*$^{+/+}$ x OT-I CD8^{+} T cell blasts at indicated times after TCR crosslinking. **d**, **f** Representative plot of ICAM-1-binding at 0min and 2min after CD3-crosslinking for OT-I x *Cas9* CD8^{+} T cells

transduced with sgRNAs against *Dnm2, Fermt3* (encoding KINDLIN-3) (**f**), or *Rasa3* (**f**). **e**, **g**, LFA-1 levels (CD11a staining) are shown positive (**e**) and negative regulators (**g**). **h**, GFP-sorted sgRNA transduced T cells were western blotted for RASA3. Data in (**a**) are normalised to internal non-targeting sgRNA for each experiment, and combined between multiple experiments. Data in (**b-c**) are representative of 3 independent experiments and are means ± SD of 3 sgRNAs. **P*<0.05; ***P*<0.01, ****P*<0.001, *****P*<0.0001 as determined by two-way ANOVA with Holm-Šídák's multiple comparison comparing samples in a timepoint to respective NT control (**a-c**).

3.6 Discussion

CRISPR/Cas9 has revolutionised the way we study signal transduction and gene function; by enabling easy, specific, and swift KO of genes, it is now possible in vitro, without generating complicated genetic mouse models, to evaluate how KO affects biological functions. Whole genome CRISPR screening takes advantage of the technique to screen the role of all genes in the genome in one experiment in a biological context. Here I will discuss the pros and cons of some of the techniques I have applied, and how my CRISPR/Cas9 screening results fit in the context of findings in the literature.

3.6.1 Requirements for a CRISPR/Cas9 screen

The critical limiting steps of a pooled CRISPR/Cas9 screen are sgRNA representation at all steps, uniform library distribution, low MOI, and a good functional assay (Figure 3-11a). Achieving sufficient representation of all the sgRNAs (often stated to be >200-fold coverage of sgRNAs) is necessary for several reasons. Firstly, as sgRNA library diversity does not equally represent all sgRNAs, high sgRNA coverage will ensure that every sgRNA is represented. Further high sgRNA representation diminishes the chance of stochastically getting a false negative or false positive hit. In my screen I had >1000-fold sgRNA coverage at all steps (at most steps way higher coverage) reducing the chance of stochastic false negative or false positive hits. What is also evident from the distribution of sgRNA counts in the samples is that there is a tail on the distributions from transduced and sorted cells (Figure 3-11b). This illustrates that certain sgRNAs were indeed enriched (increased counts) or lost (lower counts) compared to the total library.

Secondly, the library should preferably be as uniform as possible, (equal representation of sgRNAs in the library) as this reduces the stochastic variability of the screen. My designed and cloned library targeting PIP_3-binding proteins had a fairly uniform distribution of sgRNAs, but I did see a hump in the distribution, meaning some of the sgRNAs are represented at lower rates than others (Figure 3-11b). This is not a matter of concern for a CRISPR screen with high coverage at the screening steps, but could possibly be a concern at screens with borderline/low representation as sgRNAs with lower representation in the library would be at increased risk of being identified as false positive or false negative hits. All my sgRNAs were present at high numbers in the library, except for 3 sgRNAs against *Swap70* that I by accident left out during the mixing of the oligos. Those 3 sgRNAs could for future experiments be spiked into the library to get full library coverage, but there is still one sgRNA against the gene present, and for my screens that sgRNA did not seem to affect neither expansion or ICAM-1-binding indicating that SWAP70 is not involved in expansion or ICAM-1-binding. For future library cloning I would prefer cloning libraries from chip-synthesised oligos, as I did for my inositol-binding libraries as this greatly simplifies preparation of the libraries and thus limits the risks of missing sgRNAs during library preparation.

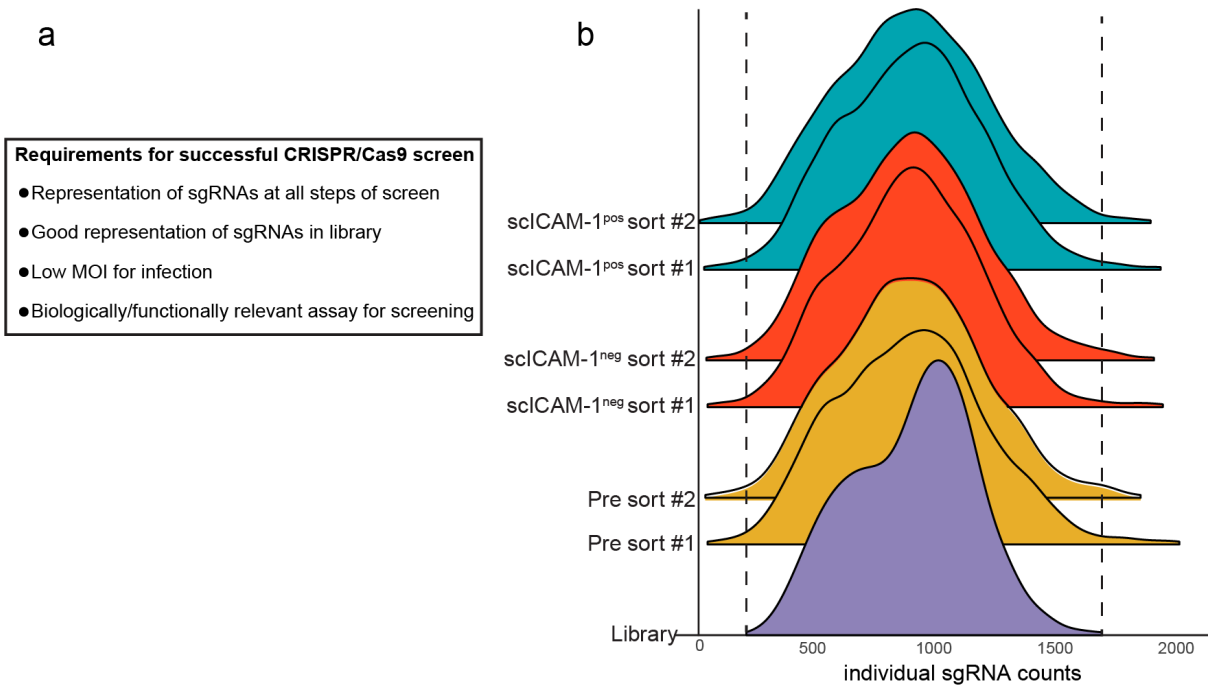

Figure 3-11. Distribution of sgRNAs in samples. **a**, 4 requirements for a successful CRISPR/Cas9 screen. **b**, Distribution of sequenced samples for CRISPR screen of ICAM-1-regulating proteins. X axis shows counts for

the different sgRNAs in each sample. Distribution shows that most sgRNA counts are distributed around ~1000 counts. Dotted lines show the 1% cut-off for the distribution of the library.

The third important requirement for successful CRISPR/Cas9 screening is a low multiplicity of infection with only one transduction; By only transducing a low number of cells (~30-40% of the cells) the chance of transducing a cell twice is reduced, and the risk of getting false positive hits due to double-transduced cells is decreased. For my experiments I ensured I only had ~30 % transduction efficiency for my CRISPR screen, with only one transduction.

Lastly, the sensitivity of the assay, and functional relevance is of importance for the biological conclusions that can be drawn from the results. A good functional assay is sensitive to the phenotypes of interest, and is scalable allowing for inputting enough cells to get representation. Classical pooled CRISPR/Cas9 screens are selection-based screens where survival in culture in presence of a drug or stimuli is the output. This type of assays are ideal for whole genome screening, as they are easily scaled up to ensure coverage of the 70-80,000 sgRNAs in a whole genome library [368]. If the assay is more complicated however, whole genome screening is often not feasible. A good example is a screen like the one I have performed, where the assay is flow cytometry-based. Sorting enough cells to get sufficient coverage for a whole genome library is very time consuming, labour intensive and expensive. Similarly, in vivo screens are limited by cell numbers, and are thus not feasible with whole genome sgRNA libraries. The simplest way around this problem is to scale down the libraries, and target a group of proteins instead of the whole genome. Using smaller sgRNA libraries is therefore for many experimental questions compared to whole genome screens, but smaller libraries do have multiple pros and cons, and deciding on the correct library size and content is therefore not trivial (Table 3-1). For the questions asked in this thesis it made sense to use a smaller library as I was specifically interested in pursuing PI3K effector proteins, and wanted to use a flow-cytometry-based screening assay and consequently was somewhat limited by the number of cells I could use in the assay.

Table 3-1. Pros and cons of smaller sgRNA libraries for CRISPR screening.

Pros	**Cons**
Allows for higher coverage with much fewer cells	Semi-biased due to only screening pre-picked genes

Is feasible for *in vivo* screens	Does not easily allow for pathway analysis as a pathway is overrepresented in the library
Allows for specifically probing a gene group of interest	Does not give as much flexibility for analysis
Easier to pick a hit of interest to pursue as you will likely not have as many hits	Will not necessarily pick up the top hits of the genome
Allows for answering more specific questions by increasing sensitivity to detect less prominent hits.	

3.6.2 LFA-1 regulators downstream of PI3K

LFA-1 activation is tightly regulated in T cells to ensure temporal and spatial control of migration and adhesion. In this chapter, I described a targeted CRISPR/Cas9 screen that allowed me to specifically probe the role of potential PI3K-effectors in LFA-1-mediated binding of ICAM-1. It remains uncertain exactly how many proteins have the capacity to bind PIP_3, but what is clear is that the roles of many of these in various biological contexts remain understudied in comparison to the canonical PI3K effectors, such as PDK1 and AKT. The library I generated, which targets 570 proteins encompassing the major PIP_3-binding proteome, will be a useful resource to explore other mechanisms downstream of the PI3Ks that cannot be simply explained by the predominant AKT pathway.

To assay LFA-1 regulation by CRISPR, I had to optimise CRISPR/Cas9 KO in the context of ICAM-1-binding, and it was quite clear that the flow cytometry-based ICAM-1-binding assay was ideal for a smaller -scale pooled CRISPR/Cas9 screen. The assay provided two clearly distinct populations by flow cytometry that could easily be sorted, with ~50% positive and 50% negative for the scICAM-1-molecule. Further the assay was highly sensitive to PI3K activity and thus would likely pick up regulators downstream of PI3K.

In our screen for proteins that regulate LFA-1, I identified multiple known regulators such as KINDLIN-3, RIAM, PI3Kδ, RAP1a, and TALIN-1. I also uncovered multiple new proteins involved in LFA-1 activation, including molecules mitochondrial components, suggesting a level of LFA-1 regulation by mitochondrial respiration and function, perhaps for energy generation required for adhesion. LFA-1 has earlier been implicated in mitochondrial translocation in T cells [414], however to my knowledge mitochondria have not been

implicated in reciprocal regulation of LFA-1, and it will be interesting to further investigate how LFA-1 and mitochondrial function are related.

Further, multiple TCR-signalling related genes (10 PIP_3-binding proteins) were identified as regulators of LFA-1, including genes encoding the known regulators KINDLIN3, RIAM, VAV1, ITK, and less well characterised proteins, such as DEF6 (a GEF for RAC) and ARHGEF6 (a GEF for RHO; also known as α-PIX). These proteins are all involved in complex signalling networks, and it is not surprising that they mediate LFA-1 activation to some extent.

Multiple protein trafficking-related proteins were also identified. This supports earlier studies indicating that LFA-1 is readily trafficked from the T cell surface via intracellular vesicles and that these vesicles are a necessary pool of LFA-1 which is delivered to the IS during conjugate formation to support the conjugate [415]. These identified proteins are therefore likely involved in regulating the location of LFA-1 within the T cells.

Lastly, I identified a range of proteins that are regulators of RAS/RAP1 signalling. The top negative regulator of LFA-1 identified after the negative control PTEN, was the dual RAS/RAP1 GAP called RASA3. As it is known from earlier studies that high RAP1-GTP levels are dependent on PI3K activity [219], it seemed like these RAP1-regulators were likely candidates for explaining the PI3K-mediated LFA-1 regulation. As RASA3 had been suggested to be a regulator of integrins in platelets [337], is highly expressed in T cells (Immgen.com), and is a particularly strong binder of PIP_3 [227], I decided to investigate the role of RASA3 further in T cell functions *in vitro* and *in vivo*.

3.6.3 Chapter summary

In this chapter, I have presented evidence that supported the notion that PI3K activity is crucial for regulating LFA-1 activity. I have further shown that CRISPR/Cas9 could be adapted for screening of PI3K effector proteins involved in LFA-1 regulation. I therefore used CRISPR/Cas9 to screen for such regulators of LFA-1 and identified both multiple known regulators and multiple unknown regulators of LFA-1-mediated ICAM-1-binding. I

subsequently confirmed some of these hits by KO of the genes individually, and found that RASA3 is a critical regulator of LFA-1-mediated ICAM-1-binding.

Chapter 4 – Biochemical characterisation of the dual RAP1/RAS-GAP, RASA3

4. Biochemical characterisation of the dual RAP1/RAS-GAP, RASA3

4.1 Introduction

After identifying RASA3 as a potent negative regulator of LFA-1-mediated ICAM-1-binding, I wanted to understand how RASA3 regulates LFA-1, and whether it is in some way regulated by PI3K signalling. To study the function of RASA3 in T cells I generated *Rasa3*$^{fl/fl}$ x *Cd4*^{Cre} mice where *Rasa3* is specifically deleted in T cells (*Rasa3*$^{T\text{-}KO}$) by crossing *Rasa3*-flox mice from Professor Wolfgang Bergmeier's laboratory at University of North Carolina, USA [352] with *Cd4*^{Cre} mice. In these mice, exon 3 is flanked by loxp sites leading to deletion upon Cre-mediated recombination. For certain experiments I further crossed these *Rasa3*$^{T\text{-}KO}$ mice to OT-I or OT-II TCR-transgenic mice allowing me to study apply TCR-specificity-dependent *in vitro* and *in vivo* models, or *Cas9*-expressing mice, allowing me to further KO potential proteins involved in the regulation of RASA3 activity or its involvement in LFA-1 regulation.

In this chapter I applied *in vitro* assays to understand the biochemical role and regulation of RASA3 in regulating LFA-1. I applied flow cytometric ICAM-1-binding assays to determine ICAM-1-binding under various conditions, including following overexpression of RASA3 mutants. I further quantified RASA3 expression by qRT-PCR and mining proteomic databases following activation to understand RASA3 regulation in stimulated T cells, and used biochemical pulldown assays to investigate the biochemical activity of RASA3. I further had assistance from Julie Hagedorn Thomsen, an MSc student I supervised, in imaging cells transduced with a fluorescently tagged RASA3 construct I generated to understand the dynamic regulation of RASA3 location in T cells. These tools combined allowed me to investigate how the intricate mechanisms involved in RASA3-mediated LFA-1 regulation.

4.2 RASA3 – a novel critical regulator of integrins in T cells

4.2.1 *Rasa3* KO and expression in T cells

Firstly, I wanted to ensure that the *Rasa3*$^{T\text{-}KO}$ mice I had generated indeed had specific deletion of RASA3 in T cells, and therefore designed primers around the floxed exon and amplified the sites by PCR of sorted T and B cells. The sorted CD4$^+$ and CD8$^+$ T cells had lost exon 3 completely, whereas the B cells had completely intact exon 3 (Figure 4-1a). Exon 3 deletion results in out of frame translation of exon 4 leading to a premature stop codon in exon 5 (Figure 4-1b) [352]. This indicated specificity of the *Cd4*^{Cre} and gave me confidence that the *Rasa3*$^{T\text{-}KO}$ mouse model would allow me to look at T cell intrinsic roles of RASA3.

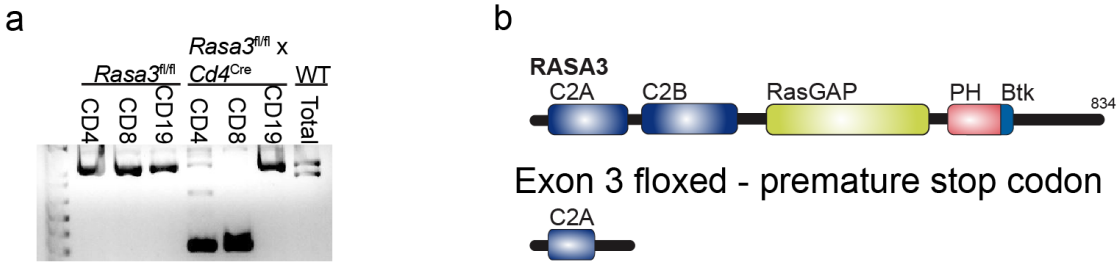

Figure 4-1. PCR of *Rasa3* exon 3 from sorted CD4$^+$, CD8$^+$, or CD19$^+$ cells. **a**, CD4$^+$CD8$^-$CD19$^-$ (CD4), CD4$^-$CD8$^+$CD19$^-$ (CD8) and CD4$^-$CD8$^-$CD19$^+$ (CD19) cells were sorted from pooled LNs and spleens from *Rasa3*$^{fl/fl}$ and *Rasa3*$^{fl/fl}$ x *Cd4*^{Cre} (*Rasa3*$^{T\text{-}KO}$) mice, and the floxed allele was amplified from genomic DNA with primers designed on either side of the floxed exon 3 (Rasa3flox_Fwd and Rasa3flox_Rev). **b**, Domain structure of full RASA3, and domain structure of truncated RASA3 following deleted exon 3. Experiment performed once with cells from one mouse for each genotype.

Mining of gene expression databases suggested that *Rasa3* mRNA is markedly downregulated following TCR stimulation [416]. To understand the dynamics of this regulation and confirm these findings, I sorted CD4$^+$ and CD8$^+$ T cells, and stimulated the T cells with αCD3/αCD28 for 0-7 days and TriZol-purified RNA from the cells for qRT-PCR. It was clear that *Rasa3* transcripts were rapidly downregulated following stimulation, and remained low during the proliferative phase of T cell expansion, but increased to some extent at the later timepoints (Figure 4-2a). Similarly, I mined RASA3 protein levels from the ImmPRess proteomics database (www.immpres.co.uk) [417], and found that both the protein copy number and concentration were markedly decreased in both CD4$^+$ and CD8$^+$ T cells after 24h stimulation

and in T cell blasts compared to their naïve counterpart (Figure 4-2b). This is in stark contrast to the majority of proteins in T cells following stimulation; the great majority of proteins are increased by copy number following stimulation [417], and this finding thus suggests that RASA3 levels are tightly regulated and show an unusual expression pattern. To evaluate whether RASA3 was degraded through a proteasomal pathway besides being regulated by transcriptional downregulation I incubated activated T cells with and without the proteasomal inhibitor MG132 and lysed cells for WB at 1h, 2h, 4h, 12h, and 24h post activation. If RASA3 was degraded by the proteasome, I would expect MG132 to block the degradation. MG132 however did not seem to affect the RASA3 levels significantly at any timepoints except for the 14h timepoint. The decreased RASA3 levels at the 14h timepoint is likely due to the cells dying from the MG132 inhibition (the 24h timepoint only had MG132 for the last 8h of incubation) (Figure 4-2c). This suggests that RASA3 is primarily regulated transcriptionally, but it is unclear what the mechanism behind this is. Evaluation of proteomics datasets from the Okkenhaug laboratory with T cells expressing hyperactive or kinase-dead PI3K had only minor alterations in RASA3 levels in *Pik3cd*^{D910A} naïve CD4^{+} T cells (Figure 4-2d), indicating that *Rasa3* is likely not regulated downstream of FOXO1 or KLF2 transcription factors. Thus, the mechanisms for the downregulation of *Rasa3* should be investigated further in future experiments.

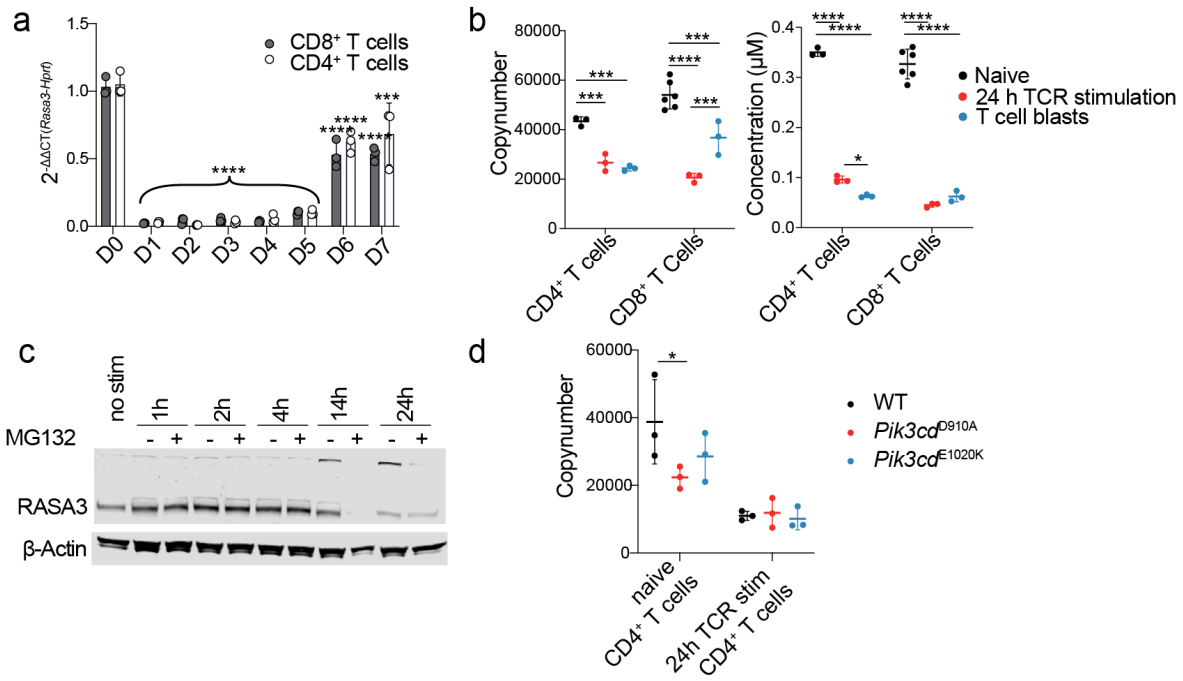

Figure 4-2. Expression of *Rasa3* in T cells. **a**, qRT-PCR quantification of *Rasa3* mRNA levels from FACS-sorted CD4⁺ and CD8⁺ T cells activated with 1 μg/ml anti-CD3 and 2 μg/ml anti-CD28 at D0-D7, normalized to *Hprt* by ΔΔCT method. Data are representative of 3 independent experiments and are means ± SD of 3 mice (**a**). **b**, RASA3 protein copy numbers and concentration mined from peptracker (ImmPRess) [417]. **c**, MACS isolated CD4⁺ T cells were stimulated with plate bound anti-CD3/anti-CD28 with or without 10 μM MG132 (protease inhibitor) to evaluate whether this could block T cell degradation. 24h timepoint was incubated with MG132 for the last 8h. Experiment performed once with one sample per timepoint. **d**, Copy numbers of RASA3 in naïve and 24h TCR stimulated WT, *Pik3cd*^{D910A}, and *Pik3cd*^{E1020K} CD4⁺ T cells (data are biological triplicates from former PhD Rafeah Alam in the Okkenhaug laboratory). **P*<0.05; ***P*<0.01, ****P*<0.001, *****P*<0.0001 as determined by two-way ANOVA with Holm-Šídák's multiple comparison comparing every timepoint to the D0 timepoint for same T cells (**a**) or all samples within condition (**b, d**).

4.2.2 Integrin regulation in *Rasa3* KO T cells

I then sought to confirm that RASA3 indeed did regulate ICAM-1-binding in this genetic mouse model. Both CD4⁺ and CD8⁺ naïve (CD44⁻) T cells lacking RASA3 exhibited highly increased ICAM-1-binding after TCR stimulation (Figure 4-3a) confirming the role for RASA3 in keeping LFA-1 in check. Consistent with the upregulation of LFA-1 on activated T cells, *wild-type* (WT) T blasts, which have been expanded after stimulation with anti-CD3 and anti-CD28 antibodies, showed markedly increased TCR-induced ICAM-1-binding compared to

naïve T cells, but expanded *Rasa3* KO T cell blasts exhibited even higher TCR-induced ICAM-1-binding than WT T cell blasts (Figure 4-3b). However, the increased ICAM-1-binding was more profound in naïve T cells, likely due to the fact that RASA3 is higher in naïve than activated T cells (see Figure 4-2a-b). To rescue this increase in ICAM-1-binding, I cloned a retroviral construct based on the MIGR1 backbone that contained mRuby fused to human RASA3 connected by a flexible linker (see Chapter 2.8.3). Increasing RASA3 expression by transduction with this retroviral mRuby-RASA3 construct (mRuby-RASA3) into WT and *Rasa3* KO activated T cells led to decreased ICAM-1-binding, bringing ICAM-1-binding down to the levels observed in naïve WT T cells (Figure 4-3b). The mRuby-RASA3 was not massively overexpressed, and thus seemed to somewhat recapitulate normal levels of RASA3 (Figure 4-3c). This suggested that the downregulation of RASA3 observed in Figure 4-2a-b might be responsible for the increased LFA-1 activity observed in activated T cells, and RASA3 is therefore possibly involved in keeping LFA-1 in check. I further investigated whether RASA3 affected ICAM-1-binding in the absence of TCR stimulation, and found that RASA3 KO indeed does result in slightly increased ICAM-1-binding in naïve T cells even at baseline (Figure 4-3d).

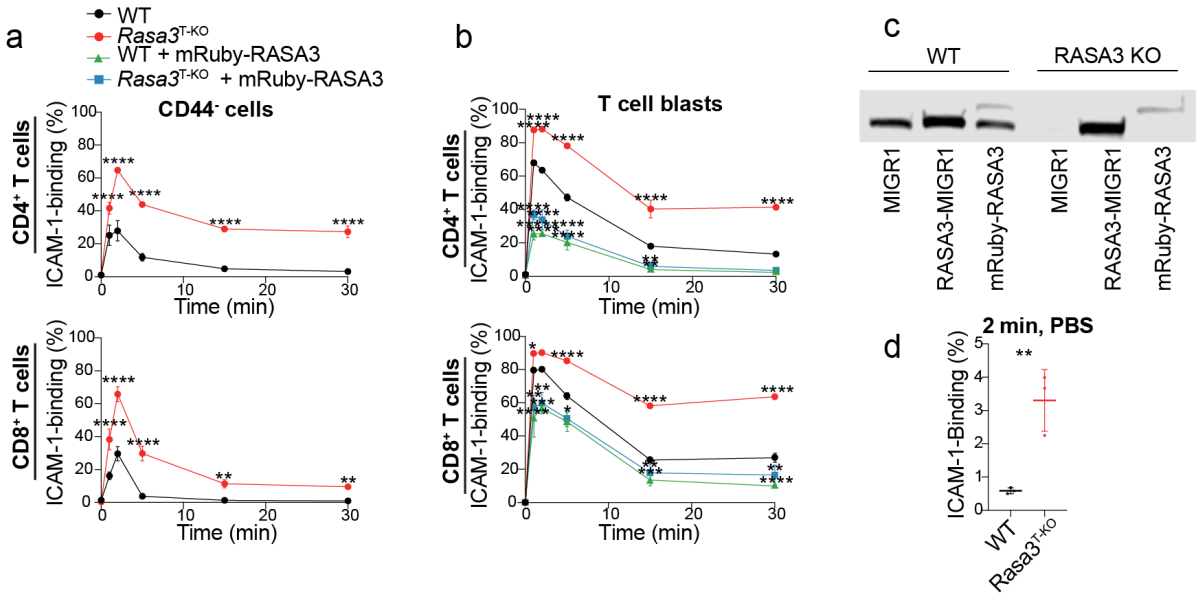

Figure 4-3. ICAM-1-binding in TCR-transduced *Rasa3* KO T cells. **a-b**, ICAM-1-binding of *Rasa3* KO CD4+ (top) and CD8+ (bottom) T cells, *ex vivo* gated on CD44- (**a**) or blasts transduced with MIGR1 or mRuby-hRASA3-expressing retroviral constructs (**b**). **c**, WB of RASA3 in WT or *Rasa3* KO CD4+ T cells transduced with MIGR1, RASA3-MIGR1, or mRuby-RASA3 (Experiment performed once). **d**, ICAM-1-binding of control and *Rasa3* KO

CD4+ T cells directly *ex vivo* and incubated for 2min at 37˚C with no stimulation (WT n=3, *Rasa3*$^{T\text{-}KO}$ n=3). Data are representative of 3 independent experiments and are means ± SD of 3 mice (**a-b, d**). **P*<0.05; ***P*<0.01, ****P*<0.001, *****P*<0.0001 as determined by two-way ANOVA with Holm-Šídák's multiple comparison (**a**-**b**) or Unpaired two-tailed Student's *t* test. Multiple comparisons are comparing samples in a timepoint to respective control (**a**-**b**).

To investigate whether *Rasa3* KO also affected ICAM-1-binding downstream of chemokines, I conducted the same ICAM-1-binding assay with the chemokines SDF1α and CXCL10 known to induce inside-out signalling to integrins in activated T cells. *Rasa3* KO T cells had increased ICAM-1-binding in response to these chemokines (Figure 4-4a), suggesting that RASA3-mediated regulation of LFA-1 is not specific to TCR stimulation. To allow for assaying binding to other integrins than LFA-1, I adapted the ICAM-1-binding assay to feature other adhesion molecules. Binding of VCAM-1, which is bound by the integrin, VLA-4, was also increased in response to chemokines in *Rasa3* KO T cells again implicating RASA3 more broadly in integrin regulation (Figure 4-4b). Together these findings paint a picture where RASA3 is a critical regulator of integrin regulation in general, dampening the activity of LFA-1 and VLA-4 (and potentially other integrins) both with and without stimulation through TCR or chemokine receptors.

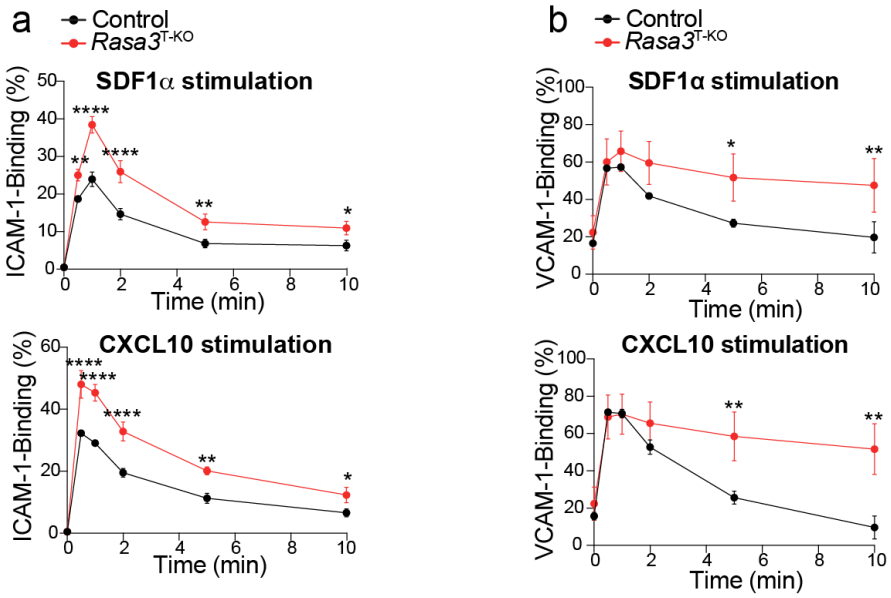

Figure 4-4. Chemokine-induced ICAM-1 and VCAM-1-binding. **a**, ICAM-1-binding of *Rasa3* KO CD4+ T cells following stimulation with SDF1α (upper) or CXCL10 (lower) (WT n=3, *Rasa3*$^{T\text{-}KO}$ n=3). **b**, VCAM-1-binding assays of T cell blasts from control and *Rasa3* KO CD4+ T mice stimulated with SDF-1α (upper) or CXCL10

(lower) (WT n=3, *Rasa3*$^{T\text{-}KO}$ n=3). Data are representative of 3 independent experiments and are means ± SD of 3 mice (**a**). **P*<0.05; ***P*<0.01, ****P*<0.001, *****P*<0.0001 as determined by two-way ANOVA with Holm-Šídák's multiple comparison. Multiple comparisons are comparing samples in a timepoint to respective control.

4.2.3 RAP1 activation in *Rasa3* KO T cells

I next wanted to understand how RASA3 regulates LFA-1. As RASA3 is a known GAP for RAP1 and RAS, I decided to evaluate to what extent RASA3 regulates these proteins in T cells, and whether RAP1 deactivation was the main regulatory mechanism driving inactivation of LFA-1 downstream of RASA3. RAP1-GTP pulldown using *Glutathione S Transferase* (GST)-bound RAP1-GTP-binding domain RalGDS (GST-RalGDS) is commonly used to pulldown the active RAP1-GTP from lysates followed by WB of RAP1. After extensive optimisation and purification of GST-RalGDS from bacteria, I conducted the RAP1-GTP pulldown assay on TCR-stimulated WT and *Rasa3* KO T cells. It was clear that *Rasa3* KO T cells had increased RAP1-GTP, even without TCR crosslinking (Figure 4-5a), consistent with increased ICAM-1-binding without TCR crosslinking (Figure 4-3c). Thus RASA3 acts as a GAP for RAP1 in T cells. RAS-GTP pulldown assays are not easy to do with primary mouse T cells, and I thus decided to investigate the RAS activity indirectly by blotting for phospho-ERK (pERK) which is phosphorylated downstream of RAS-GTP. To my surprise I found that *Rasa3* KO T cells had slightly decreased pERK indicating that RASA3 does not function as an effective GAP for RAS in T cells (Figure 4-5b). Early studies of RASA3 did indicate that RASA3 had higher activity towards RAP1 than RAS [340, 344], but this indicates very limited RAS-specific activity in T cells. The slightly decreased pERK in the *Rasa3* KO T cells is possibly a result of a negative feedback loop from RAP1-GTP to RAS [418] and thus decreased RASA3 would result in increased RAP1-GTP and via a negative feedback loop inhibit RAS activity. Nonetheless this would have to be evaluated in future studies.

To evaluate whether the GAP functions of RASA3 are responsible for its negative regulation of LFA-1, I mutated my mRuby-RASA3 construct generate a mRuby-RASA3^{R371Q} mutant which inactivates the GAP domain [342, 344]. Expression of WT RASA3 suppressed ICAM-1-binding, consistent with RASA3 being an inhibitor of LFA-1 activity (Figure 4-5c, blue). By contrast, the mutant R371Q, which inactivates the GAP activity of RASA3, completely prevented suppression of ICAM-1-binding seen with ectopic expression of WT RASA3

(Figure 4-5c, purple). Together these results suggest RASA3 mainly negatively regulates ICAM-1-binding by negatively regulating RAP1 activity via its GAP domain, consistent with the lower RAS-specific activity observed in the literature [342, 343, 419]. In contrast, CRISPR-targeting of RASA2 and 4 (also known as CAPRI), which do affect RAS in T cells [80], did not affect ICAM-1-binding to the same extent as RASA3 (Figure 4-5d). This highlights that RASA3 is the main RASA protein negatively regulating LFA-1 activity by inactivating RAP1.

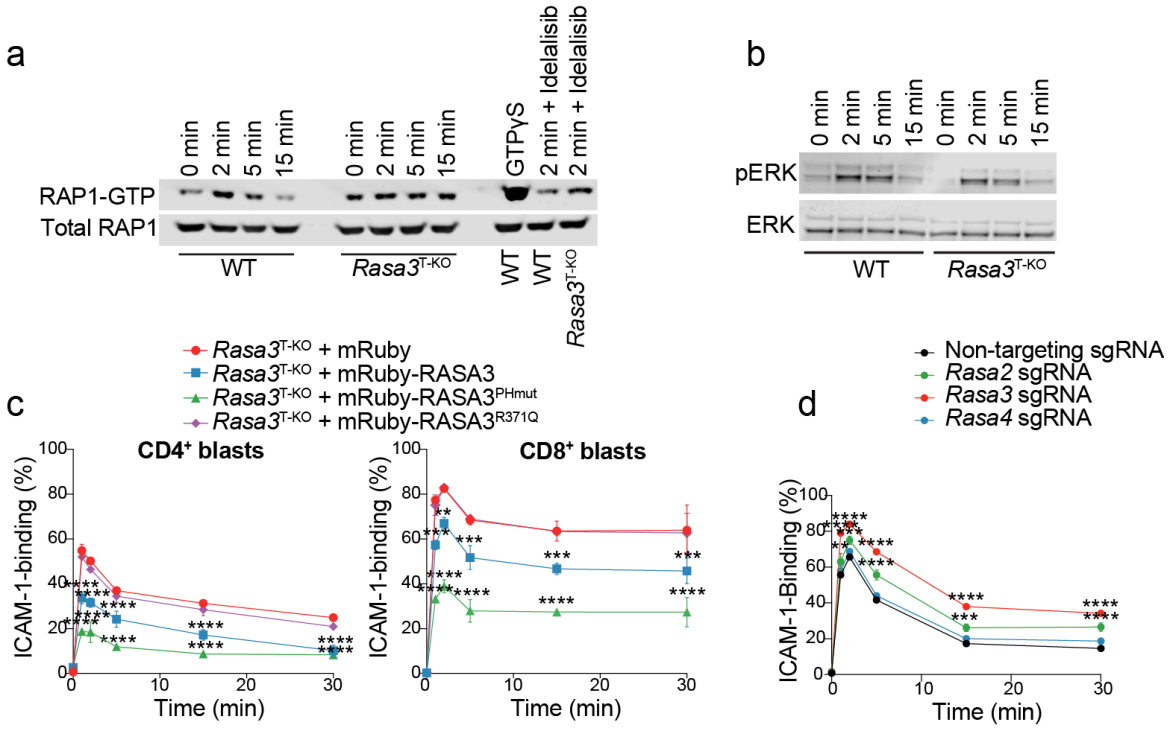

Figure 4-5. GAP functionality and PI3K inhibition of RASA3. **a**, RAP1-GTP pull-down assay using purified GST-RalGDS-RBD and glutathione agarose following crosslinking of TCR of purified WT and *Rasa3* KO T cells for indicated timepoints. p110δ-specific Idelalisib inhibitor was included and evaluated at 2min timepoint. GTPγS was used as a positive control and RAP1 from total lysates as loading control (Representative of 4 experiments). **b**, Phospho-ERK and total ERK from *Rasa3*$^{T\text{-}KO}$ T cells following crosslinking of TCR as evaluated by blotting (Representative of 3 experiments). **c**, ICAM-1-binding assessed in CD4^{+} (left) and CD8^{+} (right) *Rasa3* KO T cell blasts following expression of mRuby, mRuby-RASA3, mRuby-RASA3^{PHmut} (RASA3^{K599Q,K600Q,R601Q}) or mRuby-RASA3^{R371Q}, assayed on day 6 in culture. **d**, ICAM-1-binding assay of OT-I x *Cas9* WT CD8^{+} cells transduced with sgRNAs against *Rasa2*, *3* and *4*. Data in (**c**-**d**) are representative of 3 experiments and are showing means ± SD of 3 mice per sample. **P*<0.05; ***P*<0.01, ****P*<0.001, *****P*<0.0001 as determined by two-way ANOVA

with Holm-Šídák's multiple comparison. Multiple comparisons are comparing samples in a timepoint to its respective control (**c**-**d**).

4.3 Regulation of RASA3 by PI3K signalling

4.3.1 RASA3 is inhibited by PI3K

Previous data from platelets suggest that PI3K activity can inhibit RASA3 [337]. To investigate how PI3K affects RASA3 activity in T cells, I included the PI3Kδ-selective inhibitor, Idelalisib, during TCR-crosslinking, before pulldown of RAP1-GTP. Idelalisib decreased RAP1-GTP in WT cells, consistent with previous observations from the Okkenhaug laboratory that inhibition of PI3Kδ decreases ICAM-1-binding through a RAP1-dependent mechanism [219]. However, RAP1 activity was not affected by Idelalisib in the absence of RASA3 (Figure 4-5a, Figure 4-6a). Thus in the absence of RASA3, PI3Kδ is no longer required for TCR-dependent RAP1 activation.

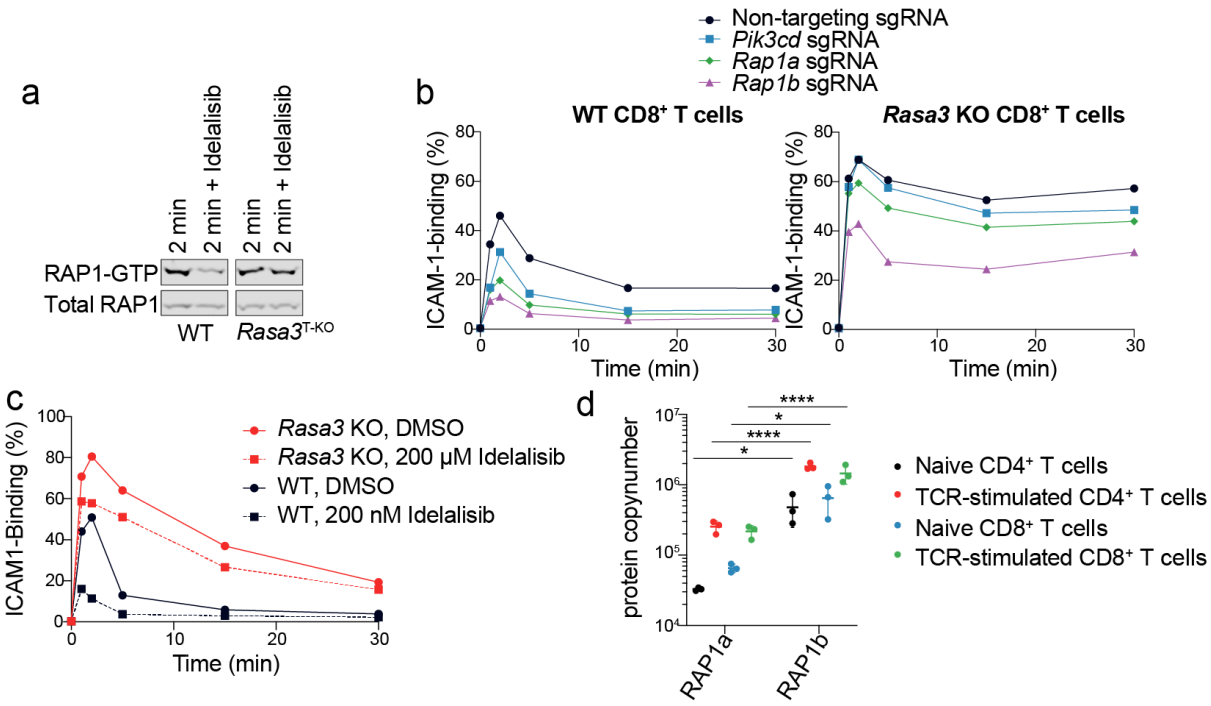

Figure 4-6. PI3K-mediated inactivation of RASA3. **a**, RAP-1-GTP pulldown of WT or *Rasa3* KO T cells stimulated with CD3 crosslinking with and without Idelalisib (p110δ inhibitor) (Representative of 3 experiments). **b**, ICAM-1-binding assay of OT-I x *Cas9* WT and *Rasa3* KO CD8+ cells transduced with sgRNAs against *Pik3cd*,

Rap1a, and *Rap1b* (representative of two experiments, n=1 per group). **c**, WT and *Rasa3* KO Day 7 blasted $CD8^+$ T cells treated with DMSO or 200 μM Idelalisib during ICAM-1-binding assay (representative of two experiments, n=2 per group). **d**, Copy numbers of RAP1a and RAP1b isoforms from proteomics dataset from former PhD student Rafeah Alam in Okkenhaug laboratory (3 biological repeats). *P<0.05; **P<0.01, ***P<0.001, ****P<0.0001 as determined by two-way ANOVA with Holm-Šídák's multiple comparison comparing RAP1 protein copy numbers between RAP1a/RAP1b within condition (**d**).

To further understand how PI3K regulates RASA3, I generated a triple mutant (K599Q, K600Q, and R601Q), which disables the PH domain of RASA3 (PHmut), and disrupts binding to PIP_3 [337] (discussed in Chapter 4.3.2). Overexpression of this mutant in *Rasa3* KO T cells decreased ICAM-1-binding even further than overexpression of WT RASA3, consistent with the idea that PIP_3-binding inactivates RASA3 activity (Figure 4-5c, green). To further investigate how KO of *Pik3cd* affected ICAM-1-binding in *Rasa3* KO T cells, I crossed the $Rasa3^{T\text{-}KO}$ mice to $Cas9^{+/+}$ x OT-I mice. In WT cells as seen in Chapter 3 *Pik3cd* KO results in decreased ICAM-1-binding (Figure 4-6b, left, blue), however in the *Rasa3* KO T cells KO of *Pik3cd* only modestly decreased ICAM-1-binding (Figure 4-6b, right, blue), again supporting the notion that PI3K-mediated activation of LFA-1 is mediated by inhibition of RASA3, and without RASA3, *Pik3cd* KO does not affect the activation of LFA-1 to the same extent. Similarly, when treating Rasa3 KO T cells with Idelalisib (p110δ inhibitor) during ICAM-1-binding, it did not limit ICAM-1-binding as much as Idelalisib treatments in WT T cells (Figure 4-6c).

To understand the respective contribution of RAP1a and RAP1b to the effects of *Rasa3* KO these two proteins were also knocked out, and ICAM-1-binding seemed to mainly be affected by *Rap1b* KO, with only a minor ICAM-1-binding decrease in *Rap1a* KO cells (Figure 4-6b). However, it is clear that there is redundancy between the RAP1 isoforms as none of the KOs completely ablated ICAM-1-binding (Figure 4-6b). The notion that RAP1b is the major isoform is in accordance with the expression levels, where RAP1b is expressed at higher levels than RAP1a (Figure 4-6d).

4.3.2 PI3K-dependent recruitment of RASA3 to the membrane

To understand mechanistically how PI3K inhibits RASA3, I decided to pursue evaluating location of RASA3 by imaging. To effectively image RASA3 I created fusion constructs containing GFP instead of mRuby, as the mRuby constructs were not bright enough for good confocal imaging. We found that RASA3 at steady state (poly-L-lysine) or ICAM-1 was mainly bound to the plasma-membrane (PM), but saw a higher concentration of RASA3 at the membrane when plating cells on anti-CD3-coated plastic (Figure 4-7a-b). Intriguingly, PI3Kδ inhibition with Idelalisib resulted in reduced PM location of RASA3 as quantified by PM/Cytosol intensity ratio (Figure 4-7a). Further, to validate the RASA3^{PHmut} constructs did not bind PIs the membrane, we imaged our GFP and mRuby RASA3^{PHmut} and found that the PHmutant of RASA3 had completely ablated membrane binding (Figure 4-7c-d). These findings indicate that PI3Kδ activity is required for effective recruitment of RASA3 to the membrane and is a likely mechanism involved in inhibition of RASA3.

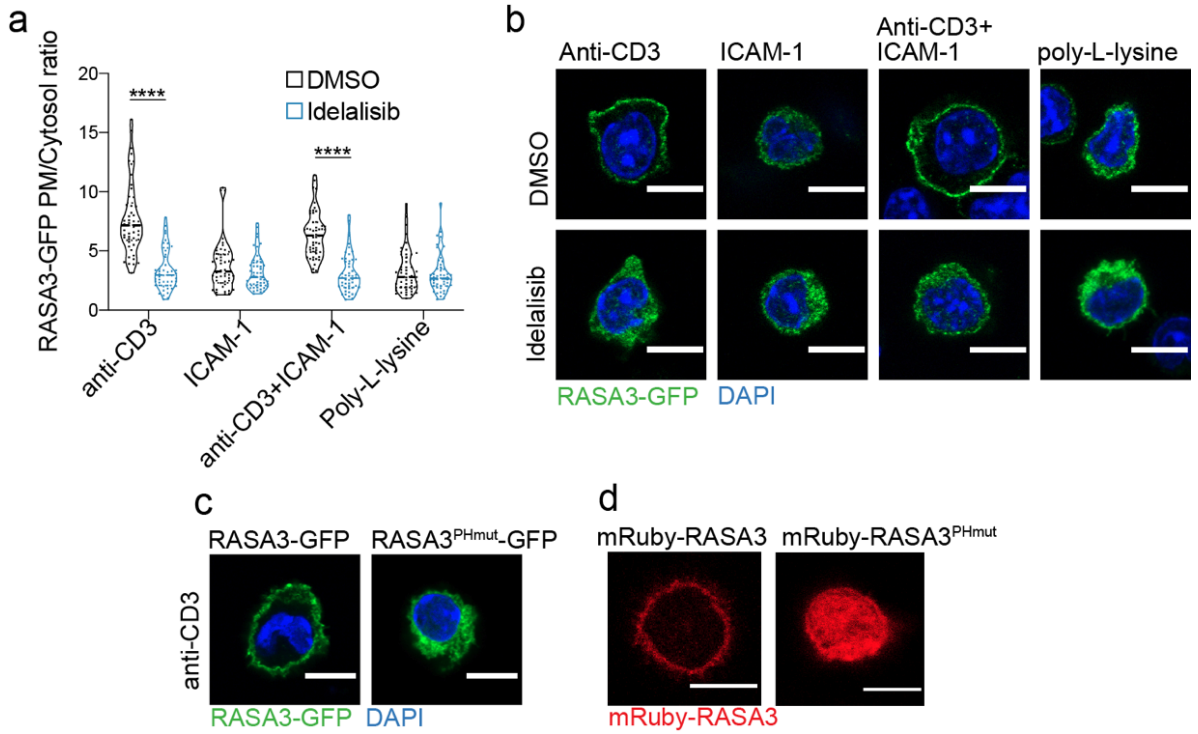

Figure 4-7. RASA3 location is PI3K dependent. **a**, Quantification of plasma membrane (PM)/cytosol intensity ratio of RASA3-GFP in CD4$^+$ T cells on indicated coating following treatment with DMSO or Idelalisib. **b**, Images of data quantified in (**a**) (scale: 7 μm). **c-d**, RASA3-GFP and RASA3^{PHmut}-GFP stained with anti-GFP antibodies

(**c**) or mRuby-RASA3 and mRuby-RASA3PHmut (**d**). Data in (**a**) are truncated violin plots of 47-50 cells per sample, pooled from 3 experiments. Data in (**b-d**) are representative of 3 experiments. *P<0.05; **P<0.01, ***P<0.001, ****P<0.0001 as determined by two-way ANOVA with Holm-Šídák's multiple comparison comparing DMSO to Idelalisib treatment within condition (**a**). Julie H. Thomsen conducted imaging and quantification of pictures in (**a**-**c**) under my supervision.

As LFA-1 is important in the formation of conjugates, we hypothesised that RASA3 would be spatiotemporally regulated in the IS during conjugate formation. Julie H. Thomsen optimised an assay for imaging of T:B cell conjugates using activated OT-II TCR transgenic $CD4^+$ T cells following transduction with the RASA3-GFP constructs with activated WT B cells and imaging by confocal microscopy. The images were taken as z-stacks through the conjugates, allowing us to evaluate RASA3 location in the z-plane at surprisingly high resolution (Figure 4-8a-b). From her imaging it was clear that RASA3 localised in the peripheral or distal SMAC, whereas LFA-1 appeared more centralised in the central or peripheral SMAC (Figure 4-8a-b). Thus, RASA3 seemed to be expelled from the IS centre and pushed to the T cells lamellipodia-like protrusions that wrap around the B cell. To investigate whether the location in the IS was PI3Kδ-dependent Julie H. Thomsen conducted the same experiment in absence or presence of Idelalisib, and found that following Idelalisib-treatment the dSMAC location of RASA3 seemed to be somewhat disrupted resulting in a greater majority of the B:T cell conjugates having colocalised RASA3 and LFA-1 as evident from an increased Pearson's correlation coefficient measuring colocalization between RASA3 and LFA-1 (Figure 4-8c-d). The effects were not statistically significant, but it was clear that only the treatments without Idelalisib had cells with very clear separation of RASA3 and LFA-1 (Figure 4-8c). Repeat experiments would help determine to what extent Idelalisib treatment affect RASA3 in the IS at different timepoints following conjugation.

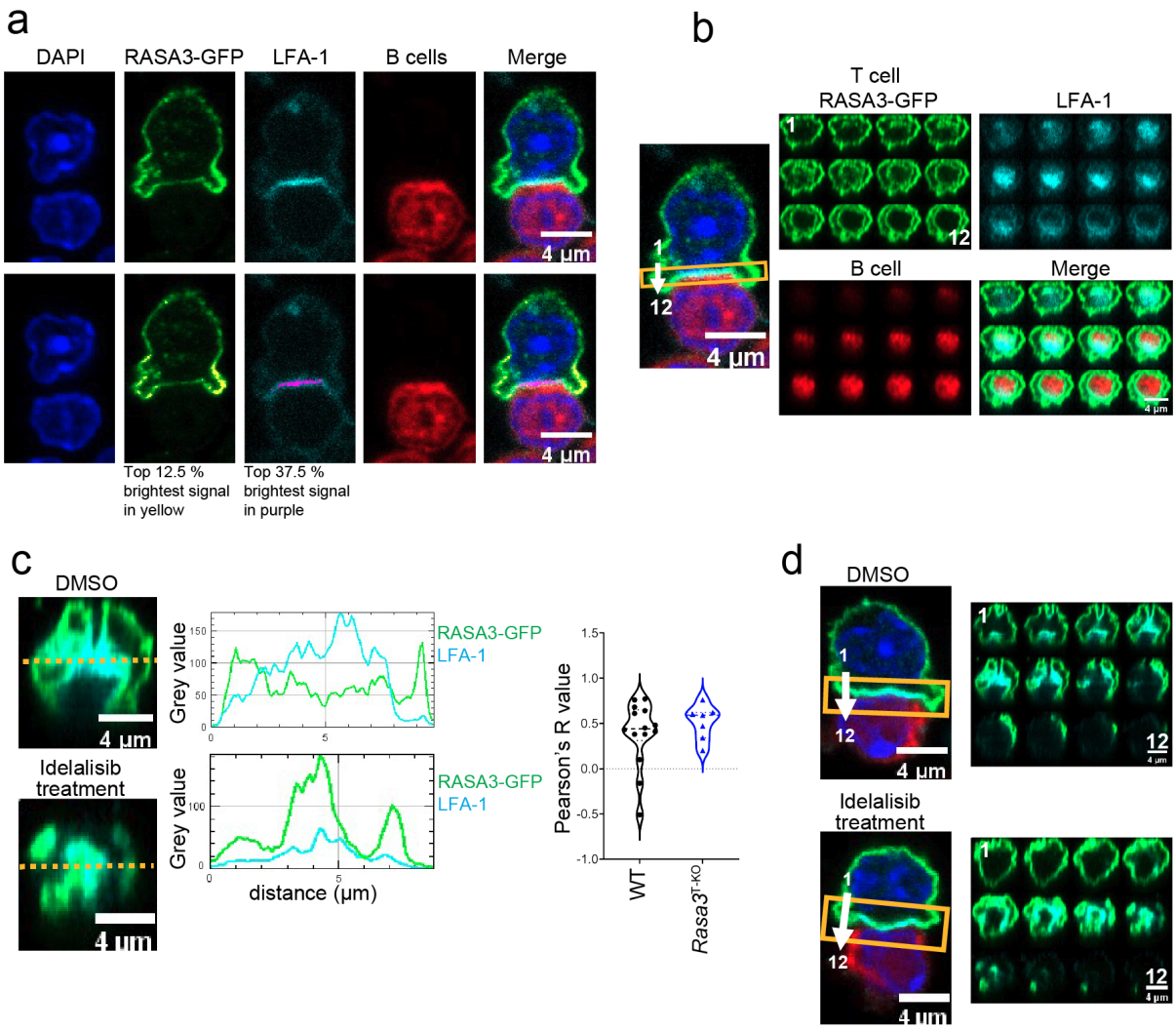

Figure 4-8. RASA3 localisation in B:T cell conjugate immunological synapses. Activated and RASA3-GFP-transduced OT-II TCR transgenic T cells mixed with LPS-activated $OVA_{323-339}$-pulsed prestained B cells, incubated 30min, stained with anti-GFP, anti-LFA-1, and DAPI and imaged by confocal microscopy in z stacks. **a**, Representative images in the X-Y plane are shown with LFA-1 capping at the synapse with (upper) and without highest intensity of LFA-1 (purple) and RASA3 (yellow) indicated in different colour. **b**, Z planes are shown for the same conjugate with montage of 12 images through the Z stack. **c**, The Z plane is further shown following treatment of the conjugates with Idelalisib (1 μM, PI3Kδ inhibitor) during conjugate formation. Colocalisation was determined by Pearson's R Correlation Coefficient for WT and *Rasa3* KO T cells. **d**, Z-stack montages are

further shown for the IS presented in (**c**). These imaging experiments were repeated 3 times by Julie H. Thomsen under my supervision.

4.4 Rasa3 KO increases T:B cell conjugation

As LFA-1 is important for conjugate formation, we were interested in whether *Rasa3* KO T cells were better at forming conjugates *in vitro*. To evaluate conjugate formation, naïve OT-II T cells were mixed with $OVA_{323-339}$-pulsed B cells and counted the formed conjugates and normalized conjugate numbers to the number of T cells on the slides. This experiment showed that there is a trend towards increased conjugate formation, albeit not statistically significant (Figure 4-9a, d). Further, the contact length of the conjugates with *Rasa3* KO T cells were significantly longer than the WT conjugates (Figure 4-9b), possibly as a result of more LFA-1 interactions in the IS resulting in a bigger synapse. We further quantified the % of the conjugates that had LFA-1 capping to the IS, and observed a trend towards more LFA-1 capping in the *Rasa3* KO T cell conjugates (Figure 4-9c,e). Together this hinted an effect on conjugate formation in *Rasa3* KO T cells with increased LFA-1 capping and a larger contact interface between the T cell and B cells. However this experiment would have to be repeated to ensure reproducibility. Further experiments evaluating the localisation in a live microscopy setting using techniques such as TIRF microscopy which produces images of lower optical thickness would be ideal for localisation studies. Further, lipid-bilayers could aid in understanding the dynamics of the RASA3 subcellular location.

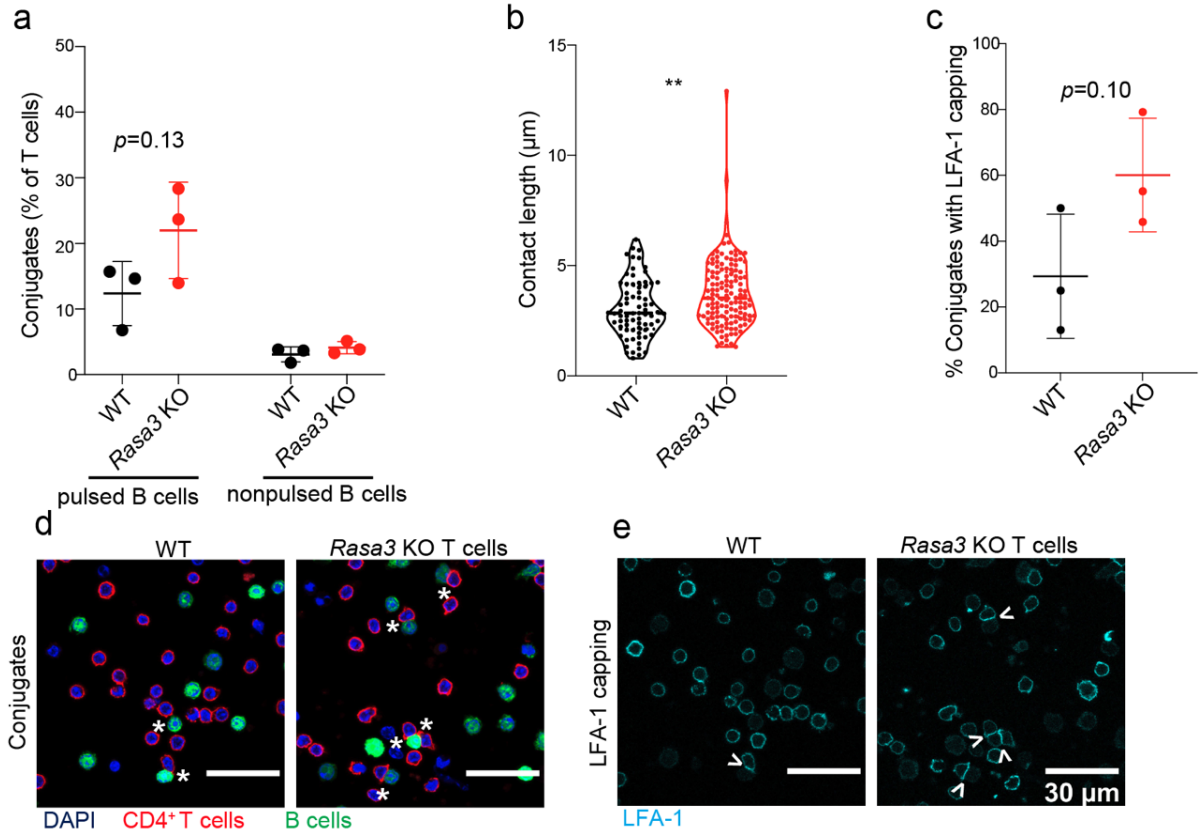

Figure 4-9. Conjugate formation with *Rasa3* KO T cells. OT-II WT and KO T cells were mixed with LPS-stimulated $OVA_{323-339}$-pulsed B cells for 30 min followed by fixation and imaging. **a**, Conjugates were counted for each sample and normalised to the T cells present on the slides with pulsed and non-pulsed B cells. Each dot represents a mouse (Error bars: mean±SD). **b**, Contact length of each conjugate in the pulsed samples (WT: n=73 cells, *Rasa3* KO: n=135 cells). **c**, % conjugates with LFA-1 capping in pulsed samples from (**a**). **d**-**e**, Representative pictures of conjugates (**d**) or LFA-1 capping (**e**). Scale bar: 30 μm. Experiments were performed twice with 3 biological repeats. *P<0.05; **P<0.01, ***P<0.001, ****P<0.0001 as determined by unpaired two-tailed Student's t test. This imaging experiment was performed by Julie H. Thomsen under my supervision and will need to be repeated.

4.5 Discussion

RASA3 has been implicated in development of, and integrin activation in platelets [337, 350, 352], but its role in regulating integrins in T cells has not been described. I have in this chapter demonstrated that RASA3 is a potent regulator of LFA-1-mediated ICAM-1-binding and adhesion negatively regulated by PI3K in T cells.

4.5.1 RASA3, keeping LFA-1 at bay through RAP1

I show that mechanistically RASA3 suppresses the activity of RAP1 which is a major activator of LFA-1, and that this inactivation of RAP1 is responsible for the effect of RASA3 on LFA-1 activation. I further describe how *Rasa3* is expressed at high levels in naïve T cells, whereas mRNA and protein copy numbers are greatly decreased within hours (and up to 5 days) following TCR stimulation. This downregulation may help lower the threshold of activation for LFA-1, potentially allowing activated T cells to respond more rapidly and migrate in response to lower concentrations of antigen or chemokines. Indeed, the threshold for activating LFA-1 is higher in naïve T cells than in activated T cell blasts. Although activated T cells also express higher levels of integrins, these findings could explain, in part, why integrin activation on resting T cells is "silenced" [249], whereas integrins on migratory effector T cells have increased capacity to bind ICAMs [420]. If this indeed is the case, RASA3 is supposedly most important in naïve cells, whereas activated T cells are less dependent on RASA3; during T cell activation and differentiation the RASA3 levels would dictate migration patterns and the propensity to engage a target or APC. This is in accordance with the observation that *Rasa3* KO *in vitro* seems to increase the propensity of naïve $CD4^+$ T cells to form conjugations although these experiments would have to be repeated.

4.5.2 PI3K-mediated inactivation of RASA3

PI3Ks function by generating PIP_3 at the plasma membrane where it serves as a lipid anchor to recruit downstream signalling proteins, usually leading to their activation. In contrast, RASA3 has been suggested to be negatively regulated by PI3K-mediated signalling in platelets [337] (See Chapter 1.4). Consistent with this idea, I observed that a PH-domain mutant of RASA3, which cannot bind PIP_3 and is hence uncoupled from inhibition by PI3K, suppressed ICAM-1-binding to a greater extent than WT RASA3. Moreover, in the absence of RASA3, PI3Kδ is no longer required for the activation of RAP1; treatment with a PI3Kδ inhibitor reduced RAP1 activation in WT cells, but this was not observed in cells lacking RASA3. The findings further show that PI3K signalling regulates the location of RASA3 in T cells. Together, these results

suggest a novel mechanism for PI3K-mediated regulation of LFA-1, involving inhibition of a PIP_3-binding protein (Figure 4-10).

It is intriguing to speculate how PI3K might negatively regulate the activity of a PIP_3-binding protein; It is notable that the location of RASA3 is PI3K dependent, both in the IS and in the membrane of cells on coated coverslips. Moreover, previous data indicate that the PH domain of RASA3 has one of the highest affinities for PIP_3 among all PH domains[227]. These observations raise several possibilities, including that RASA3 is sequestered away from RAP1 by PIP_3, that PIP_3-binding affects the conformation of RASA3, or that PIP_3 brings RASA3 close to a binding partner that helps inhibit the catalytic activity of RASA3.

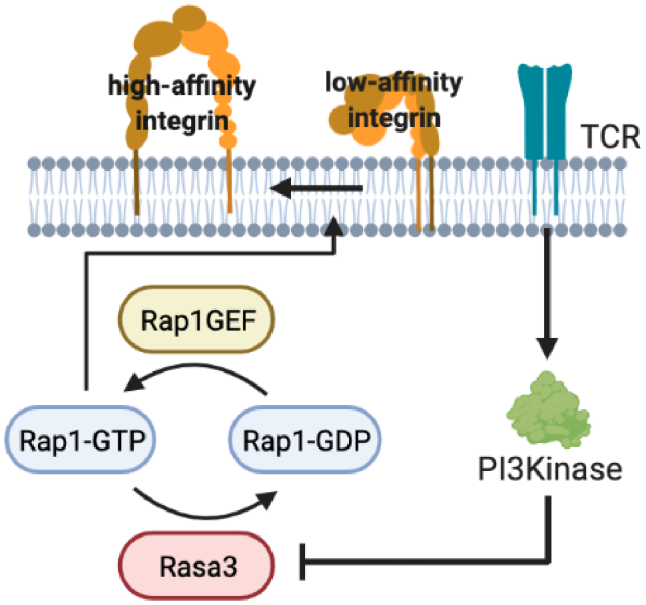

Figure 4-10. PI3K-mediated inactivation of RASA3. PI3K-mediated inactivation of RASA3 results in increased RAP1-GTP and thereby activation of LFA-1. Figure made in Biorender.

The sequestration hypothesis is supported by the observation that RASA3 in T:B cell conjugates is segregated from LFA-1 in the IS. Thus LFA-1 and the necessary effectors such as RAP1 would be located in specific subdomains of the membrane, whereas RASA3 would be sequestered in others. This hypothesis is somewhat similar to the mechanism by which CD45 is sequestered from the TCR during T cell activation [421]. However, there are major differences as RASA3 would be directly sequestered by PIP_3 and not by interaction with other proteins. PIP_3 levels in the IS are known to be depleted from the cSMAC at certain stages of

IS formation, and enriched in the pSMAC/dSMAC, which supports the sequestration hypothesis. However, this does not easily explain how RASA3 is regulated by PI3K in our soluble ICAM-1-binding assay, as the assay does not employ an IS with spatiotemporal segregation of LFA-1 from other proteins although there could still be separation of proteins in microdomains in the membrane following TCR crosslinking [422]. Another possible explanation is that PIP_3-binding affects the conformation of RASA3 directly. The conformational changes of RASA3 during RAP1-GTP catalysis have been studied, and it is clear that the RAP1 GAP function of RASA3 is dependent on the C2 domains [343, 419], but it is unclear whether binding of specific PIs directly affect the ability of RASA3 to catalyse GTP hydrolysis. Future studies should investigate to what extent PIP_3 affects the catalytic function of RASA3 *in vitro*, either by further mutagenesis and investigation of the PH domain functions, or by investigating GAP function directly in presence and absence of PIP_3 *in vitro*. Lastly, it is possible that PIP_3 acts as a mediator of RASA3 interactions with other proteins resulting in either degradation, inactivating post-translational modifications, or direct inactivation. This mechanism is supported by the fact that RASA3 has been found to bind the E3 ubiquitinase CBL-B in T cells [355]. Whether this binding is PI3K-dependent is unknown, but as CBL-B is also a binder of PI3K [81], as well as other LFA-1 regulating proteins such as CRKL [258, 293], it is possible that there is a bigger complex of proteins recruited to PIP_3 during T cell stimulation. Further, after evaluating posttranslational modification sites by the prediction site Scansite (www.Scansite.mit.edu) it is clear that there are multiple phosphorylation sites that are predicted to be phosphorylated by protein kinase A, PDK1, and/or AKT that all are regulated downstream of PI3K [423] as well as a ubiquitination site which could possibly be ubiquitinated by CBL-B. Together the presented findings do not provide sufficient data to exclude any of these mechanisms, and it is likely that a combination of the different mechanisms are in play depending on the context. LFA-1 regulation during migration might be regulated by RASA3 through different mechanisms than regulation of LFA-1 in the IS. An interesting point is that the PH domain does not seem to be required for RASA3-mediated suppression of RAP1-GTP. RAP1 is mainly membrane associated either at the plasma membrane or on internal membranes, but has been shown to primarily translocate to the plasma membrane following TCR stimulation [424], and the fact that the PH domain is not required for RASA3 function suggests that other domains mediate the membrane proximal

functions of RASA3; this could be mediated by the dual C2 domains that from other proteins are known to mediate interactions with lipids in a calcium-dependent manner [425].

4.5.3 Chapter summary

In this chapter I present evidence that RASA3 is a potent negative regulator of LFA-1 which is negatively regulated by PI3K. The findings implicate RASA3 in keeping LFA-1 in check in naïve T cells, and is spatiotemporally regulated during T cell stimulation; both on plastic and in the context of conjugation with APCs. The mechanism for PI3K-mediated negative regulation of RASA3 is not completely understood, but I have presented evidence that PI3K is involved in recruitment to subregions of the membrane thus providing evidence that RASA3 is regulated downstream of PI3K through its location.

Chapter 5 – RASA3 in T cell homeostasis and T-dependent assistance to humoral immunity

5. RASA3 in T cell homeostasis and T-dependent assistance to humoral immunity

LFA-1 is crucial for T cell homeostasis, and has been implicated in efficient development of T_{FH} cells [147] and the formation of GCs [146, 148], two processes that are intimately connected to and dependent on T cell:B cell interactions to develop T-dependent humoral immunity [426] (described in Chapter 1.1.4). In this chapter I therefore investigate how T cell specific deletion of *Rasa3* in T cells affects mice at steady state, and how *Rasa3* KO affects the process of T_{FH} cell and GC formation.

5.1 *Rasa3* KO alters T cell homeostasis

To understand the functional consequences of increased LFA-1-mediated adhesion arising from loss of *Rasa3*, I analysed thymocyte and T cell populations from *Rasa3*$^{T\text{-}KO}$ mice. Consistent with the late thymic deletion of floxed alleles deleted by *Cd4*^{Cre}, *Rasa3*$^{T\text{-}KO}$ mice had normal levels of DP and DN T cell precursors in the thymus (Figure 5-1a-d). However, I consistently observed modest increases in percentages and numbers of CD4 and especially CD8 SP thymocytes (Figure 5-1e-f).

Further evaluation revealed that *Rasa3*$^{T\text{-}KO}$ thymi contained greater percentages of the most mature (TCR^{hi}CD24^{lo}) CD4 and CD8 SP thymocytes relative to WT (Figure 5-1b, g), such that the ratio of mature SP cells (TCR^{hi}CD24^{lo}) to immature SP cells (TCR^{+}CD24^{hi}) was significantly higher (Figure 5-1h). Thus, mature SP thymocytes appeared to be accumulating relative to their immature progenitors in *Rasa3*$^{T\text{-}KO}$ thymi (Figure 5-1h). These data raise the possibility that *Rasa3* deficiency may reduce or delay egress of mature thymocytes from the thymus or that Rasa3 deficiency affects the late stages of development. To evaluate whether the *Rasa3* KO SP thymocytes that have successfully undergone positive selection seem to have received a greater TCR stimulation as a result of increased LFA-1-dependent interactions with APCs, I evaluated CD5 and CD69 levels on the SP and DP thymocytes. I found similar levels of CD5/CD69 on the DP thymocytes and CD4 SP thymocytes and slightly higher CD5 and

CD69 on the CD8 SP thymocytes although not consistently across replicates (Figure 5-1i). This higher CD5 and CD69 could indicate that the *Rasa3* KO thymocytes receive slightly higher TCR stimulation during maturation, however there are more mature SP thymocytes in the KOs, that might also skew the histograms slightly.

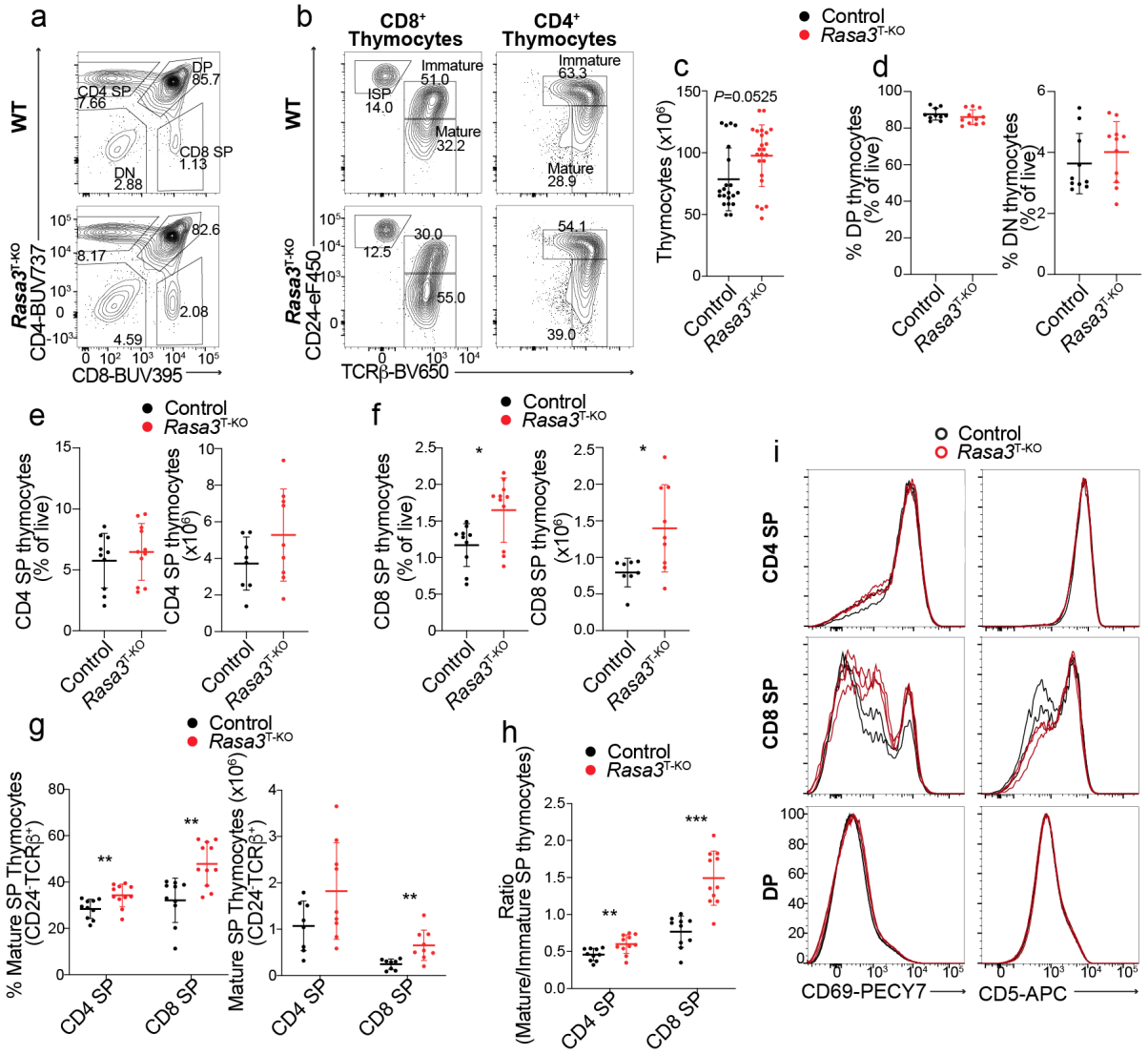

Figure 5-1. Characterisation of thymus in *Rasa3*$^{T\text{-}KO}$ mice. **a**,**b**, Representative plots of CD4 vs CD8 stains showing DN, CD4 SP, DP and CD8 (SP) cells (**a**) or mature and immature SP thymocytes (**b**) in thymi from WT control and *Rasa3*$^{fl/fl}$ x *Cd4*^{Cre} (*Rasa3*$^{T\text{-}KO}$) mice. **c**, Thymocyte (n=20) numbers from WT and *Rasa3*$^{fl/fl}$ x *Cd4*^{Cre} (*Rasa3*$^{T\text{-}KO}$) mice. **d**, Percentages of DP and DN TCRβ^{+} thymocytes (WT n=10, *Rasa3*$^{T\text{-}KO}$ n=11). **e**, **f**, Percentages and numbers of CD4 SP (**e**) and CD8 SP (**f**) thymocytes (WT n=10, *Rasa3*$^{T\text{-}KO}$ n=11). **g-h,** Percentages (left) and numbers (right) of mature and immature CD4 and CD8 SP thymocytes from WT (n=10) and *Rasa3*$^{T\text{-}KO}$ (n=11) mice (**g**), as well as ratios of mature/immature SP thymocytes (**h**). **i**, CD69 and CD5 levels on SP and DP

thymocytes (overlay of 3 WT and 3 *Rasa3*$^{T\text{-}KO}$ histograms). Data in (**c**-**h**) are pooled from 3 experiments and are means ± SD with a single dot representing one mouse. *P<0.05; **P<0.01, ***P<0.001, ****P<0.0001 as evaluated by Mann-Whitney U-tests with Holm-Šídák's multiple comparison correction.

Rasa3$^{T\text{-}KO}$ mice had normal numbers of total cells in pLN and spleen (Figure 5-2a). However, evaluation of peripheral T cells in *Rasa3*$^{T\text{-}KO}$ mice revealed reduced proportions and numbers of T cells in pLN, spleen and most notably, blood (Figure 5-2b-d). Both CD4$^+$ and CD8$^+$ T cell populations were reduced in *Rasa3*$^{T\text{-}KO}$ mice (Figure 5-2b-d). Interestingly, I observed no differences in T cell numbers in gut-associated mLNs and PPs. These results could be a result of altered patterns of entry or egress in the T cells consistent with the observations in the thymus presented in (Figure 5-1).

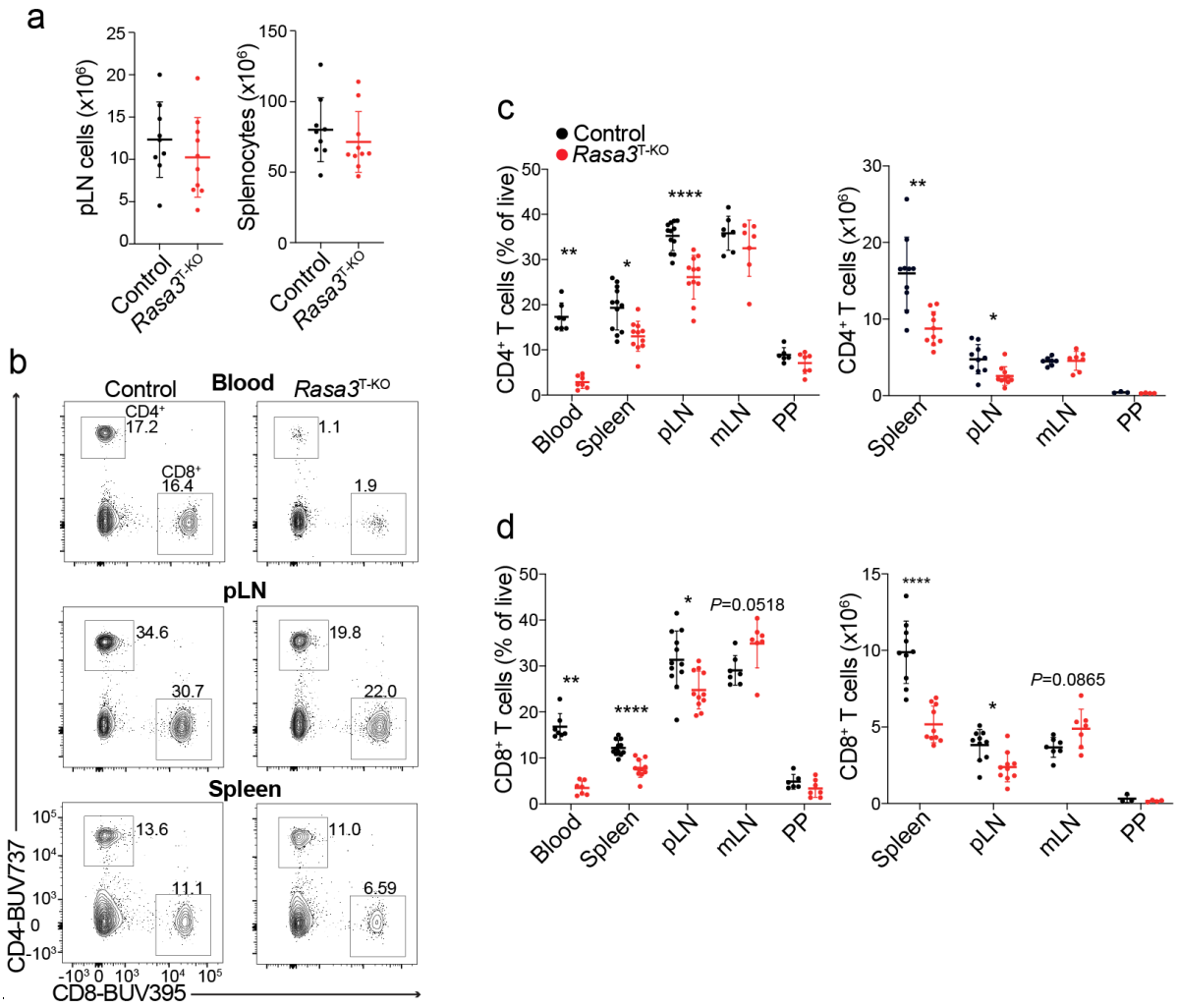

Figure 5-2. Decreased T cells in periphery of *Rasa3*$^{T\text{-}KO}$ mice. **a**, pLN and spleen cell numbers (n=9-10) numbers from WT and *Rasa3*$^{fl/fl}$ x *Cd4*^{Cre} (*Rasa3*$^{T\text{-}KO}$) mice. **b**, Representative flow cytometry plots of T cells in blood, pLN

and spleen in WT (n=12) and *Rasa3*$^{T\text{-}KO}$ mice (n=11). **c,d**, CD4$^+$ (**c**) and CD8$^+$ (**d**) T cell percentages (left), and numbers (right) from blood, spleen, pLN, mLN, and PP. Data in (**a, c-d**) are pooled from 3 experiments and are means ± SD with a single dot representing one mouse. *P<0.05; **P<0.01, ***P<0.001, ****P<0.0001 as evaluated by Mann-Whitney U-tests with Holm-Šídák's multiple comparison correction.

Phenotypic analyses revealed higher proportions of activated T cells (CD4$^+$ (Figure 5-3a-b) and CD8$^+$ T cells (Figure 5-3a,d)) in the blood and pLNs from *Rasa3*$^{T\text{-}KO}$ mice as well as lower proportions of naïve T cells (CD4$^+$ (Figure 5-3a,c) and CD8$^+$ T cells (Figure 5-3a,e)). These findings could be due to lymphopenia-induced expansion, and/or because activated T cells, which express low levels of RASA3, may be less affected than naïve T cells, which express higher levels of RASA3 (See chapter 4.2.1). The T_{reg} cell proportion of CD4$^+$ T cells in the spleen was also lower (Figure 5-3f), possibly also a consequence of RASA3 being found at high levels in T_{reg} cells [427].

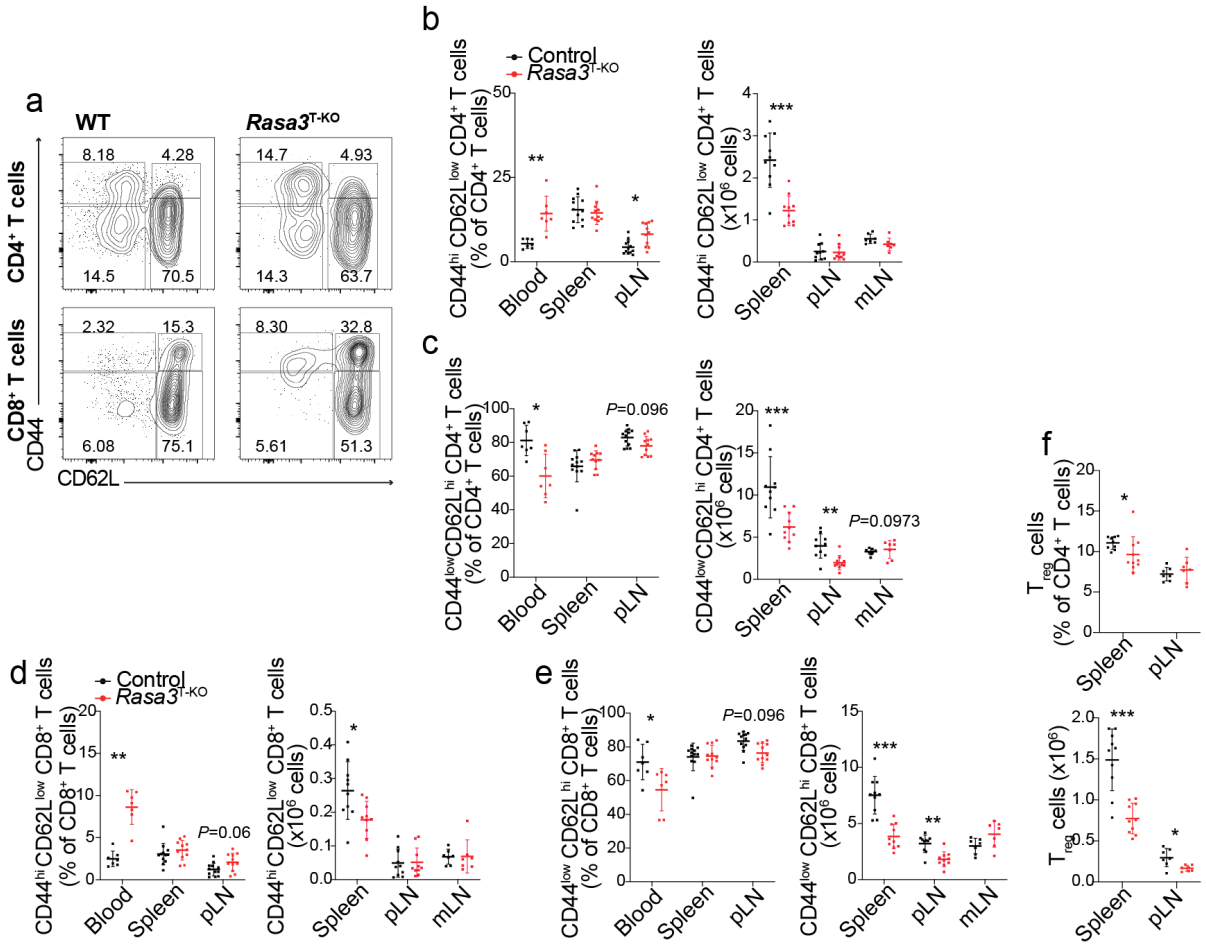

Figure 5-3. Higher proportion of activated T cells in *Rasa3*$^{T\text{-}KO}$ mice. **a**, Representative plots of CD44/CD62L profiles from CD4$^+$ (top) and CD8$^+$ (right) T cells from blood. **b**-**e**, Percentages and numbers of CD44^{hi}CD62L^{low} CD4$^+$ (**b**) and CD8$^+$ (**d**) T cells, as well as naïve CD44^{low}CD62L^{hi} CD4$^+$ (**c**) and CD8$^+$ (**e**) T cells (WT n=7-12, *Rasa3*$^{T\text{-}KO}$ n=7-12). **f**, Percentages and numbers of T_{reg} cells (% of CD4$^+$ T cells). Data in (**b-f**) are pooled from 3 or more experiments and are means ± SD with a single dot representing one mouse. **P*<0.05; ***P*<0.01, ****P*<0.001, *****P*<0.0001 as evaluated by Mann-Whitney U-test with Holm-Šídák's multiple comparison correction.

Together these findings suggest that RASA3 indeed seems to be necessary for the ability of mature T cells to exit the thymus, and subsequently for overall T cell homeostasis and location in the periphery. This is in accordance with the findings that RASA3 regulates LFA-1 which is crucial for T cell migration.

Findings by colleagues at NIH

Colleagues at NIH investigated whether *Rasa3* KO T cells had altered migration. Dr. Dominic Golec and Dr. Chung Park conducted a series of adoptive transfer experiments combined with flow cytometry, static imaging of sections, and intravital microscopy. A crucial set of experiments performed by Dr. Golec transferred WT CD45.1 and *Rasa3* KO CD45.2 $CD4^+$ T cells to CD45.1/2 WT mice and evaluated the transferred KO/WT ratio after 1h, 24h, and 72h (Appendix Figure A-1a). These experiments showed that Rasa3 KO T cells did not enter the LNs to the same extent as the WT cells; after 1h there were ~5x as many WT cells as KO cells in the SLOs. After 24h and 72h the KO/WT ratio increased, suggesting the Rasa3 KO T cells were able to enter the SLOs, albeit slower than WT cells (Appendix Figure A-1b). Dr. Golec performed similar experiments, but with injection of anti-CD62L after 24h to block further LN entry (Appendix Figure A-1c). Anti-CD62L injections would thus allow us to evaluate egress the following hours. *Rasa3* KO/WT ratios were now significantly increased, and showed that *Rasa3* KO cells were not able to egress the LNs as efficiently as WT cells (Appendix Figure A-1d). These adoptive transfer experiments therefore revealed that *Rasa3* KO T cells showed delayed and reduced entry into LNs. Further experiments revealed that *Rasa3* KO T cells stick to the HEVs during TEM resulting in a reduced rate of entry, and that the cells have reduced capacity for LN egress. These findings help explain the altered distribution of T cells in the periphery observed in intact mice presented above. These data illustrate the importance of LFA-1 deactivation in the regulation of T cell location and migration.

5.2 T cell-specific *Rasa3* KO results in decreased GC responses to immunisation

5.2.1 *Rasa3* KO results in altered distribution of T follicular cells

To evaluate the consequences of *Rasa3* loss on antibody-dependent immune responses involving T_{FH} cell and GC formation, I immunised *Rasa3*$^{T\text{-}KO}$ mice with NP-OVA emulsified in Alum adjuvants in the right hock (or AddaVax intramuscular for imaging) and investigated recruitment of T cells, generation of T_{FH} cells and GCs, and the capacity to develop antigen-specific antibody responses (Figure 5-4a). Mice were culled 8 days post immunisation at the peak of the T_{FH} cell response and the *draining popliteal LN* (dLN) and resting popliteal LN (rLN) was analysed for each mouse. Following NP-OVA immunisation, *Rasa3*$^{T\text{-}KO}$ mice had markedly fewer total cells in dLNs than WT mice (Figure 5-4b). This decrease was more pronounced than the decrease in cell numbers in non-challenged pLNs, including the rLN. To evaluate the T_{FH} cell populations in detail, I stained for T_{FH} cell markers by flow cytometry and gated as shown in (Figure 5-4c). This allowed me to evaluate the relative distribution of T_{FH} cells, T_{FR} cells, and non-T_{FR} T_{reg} cells in the rLN and dLN.

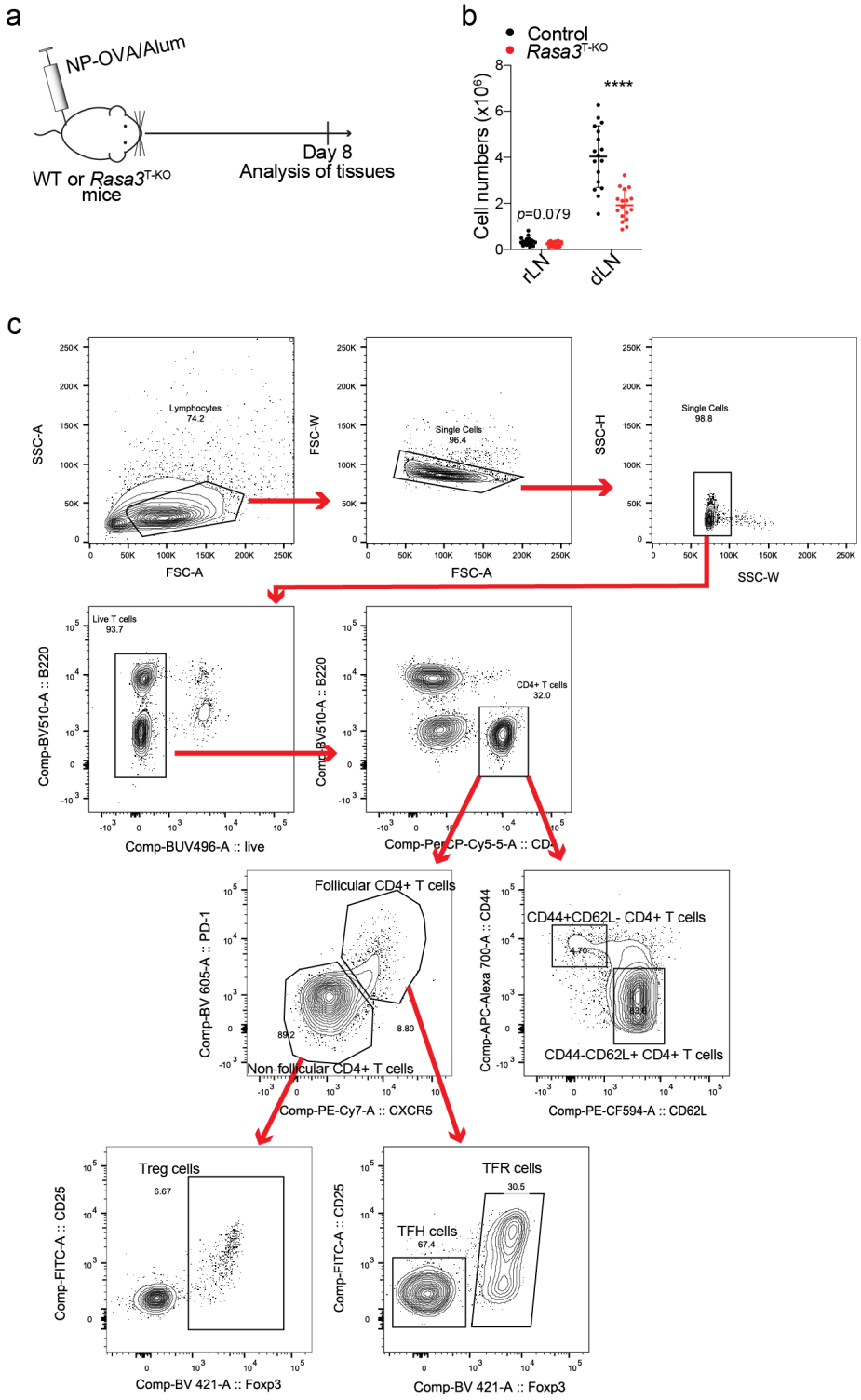

Figure 5-4. NP-OVA/Alum immunisation of WT and *Rasa3*$^{T\text{-}KO}$ mice. **a**, diagram of NP-OVA/Alum immunisation showing mice being immunised 8 days before analysis. **b,** Cell numbers in resting LNs (rLNs) and draining LNs (dLNs) from NP-OVA-immunized mice. **c**, gating strategy for T_{FH} stain of LNs from immunised mice. **c**, Flow cytometry panel of T_{FH}/T_{FR} cell populations post immunisation; red arrows showing gating hierarchy. Data in (**b**)

is pooled from 3 experiments (WT, n=17; *Rasa3*$^{T\text{-}KO}$, n=17. *P<0.05; **P<0.01, ***P<0.001, ****P<0.0001 evaluated by Mann-Whitney U-tests (**b**) with Holm-Šídák's multiple comparison correction.

When comparing WT with *Rasa3*$^{T\text{-}KO}$ mice, there were significantly lower percentage of CD4$^+$ T cells, and as a result of the lower dLN cell numbers and the lower percentage, the overall CD4$^+$ T cell numbers were very low (Figure 5-5a). This suggests that CD4$^+$ T cells exhibited deficient dLN entry and/or reduced expansion in response to immunisation. Although a higher proportion of the CD4$^+$ T cells expressed the T follicular cell markers, PD1 and CXCR5 in the *Rasa3*$^{T\text{-}KO}$ mice (Figure 5-5b), the total numbers of FoxP3$^-$ T_{FH} cells and FoxP3$^+$ T follicular regulatory (T_{FR}) cells were reduced (Figure 5-5c-d), consistent with the reduction of CD4$^+$ T cells in the dLN (Figure 5-5a). Nonetheless, LFA-1 was highly expressed on the surface of CXCR5$^+$PD1$^+$ T follicular cells compared to other CD4$^+$ T cells in both WT and mutant mice (Figure 5-5b), as previously observed [147]. Notably, I also observed a reduction of the ratio of T_{FH} cells to T_{FR} cells (Figure 5-5e) in *Rasa3*$^{T\text{-}KO}$ mice compared to WT mice. Such reduced T_{FH}/T_{FR} cell ratio can negatively affect the GC response [428, 429]. This was consistent with the percentage T_{FR} cells of CD4$^+$ T cells being increased in the *Rasa3*$^{T\text{-}KO}$ mice, whereas the T_{FH} cell percentages of CD4$^+$ T cells were not significantly increased (Figure 5-5c-d). Further, I found two-fold increase in the percentage of T_{FR} cells/FoxP3$^+$ CD4$^+$ T cells in *Rasa3*$^{T\text{-}KO}$ mice (Figure 5-5f), possibly indicative of a higher percentage of FoxP3$^+$ T_{reg} cells developing into T_{FR} cells in *Rasa3*$^{T\text{-}KO}$ mice. The increased T_{FR}/T_{reg} cell ratio is also consistent with the finding that there was a higher percentage of CXCR5$^+$PD1$^+$ CD4$^+$ follicular T cells in the *Rasa3*$^{T\text{-}KO}$ mice compared to WT mice (Figure 5-5b).

Together the presented data shows that *Rasa3*$^{T\text{-}KO}$ mice have a reduced capacity to establish T_{FH} cell responses. As the overall CD4$^+$ T cell numbers were significantly decreased, the T_{FH} cell numbers were decreased following immunisation. This decrease in T_{FH} cell numbers could be a result of either reduced migration of T cells into the LN and/or B cell zone in response to immunisation, or decreased capacity to receive sufficient proliferative signals. Further, I present data showing that there is a decreased ratio of T_{FH}/T_{FR} cells following immunisation, and increased T_{FR}/T_{reg} cell ratio suggesting that *Rasa3* KO favours increased T_{FR} cell development.

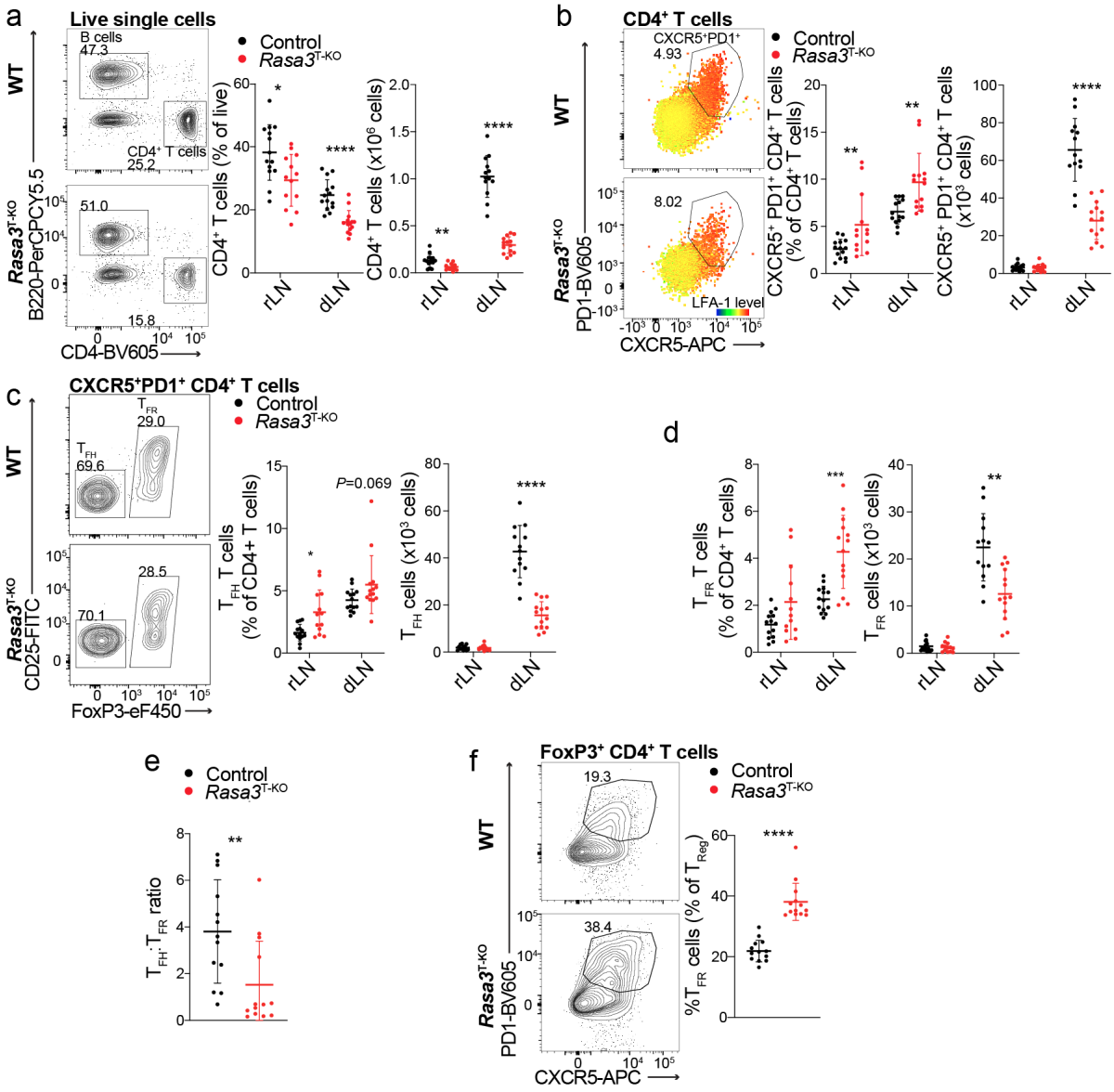

Figure 5-5. *Rasa3*$^{T\text{-}KO}$ results in altered distribution of T follicular cells. **a-f,** Flow cytometry analysis of NP-OVA/Alum immunised mice (resting LN: rLN, draining LN: dLN). **a-c**, Plots, percentages and numbers of CD4$^+$ T cells (**a**), CXCR5$^+$PD1$^+$ CD4$^+$ T cells (LFA-1 levels indicated by colour) (**b**), FoxP3/CD25 plots gated on T_{FH} cells (FoxP3$^-$CD25$^-$CXCR5$^+$PD1$^+$CD4$^+$ T cells) (**c**) and T_{FR} cells (FoxP3$^+$CXCR5$^+$PD1$^+$CD4$^+$ T cells) (**d**), ratio of T_{FH}:T_{FR} cells (**e**), and percentage T_{FR} cells of T_{reg} cells (WT n=13, *Rasa3*$^{T\text{-}KO}$ n=13). Data are pooled from 3

experiments and are means ± SD with a single dot representing one mouse. **P*<0.05; ***P*<0.01, ****P*<0.001, *****P*<0.0001 as evaluated by Mann-Whitney U-tests.

5.2.2 RASA3 is required for effective T-dependent humoral immunity

To investigate how the decreased T_{FH} cell numbers and altered T_{FH}/T_{FR} cell ratio affected the GC response, I performed flow cytometric staining for GC markers, and antigen-specific ELISAs. Staining of GC B cells allowed me to evaluate GC B cells, antigen-specific GC B cells plasma cells, and class switching by flow cytometry (Figure 5-6).

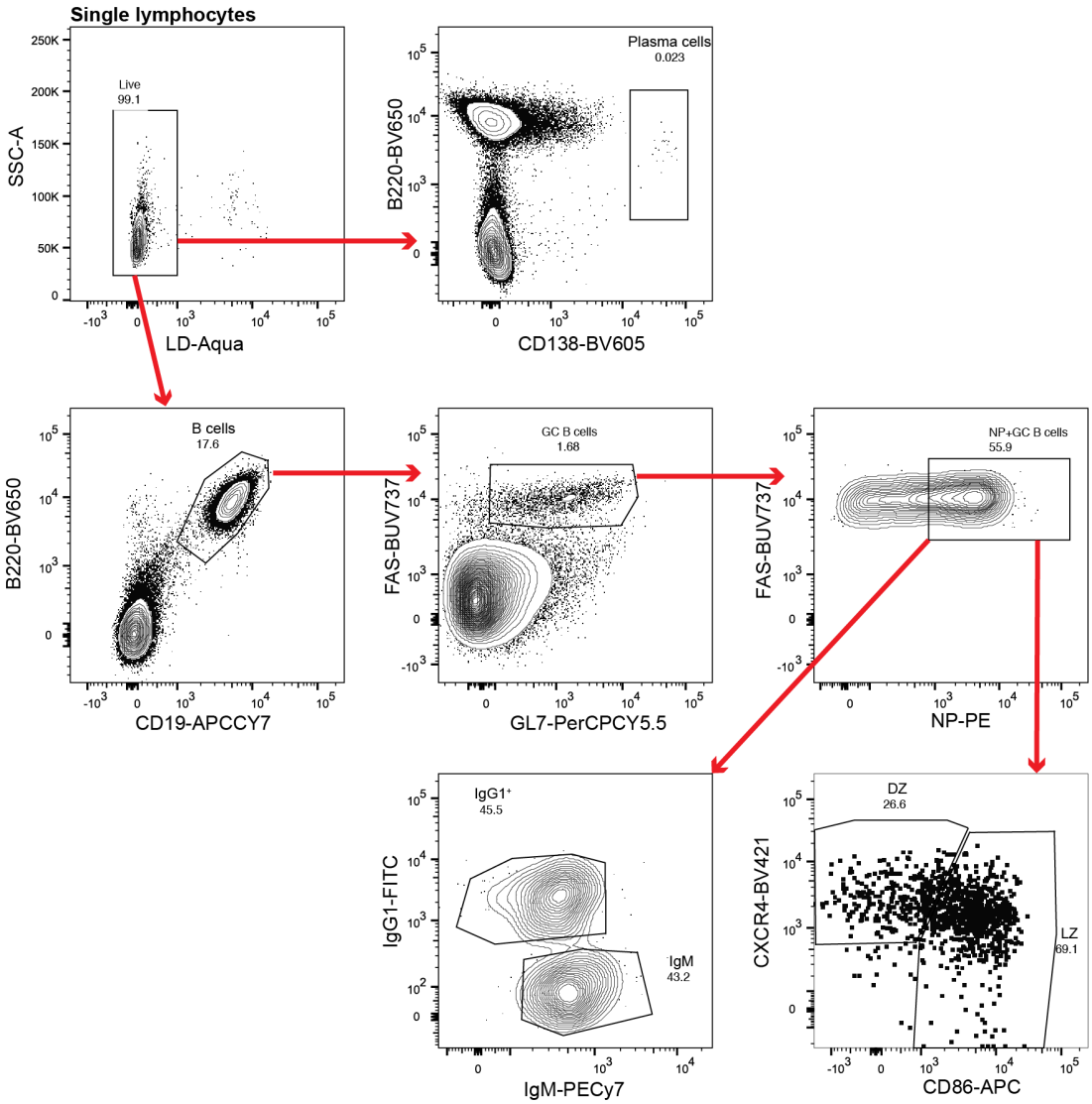

Figure 5-6. Gating strategy for GC B cell flow cytometric analysis. Gating strategy starting at single lymphocytes showing gating strategy of NP-OVA/Alum immunised dLN. For analysis of B cell populations as indicated.

In accordance with reduced T_{FH} cell numbers, I found lower B cell numbers in the NP-OVA/Alum immunised dLNs (Figure 5-7a), and lower percentages and numbers of GC B cells in *Rasa3*$^{T\text{-}KO}$ mice (Figure 5-7b). Similar results were observed when using AddaVax as adjuvant instead of Alum. AddaVax was used for Ce3D imaging experiments (experiments performed by Dr. Golec and Dr. Tibor Veres, data not shown), and elicits both T_H1 and T_H2 immune responses [430]. For AddaVax experiments NP-OVA/AddaVax was injected intramuscularly as the Ce3D protocol applied was optimised for this immunisation regimen. These results are consistent with the requirement of T_{FH} cells for GC responses [96].

GC B cells that did develop in the *Rasa3*$^{T\text{-}KO}$ mice exhibited similar percentages of NP-antigen specificity as WT GC B cells (Figure 5-7c), suggesting that *Rasa3*$^{T\text{-}KO}$ did not affect the ability of B cells to form antigen-specific responses. However, there were significantly fewer plasma cells in the dLNs, both when measured by percentages as well as numbers (Figure 5-7d).

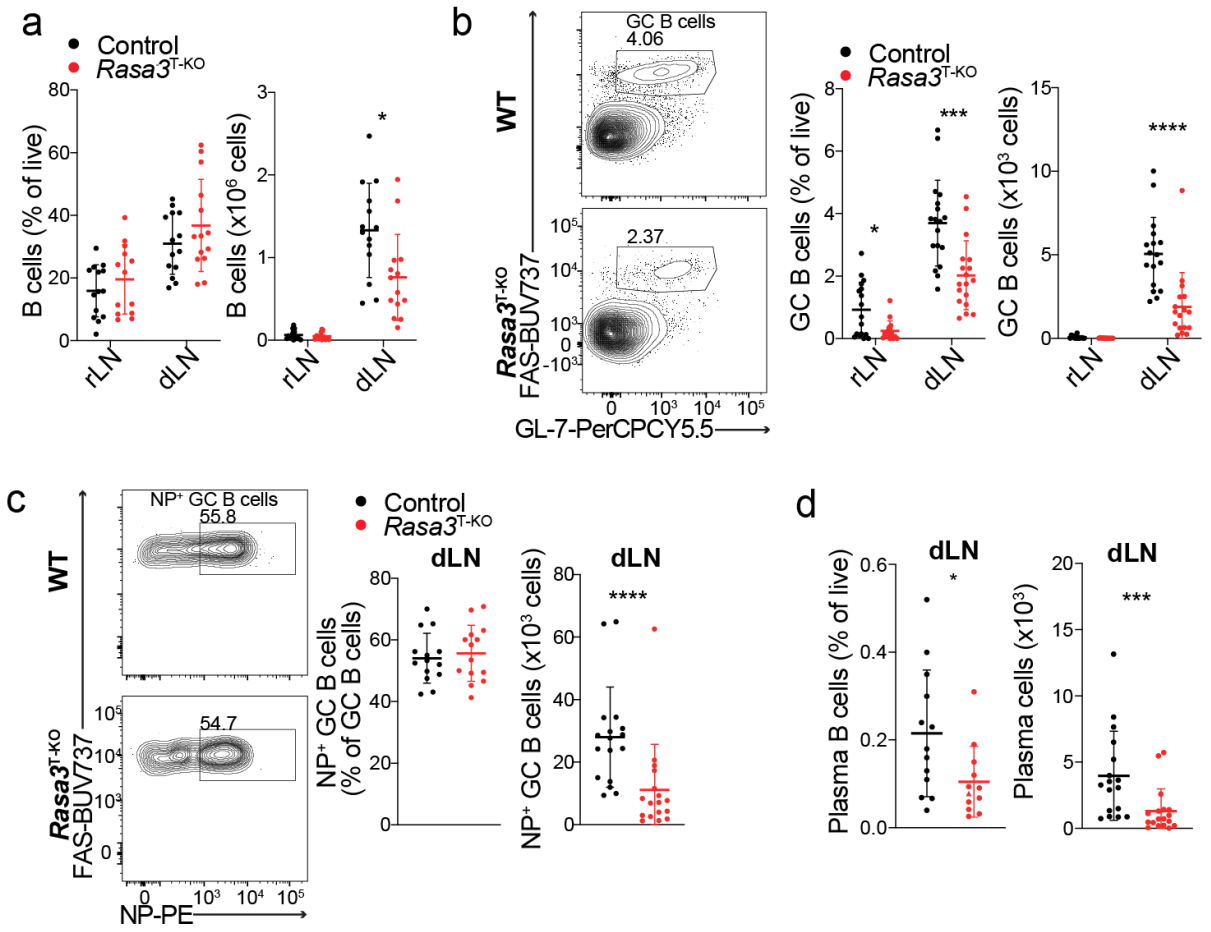

Figure 5-7. GC B cell responses in *Rasa3*$^{T\text{-}KO}$ mice. **a**, B cell percentages and numbers from rLN and dLN. **b-d**, Plots, percentages, and numbers of GC B cells (Fas$^+$GL7$^+$ B220$^+$CD19$^+$) (**b**), NP$^+$GC B cells (**c**), and CD138$^+$ plasma cells (**d**) (WT n=17, *Rasa3*$^{T\text{-}KO}$ n=17). Data are pooled from 3 experiments, means ± SD with each dot representing one mouse. **P*<0.05; ***P*<0.01, ****P*<0.001, *****P*<0.0001 evaluated by Mann-Whitney U-tests.

To evaluate whether the GCs formed in *Rasa3*$^{T\text{-}KO}$ mice were similar to WT GCs, the LN architecture was evaluated by imaging of whole LN 3D imaging. For these experiments immunisation was performed with NP-OVA emulsified in AddaVax. When evaluating the GC structure by volumetric Ce3D imaging, GCs appeared slightly smaller in volume in the *Rasa3*$^{T\text{-}KO}$ mice and had a lower density of T_{FH} cells/GC compared to WT mice, consistent with the

reduced number of T_{FH} cells (Figure 5-7c, Movie 1; https://drive.google.com/file/d/1v80VQzvDdrDPm6X7OWV4pX4EUXH9G16F/view?usp=sharing), These data indicate that RASA3 is required for optimal generation of structured GCs.

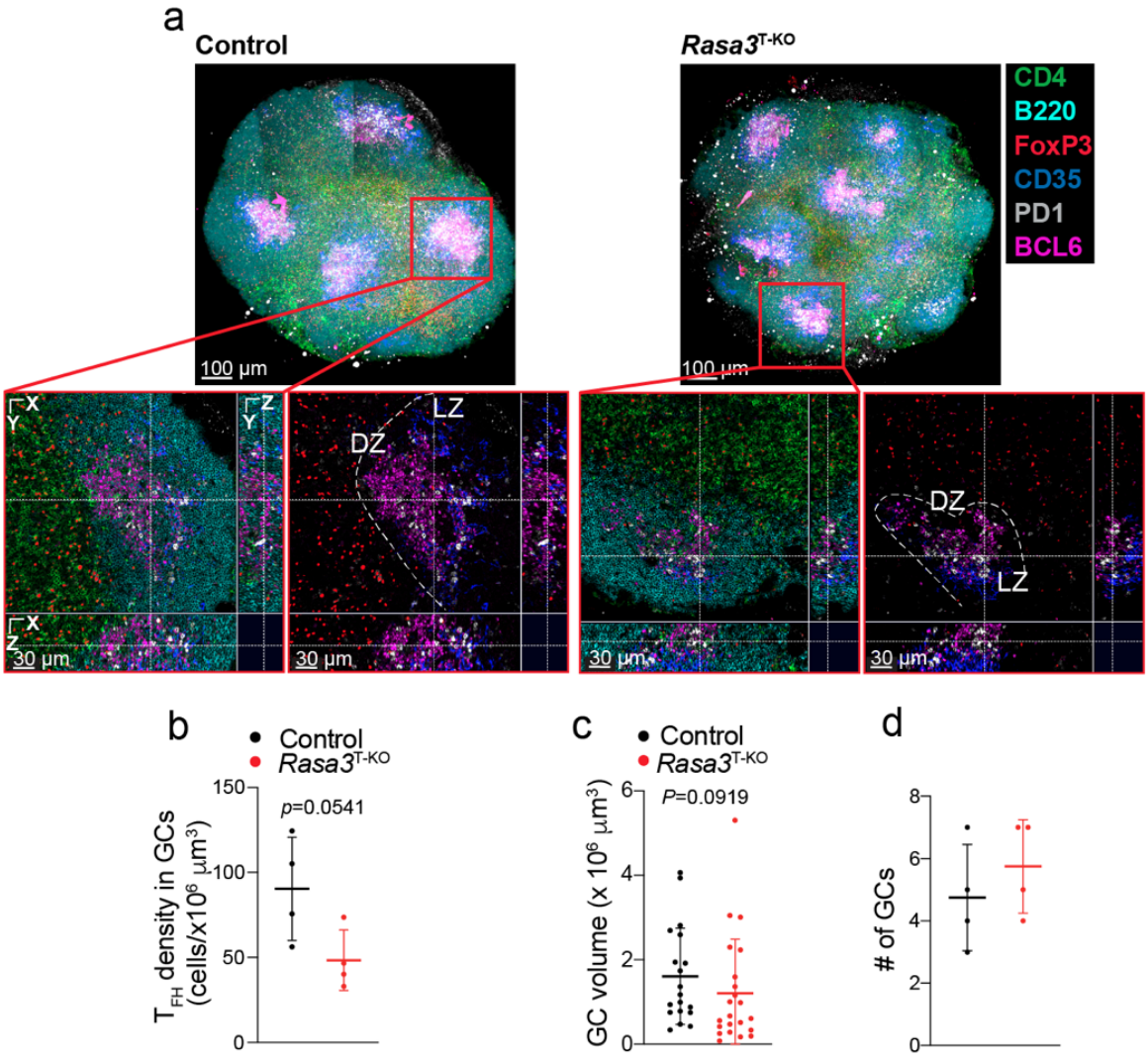

Figure 5-8. Ce3D imaging of *Rasa3*$^{T\text{-}KO}$ dLNs following immunisation. **a**, Representative Ce3D imaging of dLNs following immunisation with NP-OVA/AddaVax. LNs were stained with anti-CD4 (green), anti-B220 (teal), anti-FoxP3 (red), anti-CD35 (blue), anti-PD1 (white), and anti-BCL6 (pink). **b**, quantification of T_{FH} cell density in the GCs (WT n=4, *Rasa3*$^{T\text{-}KO}$ n=4). **c**, GC volume of individual GCs quantified from Ce3D images. **d**, Number of GCs per dLN. Data in (**b-d**) are from 1 experiment. **P*<0.05; ***P*<0.01, ****P*<0.001, *****P*<0.0001 as evaluated

by Student's *t* test (**b**, **d**) or Mann-Whitney U-test (**c**). Imaging was performed by Dr. Tibor Verez, analysis was performed by Dr. Edward Schrom and me.

CSR of GC B cells is dependent on T_{FH} cells, and is regulated by IL-4 and IL-21 cytokines secreted by T_{FH} cells [431]. *Bcl6*$^{fl/fl}$ x *Cd4*^{Cre} mice and other mice that lack T_{FH} cells (and T_{FR} cells) have markedly reduced class-switched IgG1 antibodies following immunisation [390, 432] indicating a critical role for T_{FH} cells in this process.

To investigate whether *Rasa3* KO affected CSR I quantified IgG1$^+$ versus IgM$^+$ GC B cells by flow cytometry as well as Ig levels by ELISA. I observed increased percentages of IgM$^+$ and decreased percentages of IgG1$^+$ NP-specific GC B cells indicative of defective CSR (Figure 5-9a). Total IgG and IgM levels were unaltered by *Rasa3* KO in T cells (Figure 5-9c) consistent with homeostatic B cell numbers in resting LNs being normal in *Rasa3*$^{T\text{-}KO}$ mice (Figure 5-7a) as well as B cell numbers in pLN, mLN, PP, and spleen under steady state (Figure 5-9b). Similarly, the levels of low affinity antigen-specific IgM (binding NP_{20}) were unaltered by *Rasa3*$^{T\text{-}KO}$ (Figure 5-9d). However, high-affinity IgM was modestly decreased (Figure 5-9d), and both low- and high-affinity IgG1 were markedly decreased in *Rasa3*$^{T\text{-}KO}$ mice (Figure 5-9e). Together these findings shows that *Rasa3*$^{T\text{-}KO}$ results in significantly decreased T cell assistance for class-switched antibody production.

The observed class switching and antibody defect could be a result of either the *Rasa3* KO T_{FH} cells being defective, T_{FR} cells being more suppressive than WT T_{FR} cells, the decreased T_{FH}/T_{FR} cell ratio, or the overall reduction in T_{FH} cells (and overall T cells) due to defective T cell migration, or a combination of these factors.

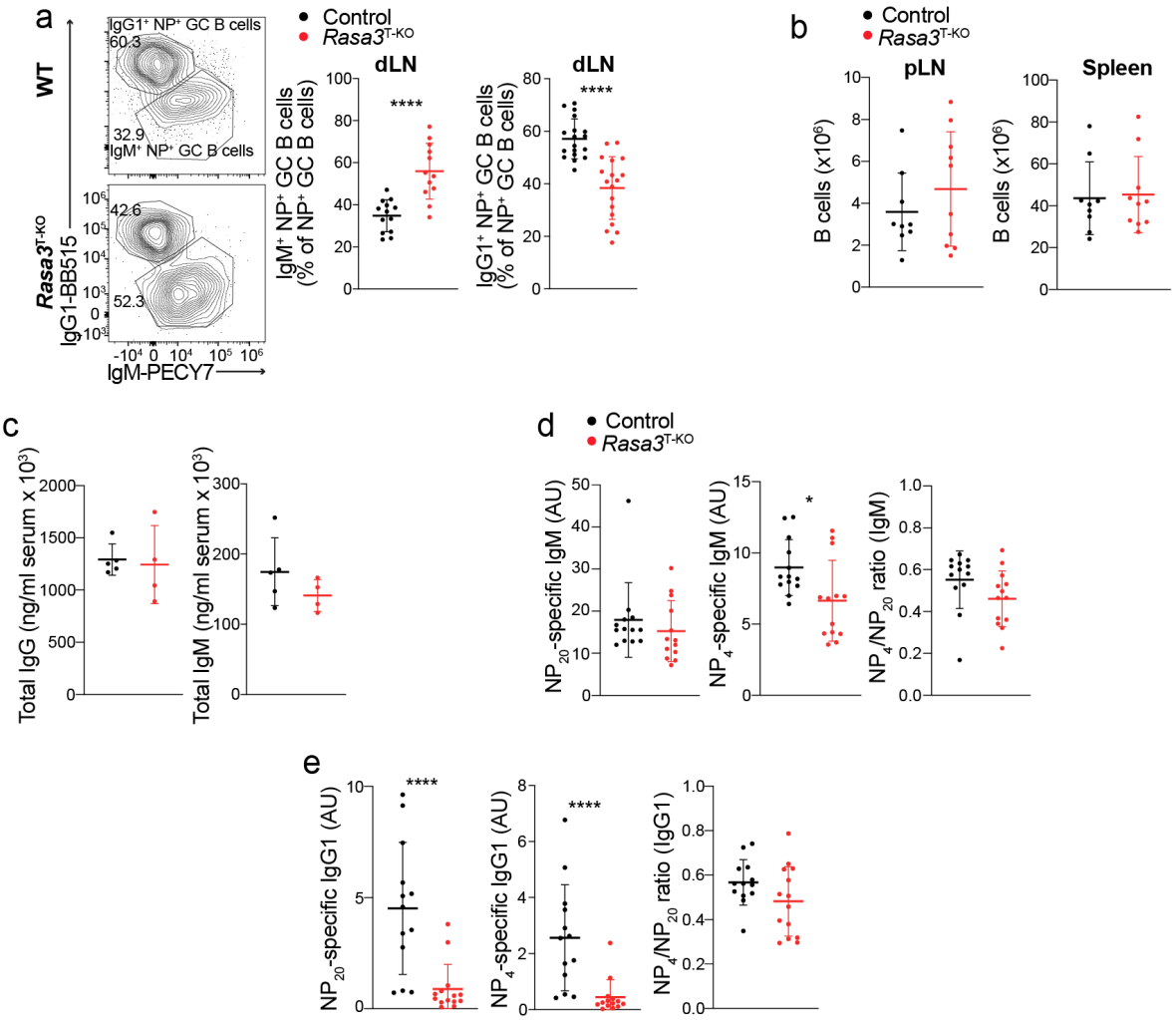

Figure 5-9. Defective class switching and antibody production in *Rasa3*$^{T\text{-}KO}$ mice. **a**, Plots, percentages, and numbers of IgG1/IgM plots and class-switched IgG1$^+$ NP-specific GC B cells (WT n=19, *Rasa3*$^{T\text{-}KO}$ n=22). **b**, B cell numbers in pLN and spleen at steady state (WT n=9, *Rasa3*$^{T\text{-}KO}$ n=10). **c**, Total serum IgG and IgM quantified by ELISA following immunisation (WT n=4, *Rasa3*$^{T\text{-}KO}$ n=5). **d-e**, NP-specific ELISAs of serum from WT and *Rasa3*$^{T\text{-}KO}$ mice immunized with NP-OVA/Alum, showing low-affinity (NP_{20}), high-affinity (NP_4), and NP_4/NP_{20} ratios of IgM (**d**) and IgG1 (**e**) (WT n=13, *Rasa3*$^{T\text{-}KO}$ n=13). Data are pooled from 3 experiments, means ± SD with each dot representing one mouse. **P*<0.05; ***P*<0.01, ****P*<0.001, *****P*<0.0001 as evaluated by Student's *t* test (**c**) or Mann-Whitney U-test (**a-c, d-e**).

A preliminary prognostic of how well the T_{FH} cells worked in intact *Rasa3*$^{T\text{-}KO}$ mice was to correlate GC B cell numbers with T_{FH} cell numbers to get a sense of how well each T_{FH} cell contributed to the GC response. In WT mice, I found both more T_{FH} cells and GC B cells than *Rasa3*$^{T\text{-}KO}$ mice, however when plotting the WT vs *Rasa3*$^{T\text{-}KO}$ mice, there seemed to be a similar

trend of T_{FH} cells/GC B cell in *Rasa3*$^{T\text{-}KO}$ and WT mice suggesting that the T_{FH} cells do function when they are present (Figure 5-10a). Another indicator that *Rasa3* KO T_{FH} cells are capable of supporting GC B cells is evaluation of GC formation in the mLN and PP in unimmunised mice, as these organs did not show a deficiency in *Rasa3* KO T cell numbers compared to WT T cells and GCs are formed there in response to antigens associated with the commensal microbiota. Both mLN and PP showed similar percentages of GC B cells in the *Rasa3*$^{T\text{-}KO}$ mice as in WT mice (Figure 5-10b). Together this suggests that the low number of T_{FH} cells found in *Rasa3*$^{T\text{-}KO}$ mice is a driving factor in the defective GC B cell response.

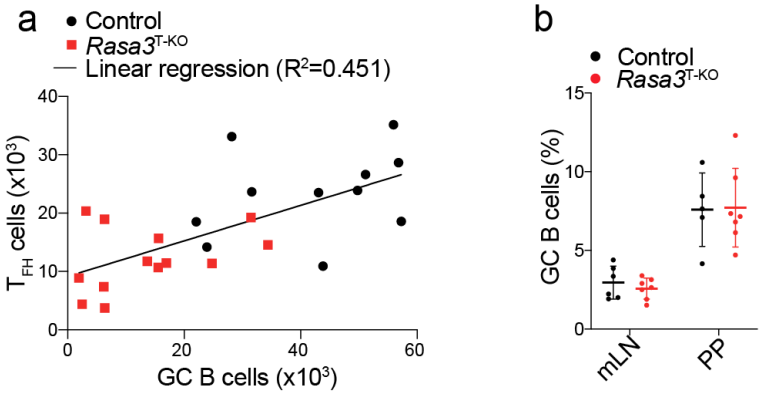

Figure 5-10. *Rasa3* KO T_{FH} cell numbers correlate with GC B cells. **a**, Correlation of T_{FH} and GC B cell numbers in dLN. Linear regression of all datapoints with an Akaike's Information Criterion comparison showing a 85.2 % chance of the two datasets being from a similar regression line (R^2=0.451). **b**, Percentage GC B cells of live B cells in mLN and PP. Data in (**a**-**b**) are pooled from 3 experiments, means in (**b**) are ± SD with each dot representing one mouse.

To examine the T_{FH} cell function in an isolated system not affected by other T cell subsets, and to allow me to artificially introduce antigen-specific T cells, I transferred 1x10^6 WT or *Rasa3* KO or WT naïve OT-II CD4$^+$ T cells into T_{FH}-deficient *Bcl6*$^{fl/fl}$ x *Cd4*^{Cre} mice (Figure 5-11a). I subsequently immunised the mice with NP-OVA/Alum 24h later and evaluated GC formation and T_{FH} cell generation after 8 days by flow cytometry. Again, fewer *Rasa3* KO T cells were found in the LNs post immunisation (Figure 5-11b), albeit slightly higher percentages of these had differentiated into T_{FH} cells (Figure 5-11c), similar to the intact mice. Furthermore, as a consequence of lower number of transferred cells arriving in the LNs of mice receiving *Rasa3* KO T cells, I found lower T_{FH} cell numbers and GC B cell numbers (Figure 5-11d). When correlating T_{FH} cell numbers with GC B cell numbers I found a correlation between T_{FH} cells

and GC B cells following transfer of WT and *Rasa3* KO OT-II $CD4^+$ T cells (Figure 5-11e), similar to my observations in the intact mice. Similar findings were also observed when a greater number of OT-II T cells were transferred in experiments repeated at NIH by Drs. Dominic Golec and Bonnie Huang (see appendix Figure A-2). Importantly, transferred OT-II naïve T cells do not differentiate into T_{FR} cells (Figure 5-11f).

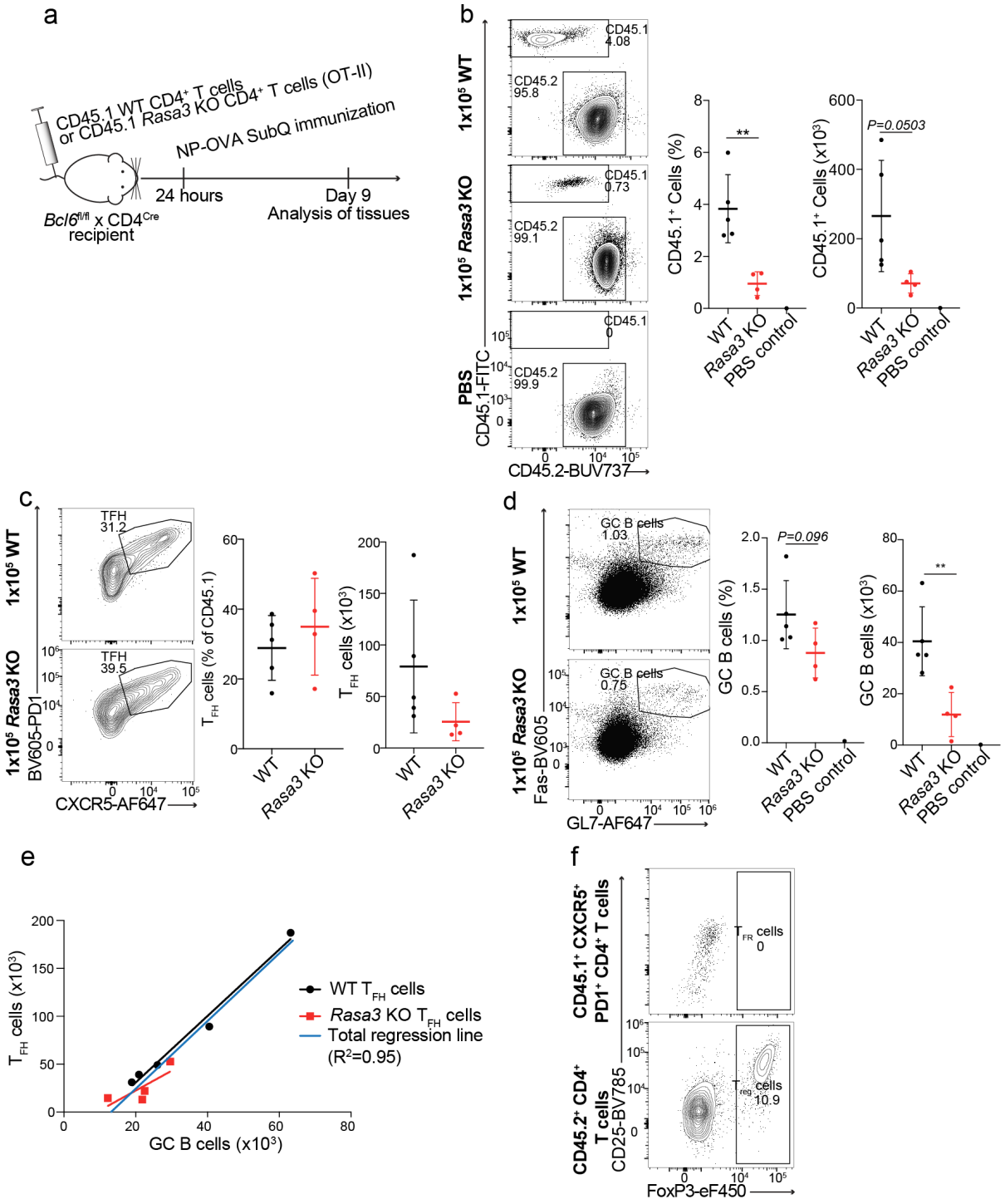

Figure 5-11. OT-II transfers to *Bcl6*$^{fl/fl}$ x *Cd4*^{Cre} mice. **a**, Diagram of OT-II transfer experiments, where I transferred 1x10^5 WT or *Rasa3* KO OT-II TCR transgenic naïve CD4$^+$ T cells into *Bcl6*$^{fl/fl}$ x *Cd4*^{Cre} mice and immunised with NP-OVA/Alum in the right hock after 24 hours and analysed tissues by flow cytometry 8 days later. **b**, representative plots, percentages, and numbers of CD45.1 vs CD45.2 cells in mice following transfer of WT cells, *Rasa3* KO cells or PBS. **c**, Representative plots, percentages, and numbers of CXCR5$^+$PD1$^+$ T$_{FH}$ cells (gated on

CD45.1 cells). **d**, Representative plots, percentages, and numbers of GC B cells (gated on B cells). **e**, Correlation of TFH cells and GC B cells. Black line is regression of mice with transferred WT cells, red line is regression of mice with KO cells, and blue line is regression line of all datapoints (R^2=0.95 for total datapoints). An Akaike's Information Criterion comparison showing a 99.8 % chance of the blue line describing the whole dataset. **f**, Representative plot of FoxP3$^+$ CD25^{hi} cells within the CD45.2$^+$ CD4$^+$ T cells and CD45.1$^+$CXCR5$^+$PD1$^+$CD4$^+$ T cells. Data are representative of 3 experiments and are means ± SD with each dot representing one mouse. **P*<0.05; ***P*<0.01, ****P*<0.001, *****P*<0.0001 as evaluated by Student's *t* test.

Besides affecting the GC B cell numbers, *Rasa3*$^{T\text{-}KO}$ also affected class switching in intact mice. To evaluate whether this was the case in my transfer model I evaluated IgG1/IgM ratios and antigen-specific IgG1 antibodies by ELISA. Surprisingly I found a higher percentage of NP-specific GC B cells in the *Bcl6*$^{fl/fl}$ x *Cd4*^{Cre} mice that had received *Rasa3* KO T cells compared to those that had received WT cells, however as a result of low GC B cell counts there were fewer NP$^+$ GC B cell numbers in the *Rasa3* KO transfers than WT transfers (Figure 5-12a). This increase in NP-specificity is possibly a result of competition for signals from T_{FH} cells being more limited in the mice with *Rasa3* KO T cells due to decreased T_{FH} cells. When the experiments were repeated with higher cell numbers (2 or 5x10^5) the difference in NP$^+$ GC B cell percentages between WT and *Rasa3* KO transfers was diminished (see appendix Figure A-2). Further, when evaluating the class switching in the transfer model, I observed no defect in class switching to IgG1$^+$ NP$^+$ GC B cells (Figure 5-12b), although I still found significantly less NP-specific high- and low-affinity IgG1 in the serum (Figure 5-12c-d), possibly as a result of fewer overall GC B cells.

Thus, *Rasa3* KO T cells can differentiate into T_{FH} cells if they are present in the LNs, and these T_{FH} cells provide help for GC formation and class-switched antibody responses. However, likely due to the decreased numbers of *Rasa3* KO CD4$^+$ T cells (i.e. T_{FH} precursors reaching the LNs), there were fewer T_{FH} cells and decreased formation of GCs resulting in decreased antigen-specific antibodies.

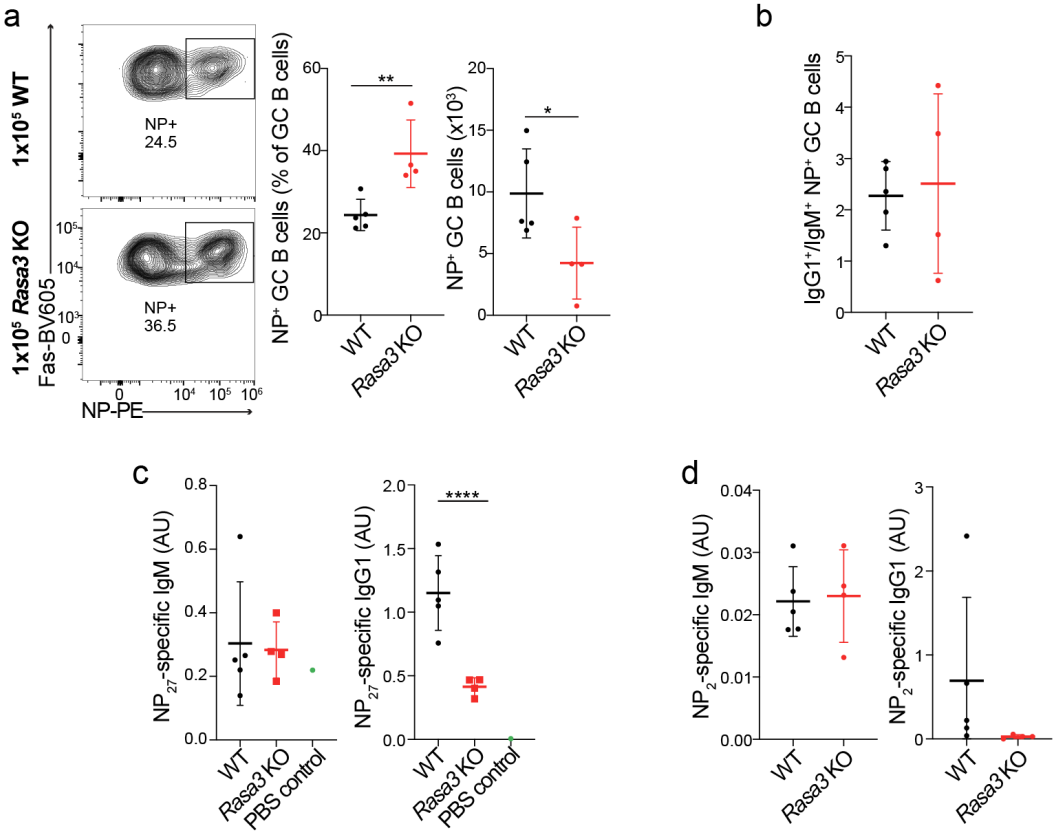

Figure 5-12. Evaluation of class switching in OT-II adoptive transfer model. **a**, Percentages, and numbers of NP⁺ GC B cells in dLNs day 8 following transfer and immunisation as described in Figure 5-11a. **b**, IgG1⁺/IgM⁺ NP⁺ GC B cell ratio. **c-d**, low- (**c**) or high-affinity (**d**) NP-specific ELISA of serum from transfers. Data are representative of 3 experiments and are means ± SD with each dot representing one mouse. **P*<0.05; ***P*<0.01, ****P*<0.001, *****P*<0.0001 as evaluated by Student's *t* test.

5.3 Discussion

RASA3 is crucial for regulating LFA-1 affinity in T cells as presented in Chapter 4. In this chapter I present data implicating RASA3 in T cell homeostasis. As LFA-1 is important for the location, development, and function of T_{FH} cells I further investigated the role of RASA3 in T-dependent humoral immunity, and found that RASA3 is crucial for effective antibody responses.

5.3.1 The role of RASA3 in T cell homeostasis and migration

The presented data supports a major role for RASA3 in T cell homeostasis, and potentially T cell egress from the thymus. I however cannot rule out that other effects such as altered selection or survival in the thymus and periphery are also affected. Intrathymic migration is tightly controlled and CCR7 deficient T cells are defective in their migration to the medulla, and develop autoimmunity as a result of defective negative selection [433, 434]. Further, thymic egress is dependent on LFA-1; knocking out the RAP1 positive regulator MST1 (which decreases LFA-1 activity) results in a build-up of mature thymocytes in the thymus, and decreased lymphocyte counts in blood and LNs [435-437]. *Mst1* KO mice that have decreased T cell LFA-1 activity thereby have strikingly similar thymic egress phenotypes to those observed in the *Rasa3*$^{T\text{-}KO}$ mice, despite having an opposite effect on LFA-1. This suggests LFA-1 has to be tightly regulated, and both too little or too much LFA-1 activity will result in build-up of mature thymocytes in the thymus. It is still possible that RASA3 affects thymic T cell development, however with the current models these defects would not be picked up in the *Rasa3*$^{T\text{-}KO}$ mice. To evaluate thymic development further, additional stains and other mouse models would have to be applied such as HY TCR transgenic mouse models that allow for evaluation of negative or positive selection in female and male mice, respectively [438].

The possible thymic egress defect in *Rasa3*$^{T\text{-}KO}$ mice could at least partly explain the peripheral lymphopenia, however it does not explain it in entirety; I observed normal T cell numbers in gut associated lymphoid organs, as well as most other peripheral tissues I have studied, whereas the lymphopenia is particularly pronounced in blood suggesting there is altered migration of the T cells in and out of peripheral organs. Nonetheless, I did not find any tissues where T cells were increased in *Rasa3*$^{T\text{-}KO}$ mice compared to WT mice supporting the finding that the T cells have defective egress from the thymus, reduced thymic development, reduced survival in the periphery, or are stuck in unidentified locations. In this regard, it is relevant that I also observe increased ICAM-1-binding in response to chemokines in the absence of *Rasa3*.

It is clear that *Rasa3* KO T cells elicit defective entry through HEVs from transfer experiments performed by Dr. Golec at NIH, KO T cells transferred do not enter LNs as readily as the co-transferred WT cells, suggesting that entry is somehow impaired, however these KO/WT ratios

normalised after 24 hours, suggesting the cells do catch up to some extent. This suggests that KO cells reside in the LNs longer than WT cells, allowing the KO cells to catch up eventually. Indeed, when LN entry is blocked with anti-CD62L, the KO/WT ratio increases; thus WT T cells seem to exit the LNs more readily than *Rasa3* KO T cells. So why are the *Rasa3* KO T cells slower at entry and egress? Intravital two-photon imaging performed by Dr. Chung Park at NIH provided some answers; it seems like the *Rasa3* KO T cells are able to initiate TEM, but the cells were often trapped in the perivascular space in the process of entering the LN. Further, the KO T cells seem to interact for longer times with the endothelium before migrating through the endothelial layer. It is likely that this is a result increased ICAM-1-binding I described in Chapter 4, leading to *Rasa3* KO T cells sticking to the HEVs longer before LFA-1 is deactivated, and resulting in prolonged LFA-1-ICAM-1 interaction. Similarly, it is likely a similar mechanism responsible for decreased LN egress; WT T cells readily undergo lymphatic egress through lymphatic endothelia, whereas *Rasa3* KO T cells may stick to the lymphatic endothelial cells and therefore do not egress as readily. In conjunction, slower intranodal migration as a result of LFA-1/ICAM-1-interactions might result in *Rasa3* KO T cells migrating more slowly through the paracortex.

Two studies of constitutively active LFA-1 mice recapitulate certain aspects of the hyperactive LFA-1 I find in our *Rasa3* KO T cells including lower LN and PP T cell counts, although one model of LFA-1 hyperactive mice exhibited splenomegaly and normal numbers of blood lymphocytes [149, 439]. In contrast, *Rasa3*$^{T\text{-}KO}$ resulted in reduced T cell numbers in blood, spleen, and LNs, perhaps because *Rasa3* KO T cells can still respond to chemokine and TCR-induced inside-out signalling, although in an altered manner. It is also of note that *Rasa3*$^{T\text{-}KO}$ did not alter T cell migration to gut-associated lymphoid tissues to the same extent as migration to spleen and pLNs. Whether this results from differing homing receptors or the inflammatory environment of the gut, which may provide other signals that regulate lymphocyte homing [440], is an intriguing question.

5.3.2 The role of RASA3 in T-dependent humoral immunity

I found profound defects in high affinity class-switched antibody responses to immunisation of *Rasa3*$^{T\text{-}KO}$ mice and impaired LN entry may be a major contributor to this phenotype. Indeed,

mLN and PPs, which did not exhibit decreased T cells in the absence of *Rasa3* had similar numbers of GC B cells as WT. However, it is also possible that *Rasa3* may impact the function of T_{FH} cells by increasing their adhesion to B cells and allowing selection of lower affinity clones; indeed, low affinity anti-NP antibodies appear to be less affected in my experiments. In addition, RASA3 may affect other T cell populations that affect responses to immunisation. In that regard, it is of interest that I observed decreased T_{FH}:T_{FR} cell ratios in the dLNs of *Rasa3*$^{T\text{-}KO}$ mice, as that T_{FR} cells have been implicated in regulating Ig class switching [441]. T_{FR} cells are not generated from OT-II TCR-transgenic T cells; this may be another reason why I see class switching defects in the intact mice, but not to the same extent following transfers of OT-II cells. My results further suggest an intriguing connection between T cell adhesion and the development of T_{FR} cells from T_{reg} cells, this could be consistent with the requirement for B cell interactions for T_{FR} cell generation as increased LFA-1 activity would possibly increase pre-T_{FR} cell-B cell interactions. It is of note that a recent paper showed that T_{FH} and T_{FR} cells express relatively lower levels of RASA3 compared to naïve T cells (similar to TCR stimulated T cells in vitro) [427]. This could explain why the relative function of individual T_{FH} cells in the *Rasa3*$^{T\text{-}KO}$ mice seems to only be modestly affected *in vivo*.

It would be interesting to investigate *in vitro* to what extent *Rasa3* KO T cells assist B cells. This can be done by sorting T_{FH} cells and mixing these with B cells in vitro and evaluating GC markers, class switched IgG1, as well as cytokines and antibodies in the supernatant [442]. One can further add T_{FR} cells to evaluate their suppressive potential. This would allow me to evaluate to what extent the T_{FH} cells assist the B cells in an isolated environment, but does not take into account differences that are a result of location within the GC which is likely a contributing factor in the *Rasa3*$^{T\text{-}KO}$ mice. Future studies of RASA3 should help address how RASA3-mediated suppression of LFA-1 is involved in the migration, homeostasis, and function of these different T cell subsets.

5.3.3 Chapter summary

In this chapter I present data from *Rasa3*$^{T\text{-}KO}$ mice under steady state, evaluating how *Rasa3* KO in T cells affects T cell homeostasis. *Rasa3*$^{T\text{-}KO}$ mice have build-up of mature thymocytes and are lymphopenic in blood and SLOs as a result of reduced entry and egress of *Rasa3* KO

T cells. The *Rasa3*$^{T\text{-}KO}$ mice establish poor GC responses following immunisation leading to reduced production of antigen-specific antibodies, which is most likely a result of reduced recruitment of T cells to the developing GCs.

Chapter 6 – Discussion

6. Discussion

LFA-1 activation is tightly regulated in T cells to ensure temporal and spatial control of migration and adhesion. LFA-1 is the main integrin expressed on T cells, and has been implicated in a multitude of functions, including T cell SLO entry and egress [245, 246], thymic development [435, 443], immunological synapse formation and cytotoxicity [296, 444], T cell location in tissues [245, 437], and T-cell mediated assistance to humoral immunity [147].

The mechanisms by which LFA-1 is activated in T cells has been extensively studied, however there are still big unknowns; one major unanswered question is how PI3K-signalling leads to activation of LFA-1 through inside-out signalling. This conundrum was studied by Dr. Fabien Garcon in the Okkenhaug lab, who found that PI3K activates LFA-1 independently of the main PI3K effector protein AKT by a mechanism that involves the activation of RAP1 [219].

In this thesis I have described a systematic screen for PI3K effector proteins involved in this process combining CRISPR/Cas9-mediated screening with a flow cytometry-based ICAM-1-binding assay (Chapter 3). In the screen for proteins that regulate LFA-1, I uncovered multiple new proteins involved in LFA-1 activation, including molecules like DNM2 that affect LFA-1 surface expression and several mitochondrial components, suggesting a level of regulation by mitochondrial respiration, perhaps for energy generation required for adhesion. I also confirmed the role of several known positive regulators, including KINDLIN-3, which is thought to be regulated in part by PIP_3 [328]. Among the negative regulators of LFA-1 affinity I identified RASA3 as the PH domain-containing protein with the greatest impact on ICAM-1-binding.

RASA3 is critical for the development and function of platelets [337, 350, 352, 353], where it has been found to regulate αIIbβ3 integrins by deactivating RAP1. Further, RASA3 has recently been implicated in regulation of pathogenic T_H17 cell development [355] (discussed further in Chapter 6.1.2). I have presented data showing that RASA3 is critical for keeping LFA-1 in check in T cells by negatively regulating RAP1 activity, both in response to TCR stimulation and chemokines. I further showed that RASA3 is negatively regulated by PI3K. RASA3 is thus the first negatively regulated PI3K effector protein in T cells described in the

literature to my knowledge (Chapter 4). Together this data indicates that RASA3 couples PI3K to RAP1 activation, and without RASA3, PI3K cannot decrease RAP1 activation (Figure 6-1a).

As RASA3 regulates LFA-1 it is perhaps not surprising that KO of *Rasa3* in T cells results in altered homeostasis of T cells. LFA-1 KO results in decreased T cell counts in pLN, mLN, and PPs, whereas T cells are slightly increased in spleen [245]; likely as a result of these cells not being able to arrest on the HEVs prior to LN entry (whereas entry to spleen is not dependent on TEM). Although *Rasa3* KO increases LFA-1 activity, similar trends are observed in *Rasa3*$^{T\text{-}KO}$ mice in pLNs, however *Rasa3*$^{T\text{-}KO}$ mice are also lymphopenic in blood and spleen, but normal cellularity in the gut-associated mLNs and PPs. Further, mature thymocytes were increased suggesting these cells are build-up in the thymus. These findings are in accordance with imaging and transfer experiments performed by collaborators and colleagues at NIH showing that *Rasa3* KO T cells have reduced entry into LNs due to the cells getting stuck during TEM (Figure 6-1b, step 1-2). These findings this describe an important role for RASA3 in T cell homeostasis by keeping integrins in check (Chapter 5.1).

LFA-1 is further crucial for several effector functions, one of those being the development and functions of T_{FH} cells in the GC reaction, where LFA-1 supports the correct location within the LN [148], the development of the T_{FH} cells [147], and the interactions with the B cells [146, 445]. Interestingly hyperactive LFA-1 results in somewhat decreased production of antigen-specific immunoglobulins following intraperitoneal TNP-CGG/Alum immunisation [149]. In this context, I investigated how *Rasa3*$^{T\text{-}KO}$ affected T-dependent humoral immunity following NP-OVA/Alum immunisation. I found that *Rasa3*$^{T\text{-}KO}$ mice showed poor GC responses after immunisation as a result of a defect in T_{FH} cell numbers in the LNs. The *Rasa3*$^{T\text{-}KO}$ mice further showed poor class switching of antigen-specific antibodies. OT-II transfer experiments suggest that these defects are a result of reduced T_{FH} cell numbers, rather than T_{FH} differentiation or functions being directly affected, consistent with the fact that *Rasa3* is expressed at low levels in T_{FH} cells [427]. Instead I suggest that the seeding of $CD4^+$ T cells in the LNs is impaired leading to reduced T_{FH} cells. Intriguingly, I also found that *Rasa3* KO T_{reg} cells seemed to more readily develop to become T_{FR} cells, suggesting an unappreciated role for integrin regulation in the process of T_{FR} cell development. In summary, RASA3 in T cells contributes to effective

development of GCs and therefore loss of *Rasa3* results in decreased T_{FH} cell-mediated assistance to GC B cells (Chapter 5.2) (Figure 6-1b, step 3).

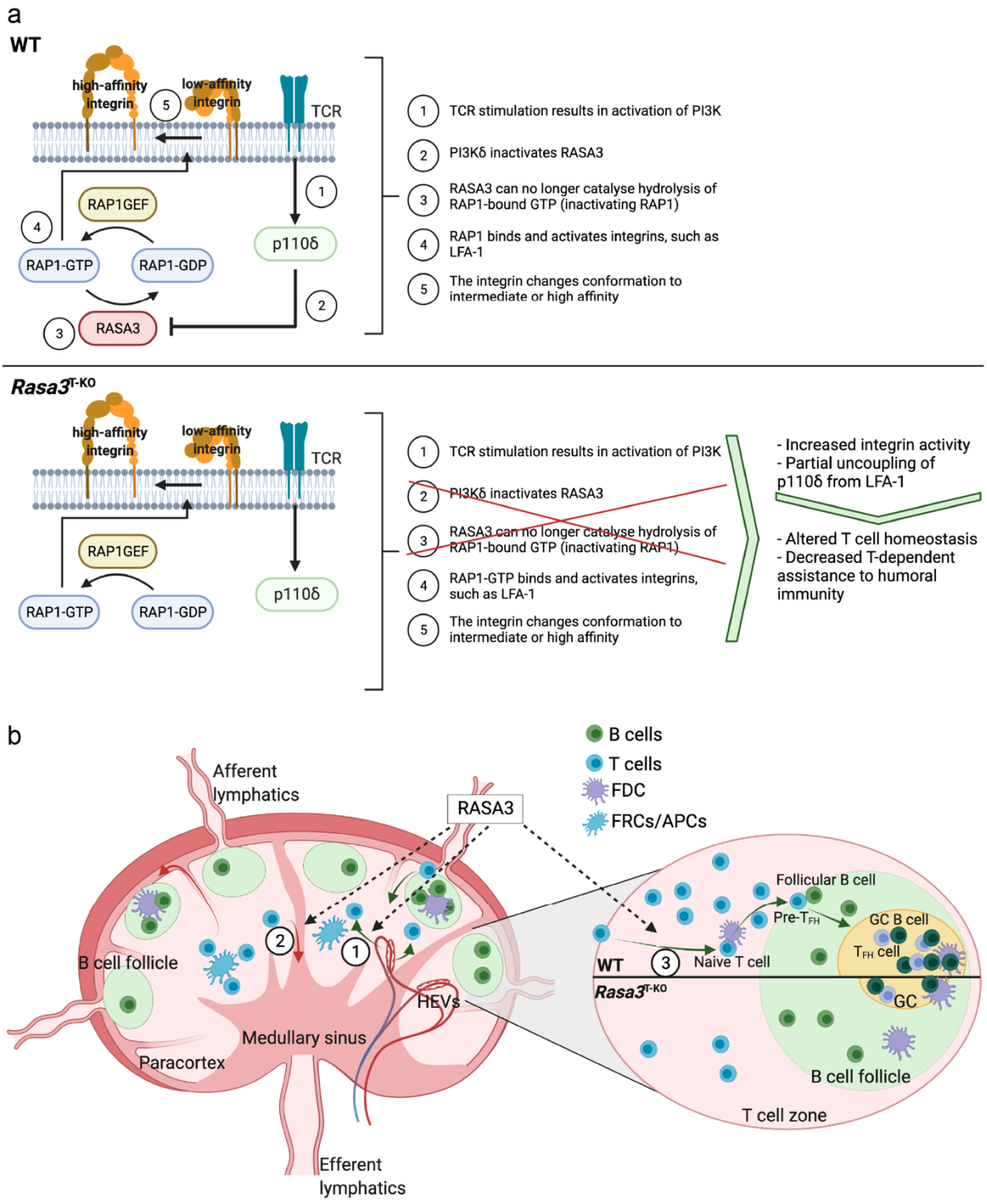

Figure 6-1. RASA3 is required for LFA-1 deactivation, T cell homeostasis, and effective T-dependent humoral responses. **a**, diagram showing proposed mechanism by which PI3K regulates LFA-1 activity by deactivating RASA3-mediated inactivation of RAP1. **b**, Figure showing functions of RASA3 in LN migration and the germinal centre reaction. RASA3 is required for effective LN entry through HEVs (1), effective LN egress (2), and sufficient development of T_{FH} cells during the GC reaction (likely as a consequence of reduced recruitment of T cells) (3).

6.1.1 RASA3 in PI3K-mediated T cell migration

These findings are critical in our understanding of how PI3K regulates T cell migration. As RASA3 is inhibited by PI3K, RASA3 inhibition likely contributes to PI3K effects on migration. Thus *Rasa3* KO in T cells would to some extent recapitulate a decoupling of PI3K from LFA-1. Indeed when evaluating T cell populations in PI3K hyperactive *Pik3cd*^{E1020K} mice and patients, there are reduced circulating lymphocytes and T cells are skewed to an activated phenotype as observed in the *Rasa3*$^{T\text{-}KO}$ mice. However, in SLOs there are increased lymphocyte numbers consistent with hyperactive *Pik3cd*^{E1020K} resulting in hyperproliferative T cells [136, 232]. Most of the PI3K phenotypes are however explained by multiple PI3K effector proteins being dysregulated, including AKT, and *Rasa3*$^{T\text{-}KO}$ mice will therefore not recapitulate all features of *Pik3cd*^{E1020K} mice.

As RASA3 is negatively regulated by PI3K, RASA3 manipulation in T cells could possibly allow for evaluation of PI3K functions that are dependent on LFA-1 activity; thus, KO of *Rasa3* in *Pik3cd*^{D910A} (kinase-dead) T cells would allow for evaluation of PI3K KO without potential effects contributed by defective LFA-1 [219]. Similarly, a mouse model with expression of a PHmutant of *Rasa3* would possibly allow for evaluation of effects of PI3K activation without LFA-1 hyperactivation as observed in Chapter 3.3. These studies would help elucidate effects of PI3K inhibition on T cell functions and the extent to which reduced integrin affinity explain these, which is relevant in the context of the range of studies and clinical trials evaluating the use of these in treatment of cancers [446].

6.1.2 LFA-1 and RASA3 in EAE

Although the presented data indicate that *Rasa3* is rapidly downregulated in newly activated T cells, *Rasa3* is also highly expressed in subsets of T_H17 cells [355, 447], memory T cells [448] and regulatory T cells [427]. These observations suggest that LFA-1 activity modulation by RASA3 might differentially affect T cell subsets during distinct immune challenges. A recent study has shown that *Rasa3* is highly expressed in pathogenic T_H17 cells and T cell-specific *Rasa3* deletion reduced the severity of Experimental Autoimmune Encephalomyelitis (EAE) [355] confirming the importance of RASA3 in T cell functions. The authors argued that these findings were the consequence of RASA3 suppressing T_H2-biased transcription programs by affecting CBL-B-mediated degradation of IRF4. However, it is of note that CBL-B also regulates T cell adhesion [280]. Thus, it is likely that the effects of *Rasa3*-deletion on EAE may also result in part from potential effects of increased adhesiveness on trafficking of pathogenic T_H17 cells into the CNS. These results would be consistent with LFA-1 affecting EAE in other studies [449-451]. The exact mechanism by which LFA-1 affects EAE remains elusive, and some studies indicated that LFA-1 KO resulted in increased EAE severity due to decreased suppressive T_{reg} cells [450], whereas others suggested LFA-1 KO or blockade decreases EAE due to decreased migration to CNS [449, 451, 452]. To my knowledge, hyperactive LFA-1 has not been studied in the context of EAE. However, expression of hyperactive RAP1 in T cells attenuates EAE [453] and mice lacking RAP1 in T cells develop colitis, associated with increased migration of pathogenic T_H17 and T_H1 cells into the intestines [454]. These findings are thus consistent with *Rasa3* KO decreasing EAE severity by regulating RAP1 and LFA-1 activity.

6.2 Future directions

The data presented open for multiple questions to be further investigated;

- Do class II and III PI3Ks and their effector proteins also regulate LFA-1?
- How is RASA3 inactivated by PI3K?
- To what extent does RASA3 affect T_{FH}/T_{FR} cell functions directly?

The CRISPR/Cas9 libraries would ideally be used in a bigger screen of all LFA-1 regulating proteins downstream of PIs in general and not just PIP_3. A such screen would likely uncover proteins involved in vesicular trafficking of LFA-1 more so than LFA-1 activity as PI(3)P, and $PI(3,4)P_2$ produced by class II and class III PI3Ks is required for vesicular trafficking. To incorporate this in a future CRISPR screen it would be of interest to do further screening sorting cells based on surface LFA-1 levels and sequence the cells and thereby identify sgRNAs that affect the levels of LFA-1 on the surface. I have as described already cloned a bigger library targeting all phospholipid-binding proteins ready to be used for such a screen. Further it would be of interest to conduct a CRISPR screen of other integrins such as VLA-4, or $\alpha4\beta7$ to understand whether any of the genes identified are involved in regulation of one integrin, but the other. Such proteins would be of interest as targets for therapies where specific ablation or activation of one integrin, but not the others is favorable.

RASA3 is unique among known PIP_3-binding proteins in that it is inactivated by PI3K. The mechanism involved in such inactivation is still unknown. Is RASA3 catalytic activity directly affected by PIP_3-binding through a conformational change? This seems unlikely, as RASA3 has affinity to PIP_2 as well, and the binding pocked of the protein is not likely to be specifically modulated by PIP_3 and not PIP_2. Further RASA3 with the PH domain of RASA2 (which does not have RAP1-GAP activity) still has catalytic activity[344], suggesting the PH domain is irrelevant for its conformational stability. One way to model this would be to perform in vitro assays investigating whether PIP_3 alters the activity of purified RASA3. Such experiments have been performed to some extent, showing that RASA3 bound to PIs seem to have no RAS-GAP activity, whereas addition of the competing soluble inositide $I(1,3,4,5)P_4$, which RASA3 has high affinity towards, restored activity of RASA3 [340]. This suggests a model where RASA3 is inactive in its membrane-bound form, and active in its soluble form. Since RASA3 has high affinity to PIP_3, PI3K would recruit any cytosolic active RASA3 to the membrane, thereby inactivating it. Other possible models discussed in the thesis involved sequestration in microdomains or compartments of the membrane distant from RAP1 and LFA-1. This model is backed up by data showing that in T cell conjugates, RASA3 is pulled away from LFA-1 in the IS, and inhibition of PI3K seems to disrupt this sequestration. Lastly, it is possible that PIP_3-binding brings RASA3 close to another modifying protein as discussed in Chapter 4.5.2.

To understand the specifics of these proposed mechanisms, detailed imaging would be required, such as lipid-bilayer assisted artificial IS formation with high resolution TIRF microscopy. Further it would be interesting to perform BioID-labelling of RASA3 to investigate protein interaction partners [455], and combine this technique with subcellular fractionation [456], and thereby evaluate which proteins might be binding RASA3 and inhibiting it.

My studies of the role of RASA3 on T-dependent humoral immunity indicated that the main involvement of RASA3 in the GC reaction is through modulation of T_{FH} numbers. However, we do still not definitively know whether RASA3 also affects other aspects of the T_{FH}-assisted GC response. The fact that I found class switching defects in intact animals, but not to the same extent following transfers, suggests that other cells than T_{FH} cells are affected by *Rasa3* KO. This could be an effect of RASA3 on T_{FR} cells and I have presented some evidence that *Rasa3* KO results in increased T_{FR}/T_{reg} cell, which could indicate that loss of *Rasa3* results in increased differentiation of T_{FR} cells. Alternatively loss of *Rasa3* affects LN entry of T_{reg} cells whilst affecting T_{FR} cells to a lesser extent, thereby skewing the ratio towards T_{FR} cells. To further understand this, it would be of interest to KO *Rasa3* specifically in FoxP3^{+} T cells using a FoxP3^{Cre} and investigate how that affected the GC responses to immunisation. I did attempt this, but unfortunately had problems with germline deletion of *Rasa3*. Another possibility is that *Rasa3* KO affects the numbers of T_{FH} cells by inducing CD8-mediated killing of T_{FH} cells or GC B cells unspecifically. This would mean T_{FH} cell numbers would decrease thereby inhibiting the GC response. It would be of interest to investigate this by depleting *Rasa3*$^{T\text{-}KO}$ mice for CD8^{+} T cells before or just following immunisation, thereby allowing GC formation without presence of CD8^{+} T cells.

These are some of many studies that could be performed to further understand the presented findings in this PhD (Figure 6-2). Consequently these studies would further elucidate on the roles of RASA3 in T cell biology. Interestingly RASA3 is also expressed at high levels in B cells, and as B cells also depend on LFA-1 regulated by somewhat overlapping mechanisms it would also be of interest to investigate how *Rasa3* KO affects the function of B cells.

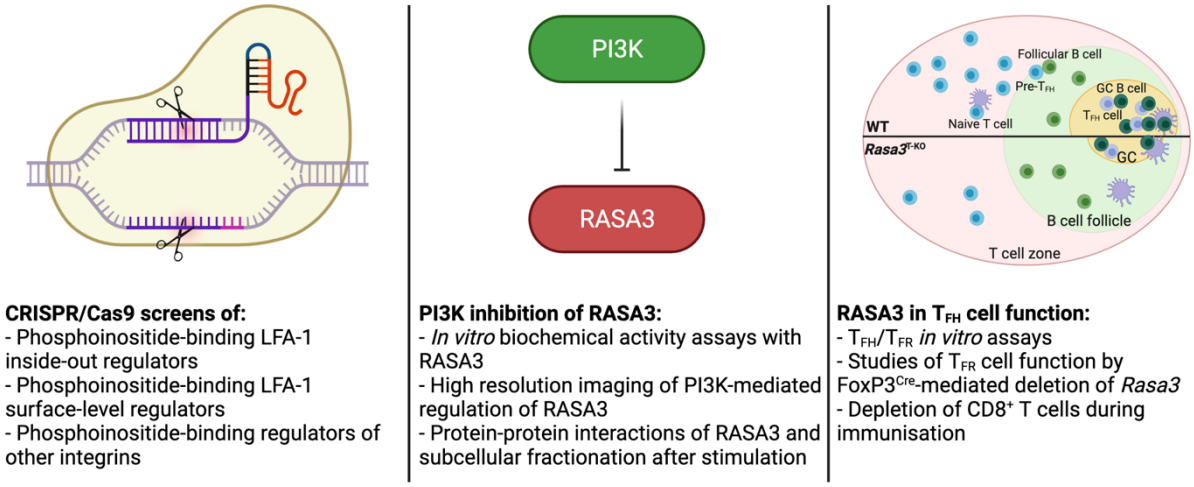

Figure 6-2. Future experiments for studies of RASA3. CRISPR/Cas9 screens, studies of RASA3, and further studies of T_{FH} functions are among experiments that would be of interest in future studies of RASA3 function in T cells.

6.3 Concluding remarks

Understanding how LFA-1 is regulated in T cells is of great interest both for the fundamental understanding of T cell migration and effector functions, and for therapeutic development. Using a targeted CRISPR/Cas9-mediated mutagenesis screen that allowed me to focus on PI3K effector proteins, I have identified multiple novel regulators of LFA-1-mediated ICAM-1-binding in T cells. These included molecules like DNM2 that affect LFA-1 surface expression and several mitochondrial components, suggesting a level of regulation by mitochondrial respiration, perhaps for energy generation required for adhesion. Importantly, my findings revealed that RASA3 is a novel PI3K-inhibited regulator of LFA-1 adhesion that represses ICAM-1-binding by decreasing the levels of GTP-bound RAP1 and severely affects T cell homeostasis as well as responses to vaccination. The findings therefore provide new insight into PI3K contributions to T cell signalling, as well as the dynamic regulation of lymphocyte homing required for proper immunity.

References

1. Kumar, B.V., T.J. Connors, and D.L. Farber, *Human T Cell Development, Localization, and Function throughout Life*. Immunity, 2018. **48**(2): p. 202-213.
2. Misslitz, A., et al., *Thymic T cell development and progenitor localization depend on CCR7*. J Exp Med, 2004. **200**(4): p. 481-91.
3. Allende, M.L., et al., *Expression of the sphingosine 1-phosphate receptor, S1P1, on T-cells controls thymic emigration*. J Biol Chem, 2004. **279**(15): p. 15396-401.
4. Kotturi, M.F., et al., *Naive precursor frequencies and MHC binding rather than the degree of epitope diversity shape CD8+ T cell immunodominance*. Journal of immunology, 2008. **181**(3): p. 2124-33.
5. Obar, J.J., K.M. Khanna, and L. Lefrançois, *Endogenous Naive CD8+ T Cell Precursor Frequency Regulates Primary and Memory Responses to Infection*. Immunity, 2008. **28**(6): p. 859-869.
6. Malek, A.M., *Hemodynamic Shear Stress and Its Role in Atherosclerosis*. JAMA, 1999. **282**(21): p. 2035.
7. Von Andrian, U.H. and C.R. Mackay, *T-cell function and migration: Two sides of the same coin*. 2000, Massachusetts Medical Society. p. 1020-1034.
8. Girard, J.-p., C. Moussion, and R. Förster, *HEVs, lymphatics and homeostatic immune cell trafficking in lymph nodes*. Nature reviews. Immunology, 2012. **12**(11): p. 762-73.
9. Arbonés, M.L., et al., *Lymphocyte homing and leukocyte rolling and migration are impaired in L-selectin-deficient mice*. Immunity, 1994. **1**(4): p. 247-260.
10. Gallatin, W.M., I.L. Weissman, and E.C. Butcher, *A cell-surface molecule involved in organ-specific homing of lymphocytes*. Nature, 1983. **304**(5921): p. 30-4.
11. Uchimura, K., et al., *A major class of L-selectin ligands is eliminated in mice deficient in two sulfotransferases expressed in high endothelial venules*. Nature Immunology, 2005. **6**(11): p. 1105-1113.
12. Malý, P., et al., *The α(1,3)Fucosyltransferase Fuc-TVII Controls Leukocyte Trafficking through an Essential Role in L-, E-, and P-selectin Ligand Biosynthesis*. Cell, 1996. **86**(4): p. 643-653.
13. Kawashima, H., et al., *N-acetylglucosamine-6-O-sulfotransferases 1 and 2 cooperatively control lymphocyte homing through L-selectin ligand biosynthesis in high endothelial venules*. Nature Immunology, 2005. **6**(11): p. 1096-1104.
14. Monneau, Y., F. Arenzana-Seisdedos, and H. Lortat-Jacob, *The sweet spot: how GAGs help chemokines guide migrating cells*. Journal of Leukocyte Biology, 2016. **99**(6): p. 935-953.
15. Baekkevold, E.S., et al., *The CCR7 ligand elc (CCL19) is transcytosed in high endothelial venules and mediates T cell recruitment*. J Exp Med, 2001. **193**(9): p. 1105-12.

16. Forster, R., et al., *CCR7 coordinates the primary immune response by establishing functional microenvironments in secondary lymphoid organs*. Cell, 1999. **99**(1): p. 23-33.

17. Bao, X., et al., *Endothelial heparan sulfate controls chemokine presentation in recruitment of lymphocytes and dendritic cells to lymph nodes*. Immunity, 2010. **33**(5): p. 817-829.

18. Bajénoff, M., et al., *Stromal Cell Networks Regulate Lymphocyte Entry, Migration, and Territoriality in Lymph Nodes*. Immunity, 2006. **25**(6): p. 989-1001.

19. von Andrian, U.H. and T.R. Mempel, *Homing and cellular traffic in lymph nodes*. Nat Rev Immunol, 2003. **3**(11): p. 867-78.

20. Braun, A., et al., *Afferent lymph–derived T cells and DCs use different chemokine receptor CCR7–dependent routes for entry into the lymph node and intranodal migration*. Nature Immunology, 2011. **12**(9): p. 879-887.

21. Mackay, C.R., W.L. Marston, and L. Dudler, *Naive and memory T cells show distinct pathways of lymphocyte recirculation*. Journal of Experimental Medicine, 1990. **171**(3): p. 801-817.

22. Boscacci, R.T., et al., *Comprehensive analysis of lymph node stroma-expressed Ig superfamily members reveals redundant and nonredundant roles for ICAM-1, ICAM-2, and VCAM-1 in lymphocyte homing*. Blood, 2010. **116**(6): p. 915-925.

23. Link, A., et al., *Fibroblastic reticular cells in lymph nodes regulate the homeostasis of naive T cells*. Nature Immunology, 2007. **8**(11): p. 1255-1265.

24. Pham, T.H.M., et al., *S1P1 Receptor Signaling Overrides Retention Mediated by Gαi-Coupled Receptors to Promote T Cell Egress*. Immunity, 2008. **28**(1): p. 122-133.

25. Sixt, M., et al., *The conduit system transports soluble antigens from the afferent lymph to resident dendritic cells in the T cell area of the lymph node*. Immunity, 2005. **22**(1): p. 19-29.

26. Bajénoff, M., et al., *Stromal Cell Networks Regulate Lymphocyte Entry, Migration, and Territoriality in Lymph Nodes*. Immunity, 2006. **25**(6): p. 989-1001.

27. Schwab, S.R., *Lymphocyte Sequestration Through S1P Lyase Inhibition and Disruption of S1P Gradients*. Science, 2005. **309**(5741): p. 1735-1739.

28. Pham, T.H.M., et al., *Lymphatic endothelial cell sphingosine kinase activity is required for lymphocyte egress and lymphatic patterning*. Journal of Experimental Medicine, 2010. **207**(1): p. 17-27.

29. Cyster, J.G. and S.R. Schwab, *Sphingosine-1-phosphate and lymphocyte egress from lymphoid organs*. Annu Rev Immunol, 2012. **30**: p. 69-94.

30. Grigorova, I.L., et al., *Cortical sinus probing, S1P1-dependent entry and flow-based capture of egressing T cells*. Nature Immunology, 2009. **10**(1): p. 58-65.

31. Chauveau, A., et al., *Visualization of T Cell Migration in the Spleen Reveals a Network of Perivascular Pathways that Guide Entry into T Zones*. Immunity, 2020. **52**(5): p. 794-807.e7.

32. Pappu, R., et al., *Promotion of Lymphocyte Egress into Blood and Lymph by Distinct Sources of Sphingosine-1-Phosphate*. Science, 2007. **316**(5822): p. 295-298.

33. Ramos-Perez, W.D., et al., *A map of the distribution of sphingosine 1-phosphate in the spleen*. Nature Immunology, 2015. **16**(12): p. 1245-1252.

34. Schaller, M.A., L.E. Kallal, and N.W. Lukacs, *A key role for CC chemokine receptor 1 in T-cell-mediated respiratory inflammation*. Am J Pathol, 2008. **172**(2): p. 386-94.

35. Bonecchi, R., et al., *Differential expression of chemokine receptors and chemotactic responsiveness of type 1 T helper cells (Th1s) and Th2s*. J Exp Med, 1998. **187**(1): p. 129-34.

36. Sallusto, F., et al., *Flexible programs of chemokine receptor expression on human polarized T helper 1 and 2 lymphocytes*. J Exp Med, 1998. **187**(6): p. 875-83.

37. Mikhak, Z., et al., *Contribution of CCR4 and CCR8 to antigen-specific T(H)2 cell trafficking in allergic pulmonary inflammation*. J Allergy Clin Immunol, 2009. **123**(1): p. 67-73 e3.

38. Qin, S., et al., *The chemokine receptors CXCR3 and CCR5 mark subsets of T cells associated with certain inflammatory reactions*. J Clin Invest, 1998. **101**(4): p. 746-54.

39. Loetscher, P., et al., *CCR5 is characteristic of Th1 lymphocytes*. Nature, 1998. **391**(6665): p. 344-5.

40. Contento, R.L., et al., *CXCR4-CCR5: a couple modulating T cell functions*. Proc Natl Acad Sci U S A, 2008. **105**(29): p. 10101-6.

41. Oo, Y.H., et al., *CXCR3-dependent recruitment and CCR6-mediated positioning of Th-17 cells in the inflamed liver*. J Hepatol, 2012. **57**(5): p. 1044-51.

42. Comerford, I., et al., *A myriad of functions and complex regulation of the CCR7/CCL19/CCL21 chemokine axis in the adaptive immune system*. Cytokine Growth Factor Rev, 2013. **24**(3): p. 269-83.

43. Duhen, T., et al., *Functionally distinct subsets of human FOXP3+ Treg cells that phenotypically mirror effector Th cells*. Blood, 2012. **119**(19): p. 4430-40.

44. Eyerich, S., et al., *Th22 cells represent a distinct human T cell subset involved in epidermal immunity and remodeling*. J Clin Invest, 2009. **119**(12): p. 3573-85.

45. Groom, J.R. and A.D. Luster, *CXCR3 in T cell function*. Exp Cell Res, 2011. **317**(5): p. 620-31.

46. Crotty, S., *Follicular helper CD4 T cells (TFH)*. Annual review of immunology, 2011. **29**: p. 621-63.

47. Gerlach, C., et al., *The Chemokine Receptor CX3CR1 Defines Three Antigen-Experienced CD8 T Cell Subsets with Distinct Roles in Immune Surveillance and Homeostasis*. Immunity, 2016. **45**(6): p. 1270-1284.

48. Li, Z., et al., *Roles of PLC-beta2 and -beta3 and PI3Kgamma in chemoattractant-mediated signal transduction*. Science, 2000. **287**(5455): p. 1046-9.

49. Kolanus, W. and B. Seed, *Integrins and inside-out signal transduction: converging signals from PKC and PIP3*. Curr Opin Cell Biol, 1997. **9**(5): p. 725-31.

50. Volkov, Y., et al., *Crucial importance of PKC-β(I) in LFA-1–mediated locomotion of activated T cells*. Nature Immunology, 2001. **2**(6): p. 508-514.

51. Balla, T., *Putting G protein-coupled receptor-mediated activation of phospholipase C in the limelight*. J Gen Physiol, 2010. **135**(2): p. 77-80.

52. Ganju, R.K., et al., *The alpha-chemokine, stromal cell-derived factor-1alpha, binds to the transmembrane G-protein-coupled CXCR-4 receptor and activates multiple signal transduction pathways*. J Biol Chem, 1998. **273**(36): p. 23169-75.

53. Afonso, P.V. and C.A. Parent, *PI3K and Chemotaxis: A Priming Issue?* Science Signaling, 2011. **4**(170): p. pe22-pe22.

54. Sasaki, T., et al., *Function of PI3Kgamma in thymocyte development, T cell activation, and neutrophil migration*. Science, 2000. **287**(5455): p. 1040-6.

55. Kaneda, M.M., et al., *PI3Kgamma is a molecular switch that controls immune suppression*. Nature, 2016. **539**(7629): p. 437-442.

56. Rickert, P., et al., *Leukocytes navigate by compass: roles of PI3Kgamma and its lipid products*. Trends Cell Biol, 2000. **10**(11): p. 466-73.

57. Okada, T., et al., *Chemokine Requirements for B Cell Entry to Lymph Nodes and Peyer's Patches*. Journal of Experimental Medicine, 2002. **196**(1): p. 65-75.

58. Britschgi, M.R., et al., *Dynamic Modulation of CCR7 Expression and Function on Naive T Lymphocytes In Vivo*. The Journal of Immunology, 2008. **181**(11): p. 7681-7688.

59. Zhu, J. and W.E. Paul, *Heterogeneity and plasticity of T helper cells*. Cell Res, 2010. **20**(1): p. 4-12.

60. Sakaguchi, S., et al., *Regulatory T cells and immune tolerance*. Cell, 2008. **133**(5): p. 775-87.

61. Brunkow, M.E., et al., *Disruption of a new forkhead/winged-helix protein, scurfin, results in the fatal lymphoproliferative disorder of the scurfy mouse*. Nat Genet, 2001. **27**(1): p. 68-73.

62. Wildin, R.S., et al., *X-linked neonatal diabetes mellitus, enteropathy and endocrinopathy syndrome is the human equivalent of mouse scurfy*. Nat Genet, 2001. **27**(1): p. 18-20.

63. Levy-Lahad, E. and R.S. Wildin, *Neonatal diabetes mellitus, enteropathy, thrombocytopenia, and endocrinopathy: Further evidence for an X-linked lethal syndrome*. J Pediatr, 2001. **138**(4): p. 577-80.

64. Josefowicz, S.Z., L.F. Lu, and A.Y. Rudensky, *Regulatory T cells: mechanisms of differentiation and function*. Annu Rev Immunol, 2012. **30**: p. 531-64.

65. Ridge, J.P., F. Di Rosa, and P. Matzinger, *A conditioned dendritic cell can be a temporal bridge between a CD4+ T-helper and a T-killer cell*. Nature, 1998. **393**(6684): p. 474-478.

66. Bennett, S.R.M., et al., *Help for cytotoxic-T-cell responses is mediated by CD40 signalling*. Nature, 1998. **393**(6684): p. 478-480.

67. Guerder, S. and P. Matzinger, *A fail-safe mechanism for maintaining self-tolerance*. Journal of Experimental Medicine, 1992. **176**(2): p. 553-564.

68. Sallusto, F., et al., *Two subsets of memory T lymphocytes with distinct homing potentials and effector functions*. Nature, 1999. **401**(6754): p. 708-12.

69. Ley, K. and G.S. Kansas, *Selectins in T-cell recruitment to non-lymphoid tissues and sites of inflammation*. Nature Reviews Immunology, 2004. **4**(5): p. 325-336.

70. Luster, A.D., R. Alon, and U.H. Von Andrian, *Immune cell migration in inflammation: present and future therapeutic targets*. Nature Immunology, 2005. **6**(12): p. 1182-1190.

71. Nourshargh, S. and R. Alon, *Leukocyte migration into inflamed tissues*. Immunity, 2014. **41**(5): p. 694-707.

72. Smith-Garvin, J.E., G.A. Koretzky, and M.S. Jordan, *T cell activation*. Annu Rev Immunol, 2009. **27**(1): p. 591-619.

73. Stepanek, O., et al., *Coreceptor Scanning by the T Cell Receptor Provides a Mechanism for T Cell Tolerance*. Cell, 2014. **159**(2): p. 333-345.

74. Holdorf, A.D., et al., *Regulation of Lck activity by CD4 and CD28 in the immunological synapse*. Nat Immunol, 2002. **3**(3): p. 259-64.

75. Chakraborty, A.K. and A. Weiss, *Insights into the initiation of TCR signaling*. Nat Immunol, 2014. **15**(9): p. 798-807.

76. Lo, W.-L. and A. Weiss, *Adapting T Cell Receptor Ligand Discrimination Capability via LAT*. Frontiers in Immunology, 2021. **12**.

77. Zhang, W., et al., *LAT: The ZAP-70 tyrosine kinase substrate that links T cell receptor to cellular activation*. Cell, 1998. **92**(1): p. 83-92.

78. Balagopalan, L., et al., *The Linker for Activation of T Cells (LAT) Signaling Hub: From Signaling Complexes to Microclusters*. Journal of Biological Chemistry, 2015. **290**(44): p. 26422-26429.

79. Yablonski, D., et al., *Uncoupling of nonreceptor tyrosine kinases from PLC-gamma1 in an SLP-76-deficient T cell*. Science, 1998. **281**(5375): p. 413-6.

80. Bivona, T.G., et al., *Phospholipase Cgamma activates Ras on the Golgi apparatus by means of RasGRP1*. Nature, 2003. **424**(6949): p. 694-8.

81. Luff, D.H., et al., *PI3Kdelta Forms Distinct Multiprotein Complexes at the TCR Signalosome in Naive and Differentiated CD4(+) T Cells*. Front Immunol, 2021. **12**: p. 631271.

82. Okkenhaug, K., K. Ali, and B. Vanhaesebroeck, *Antigen receptor signalling: a distinctive role for the p110delta isoform of PI3K*. Trends Immunol, 2007. **28**(2): p. 80-7.

83. Gaud, G., R. Lesourne, and P.E. Love, *Regulatory mechanisms in T cell receptor signalling*. Nature Reviews Immunology, 2018. **18**(8): p. 485-497.

84. Chiang, G.G. and B.M. Sefton, *Specific dephosphorylation of the Lck tyrosine protein kinase at Tyr-394 by the SHP-1 protein-tyrosine phosphatase*. J Biol Chem, 2001. **276**(25): p. 23173-8.

85. Stefanova, I., et al., *TCR ligand discrimination is enforced by competing ERK positive and SHP-1 negative feedback pathways*. Nat Immunol, 2003. **4**(3): p. 248-54.

86. You, R.-I. and C.-L. Chu, *SHP-1 (PTPN6) keeps the inflammation at bay: limiting IL-1α-mediated neutrophilic dermatoses by preventing Syk kinase activation*. Cellular & Molecular Immunology, 2017. **14**(11): p. 881-883.

87. Cai, Y.C., et al., *Selective CD28pYMNM mutations implicate phosphatidylinositol 3-kinase in CD86-CD28-mediated costimulation*. Immunity, 1995. **3**(4): p. 417-26.

88. Pages, F., et al., *Binding of phosphatidylinositol-3-OH kinase to CD28 is required for T-cell signalling*. Nature, 1994. **369**(6478): p. 327-9.

89. Garçon, F., et al., *CD28 provides T-cell costimulation and enhances PI3K activity at the immune synapse independently of its capacity to interact with the p85/p110 heterodimer*. Blood, 2008. **111**(3): p. 1464-1471.

90. Dobbins, J., et al., *Binding of the cytoplasmic domain of CD28 to the plasma membrane inhibits Lck recruitment and signaling*. Sci Signal, 2016. **9**(438): p. ra75.

91. Acuto, O. and F. Michel, *CD28-mediated co-stimulation: a quantitative support for TCR signalling*. Nature Reviews Immunology, 2003. **3**(12): p. 939-951.

92. Linterman, M.A., et al., *CD28 expression is required after T cell priming for helper T cell responses and protective immunity to infection*. Elife, 2014. **3**.

93. Bour-Jordan, H. and J.A. Bluestone, *Regulating the regulators: costimulatory signals control the homeostasis and function of regulatory T cells*. Immunological Reviews, 2009. **229**(1): p. 41-66.

94. Fröhlich, M., et al., *Interrupting CD28 costimulation before antigen rechallenge affects CD8+T-cell expansion and effector functions during secondary response in mice*. European Journal of Immunology, 2016. **46**(7): p. 1644-1655.

95. De Silva, N.S. and U. Klein, *Dynamics of B cells in germinal centres*. Nature Reviews Immunology, 2015. **15**(3): p. 137-148.

96. Victora, G.D. and M.C. Nussenzweig, *Germinal centers*. Annu Rev Immunol, 2012. **30**: p. 429-57.

97. Batista, F.D. and N.E. Harwood, *The who, how and where of antigen presentation to B cells*. Nat Rev Immunol, 2009. **9**(1): p. 15-27.

98. Phan, T.G., et al., *Subcapsular encounter and complement-dependent transport of immune complexes by lymph node B cells*. Nat Immunol, 2007. **8**(9): p. 992-1000.

99. Carrasco, Y.R. and F.D. Batista, *B cells acquire particulate antigen in a macrophage-rich area at the boundary between the follicle and the subcapsular sinus of the lymph node*. Immunity, 2007. **27**(1): p. 160-71.

100. Pereira, J.P., et al., *EBI2 mediates B cell segregation between the outer and centre follicle*. Nature, 2009. **460**(7259): p. 1122-6.

101. Liu, C., et al., *Oxysterols direct B-cell migration through EBI2*. Nature, 2011. **475**(7357): p. 519-23.

102. Reif, K., et al., *Balanced responsiveness to chemoattractants from adjacent zones determines B-cell position*. Nature, 2002. **416**(6876): p. 94-9.

103. Li, J., et al., *EBI2 augments Tfh cell fate by promoting interaction with IL-2-quenching dendritic cells*. Nature, 2016. **533**(7601): p. 110-114.

104. Ansel, K.M., et al., *In vivo-activated CD4 T cells upregulate CXC chemokine receptor 5 and reprogram their response to lymphoid chemokines*. J Exp Med, 1999. **190**(8): p. 1123-34.

105. Yi, T., et al., *Oxysterol gradient generation by lymphoid stromal cells guides activated B cell movement during humoral responses*. Immunity, 2012. **37**(3): p. 535-48.

106. Haynes, N.M., et al., *Role of CXCR5 and CCR7 in follicular Th cell positioning and appearance of a programmed cell death gene-1high germinal center-associated subpopulation*. J Immunol, 2007. **179**(8): p. 5099-108.

107. Cannons, J.L., et al., *Optimal Germinal Center Responses Require a Multistage T Cell:B Cell Adhesion Process Involving Integrins, SLAM-Associated Protein, and CD84*. Immunity, 2010. **32**(2): p. 253-265.

108. Qi, H., et al., *SAP-controlled T–B cell interactions underlie germinal centre formation*. Nature, 2008. **455**(7214): p. 764-769.

109. Kerfoot, S.M., et al., *Germinal center B cell and T follicular helper cell development initiates in the interfollicular zone*. Immunity, 2011. **34**(6): p. 947-60.

110. Crotty, S., *T Follicular Helper Cell Biology: A Decade of Discovery and Diseases*. Immunity, 2019. **50**(5): p. 1132-1148.

111. Vinuesa, C.G., et al., *Follicular Helper T Cells*. Annu Rev Immunol, 2016. **34**: p. 335-68.

112. Roco, J.A., et al., *Class-Switch Recombination Occurs Infrequently in Germinal Centers*. Immunity, 2019. **51**(2): p. 337-350 e7.

113. Bannard, O., et al., *Germinal center centroblasts transition to a centrocyte phenotype according to a timed program and depend on the dark zone for effective selection*. Immunity, 2013. **39**(5): p. 912-24.

114. Sundling, C., et al., *Positive selection of IgG(+) over IgM(+) B cells in the germinal center reaction*. Immunity, 2021.

115. Liu, D., et al., *T–B-cell entanglement and ICOSL-driven feed-forward regulation of germinal centre reaction*. Nature, 2015. **517**(7533): p. 214-218.

116. Allen, C.D., et al., *Imaging of germinal center selection events during affinity maturation*. Science, 2007. **315**(5811): p. 528-31.

117. Liu, B., et al., *Affinity-coupled CCL22 promotes positive selection in germinal centres*. Nature, 2021. **592**(7852): p. 133-137.

118. Chung, Y., et al., *Follicular regulatory T cells expressing Foxp3 and Bcl-6 suppress germinal center reactions*. Nat Med, 2011. **17**(8): p. 983-8.

119. Wollenberg, I., et al., *Regulation of the germinal center reaction by Foxp3+ follicular regulatory T cells*. J Immunol, 2011. **187**(9): p. 4553-60.

120. Linterman, M.A., et al., *Foxp3+ follicular regulatory T cells control the germinal center response*. Nat Med, 2011. **17**(8): p. 975-82.

121. Aloulou, M., et al., *Follicular regulatory T cells can be specific for the immunizing antigen and derive from naive T cells*. Nat Commun, 2016. **7**: p. 10579.

122. Maceiras, A.R., et al., *T follicular helper and T follicular regulatory cells have different TCR specificity*. Nat Commun, 2017. **8**: p. 15067.

123. Vaeth, M., et al., *Follicular regulatory T cells control humoral autoimmunity via NFAT2-regulated CXCR5 expression*. J Exp Med, 2014. **211**(3): p. 545-61.

124. Sage, P.T., et al., *The coinhibitory receptor CTLA-4 controls B cell responses by modulating T follicular helper, T follicular regulatory, and T regulatory cells*. Immunity, 2014. **41**(6): p. 1026-39.

125. Fonseca, V.R., F. Ribeiro, and L. Graca, *T follicular regulatory (Tfr) cells: Dissecting the complexity of Tfr-cell compartments*. Immunological Reviews, 2019. **288**(1): p. 112-127.

126. McCarron, M.J. and J.C. Marie, *TGF-beta prevents T follicular helper cell accumulation and B cell autoreactivity*. J Clin Invest, 2014. **124**(10): p. 4375-86.

127. Sage, P.T., et al., *Circulating T follicular regulatory and helper cells have memory-like properties*. J Clin Invest, 2014. **124**(12): p. 5191-204.

128. Huynh, A., et al., *Control of PI(3) kinase in Treg cells maintains homeostasis and lineage stability*. Nat Immunol, 2015. **16**(2): p. 188-96.

129. Shrestha, S., et al., *Treg cells require the phosphatase PTEN to restrain TH1 and TFH cell responses*. Nat Immunol, 2015. **16**(2): p. 178-87.

130. Sage, P.T. and A.H. Sharpe, *T follicular regulatory cells*. Immunological Reviews, 2016. **271**(1): p. 246-259.

131. Choi, S., Youn, et al., *ICOS Receptor Instructs T Follicular Helper Cell versus Effector Cell Differentiation via Induction of the Transcriptional Repressor Bcl6*. Immunity, 2011. **34**(6): p. 932-946.

132. Webb, L.M.C. and M.A. Linterman, *Signals that drive T follicular helper cell formation*. Immunology, 2017. **152**(2): p. 185-194.

133. Xu, H., et al., *Follicular T-helper cell recruitment governed by bystander B cells and ICOS-driven motility*. Nature, 2013. **496**(7446): p. 523-7.

134. Gigoux, M., et al., *Inducible costimulator promotes helper T-cell differentiation through phosphoinositide 3-kinase*. Proceedings of the National Academy of Sciences of the United States of America, 2009. **106**(48): p. 20371-20376.

135. Rolf, J., et al., *Phosphoinositide 3-kinase activity in T cells regulates the magnitude of the germinal center reaction*. J Immunol, 2010. **185**(7): p. 4042-52.

136. Preite, S., et al., *Hyperactivated PI3Kdelta promotes self and commensal reactivity at the expense of optimal humoral immunity*. Nat Immunol, 2018. **19**(9): p. 986-1000.

137. Preite, S., et al., *PI3K Orchestrates T Follicular Helper Cell Differentiation in a Context Dependent Manner: Implications for Autoimmunity*. Frontiers in Immunology, 2019. **9**.

138. Stone, E.L., et al., *ICOS coreceptor signaling inactivates the transcription factor FOXO1 to promote Tfh cell differentiation*. Immunity, 2015. **42**(2): p. 239-251.

139. Preite, S., et al., *T and B-cell signaling in activated PI3K delta syndrome: From immunodeficiency to autoimmunity*. Immunological Reviews, 2019. **291**(1): p. 154-173.

140. Kopf, M., et al., *OX40-deficient mice are defective in Th cell proliferation but are competent in generating B cell and CTL Responses after virus infection*. Immunity, 1999. **11**(6): p. 699-708.

141. Jacquemin, C., et al., *OX40 Ligand Contributes to Human Lupus Pathogenesis by Promoting T Follicular Helper Response*. Immunity, 2015. **42**(6): p. 1159-70.

142. Brocker, T., et al., *CD4 T cell traffic control: in vivo evidence that ligation of OX40 on CD4 T cells by OX40-ligand expressed on dendritic cells leads to the accumulation of CD4 T cells in B follicles*. Eur J Immunol, 1999. **29**(5): p. 1610-6.

143. Bartleson, J.M., et al., *Strength of tonic T cell receptor signaling instructs T follicular helper cell-fate decisions*. Nat Immunol, 2020. **21**(11): p. 1384-1396.

144. Merkenschlager, J., et al., *Dynamic regulation of TFH selection during the germinal centre reaction*. Nature, 2021. **591**(7850): p. 458-463.

145. Ise, W., et al., *T Follicular Helper Cell-Germinal Center B Cell Interaction Strength Regulates Entry into Plasma Cell or Recycling Germinal Center Cell Fate*. Immunity, 2018. **48**(4): p. 702-715.e4.

146. Zaretsky, I., et al., *ICAMs support B cell interactions with T follicular helper cells and promote clonal selection*. Journal of Experimental Medicine, 2017. **214**(11): p. 3435-3448.

147. Meli, A.P., et al., *The Integrin LFA-1 Controls T Follicular Helper Cell Generation and Maintenance*. Immunity, 2016. **45**(4): p. 831-846.

148. Janssen, E., et al., *DOCK8 is essential for LFA-1–dependent positioning of T follicular helper cells in germinal centers*. JCI Insight, 2020. **5**(15).

149. Semmrich, M., et al., *Importance of integrin LFA-1 deactivation for the generation of immune responses*. Journal of Experimental Medicine, 2005. **201**(12): p. 1987-1998.

150. Mulgrew-Nesbitt, A., et al., *The role of electrostatics in protein-membrane interactions*. 2006. p. 812-826.

151. Okkenhaug, K., *Signaling by the phosphoinositide 3-kinase family in immune cells*. Annu Rev Immunol, 2013. **31**: p. 675-704.

152. Gaidarov, I., et al., *The Class II Phosphoinositide 3-Kinase C2α Is Activated by Clathrin and Regulates Clathrin-Mediated Membrane Trafficking*. Molecular Cell, 2001. **7**(2): p. 443-449.

153. Maffucci, T., et al., *Class II phosphoinositide 3-kinase defines a novel signaling pathway in cell migration*. The Journal of cell biology, 2005. **169**: p. 789-799.

154. Srivastava, S., L. Di, and O. Zhdanova, *The class II phosphatidylinositol 3 kinase C2β is required for the activation of the K+ channel KCa3. 1 and CD4 T-cells*. Molecular biology of the cell, 2009. **20**: p. 3783-3791.

155. Nascimbeni, A.C., P. Codogno, and E. Morel, *Phosphatidylinositol-3-phosphate in the regulation of autophagy membrane dynamics*. FEBS J, 2017. **284**(9): p. 1267-1278.

156. Parekh, V.V., et al., *Impaired autophagy, defective T cell homeostasis, and a wasting syndrome in mice with a T cell-specific deletion of Vps34*. Journal of immunology, 2013. **190**(10): p. 5086-101.

157. Yang, G., et al., *Autophagy-related protein PIK3C3/VPS34 controls T cell metabolism and function*. Autophagy, 2020: p. 1-12.

158. Roy, N.H., et al., *LFA-1 signals to promote actin polymerization and upstream migration in T cells*. Journal of Cell Science, 2020. **133**(17): p. jcs248328.

159. Songyang, Z., et al., *SH2 domains recognize specific phosphopeptide sequences*. Cell, 1993. **72**(5): p. 767-78.

160. Janas, M.L., et al., *Thymic development beyond beta-selection requires phosphatidylinositol 3-kinase activation by CXCR4*. J Exp Med, 2010. **207**(1): p. 247-61.

161. Ji, H., et al., *Inactivation of PI3Kgamma and PI3Kdelta distorts T-cell development and causes multiple organ inflammation*. Blood, 2007. **110**(8): p. 2940-7.

162. Webb, L.M., et al., *Cutting edge: T cell development requires the combined activities of the p110gamma and p110delta catalytic isoforms of phosphatidylinositol 3-kinase*. J Immunol, 2005. **175**(5): p. 2783-7.

163. Trampont, P.C., et al., *CXCR4 acts as a costimulator during thymic β-selection*. Nature Immunology, 2010. **11**(2): p. 162-170.

164. Hagenbeek, T.J., et al., *The loss of PTEN allows TCR alphabeta lineage thymocytes to bypass IL-7 and Pre-TCR-mediated signaling*. J Exp Med, 2004. **200**(7): p. 883-94.

165. Suzuki, A., et al., *T Cell-Specific Loss of Pten Leads to Defects in Central and Peripheral Tolerance*. Immunity, 2001. **14**(5): p. 523-534.

166. Okkenhaug, K., et al., *The p110delta isoform of phosphoinositide 3-kinase controls clonal expansion and differentiation of Th cells*. J Immunol, 2006. **177**(8): p. 5122-8.

167. Conley, M.E., et al., *Agammaglobulinemia and absent B lineage cells in a patient lacking the p85alpha subunit of PI3K*. J Exp Med, 2012. **209**(3): p. 463-70.

168. Sogkas, G., et al., *Primary immunodeficiency disorder caused by phosphoinositide 3-kinase delta deficiency*. J Allergy Clin Immunol, 2018. **142**(5): p. 1650-1653 e2.

169. Swan, D.J., et al., *Immunodeficiency, autoimmune thrombocytopenia and enterocolitis caused by autosomal recessive deficiency of PIK3CD-encoded phosphoinositide 3-kinase delta*. Haematologica, 2019. **104**(10): p. e483-e486.

170. Vanhaesebroeck, B. and D.R. Alessi, *The PI3K-PDK1 connection: more than just a road to PKB*. Biochem J, 2000. **346 Pt 3**: p. 561-76.

171. Yang, G., et al., *A Positive Feedback Loop between Akt and mTORC2 via SIN1 Phosphorylation*. Cell Rep, 2015. **12**(6): p. 937-43.

172. Brunet, A., et al., *Akt promotes cell survival by phosphorylating and inhibiting a Forkhead transcription factor*. Cell, 1999. **96**(6): p. 857-68.

173. Kops, G.J., et al., *Direct control of the Forkhead transcription factor AFX by protein kinase B*. Nature, 1999. **398**(6728): p. 630-4.

174. Charvet, C., et al., *Vav1 promotes T cell cycle progression by linking TCR/CD28 costimulation to FOXO1 and p27kip1 expression*. J Immunol, 2006. **177**(8): p. 5024-31.

175. Aoki, M., H. Jiang, and P.K. Vogt, *Proteasomal degradation of the FoxO1 transcriptional regulator in cells transformed by the P3k and Akt oncoproteins*. Proc Natl Acad Sci U S A, 2004. **101**(37): p. 13613-7.

176. Hay, N., *Interplay between FOXO, TOR, and Akt*. Biochimica et biophysica acta, 2011. **1813**(11): p. 1965-70.

177. Kim, E.H. and M. Suresh, *Role of PI3K/Akt signaling in memory CD8 T cell differentiation*. Frontiers in immunology, 2013. **4**(February): p. 20-20.

178. Ouyang, W., et al., *Foxo proteins cooperatively control the differentiation of Foxp3+ regulatory T cells*. Nature immunology, 2010. **11**(7): p. 618-27.

179. Ouyang, W., et al., *Novel Foxo1-dependent transcriptional programs control Treg cell function*. Nature, 2012. **491**(7425): p. 554-559.

180. Manning, B.D., *Balancing Akt with S6K: implications for both metabolic diseases and tumorigenesis*. J Cell Biol, 2004. **167**(3): p. 399-403.

181. Hukelmann, J.L., et al., *The cytotoxic T cell proteome and its shaping by the kinase mTOR*. Nat Immunol, 2016. **17**(1): p. 104-12.

182. Delgoffe, G.M., et al., *The mTOR kinase differentially regulates effector and regulatory T cell lineage commitment*. Immunity, 2009. **30**(6): p. 832-44.

183. Sauer, S., et al., *T cell receptor signaling controls Foxp3 expression via PI3K, Akt, and mTOR*. Proceedings of the National Academy of Sciences of the United States of America, 2008. **105**(22): p. 7797-802.

184. Chi, H., *Regulation and function of mTOR signalling in T cell fate decisions*. Nat Rev Immunol, 2012. **12**(5): p. 325-38.

185. Finlay, D.K., et al., *PDK1 regulation of mTOR and hypoxia-inducible factor 1 integrate metabolism and migration of CD8+ T cells*. J Exp Med, 2012. **209**(13): p. 2441-53.

186. Roberts, M.S., et al., *Protein kinase B/Akt acts via glycogen synthase kinase 3 to regulate recycling of αvβ3 and α5β1 integrins*. Molecular and cellular biology, 2004. **24**(4): p. 1505-1515.

187. Stark, A.K., et al., *Loss of Phosphatidylinositol 3-Kinase Activity in Regulatory T Cells Leads to Neuronal Inflammation*. J Immunol, 2020. **205**(1): p. 78-89.

188. Soond, D.R., et al., *Pten loss in CD4 T cells enhances their helper function but does not lead to autoimmunity or lymphoma*. J Immunol, 2012. **188**(12): p. 5935-43.

189. Soond, D.R., et al., *PI3K p110delta regulates T-cell cytokine production during primary and secondary immune responses in mice and humans*. Blood, 2010. **115**(11): p. 2203-13.

190. Patton, D.T., et al., *Cutting edge: the phosphoinositide 3-kinase p110 delta is critical for the function of CD4+CD25+Foxp3+ regulatory T cells*. J Immunol, 2006. **177**(10): p. 6598-602.

191. Macintyre, A.N., et al., *Protein kinase B controls transcriptional programs that direct cytotoxic T cell fate but is dispensable for T cell metabolism*. Immunity, 2011. **34**(2): p. 224-36.

192. Pearce, V.Q., et al., *PI3Kdelta Regulates the Magnitude of CD8+ T Cell Responses after Challenge with Listeria monocytogenes*. J Immunol, 2015. **195**(7): p. 3206-17.

193. Kurebayashi, Y., et al., *PI3K-Akt-mTORC1-S6K1/2 axis controls Th17 differentiation by regulating Gfi1 expression and nuclear translocation of RORgamma*. Cell Rep, 2012. **1**(4): p. 360-73.

194. Nashed, B.F., et al., *Role of the phosphoinositide 3-kinase p110delta in generation of type 2 cytokine responses and allergic airway inflammation*. European journal of immunology, 2007. **37**(2): p. 416-24.

195. Haylock-Jacobs, S., et al., *PI3Kdelta drives the pathogenesis of experimental autoimmune encephalomyelitis by inhibiting effector T cell apoptosis and promoting Th17 differentiation*. J Autoimmun, 2011. **36**(3-4): p. 278-87.

196. Wan, Q., et al., *Cytokine signals through PI-3 kinase pathway modulate Th17 cytokine production by CCR6+ human memory T cells*. The Journal of experimental medicine, 2011. **208**(9): p. 1875-87.

197. Putz, E.M., et al., *PI3Kδ is essential for tumor clearance mediated by cytotoxic T lymphocytes*. PloS one, 2012. **7**(7): p. e40852-e40852.

198. Ali, K., et al., *Inactivation of PI(3)K p110δ breaks regulatory T-cell-mediated immune tolerance to cancer*. Nature, 2014. **509**(7505): p. 407-11.

199. Ladygina, N., et al., *PI3Kγ kinase activity is required for optimal T-cell activation and differentiation*. European journal of immunology, 2013. **43**(12): p. 3183-96.

200. Martin, A.L., et al., *Selective Regulation of CD8 Effector T Cell Migration by the p110γ Isoform of Phosphatidylinositol 3-Kinase*. The Journal of Immunology, 2008. **180**(4): p. 2081-2088.

201. Thomas, M.S., et al., *The p110gamma isoform of phosphatidylinositol 3-kinase regulates migration of effector CD4 T lymphocytes into peripheral inflammatory sites*. J Leukoc Biol, 2008. **84**(3): p. 814-23.

202. Hedrick, S.M., et al., *FOXO transcription factors throughout T cell biology*. Nat Rev Immunol, 2012. **12**(9): p. 649-61.

203. Carlson, C.M., et al., *Kruppel-like factor 2 regulates thymocyte and T-cell migration*. Nature, 2006. **442**(7100): p. 299-302.

204. Fabre, S., et al., *FOXO1 regulates L-Selectin and a network of human T cell homing molecules downstream of phosphatidylinositol 3-kinase*. J Immunol, 2008. **181**(5): p. 2980-9.

205. Galkina, E., et al., *L-selectin shedding does not regulate constitutive T cell trafficking but controls the migration pathways of antigen-activated T lymphocytes*. J Exp Med, 2003. **198**(9): p. 1323-35.

206. Venturi, G.M., et al., *Leukocyte migration is regulated by L-selectin endoproteolytic release*. Immunity, 2003. **19**(5): p. 713-24.

207. Finlay, D. and D. Cantrell, *Phosphoinositide 3-kinase and the mammalian target of rapamycin pathways control T cell migration*. Ann N Y Acad Sci, 2010. **1183**: p. 149-57.

208. Sinclair, L.V., et al., *Phosphatidylinositol-3-OH kinase and nutrient-sensing mTOR pathways control T lymphocyte trafficking*. Nature Immunology, 2008. **9**(5): p. 513-521.

209. Diaz-Rodriguez, E., et al., *Extracellular signal-regulated kinase phosphorylates tumor necrosis factor alpha-converting enzyme at threonine 735: a potential role in regulated shedding*. Mol Biol Cell, 2002. **13**(6): p. 2031-44.

210. Fan, H. and R. Derynck, *Ectodomain shedding of TGF-alpha and other transmembrane proteins is induced by receptor tyrosine kinase activation and MAP kinase signaling cascades*. EMBO J, 1999. **18**(24): p. 6962-72.

211. Soond, S.M., et al., *ERK-mediated phosphorylation of Thr735 in TNFalpha-converting enzyme and its potential role in TACE protein trafficking*. J Cell Sci, 2005. **118**(Pt 11): p. 2371-80.

212. Finlay, D.K., et al., *Phosphoinositide-dependent kinase 1 controls migration and malignant transformation but not cell growth and proliferation in PTEN-null lymphocytes*. Journal of Experimental Medicine, 2009. **206**(11): p. 2441-2454.

213. Rao, V.K., et al., *Effective "activated PI3Kdelta syndrome"-targeted therapy with the PI3Kdelta inhibitor leniolisib*. Blood, 2017. **130**(21): p. 2307-2316.

214. Reif, K., et al., *Cutting edge: differential roles for phosphoinositide 3-kinases, p110gamma and p110delta, in lymphocyte chemotaxis and homing*. J Immunol, 2004. **173**(4): p. 2236-40.

215. Smith, L.D., et al., *PI3Kgamma is the dominant isoform involved in migratory responses of human T lymphocytes: effects of ex vivo maintenance and limitations of non-viral delivery of siRNA*. Cell Signal, 2007. **19**(12): p. 2528-39.

216. Asperti-Boursin, F., et al., *CCR7 ligands control basal T cell motility within lymph node slices in a phosphoinositide 3-kinase-independent manner*. J Exp Med, 2007. **204**(5): p. 1167-79.

217. Matheu, M.P., et al., *Class IA phosphoinositide 3-kinase modulates basal lymphocyte motility in the lymph node*. J Immunol, 2007. **179**(4): p. 2261-9.

218. Jarmin, S.J., et al., *T cell receptor-induced phosphoinositide-3-kinase p110delta activity is required for T cell localization to antigenic tissue in mice*. J Clin Invest, 2008. **118**(3): p. 1154-64.

219. Garcon, F. and K. Okkenhaug, *PI3Kdelta promotes CD4(+) T-cell interactions with antigen-presenting cells by increasing LFA-1 binding to ICAM-1*. Immunol Cell Biol, 2016. **94**(5): p. 486-95.

220. Mirenda, V., et al., *Physiologic and aberrant regulation of memory T-cell trafficking by the costimulatory molecule CD28*. Blood, 2007. **109**(7): p. 2968-2977.

221. Lucas, C.L., et al., *Heterozygous splice mutation in PIK3R1 causes human immunodeficiency with lymphoproliferation due to dominant activation of PI3K*. J Exp Med, 2014. **211**(13): p. 2537-47.

222. Angulo, I., et al., *Phosphoinositide 3-kinase δ gene mutation predisposes to respiratory infection and airway damage*. Science (New York, N.Y.), 2013. **342**(6160): p. 866-71.

223. Haslam, R.J., H.B. Koide, and B.A. Hemmings, *Pleckstrin domain homology*. Nature, 1993. **363**: p. 309-10.

224. Mayer, B.J., et al., *A Putative Modular Domain Present in diverse signaling proteins*. Cell, 1993. **73**: p. 629-630.

225. Harlan, J.E., et al., *Pleckstrin homology domains bind to phosphatidylinositol-4, 5-bisphosphate*. Nature, 1994. **371**: p. 168-70.

226. Park, W.S., et al., *Comprehensive Identification of PIP3-Regulated PH Domains from C. elegans to H. sapiens by Model Prediction and Live Imaging*. Molecular Cell, 2008. **30**(3): p. 381-392.

227. Jungmichel, S., et al., *Specificity and commonality of the phosphoinositide-binding proteome analyzed by quantitative mass spectrometry*. Cell Rep, 2014. **6**(3): p. 578-91.

228. Côté, J.-F., et al., *A novel and evolutionarily conserved PtdIns(3,4,5)P3-binding domain is necessary for DOCK180 signalling*. Nature Cell Biology, 2005. **7**(8): p. 797-807.

229. Lucas, C.L., et al., *Dominant-activating germline mutations in the gene encoding the PI(3)K catalytic subunit p110δ result in T cell senescence and human immunodeficiency*. Nature immunology, 2014. **15**(1): p. 88-97.

230. Coulter, T.I., et al., *Clinical spectrum and features of activated phosphoinositide 3-kinase delta syndrome: A large patient cohort study*. J Allergy Clin Immunol, 2017. **139**(2): p. 597-606 e4.

231. Deau, M.C., et al., *A human immunodeficiency caused by mutations in the PIK3R1 gene*. J Clin Invest, 2014. **124**(9): p. 3923-8.

232. Stark, A.K., et al., *PI3Kδ hyper-activation promotes development of B cells that exacerbate Streptococcus pneumoniae infection in an antibody-independent manner*. Nature Communications, 2018. **9**(1): p. 1-16.

233. Avery, D.T., et al., *Germline-activating mutations in PIK3CD compromise B cell development and function*. J Exp Med, 2018. **215**(8): p. 2073-2095.

234. Lucas, C.L., et al., *PI3Kδ and primary immunodeficiencies*. Nature Publishing Group, 2016. **4**(11): p. 702-714.

235. Tangye, S.G., et al., *Immune Dysregulation and Disease Pathogenesis due to Activating Mutations in PIK3CD-the Goldilocks' Effect*. J Clin Immunol, 2019. **39**(2): p. 148-158.

236. Gaullier, J.M., et al., *FYVE fingers bind PtdIns(3)P*. Nature, 1998. **394**(6692): p. 432-3.

237. Ago, T., et al., *Phosphorylation of p47phox directs phox homology domain from SH3 domain toward phosphoinositides, leading to phagocyte NADPH oxidase activation*. Proc Natl Acad Sci U S A, 2003. **100**(8): p. 4474-9.

238. Karathanassis, D., et al., *Binding of the PX domain of p47(phox) to phosphatidylinositol 3,4-bisphosphate and phosphatidic acid is masked by an intramolecular interaction*. EMBO J, 2002. **21**(19): p. 5057-68.

239. Balla, T., *Phosphoinositides: tiny lipids with giant impact on cell regulation*. Physiol Rev, 2013. **93**(3): p. 1019-137.

240. Hogg, N., *T-cell integrins: more than just sticking points*. Journal of Cell Science, 2003. **116**(23): p. 4695-4705.

241. Mair, I., et al., *A Context-Dependent Role for alphav Integrins in Regulatory T Cell Accumulation at Sites of Inflammation*. Front Immunol, 2018. **9**: p. 264.

242. Ostermann, G., et al., *JAM-1 is a ligand of the β2 integrin LFA-1 involved in transendothelial migration of leukocytes*. Nature Immunology, 2002. **3**(2): p. 151-158.

243. Marlin, S.D. and T.A. Springer, *Purified intercellular adhesion molecule-1 (ICAM-1) is a ligand for lymphocyte function-associated antigen 1 (LFA-1)*. Cell, 1987. **51**(5): p. 813-9.

244. Walling, B.L. and M. Kim, *LFA-1 in T Cell Migration and Differentiation*. Frontiers in Immunology, 2018. **9**(May): p. 1-10.

245. Berlin-Rufenach, C., et al., *Lymphocyte migration in lymphocyte function-associated antigen (LFA)-1-deficient mice*. J Exp Med, 1999. **189**(9): p. 1467-78.

246. Andrew, D.P., et al., *Transendothelial migration and trafficking of leukocytes in LFA-1-deficient mice*. Eur J Immunol, 1998. **28**(6): p. 1959-69.

247. Reichardt, P., et al., *A role for LFA-1 in delaying T-lymphocyte egress from lymph nodes*. EMBO J, 2013. **32**(6): p. 829-43.

248. Katakai, T., K. Habiro, and T. Kinashi, *Dendritic cells regulate high-speed interstitial T cell migration in the lymph node via LFA-1/ICAM-1*. J Immunol, 2013. **191**(3): p. 1188-99.

249. Woolf, E., et al., *Lymph node chemokines promote sustained T lymphocyte motility without triggering stable integrin adhesiveness in the absence of shear forces*. Nat Immunol, 2007. **8**(10): p. 1076-85.

250. Westermann, J., et al., *Naive, effector, and memory T lymphocytes efficiently scan dendritic cells in vivo: contact frequency in T cell zones of secondary lymphoid organs*

does not depend on LFA-1 expression and facilitates survival of effector T cells. J Immunol, 2005. **174**(5): p. 2517-24.

251. Lammermann, T., et al., *Rapid leukocyte migration by integrin-independent flowing and squeezing*. Nature, 2008. **453**(7191): p. 51-5.

252. Shimizu, Y., et al., *Regulated expression and binding of three VLA (beta 1) integrin receptors on T cells*. Nature, 1990. **345**(6272): p. 250-3.

253. Baron, J.L., et al., *Surface expression of alpha 4 integrin by CD4 T cells is required for their entry into brain parenchyma*. Journal of Experimental Medicine, 1993. **177**(1): p. 57-68.

254. Berlin, C., et al., *Alpha 4 beta 7 integrin mediates lymphocyte binding to the mucosal vascular addressin MAdCAM-1*. Cell, 1993. **74**(1): p. 185-95.

255. Ghandour, H., et al., *Essential role for Rap1 GTPase and its guanine exchange factor CalDAG-GEFI in LFA-1 but not VLA-4 integrin-mediated human T-cell adhesion*. Blood, 2007.

256. Burbach, B.J., et al., *T-cell receptor signaling to integrins*. Immunol Rev, 2007. **218**(1): p. 65-81.

257. Nolz, J.C., et al., *The WAVE2 complex regulates T cell receptor signaling to integrins via Abl- and CrkL-C3G-mediated activation of Rap1*. J Cell Biol, 2008. **182**(6): p. 1231-44.

258. Braiman, A. and N. Isakov, *The role of Crk adaptor proteins in T-cell adhesion and migration*. Frontiers in Immunology, 2015. **6**(OCT): p. 1-7.

259. Shimonaka, M., et al., *Rap1 translates chemokine signals to integrin activation, cell polarization, and motility across vascular endothelium under flow*. Journal of Cell Biology, 2003. **161**(2): p. 417-427.

260. Katagiri, K., et al., *Rap1 Is a Potent Activation Signal for Leukocyte Function-Associated Antigen 1 Distinct from Protein Kinase C and Phosphatidylinositol-3-OH Kinase*. Molecular and cellular biology, 2000. **20**(6): p. 1956-1969.

261. Katagiri, K., et al., *RAPL, a Rap1-binding molecule that mediates Rap1-induced adhesion through spatial regulation of LFA-1*. Nat Immunol, 2003. **4**(8): p. 741-8.

262. Kinashi, T., *Intracellular signalling controlling integrin activation in lymphocytes*. Nat Rev Immunol, 2005. **5**(7): p. 546-59.

263. Lafuente, E.M., et al., *RIAM, an Ena/VASP and Profilin ligand, interacts with Rap1-GTP and mediates Rap1-induced adhesion*. Dev Cell, 2004. **7**(4): p. 585-95.

264. Lee, H.S., et al., *RIAM activates integrins by linking talin to ras GTPase membrane-targeting sequences*. J Biol Chem, 2009. **284**(8): p. 5119-27.

265. Yang, J., et al., *Conformational activation of talin by RIAM triggers integrin-mediated cell adhesion*. Nat Commun, 2014. **5**: p. 5880.

266. Tadokoro, S., et al., *Talin binding to integrin beta tails: a final common step in integrin activation*. Science, 2003. **302**(5642): p. 103-6.

267. Wegener, K.L., et al., *Structural basis of integrin activation by talin*. Cell, 2007. **128**(1): p. 171-82.

268. Wynne, J.P., et al., *Rap1-interacting adapter molecule (RIAM) associates with the plasma membrane via a proximity detector*. J Cell Biol, 2012. **199**(2): p. 317-30.

269. Kliche, S., et al., *The ADAP/SKAP55 signaling module regulates T-cell receptor-mediated integrin activation through plasma membrane targeting of Rap1*. Mol Cell Biol, 2006. **26**(19): p. 7130-44.

270. Raab, M., et al., *SKAP1 protein PH domain determines RapL membrane localization and Rap1 protein complex formation for T cell receptor (TCR) activation of LFA-1*. J Biol Chem, 2011. **286**(34): p. 29663-70.

271. Raab, M., et al., *T cell receptor "inside-out" pathway via signaling module SKAP1-RapL regulates T cell motility and interactions in lymph nodes*. Immunity, 2010. **32**(4): p. 541-56.

272. Lefort, C.T., et al., *Distinct roles for talin-1 and kindlin-3 in LFA-1 extension and affinity regulation*. Blood, 2012. **119**(18): p. 4275-82.

273. Manevich-Mendelson, E., et al., *Loss of Kindlin-3 in LAD-III eliminates LFA-1 but not VLA-4 adhesiveness developed under shear flow conditions*. Blood, 2009. **114**(11): p. 2344-53.

274. Moretti, F.A., et al., *Kindlin-3 regulates integrin activation and adhesion reinforcement of effector T cells*. Proc Natl Acad Sci U S A, 2013. **110**(42): p. 17005-10.

275. Cherry, L.K., et al., *RhoH is required to maintain the integrin LFA-1 in a nonadhesive state on lymphocytes*. Nat Immunol, 2004. **5**(9): p. 961-7.

276. Wang, H., et al., *RhoH modulates pre-TCR and TCR signalling by regulating LCK*. Cell Signal, 2011. **23**(1): p. 249-58.

277. Gu, Y., et al., *RhoH GTPase recruits and activates Zap70 required for T cell receptor signaling and thymocyte development*. Nat Immunol, 2006. **7**(11): p. 1182-90.

278. Baker, C.M., et al., *Opposing roles for RhoH GTPase during T-cell migration and activation*. Proc Natl Acad Sci U S A, 2012. **109**(26): p. 10474-9.

279. Zhang, W., et al., *Negative regulation of T cell antigen receptor-mediated Crk-L-C3G signaling and cell adhesion by Cbl-b*. J Biol Chem, 2003. **278**(26): p. 23978-83.

280. Choi, E.Y., et al., *Regulation of LFA-1-dependent inflammatory cell recruitment by Cbl-b and 14-3-3 proteins*. Blood, 2008. **111**(7): p. 3607-14.

281. Duchniewicz, M., et al., *Rap1A-Deficient T and B Cells Show Impaired Integrin-Mediated Cell Adhesion*. Molecular and Cellular Biology, 2006. **26**(2): p. 643-653.

282. Ghandour, H., et al., *Essential role for Rap1 GTPase and its guanine exchange factor CalDAG-GEFI in LFA-1 but not VLA-4 integrin–mediated human T-cell adhesion*. Blood, 2007. **110**(10): p. 3682-3690.

283. Klapproth, S., et al., *Loss of the Rap1 effector RIAM results in leukocyte adhesion deficiency due to impaired β2 integrin function in mice*. Blood, 2015. **126**(25): p. 2704-2712.

284. Hogg, N., I. Patzak, and F. Willenbrock, *The insider's guide to leukocyte integrin signalling and function*. Nature reviews. Immunology, 2011. **11**(6): p. 416-26.

285. Evans, R., et al., *The integrin LFA-1 signals through ZAP-70 to regulate expression of high-affinity LFA-1 on T lymphocytes*. Blood, 2011. **117**(12): p. 3331-42.

286. Ebisuno, Y., et al., *Rap1 controls lymphocyte adhesion cascade and interstitial migration within lymph nodes in RAPL-dependent and -independent manners*. Blood, 2010. **115**(4): p. 804-14.

287. Moser, M., et al., *Kindlin-3 is essential for integrin activation and platelet aggregation*. Nat Med, 2008. **14**(3): p. 325-30.

288. Critchley, D.R. and A.R. Gingras, *Talin at a glance*. J Cell Sci, 2008. **121**(Pt 9): p. 1345-7.

289. García-Bernal, D., et al., *Chemokine-Induced Zap70 Kinase-Mediated Dissociation of the Vav1-Talin Complex Activates α4β1 Integrin for T Cell Adhesion*. Immunity, 2009. **31**(6): p. 953-964.

290. Verma, N.K. and D. Kelleher, *Adaptor regulation of LFA-1 signaling in T lymphocyte migration: Potential druggable targets for immunotherapies?* Eur J Immunol, 2014. **44**(12): p. 3484-99.

291. Sanchez-Martin, L., et al., *Signaling through the leukocyte integrin LFA-1 in T cells induces a transient activation of Rac-1 that is regulated by Vav and PI3K/Akt-1*. J Biol Chem, 2004. **279**(16): p. 16194-205.

292. Kim, S.H.J. and D.A. Hammer, *Integrin crosstalk allows CD4+ T lymphocytes to continue migrating in the upstream direction after flow*. Integr Biol (Camb), 2019. **11**(10): p. 384-393.

293. Roy, N.H., et al., *Crk adaptor proteins mediate actin-dependent T cell migration and mechanosensing induced by the integrin LFA-1*. Science Signaling, 2018. **11**(560): p. 22-28.

294. Mastrogiovanni, M., et al., *Coordinating Cytoskeleton and Molecular Traffic in T Cell Migration, Activation, and Effector Functions*. Front Cell Dev Biol, 2020. **8**: p. 591348.

295. Finetti, F. and C.T. Baldari, *The immunological synapse as a pharmacological target*. Pharmacol Res, 2018. **134**: p. 118-133.

296. Contento, R.L., et al., *Adhesion shapes T cells for prompt and sustained T-cell receptor signalling*. EMBO J, 2010. **29**(23): p. 4035-47.

297. Lee, K.H., et al., *T cell receptor signaling precedes immunological synapse formation*. Science, 2002. **295**(5559): p. 1539-42.

298. Grakoui, A., et al., *The immunological synapse: a molecular machine controlling T cell activation*. Science, 1999. **285**(5425): p. 221-7.

299. Monks, C.R., et al., *Three-dimensional segregation of supramolecular activation clusters in T cells*. Nature, 1998. **395**(6697): p. 82-6.

300. Nguyen, K., N.R. Sylvain, and S.C. Bunnell, *T cell costimulation via the integrin VLA-4 inhibits the actin-dependent centralization of signaling microclusters containing the adaptor SLP-76*. Immunity, 2008. **28**(6): p. 810-21.

301. Mossman, K.D., et al., *Altered TCR signaling from geometrically repatterned immunological synapses*. Science, 2005. **310**(5751): p. 1191-3.

302. Le Floc'h, A., et al., *Annular PIP3 accumulation controls actin architecture and modulates cytotoxicity at the immunological synapse*. J Exp Med, 2013. **210**(12): p. 2721-37.

303. Costello, P.S., M. Gallagher, and D.A. Cantrell, *Sustained and dynamic inositol lipid metabolism inside and outside the immunological synapse*. Nat Immunol, 2002. **3**(11): p. 1082-9.

304. Gawden-Bone, C.M., et al., *PIP5 Kinases Regulate Membrane Phosphoinositide and Actin Composition for Targeted Granule Secretion by Cytotoxic Lymphocytes*. Immunity, 2018. **49**(3): p. 427-437 e4.

305. Basu, R., et al., *Cytotoxic T Cells Use Mechanical Force to Potentiate Target Cell Killing*. Cell, 2016. **165**(1): p. 100-110.

306. Shi, J., et al., *Wortmannin, a Phosphatidylinositol 3-Kinase Inhibitor, Blocks Antigen-Mediated, but Not CD3 Monoclonal Antibody-Induced, Activation of Murine CD4+ T cells*. Journal of immunology, 1997. **158**(10): p. 4688-95.

307. O'Rourke, A.M., H. Shao, and J. Kaye, *A role for p21ras/MAP kinase in TCR-mediated activation of LFA-1*. J Immunol, 1998. **161**(11): p. 5800-3.

308. Zell, T., et al., *CD28-mediated up-regulation of beta 1-integrin adhesion involves phosphatidylinositol 3-kinase*. J Immunol, 1996. **156**(3): p. 883-6.

309. Chan, A.S., et al., *CD7-mediated regulation of integrin adhesiveness on human T cells involves tyrosine phosphorylation-dependent activation of phosphatidylinositol 3-kinase*. J Immunol, 1997. **159**(2): p. 934-42.

310. Letschka, T., et al., *PKC-theta selectively controls the adhesion-stimulating molecule Rap1*. Blood, 2008. **112**(12): p. 4617-27.

311. Constantin, G., et al., *Chemokines trigger immediate beta2 integrin affinity and mobility changes: differential regulation and roles in lymphocyte arrest under flow*. Immunity, 2000. **13**(6): p. 759-69.

312. Nombela-Arrieta, C., et al., *Differential requirements for DOCK2 and phosphoinositide-3-kinase gamma during T and B lymphocyte homing*. Immunity, 2004. **21**(3): p. 429-41.

313. Nombela-Arrieta, C., et al., *A central role for DOCK2 during interstitial lymphocyte motility and sphingosine-1-phosphate-mediated egress*. J Exp Med, 2007. **204**(3): p. 497-510.

314. Grabovsky, V., et al., *Subsecond induction of alpha4 integrin clustering by immobilized chemokines stimulates leukocyte tethering and rolling on endothelial vascular cell adhesion molecule 1 under flow conditions*. J Exp Med, 2000. **192**(4): p. 495-506.

315. Nagel, W., et al., *Phosphoinositide 3-OH kinase activates the beta2 integrin adhesion pathway and induces membrane recruitment of cytohesin-1*. J Biol Chem, 1998. **273**(24): p. 14853-61.

316. Kolanus, W., et al., *αLβ2 Integrin/LFA-1 Binding to ICAM-1 Induced by Cytohesin-1, a Cytoplasmic Regulatory Molecule*. Cell, 1996. **86**(2): p. 233-242.

317. Nagel, W., et al., *The PH domain and the polybasic c domain of cytohesin-1 cooperate specifically in plasma membrane association and cellular function*. Mol Biol Cell, 1998. **9**(8): p. 1981-94.

318. Geiger, C., et al., *Cytohesin-1 regulates beta-2 integrin-mediated adhesion through both ARF-GEF function and interaction with LFA-1*. EMBO J, 2000. **19**(11): p. 2525-36.

319. Weber, K.S.C., et al., *Cytohesin-1 is a dynamic regulator of distinct LFA-1 functions in leukocyte arrest and transmigration triggered by chemokines*. Current Biology, 2001. **11**(24): p. 1969-1974.

320. Quast, T., et al., *Cytohesin-1 controls the activation of RhoA and modulates integrin-dependent adhesion and migration of dendritic cells*. Blood, 2009. **113**(23): p. 5801-10.

321. El Azreq, M.A., V. Garceau, and S.G. Bourgoin, *Cytohesin-1 regulates fMLF-mediated activation and functions of the beta2 integrin Mac-1 in human neutrophils*. J Leukoc Biol, 2011. **89**(6): p. 823-36.

322. Jo, E.K., H. Wang, and C.E. Rudd, *An essential role for SKAP-55 in LFA-1 clustering on T cells that cannot be substituted by SKAP-55R*. J Exp Med, 2005. **201**(11): p. 1733-9.

323. Menasche, G., et al., *RIAM links the ADAP/SKAP-55 signaling module to Rap1, facilitating T-cell-receptor-mediated integrin activation*. Mol Cell Biol, 2007. **27**(11): p. 4070-81.

324. Witte, A., et al., *D120 and K152 within the PH Domain of T Cell Adapter SKAP55 Regulate Plasma Membrane Targeting of SKAP55 and LFA-1 Affinity Modulation in Human T Lymphocytes*. Mol Cell Biol, 2017. **37**(7): p. MCB.00509-16.

325. Ophir, M.J., B.C. Liu, and S.C. Bunnell, *The N terminus of SKAP55 enables T cell adhesion to TCR and integrin ligands via distinct mechanisms*. J Cell Biol, 2013. **203**(6): p. 1021-41.

326. Svensson, L., et al., *Leukocyte adhesion deficiency-III is caused by mutations in KINDLIN3 affecting integrin activation*. Nat Med, 2009. **15**(3): p. 306-12.

327. Moser, M., et al., *Kindlin-3 is required for beta2 integrin-mediated leukocyte adhesion to endothelial cells*. Nat Med, 2009. **15**(3): p. 300-5.

328. Hart, R., et al., *The kindlin 3 pleckstrin homology domain has an essential role in lymphocyte function-associated antigen 1 (LFA-1) integrin-mediated B cell adhesion and migration*. J Biol Chem, 2013. **288**(21): p. 14852-62.

329. Eppler, F.J., T. Quast, and W. Kolanus, *Dynamin2 controls Rap1 activation and integrin clustering in human T lymphocyte adhesion*. PLoS One, 2017. **12**(3): p. e0172443.

330. Labno, C.M., et al., *Itk Functions to Control Actin Polymerization at the Immune Synapse through Localized Activation of Cdc42 and WASP*. Current Biology, 2003. **13**(18): p. 1619-1624.

331. Finkelstein, L.D., Y. Shimizu, and P.L. Schwartzberg, *Tec Kinases Regulate TCR-Mediated Recruitment of Signaling Molecules and Integrin-Dependent Cell Adhesion*. The Journal of Immunology, 2005. **175**(9): p. 5923-5930.

332. Huang, Y.H., et al., *Positive regulation of Itk PH domain function by soluble IP4*. Science, 2007. **316**(5826): p. 886-9.

333. Krawczyk, C., et al., *Vav1 controls integrin clustering and MHC/peptide-specific cell adhesion to antigen-presenting cells*. Immunity, 2002. **16**(3): p. 331-43.

334. Prisco, A., et al., *Lineage-specific requirement for the PH domain of Vav1 in the activation of CD4+ but not CD8+ T cells*. Immunity, 2005. **23**(3): p. 263-74.

335. Sanematsu, F., et al., *Phosphatidic acid-dependent recruitment and function of the Rac activator DOCK1 during dorsal ruffle formation*. J Biol Chem, 2013. **288**(12): p. 8092-8100.

336. Sanui, T., et al., *DOCK2 is essential for antigen-induced translocation of TCR and lipid rafts, but not PKC-theta and LFA-1, in T cells*. Immunity, 2003. **19**(1): p. 119-29.

337. Battram, A.M., et al., *The phosphatidylinositol 3,4,5-trisphosphate (PI(3,4,5)P3) binder Rasa3 regulates phosphoinositide 3-kinase (PI3K)-dependent integrin αIIbβ3 outside-in signaling*. Journal of Biological Chemistry, 2017. **292**(5): p. 1691-1704.

338. Cullen, P.J., et al., *Specificity of the purified inositol (1,3,4,5) tetrakisphosphate-binding protein from porcine platelets*. FEBS Lett, 1995. **358**(3): p. 240-2.

339. Cullen, P.J., A.P. Dawson, and R.F. Irvine, *Purification and characterization of an Ins(1,3,4,5)P4 binding protein from pig platelets: possible identification of a novel non-neuronal Ins(1,3,4,5)P4 receptor*. Biochem J, 1995. **305 (Pt 1)**: p. 139-43.

340. Cullen, P.J., et al., *Identification of a specific Ins(1,3,4,5)P4-binding protein as a member of the GAP1 family*. Nature, 1995. **376**(6540): p. 527-30.

341. Nafisi, H., et al., *GAP1(IP4BP)/RASA3 mediates Galphai-induced inhibition of mitogen-activated protein kinase*. J Biol Chem, 2008. **283**(51): p. 35908-17.

342. Kupzig, S., et al., *GAP1 family members constitute bifunctional Ras and Rap GTPase-activating proteins*. J Biol Chem, 2006. **281**(15): p. 9891-900.

343. Sot, B., et al., *Unravelling the mechanism of dual-specificity GAPs*. EMBO J, 2010. **29**(7): p. 1205-14.

344. Kupzig, S., et al., *The Ability of GAP1IP4BP To Function as a Rap1 GTPase-Activating Protein (GAP) Requires Its Ras GAP-Related Domain and an Arginine Finger Rather than an Asparagine Thumb*. Molecular and Cellular Biology, 2009. **29**(14): p. 3929-3940.

345. Fagerberg, L., et al., *Analysis of the Human Tissue-specific Expression by Genome-wide Integration of Transcriptomics and Antibody-based Proteomics*. Mol Cell Proteomics, 2014. **13**(2): p. 397-406.

346. Lockyer, P.J., et al., *Distinct subcellular localisations of the putative inositol 1,3,4,5-tetrakisphosphate receptors GAP1IP4BP and GAP1m result from the GAP1IP4BP PH domain directing plasma membrane targeting*. Curr Biol, 1997. **7**(12): p. 1007-10.

347. Cozier, G.E., et al., *GAP1IP4BP contains a novel group I pleckstrin homology domain that directs constitutive plasma membrane association*. J Biol Chem, 2000. **275**(36): p. 28261-8.

348. Hammond, G.R., et al., *Reversible binding and rapid diffusion of proteins in complex with inositol lipids serves to coordinate free movement with spatial information*. J Cell Biol, 2009. **184**(2): p. 297-308.

349. Blanc, L., et al., *Critical function for the Ras-GTPase activating protein RASA3 in vertebrate erythropoiesis and megakaryopoiesis*. Proc Natl Acad Sci U S A, 2012. **109**(30): p. 12099-104.

350. Molina-Ortiz, P., et al., *Rasa3 Controls Megakaryocyte Rap1 Activation, Integrin Signaling and Differentiation into Proplatelet*. PLoS Genetics, 2014. **10**(6).

351. Iwashita, S., et al., *Versatile roles of R-Ras GAP in neurite formation of PC12 cells and embryonic vascular development*. J Biol Chem, 2007. **282**(6): p. 3413-7.

352. Stefanini, L., et al., *RASA3 is a critical inhibitor of RAP1-dependent platelet activation*. Journal of Clinical Investigation, 2015. **125**(4): p. 1419-1432.

353. Molina-Ortiz, P., et al., *Rasa3 controls turnover of endothelial cell adhesion and vascular lumen integrity by a Rap1-dependent mechanism*. PLoS Genet, 2018. **14**(1): p. e1007195.

354. Durrant, T.N., et al., *Identification of PtdIns(3,4)P2 effectors in human platelets using quantitative proteomics*. Biochim Biophys Acta Mol Cell Biol Lipids, 2020. **1865**(2): p. 158575.

355. Wu, B., et al., *RAS P21 Protein Activator 3 (RASA3) Specifically Promotes Pathogenic T Helper 17 Cell Generation by Repressing T-Helper-2-Cell-Biased Programs*. Immunity, 2018. **49**(5): p. 886-898.e5.

356. Lawson, K.A., et al., *Functional genomic landscape of cancer-intrinsic evasion of killing by T cells*. Nature, 2020. **586**(7827): p. 120-126.

357. Li, B., et al., *Genome-wide CRISPR screen identifies host dependency factors for influenza A virus infection*. Nat Commun, 2020. **11**(1): p. 164.

358. Park, R.J., et al., *A genome-wide CRISPR screen identifies a restricted set of HIV host dependency factors*. Nat Genet, 2017. **49**(2): p. 193-203.

359. Zhu, Y., et al., *A genome-wide CRISPR screen identifies host factors that regulate SARS-CoV-2 entry*. Nat Commun, 2021. **12**(1): p. 961.

360. Cortez, J.T., et al., *CRISPR screen in regulatory T cells reveals modulators of Foxp3*. Nature, 2020. **582**(7812): p. 416-420.

361. Shifrut, E., et al., *Genome-wide CRISPR Screens in Primary Human T Cells Reveal Key Regulators of Immune Function*. Cell, 2018. **175**(7): p. 1958-1971 e15.

362. Rupp, L.J., et al., *CRISPR/Cas9-mediated PD-1 disruption enhances anti-tumor efficacy of human chimeric antigen receptor T cells*. Sci Rep, 2017. **7**(1): p. 737.

363. Makarova, K.S., et al., *A putative RNA-interference-based immune system in prokaryotes: computational analysis of the predicted enzymatic machinery, functional analogies with eukaryotic RNAi, and hypothetical mechanisms of action*. Biol Direct, 2006. **1**: p. 7.

364. Barrangou, R., et al., *CRISPR provides acquired resistance against viruses in prokaryotes*. Science, 2007. **315**(5819): p. 1709-12.

365. Garneau, J.E., et al., *The CRISPR/Cas bacterial immune system cleaves bacteriophage and plasmid DNA*. Nature, 2010. **468**(7320): p. 67-71.

366. Anders, C., et al., *Structural basis of PAM-dependent target DNA recognition by the Cas9 endonuclease*. Nature, 2014. **513**(7519): p. 569-73.

367. Jinek, M., et al., *A programmable dual-RNA-guided DNA endonuclease in adaptive bacterial immunity*. Science, 2012. **337**(6096): p. 816-21.

368. Doench, J.G., et al., *Optimized sgRNA design to maximize activity and minimize off-target effects of CRISPR-Cas9*. Nature Biotechnology, 2016. **34**(2): p. 184-191.

369. Cong, L., et al., *Multiplex Genome Engineering Using CRISPR/Cas Systems*. Science, 2013. **339**(6121): p. 819-823.

370. Jinek, M., et al., *RNA-programmed genome editing in human cells*. Elife, 2013. **2**(2): p. e00471.

371. Cho, S.W., et al., *Targeted genome engineering in human cells with the Cas9 RNA-guided endonuclease*. Nat Biotechnol, 2013. **31**(3): p. 230-2.

372. Mali, P., et al., *RNA-guided human genome engineering via Cas9*. Science, 2013. **339**(6121): p. 823-6.

373. Zhang, T., T.C. Tsang, and D.T. Harris, *Efficient transduction of murine primary T cells requires a combination of high viral titer, preferred tropism, and proper timing of transduction*. J Hematother Stem Cell Res, 2003. **12**(1): p. 123-30.

374. Kerkar, S.P., et al., *Genetic engineering of murine CD8+ and CD4+ T cells for preclinical adoptive immunotherapy studies*. J Immunother, 2011. **34**(4): p. 343-52.

375. Schumann, K., et al., *Generation of knock-in primary human T cells using Cas9 ribonucleoproteins*. Proceedings of the National Academy of Sciences, 2015. **112**(33): p. 10437-10442.

376. Seki, A. and S. Rutz, *Optimized RNP transfection for highly efficient CRISPR/Cas9-mediated gene knockout in primary T cells*. J Exp Med, 2018. **215**(3): p. 985-997.

377. Chu, V.T., et al., *Efficient generation of Rosa26 knock-in mice using CRISPR/Cas9 in C57BL/6 zygotes*. BMC Biotechnology, 2016. **16**(1): p. 4-4.

378. Platt, Randall J., et al., *CRISPR-Cas9 Knockin Mice for Genome Editing and Cancer Modeling*. Cell, 2014. **159**(2): p. 440-455.

379. Huang, B., K.H. Johansen, and P.L. Schwartzberg, *Efficient CRISPR/Cas9-Mediated Mutagenesis in Primary Murine T Lymphocytes*. Curr Protoc Immunol, 2019. **124**(1): p. e62.

380. LaFleur, M.W., et al., *A CRISPR-Cas9 delivery system for in vivo screening of genes in the immune system*. Nat Commun, 2019. **10**(1): p. 1668.

381. Evers, B., et al., *CRISPR knockout screening outperforms shRNA and CRISPRi in identifying essential genes*. Nat Biotechnol, 2016. **34**(6): p. 631-3.

382. Koike-Yusa, H., et al., *Genome-wide recessive genetic screening in mammalian cells with a lentiviral CRISPR-guide RNA library*. Nat Biotechnol, 2014. **32**(3): p. 267-73.

383. Shalem, O., N.E. Sanjana, and F. Zhang, *High-throughput functional genomics using CRISPR-Cas9*. Nat Rev Genet, 2015. **16**(5): p. 299-311.

384. Dixit, A., et al., *Perturb-Seq: Dissecting Molecular Circuits with Scalable Single-Cell RNA Profiling of Pooled Genetic Screens*. Cell, 2016. **167**(7): p. 1853-1866 e17.

385. Datlinger, P., et al., *Pooled CRISPR screening with single-cell transcriptome readout*. Nat Methods, 2017. **14**(3): p. 297-301.

386. Song, Q., et al., *Direct-seq: programmed gRNA scaffold for streamlined scRNA-seq in CRISPR screen*. Genome Biol, 2020. **21**(1): p. 136.

387. Wroblewska, A., et al., *Protein Barcodes Enable High-Dimensional Single-Cell CRISPR Screens*. Cell, 2018. **175**(4): p. 1141-1155 e16.

388. Barnden, M.J., et al., *Defective TCR expression in transgenic mice constructed using cDNA-based alpha- and beta-chain genes under the control of heterologous regulatory elements*. Immunol Cell Biol, 1998. **76**(1): p. 34-40.

389. Okkenhaug, K., et al., *Impaired B and T cell antigen receptor signaling in p110delta PI 3-kinase mutant mice*. Science, 2002. **297**(5583): p. 1031-4.

390. Hollister, K., et al., *Insights into the role of Bcl6 in follicular Th cells using a new conditional mutant mouse model*. J Immunol, 2013. **191**(7): p. 3705-11.

391. Konstandin, M.H., et al., *A novel flow-cytometry-based assay for quantification of affinity and avidity changes of integrins*. Journal of Immunological Methods, 2006. **310**(1-2): p. 67-77.

392. Kochl, R., et al., *WNK1 kinase balances T cell adhesion versus migration in vivo*. Nat Immunol, 2016. **17**(9): p. 1075-1083.

393. Phelan, J.D., et al., *A multiprotein supercomplex controlling oncogenic signalling in lymphoma*. Nature, 2018. **560**(7718): p. 387-391.

394. Webster, D.E., S. Roulland, and J.D. Phelan, *Protocols for CRISPR-Cas9 screening in lymphoma cell lines*. 2019, Humana Press Inc. p. 337-350.

395. Li, W., et al., *MAGeCK enables robust identification of essential genes from genome-scale CRISPR/Cas9 knockout screens*. Genome biology, 2014. **15**(12): p. 554-554.

396. Li, W., R.N. Germain, and M.Y. Gerner, *High-dimensional cell-level analysis of tissues with Ce3D multiplex volume imaging*. Nat Protoc, 2019. **14**(6): p. 1708-1733.

397. Waldo, G.S., et al., *Rapid protein-folding assay using green fluorescent protein*. Nat Biotechnol, 1999. **17**(7): p. 691-5.

398. Wang, B., et al., *Integrative analysis of pooled CRISPR genetic screens using MAGeCKFlute*. Nature Protocols, 2019. **14**(3): p. 756-780.

399. Hagani, A.B., et al., *Activation conditions determine susceptibility of murine primary T-lymphocytes to retroviral infection*. J Gene Med, 1999. **1**(5): p. 341-51.

400. Mitchell, A.L., et al., *InterPro in 2019: improving coverage, classification and access to protein sequence annotations*. Nucleic Acids Res, 2019. **47**(D1): p. D351-D360.

401. Wang, X., et al., *The Tumor Suppressor PTEN Regulates T Cell Survival and Antigen Receptor Signaling by Acting as a Phosphatidylinositol 3-Phosphatase*. The Journal of Immunology, 2000. **164**(4): p. 1934-1939.

402. Yu, Y., et al., *Phosphoproteomic analysis identifies Grb10 as an mTORC1 substrate that negatively regulates insulin signaling*. Science, 2011. **332**(6035): p. 1322-6.

403. Swat, W., et al., *Essential role of PI3Kdelta and PI3Kgamma in thymocyte survival*. Blood, 2006. **107**(6): p. 2415-22.

404. Di Cristofano, A., et al., *Impaired Fas response and autoimmunity in Pten+/- mice*. Science, 1999. **285**(5436): p. 2122-5.

405. Moser, M., et al., *The tail of integrins, talin, and kindlins*. 2009, American Association for the Advancement of Science. p. 895-899.

406. Calderwood, D.A., I.D. Campbell, and D.R. Critchley, *Talins and kindlins: Partners in integrin-mediated adhesion*. 2013.

407. Gomez, T.S., et al., *Dynamin 2 regulates T cell activation by controlling actin polymerization at the immunological synapse*. Nature Immunology, 2005. **6**(3): p. 261-270.

408. Miletic, A.V., et al., *Vav links the T cell antigen receptor to the actin cytoskeleton and T cell activation independently of intrinsic Guanine nucleotide exchange activity*. PloS one, 2009. **4**(8): p. e6599-e6599.

409. Ardouin, L., et al., *Vav1 transduces TCR signals required for LFA-1 function and cell polarization at the immunological synapse*. Eur J Immunol, 2003. **33**(3): p. 790-7.

410. Wen, L., et al., *Kindlin-3 recruitment to the plasma membrane precedes high-affinity beta2-integrin and neutrophil arrest from rolling*. Blood, 2021. **137**(1): p. 29-38.

411. Ni, T., et al., *Structure and lipid-binding properties of the kindlin-3 pleckstrin homology domain*. Biochem J, 2017. **474**(4): p. 539-556.

412. Bethoney, K.A., et al., *A possible effector role for the pleckstrin homology (PH) domain of dynamin*. Proc Natl Acad Sci U S A, 2009. **106**(32): p. 13359-64.

413. Han, J., et al., *Role of substrates and products of PI 3-kinase in regulating activation of Rac-related guanosine triphosphatases by Vav*. Science, 1998. **279**(5350): p. 558-60.

414. Morlino, G., et al., *Miro-1 links mitochondria and microtubule Dynein motors to control lymphocyte migration and polarity*. Mol Cell Biol, 2014. **34**(8): p. 1412-26.

415. Capece, T., et al., *A novel intracellular pool of LFA-1 is critical for asymmetric CD8(+) T cell activation and differentiation*. J Cell Biol, 2017. **216**(11): p. 3817-3829.

416. Heng, T.S., M.W. Painter, and C. Immunological Genome Project, *The Immunological Genome Project: networks of gene expression in immune cells*. Nat Immunol, 2008. **9**(10): p. 1091-4.

417. Howden, A.J.M., et al., *Quantitative analysis of T cell proteomes and environmental sensors during T cell differentiation*. Nat Immunol, 2019. **20**(11): p. 1542-1554.

418. Nussinov, R., et al., *The Mystery of Rap1 Suppression of Oncogenic Ras*. Trends Cancer, 2020. **6**(5): p. 369-379.

419. Sot, B., et al., *Ras GTPase activating (RasGAP) activity of the dual specificity GAP protein Rasal requires colocalization and C2 domain binding to lipid membranes*. Proc Natl Acad Sci U S A, 2013. **110**(1): p. 111-6.

420. Scholer, A., et al., *Intercellular Adhesion Molecule-1-Dependent Stable Interactions between T Cells and Dendritic Cells Determine CD8+ T Cell Memory*. Immunity, 2008. **28**(2): p. 258-270.

421. Johnson, K.G., et al., *A supramolecular basis for CD45 tyrosine phosphatase regulation in sustained T cell activation*. Proc Natl Acad Sci U S A, 2000. **97**(18): p. 10138-43.

422. Douglass, A.D. and R.D. Vale, *Single-molecule microscopy reveals plasma membrane microdomains created by protein-protein networks that exclude or trap signaling molecules in T cells*. Cell, 2005. **121**(6): p. 937-50.

423. Bjorgo, E., et al., *Cross talk between phosphatidylinositol 3-kinase and cyclic AMP (cAMP)-protein kinase a signaling pathways at the level of a protein kinase B/beta-arrestin/cAMP phosphodiesterase 4 complex*. Mol Cell Biol, 2010. **30**(7): p. 1660-72.

424. Medeiros, R.B., et al., *Protein kinase D1 and the beta 1 integrin cytoplasmic domain control beta 1 integrin function via regulation of Rap1 activation*. Immunity, 2005. **23**(2): p. 213-26.

425. Nalefski, E.A. and J.J. Falke, *The C2 domain calcium-binding motif: structural and functional diversity*. Protein Sci, 1996. **5**(12): p. 2375-90.

426. Qi, H., et al., *SAP-controlled T-B cell interactions underlie germinal centre formation*. Nature, 2008. **455**(7214): p. 764-9.

427. Georgiev, H., et al., *Shared and Unique Features Distinguishing Follicular T Helper and Regulatory Cells of Peripheral Lymph Node and Peyer's Patches*. Front Immunol, 2018. **9**: p. 714.

428. Sage, P.T., et al., *Defective TFH Cell Function and Increased TFR Cells Contribute to Defective Antibody Production in Aging*. Cell Rep, 2015. **12**(2): p. 163-71.

429. Sage, P.T., et al., *The receptor PD-1 controls follicular regulatory T cells in the lymph nodes and blood*. Nat Immunol, 2013. **14**(2): p. 152-61.

430. Robinson, C., et al., *Alum adjuvant is more effective than MF59 at prompting early germinal center formation in response to peptide-protein conjugates and enhancing*

efficacy of a vaccine against opioid use disorders. Hum Vaccin Immunother, 2019. **15**(4): p. 909-917.

431. Avery, D.T., et al., *IL-21-induced isotype switching to IgG and IgA by human naive B cells is differentially regulated by IL-4*. J Immunol, 2008. **181**(3): p. 1767-79.

432. Kobayashi, T., et al., *Follicular helper T cells mediate IgE antibody response to airborne allergens*. J Allergy Clin Immunol, 2017. **139**(1): p. 300-313 e7.

433. Davalos-Misslitz, A.C., et al., *Impaired responsiveness to T-cell receptor stimulation and defective negative selection of thymocytes in CCR7-deficient mice*. Blood, 2007. **110**(13): p. 4351-9.

434. Kurobe, H., et al., *CCR7-dependent cortex-to-medulla migration of positively selected thymocytes is essential for establishing central tolerance*. Immunity, 2006. **24**(2): p. 165-77.

435. Ueda, Y., et al., *Mst1 regulates integrin-dependent thymocyte trafficking and antigen recognition in the thymus*. Nat Commun, 2012. **3**: p. 1098.

436. Dong, Y., et al., *A cell-intrinsic role for Mst1 in regulating thymocyte egress*. J Immunol, 2009. **183**(6): p. 3865-72.

437. Katagiri, K., et al., *Mst1 controls lymphocyte trafficking and interstitial motility within lymph nodes*. EMBO J, 2009. **28**(9): p. 1319-31.

438. Strasser, A., et al., *Positive and negative selection of T cells in T-cell receptor transgenic mice expressing a bcl-2 transgene*. Proc Natl Acad Sci U S A, 1994. **91**(4): p. 1376-80.

439. Park, E.J., et al., *Distinct roles for LFA-1 affinity regulation during T-cell adhesion, diapedesis, and interstitial migration in lymph nodes*. Blood, 2010. **115**(8): p. 1572-81.

440. Guarda, G., et al., *L-selectin-negative CCR7- effector and memory CD8+ T cells enter reactive lymph nodes and kill dendritic cells*. Nat Immunol, 2007. **8**(7): p. 743-52.

441. Sage, P.T. and A.H. Sharpe, *The multifaceted functions of follicular regulatory T cells*. Curr Opin Immunol, 2020. **67**: p. 68-74.

442. Sage, P.T. and A.H. Sharpe, *In vitro assay to sensitively measure T(FR) suppressive capacity and T(FH) stimulation of B cell responses*. Methods Mol Biol, 2015. **1291**: p. 151-60.

443. Kurzinger, K., et al., *A novel lymphocyte function-associated antigen (LFA-1): cellular distribution, quantitative expression, and structure*. J Immunol, 1981. **127**(2): p. 596-602.

444. Harjunpää, H., et al., *Cell adhesion molecules and their roles and regulation in the immune and tumor microenvironment*. Frontiers in Immunology, 2019. **10**(MAY).

445. Carrasco, Y.R., et al., *LFA-1/ICAM-1 interaction lowers the threshold of B cell activation by facilitating B cell adhesion and synapse formation*. Immunity, 2004. **20**(5): p. 589-599.

446. Vanhaesebroeck, B., et al., *PI3K inhibitors are finally coming of age*. Nature Reviews Drug Discovery, 2021: p. In press.

447. Lee, Y., et al., *Induction and molecular signature of pathogenic T H 17 cells*. Nature Immunology, 2012. **13**(10): p. 991-999.

448. McKinstry, K.K., et al., *Rapid default transition of CD4 T cell effectors to functional memory cells*. Journal of Experimental Medicine, 2007. **204**(9): p. 2199-2211.

449. Dugger, K.J., et al., *Effector and suppressor roles for LFA-1 during the development of experimental autoimmune encephalomyelitis*. Journal of Neuroimmunology, 2009. **206**(1-2): p. 22-27.

450. Gultner, S., et al., *Reduced Treg frequency in LFA-1-deficient mice allows enhanced T effector differentiation and pathology in EAE*. Eur J Immunol, 2010. **40**(12): p. 3403-12.

451. Welsh, C.T., et al., *Augmentation of adoptively transferred experimental allergic encephalomyelitis by administration of a monoclonal antibody specific for LFA-1α*. Journal of Neuroimmunology, 1993. **43**(1-2): p. 161-167.

452. Wang, Y., et al., *A critical role of LFA-1 in the development of Th17 cells and induction of experimental autoimmune encephalomyelytis*. Biochem Biophys Res Commun, 2007. **353**(4): p. 857-62.

453. Salinas, G.F., et al., *Sustained Rap1 activation in autoantigen-specific T lymphocytes attenuates experimental autoimmune encephalomyelitis*. J Neuroimmunol, 2012. **250**(1-2): p. 35-43.

454. Ishihara, S., et al., *Dual functions of Rap1 are crucial for T-cell homeostasis and prevention of spontaneous colitis*. Nat Commun, 2015. **6**: p. 8982.

455. Roux, K.J., et al., *BioID: A Screen for Protein-Protein Interactions*. Curr Protoc Protein Sci, 2018. **91**: p. 19 23 1-19 23 15.

456. Geladaki, A., et al., *Combining LOPIT with differential ultracentrifugation for high-resolution spatial proteomics*. Nat Commun, 2019. **10**(1): p. 331.

7. Appendix

In these appendices, I present data not included in the main body of the thesis as the experiments were conducted by colleagues or collaborators without my direct involvement, but still related to the presented project. I further include oligos used in the thesis.

7.1 Appendix data

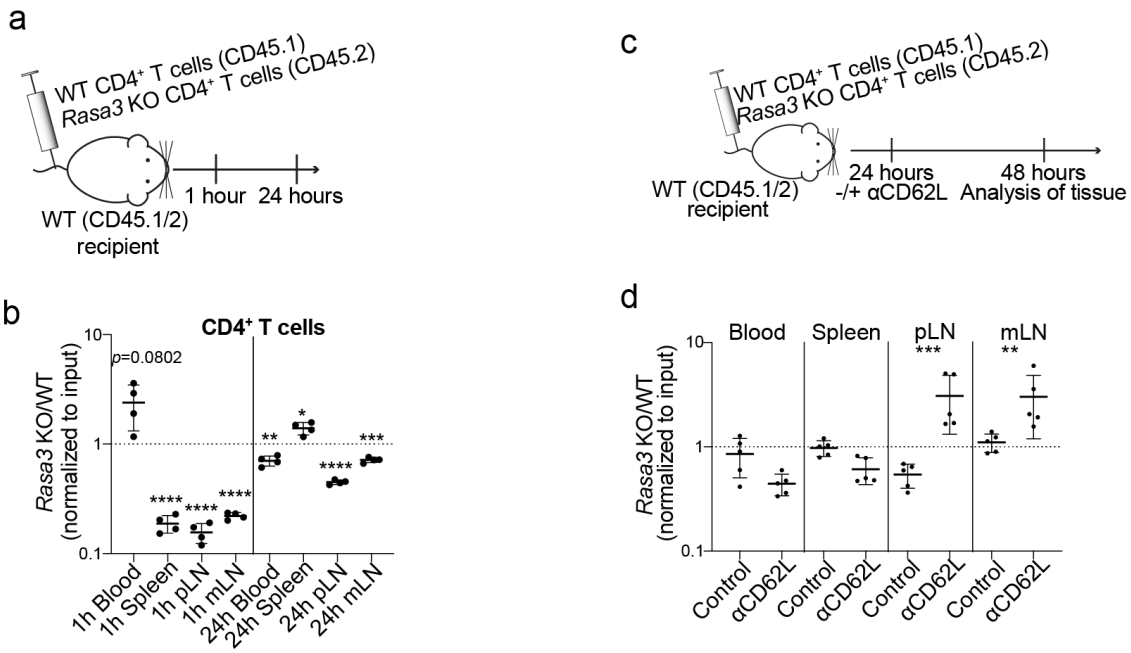

Figure A-1. Migration following competitive transfer of *Rasa3* KO T cells. **a**, Diagram showing transfer experiments. 2x10^6 CD45.1 WT CD4$^+$ T cells and 2x10^6 CD45.2 *Rasa3* KO CD4$^+$ T cells were transferred i.v. and cells were quantified 1h and 24h later by flow cytometry. **b**, *Rasa3* KO/WT ratio were calculated, and normalised to input ratios. **c**, Diagram of egress transfer experiments. 2x10^6 CD45.1 WT CD4$^+$ T cells and 2x10^6 CD45.2 *Rasa3* KO CD4$^+$ T cells were transferred i.v. 24h later, mice were injected with 250μg anti-CD62L or PBS, and cells were quantified 24h later by flow cytometry. **d**, *Rasa3* KO/WT ratio were calculated, and normalised to input ratios with and without anti-CD62L. *P<0.05; **P<0.01, ***P<0.001, ****P<0.0001 as evaluated by One-sample Student's t test comparing samples to a mean of 1 (**b**) or comparing sample to its respective control (**d**). This experiment was performed by Dr. Dominic Golec.

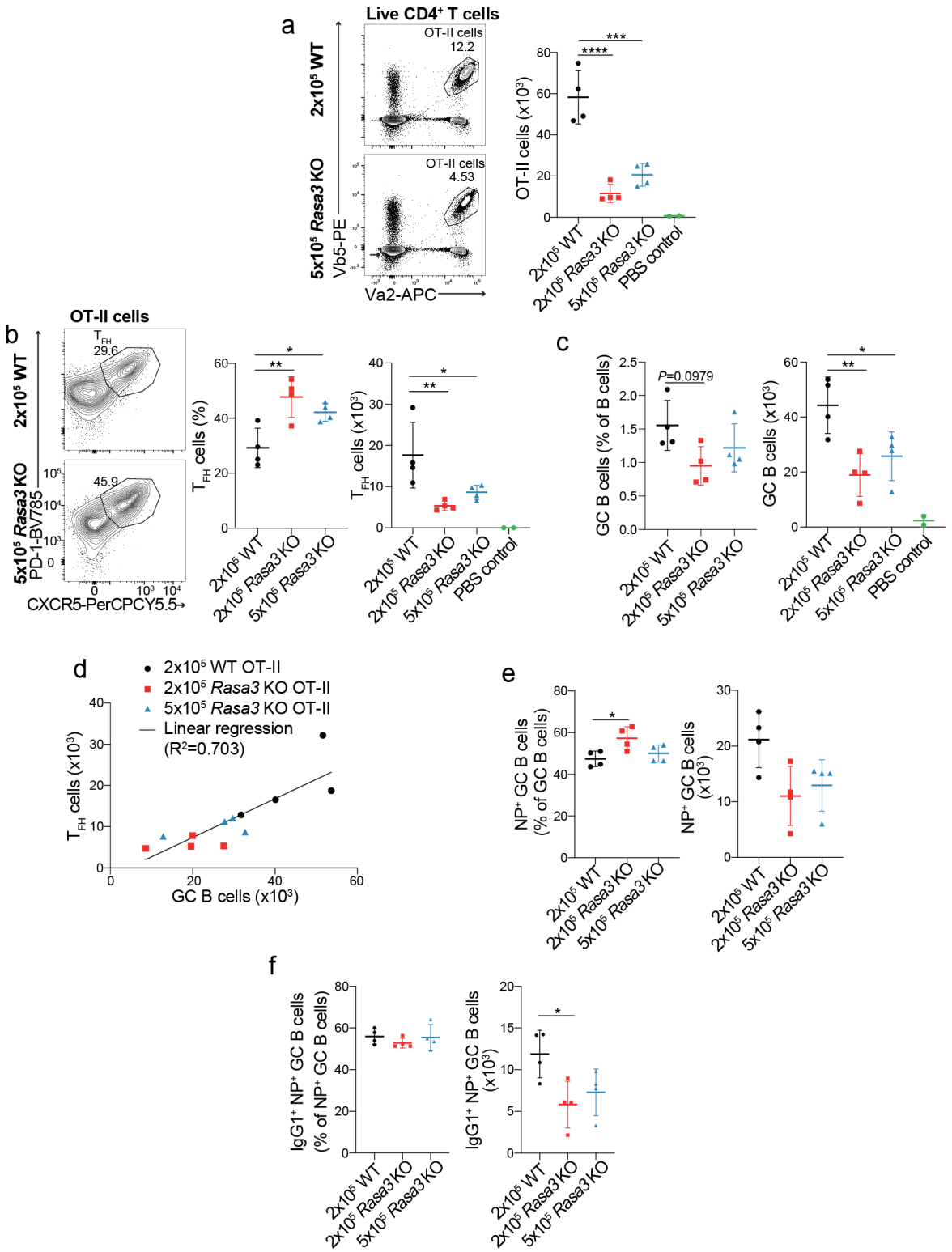

Figure A-2. OT-II transfer with varying *Rasa3* KO T cell numbers conducted at NIH. OT-II naïve CD4+ T cells (see numbers and genotype in figure) were transferred to *Bcl6*$^{fl/fl}$ x *Cd4*^{Cre} mice and the mice were immunised 24 hours later in hock with NP-OVA/Alum and culled 8 days after that. **a-c**, Percentages, and numbers of OT-II cells

(**a**) T_{FH} cells (**b**), GC B cells (**c**) on day 8, measured by flow cytometry. **d**, Correlation of GC B cell numbers and T_{FH} cell numbers following transfers in (**a**-**c**). **e**-**f** Percentages and numbers of NP^+ GC B cells (**e**) and $IgG1^+$ NP^+ GC B cells (**f**) in dLNs day 8 following transfer and immunisation. n=4 per group, each dot is one mouse, error bar: mean±SD. **P*<0.05; ***P*<0.01, ****P*<0.001, *****P*<0.0001 as evaluated by Mann-Whitney U-tests with Holm-Šídák's multiple comparison correction (**a**-**c**, **e**-**f**). This experiment was performed by Dr. Dominic Golec and Dr. Bonnie Huang.

7.2 Oligos

All sgRNAs used in the thesis can be found on
https://drive.google.com/file/d/19mibsjHj4B4z4odbZcdZxh0iAWxW7o1B/view?usp=sharing

qRT-PCR and PCR primers	
Hprt1_Fwd	CTTCCTCCTCAGACCGCTTT
Hprt1_Rev	ACCTGGTTCATCATCGCTAA
Rasa3_fwd	GAGGATCAAGATTGGTGAAGCC
Rasa3_rev	AGTAGCAGTCCCTCATCTTGTTTG
Rasa3flox_Fwd	CCAGTGTTACGGTCGTCTGC
Rasa3flox_Rev	GTGTCCTCTTCCTAGTGTCGT
Cloning primers	
mRuby_fwd HiFi assembly	TAGATCTCTCGAGGTTAACGGCCACCATGAACAGCCTGATCAAAGAAAAC
mRuby_rev HiFi assembly	CACTTCCTCCTCCTCCCCCTCCGCCCAGGCCG
hRasa3_Fwd HiFi assembly	AAGTTCGCCGGCCTGGGCGGAGGAGGTTCCGGAGGTGGAGGAAGTATGGCGGTGGAGGAC GAGGG
hRasa3_Rev HiFi assembly	TCGATAAGCTTGGCTGCAGGATTAAATGGAATGAGTGGAGGTCTCG
hRasa3_R371Q_mut	CGCCAGTGAGTTTCCTTGGAAGATGGTGTTGGG
hRasa3_K599Q_K600Q_R601Q_mut	GGTCAAGCGAAACCATTGCTGCTGAAAATTCTTCATCCCAAAGCGCTTCCGTCC
Kozak_fragment	CCTTCTCTAGGCGCCGGAATTAGATCTCTCGAGGTTAACGAGGCCTCAATTGGCCGCCACCA TGGTGAGCAAGGGCGAGGAGCTGTTCACCGGGGTGGTGCCCA
hRasa3-GFP_Fwd	GGCCGCCACCATGGCGGTGGAGGACGAG
hRasa3-GFP_Rev	GAATTCGCCAGAACCAGCAGCGGAGCCAGCGGATCCAATGGAATGAGTGGAGGTCTCG
MGR1_Fwd	GGATCCGCTGGCTCCGCTGCTGGTTCTGGCGAATTCATGGTGAGCAAGGGCGAG
MGR1_Rev	CCACCGCCATGGTGGCGGCCAATTGAGG
Primers for CRISPR library cloning and screening	
guide_ID_Fwd	GAACCTCCTCGTTCGACCCC
guide_ID_Rev	GCACACCGGCCTTATTCCA
ARRAY-Fwd	ACTGTAAAGTAATTGTGTGTTTTGAGACTATAAATATCAATTGGAGAAAAGCCTTGTTTG
ARRAY-Rev	TTTTTCAAGTTGATAACGGACTAGCCTTATTTTAACTTGCTAGGATCCTAGCTCTAAAAC